

Effect of Oxidation on the Compression Behaviour of Organic Soils

Zain, N.H.M.

DOI

[10.4233/uuid:aa7fe90a-7bf5-4c91-aa3e-c6a594a7d59d](https://doi.org/10.4233/uuid:aa7fe90a-7bf5-4c91-aa3e-c6a594a7d59d)

Publication date

2019

Document Version

Final published version

Citation (APA)

Zain, N. H. M. (2019). *Effect of Oxidation on the Compression Behaviour of Organic Soils*. [Dissertation (TU Delft), Delft University of Technology]. <https://doi.org/10.4233/uuid:aa7fe90a-7bf5-4c91-aa3e-c6a594a7d59d>

Important note

To cite this publication, please use the final published version (if applicable). Please check the document version above.

Copyright

Other than for strictly personal use, it is not permitted to download, forward or distribute the text or part of it, without the consent of the author(s) and/or copyright holder(s), unless the work is under an open content license such as Creative Commons.

Takedown policy

Please contact us and provide details if you believe this document breaches copyrights. We will remove access to the work immediately and investigate your claim.

**EFFECT OF OXIDATION ON THE COMPRESSION
BEHAVIOUR OF ORGANIC SOILS**

EFFECT OF OXIDATION ON THE COMPRESSION BEHAVIOUR OF ORGANIC SOILS

Proefschrift

ter verkrijging van de graad van doctor
aan de Technische Universiteit Delft,
op gezag van de Rector Magnificus prof. dr. ir. T.H.J.J. van der Hagen,
voorzitter van het College voor Promoties,
in het openbaar te verdedigen op dinsdag 9 Juli 2019 om 10:00 uur

door

Nor Hazwani Md. ZAIN

Master of Science in Geotechnical Engineering,
Faculty of Civil Engineering,
Universiti Teknologi MARA (UiTM), Shah Alam, Selangor, Malaysia,
geboren te Kuala Lumpur, Malaysia.

Dit proefschrift is goedgekeurd door de

promotor: prof. dr. ir. C. Jommi
copromotor: dr. ir. L.A. van Paassen

Samenstelling promotiecommissie:

Rector Magnificus	voorzitter
Prof. dr. ir. C. Jommi	Technische Universiteit Delft, promotor
Dr. ir. L.A. van Paassen	Arizona State University, USA, copromotor

Onafhankelijke leden:

Prof. dr. C. Zapata	Arizona State University, USA
Prof. dr. G. Della Vecchia	Politecnico di Milano, Italy
Prof. dr. M. Hattab	Université de Lorraine, France
Prof. dr. M.A. Hicks	Technische Universiteit Delft
Dr. C. Chassagne	Technische Universiteit Delft

Overige leden:

Prof. dr. ir. M. Kok	Technische Universiteit Delft
----------------------	-------------------------------



Keywords: decomposition, oxidation, settlement, consolidation, organic soils, compressibility

Printed by: Ipskamp Printing

Front & Back: www.greifswaldmoor.de

Copyright © 2019 by N.H.M. ZAIN

Email: hazwani_zain@yahoo.co.uk

ISBN 978-94-028-1596-2

An electronic version of this dissertation is available at

<http://repository.tudelft.nl/>.

To my beloved family and friends

CONTENTS

1	Introduction	1
1.1	Problem Background	2
1.2	Scientific Gap	7
1.3	Proposed Solution	8
1.4	Main Question	8
1.5	Methods	8
1.6	Thesis Outline	9
2	Organic soils and Peat	11
2.1	Definition and organic content classification	12
2.2	Botanical classification	16
2.2.1	von Post classification system	16
2.2.2	Radforth classification system	19
2.2.3	Fibre content and degree of humification classification	22
2.3	Dutch Classification System.	24
2.4	Soil Formations	25
2.5	Structural arrangement and Soil Model	28
2.6	Humification and Oxidation	32
2.7	Soil organic colloids.	33
2.8	Physical Properties	33
2.8.1	water content	33
2.8.2	organic content	36
2.8.3	specific gravity	36
2.8.4	void ratio.	37
2.8.5	bulk density	38
2.8.6	dry density.	39
2.8.7	liquid limit	39
2.8.8	plastic limit and plasticity index	41
2.9	Chemical Properties	41
2.9.1	acidity	42
2.9.2	Cation Exchange Capacity	44
2.10	Engineering Properties	44
2.10.1	Primary Consolidation	45

2.10.2	Secondary compression behaviour	52
2.10.3	Tertiary compression	66
2.11	Influence of organic content and decomposition degree on physical and engineering properties of organic soils and peat.	67
2.12	Literature review on stimulated decomposition on physical and engineering properties	85
2.13	Organic matter	91
2.13.1	Organic matter and Organic Carbon	91
2.13.2	Sources and forms of carbon.	92
2.13.3	Types and classification	92
2.13.4	Structural compounds	94
2.13.5	Laboratory methods	96
2.14	Decomposition Process	97
2.15	Factors affecting decomposition processes	100
2.16	The Ideal gas law	103
2.17	Dalton's law of partial pressures.	103
2.18	Chemical kinetics	105
2.18.1	Rate law	105
2.18.2	Integrated Rate law	106
2.19	Henry's law	109
2.20	Basic principles of gas-liquid transfer	109
2.21	Influence of carbon dioxide production on pH	111
2.22	Law of reaction rate of oxidation organic matter	111
2.23	Soil shrinkage.	113
2.24	Soil water retention characteristics	114
2.24.1	Soil suction	114
2.25	Soil water retention curve.	115
2.26	Hysteresis	116
2.27	Volume-Mass relation.	117
2.27.1	Porosity	118
2.27.2	Void ratio	118
2.27.3	Degree of saturation	118
2.27.4	Volumetric water content	118
2.27.5	Gravimetric water content	119
2.27.6	Volumetric gas content.	119
3	Oxidation effect on compression behaviour of organic soil	121
3.1	Abstract	122
3.2	Introduction	122
3.3	Materials and Methods	124

3.4	Results and analysis	127
3.5	Discussion	141
3.6	Conclusion	142
3.7	Acknowledgements	143
4	Oxidation effect on consolidation and creep of organic soils	145
4.1	Introduction	146
4.2	Materials and Methods	148
4.3	Specimen Preparation	148
4.4	Testing Programme	149
4.5	Results and Discussions.	150
4.6	Conclusion	168
4.7	Acknowledgements	169
5	Evaluating the kinetics of oxidation of organic matter in peatlands	171
5.1	Abstract	172
5.2	Introduction	172
5.3	Conceptual model of aerobic oxidation of organic material	175
5.3.1	Effect of oxygen availability on the aerobic oxidation rate	177
5.3.2	Chemical oxidation with hydrogen peroxide	178
5.4	Materials and methods	179
5.4.1	Soil material	180
5.4.2	Estimating carbon dioxide production from oxidation and settle- ment rates	184
5.5	Results and discussion	185
5.5.1	Oedometer results	190
5.6	Conclusions.	196
5.7	Acknowledgements	196
6	Effect of oxidation on shrinkage and water retention behaviour	197
6.1	Abstract	198
6.2	Introduction	198
6.3	Materials and Method.	201
6.3.1	Project area, field measurements and soil collection	201
6.3.2	Classification test	203
6.3.3	Oxidation procedure	203
6.3.4	Hyprop tests	204
6.3.5	Macro CT Scans	204
6.4	Results and Discussion	207
6.4.1	Soil Classification and Physical Properties	207
6.4.2	Hyprop test results.	208

6.4.3	CT Scan measurement and soil shrinkage curves	210
6.5	Conclusion	212
7	Conclusions and recommendations	215
7.1	Conclusions.	215
7.2	Recommendations	218
	References	219
A	Amount of Hydrogen Peroxide	235
B	Chemical reactions	237
B.1	Pyrite oxidation reaction	237
	Summary	239
	Samenvatting	243
	Acknowledgements	247
	Curriculum Vitae	249

1

INTRODUCTION

*All human knowledge begins with intuitions,
proceeds from thence to concepts,
and ends with ideas.*

Immanuel Kant

*Look deep into nature
then you will understand everything better.*

Albert Einstein

1.1. PROBLEM BACKGROUND

ORGANIC soils such as peat cover about 5% to 8% of the earth's land surface. These soils particularly occur in the wetlands of the world, which consist for nearly 60% of peat (Huat et al., 2011). According to Joosten & Clarke (2002), peatlands cover some 400 million hectares globally, which constitute 3% of the total land surface area. Most of the peatlands are in North America and in Northern Asia and Europe in countries like Canada and Russia having 170 and 150 million hectares respectively, whereas 10% of peatlands are located in the tropics, with 26 million hectares found in Indonesia and 3 million hectares found in Malaysia. The distribution of peatlands around the world is shown in Figure 1.1.

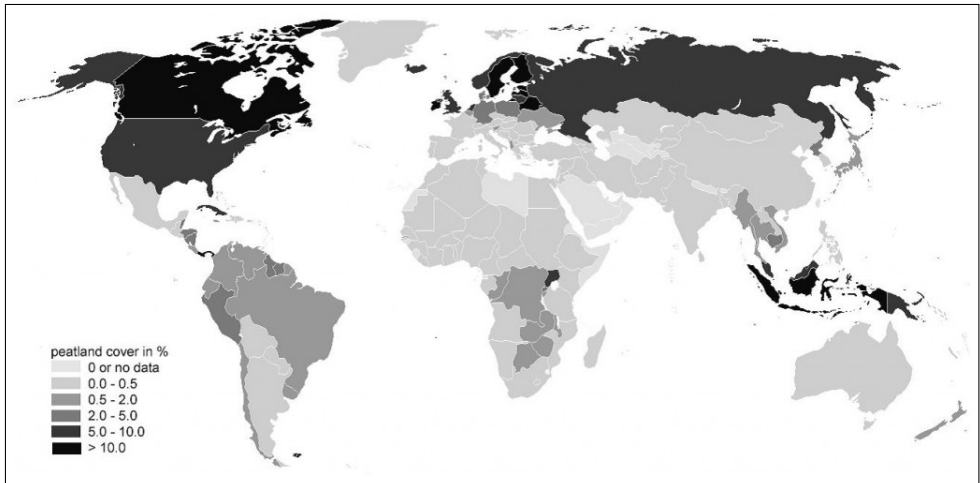


Figure 1.1: The coverage of peatland areas around the world (Huat et al., 2014)

The definition of peat is based on the amount of organic matter and varies between disciplines. In soil science, peat is described as a soil, which has more than 35% organic content while in geotechnical engineering, a distinction is made between organic soils and peat where organic soil contains more than 35% organic matter and peat exceeds more than 75% organic matter (Huat et al., 2014). This research project uses the definition and classification of peat and organic soils as common in geotechnical engineering. Peat or organic soils are normally derived from the accumulation of incompletely decomposed plant materials, such as sedges, trees, mosses and other plants that have been preserved under wet anoxic conditions (Huat et al., 2014). The colour of this material is usually brown or black depending on the degree of decomposition or humification and it has a very distinct odour. A commonly used classification which is used to distinguish different types of peat and organic soils is the “von Post scale” classification (Hobbs, 1986), which is based on fibre content, organic content and ash content.

In the Netherlands, peat soils cover about 200 thousand hectares and are mostly found in the western coastal region (Bord na Mona, 1985). Many of the peatlands have been excavated from the Middle Ages until the mid 20th century and used as a source of

energy (Zeeuw, 1978). The currently remaining peatlands are mostly used for agricultural activities such as dairy farming (Hoogland et al., 2012). Groundwater in these areas has been lowered in order to reduce the water content and increase bearing capacity of these natural peatlands and allow access to cattle, sheep and equipment. Gravimetric water content in undrained peat may reach up to 1500% depending on the type of peat and origin. The drainage of peat by groundwater lowering either naturally or artificially (anthropogenic activities) may pose several problems to land users and the global environment, including land subsidence and emission of greenhouse gasses. Land subsidence in peatlands is attributed to three mechanisms (Wösten et al., 1997):

- (a) Consolidation, which is the reduction in soil volume or compression of soil as a result of an increased surcharge load;
- (b) Oxidation, which causes volume reduction of peat above the groundwater level due to loss of organic matter due to decomposition by biochemical processes;
- (c) Shrinkage, volume reduction of peat above the groundwater level due to desiccation.

The intensity of each of these processes is affected by the groundwater level. Groundwater lowering reduces the buoyancy of the top soil, and consequently increases the overburden pressure on the underlying soil layers. Lowering groundwater level also accelerates the decomposition process in peat as desaturation of the soil allows oxygen to penetrate the soil and accelerate oxidation of the organic matter. Whereas shrinkage as a result of desiccation occurs mostly in the layers above groundwater level.

Globally recorded subsidence rates in drained peat areas range from about 1 mm to 2 mm per year in peatlands of the western part of The Netherlands at a very shallow depth of drainage of 0.1 m to 0.2 m, to 2 cm to 3 cm per year in the temperate Sacramento-San Joaquin delta in California, and to more than 5 cm per year in tropical peatlands such as in Malaysia (Camporese et al., 2006). Figure 1.2 shows the relationships between the long term average subsidence rate and depth of groundwater levels among various countries in the world ranging from temperate to tropical areas. It depicts that for each groundwater level, higher average settlement rates are observed, due to increase in temperature and absence of winter-summer periodicity (Wösten et al., 1997). The settlement rate in the Netherlands due to agricultural activities on peatlands reaches up to 10 mm per year (Hoogland et al., 2012).

Land subsidence may cause serious problems for society. Subsidence of low-lying peatlands below the level of surrounding surface water may increase flood risk or potential deterioration of land and groundwater quality in case of flooding or due to upward seepage of groundwater. Flood risk may further increase considering climate change takes place which causes the sea level to rise. To avoid accumulation of water in these areas, continuous water pumping is imperative to avoid any potential flood risk. As a result of land subsidence more energy and cost are required in order to manage this problem. Still continuous drainage is considered a viable way to enable efficient usage of these low lying areas (Dawson et al., 2010). Further advancement in drainage technology may reduce costs of drainage and improve the accessibility, but may also increase

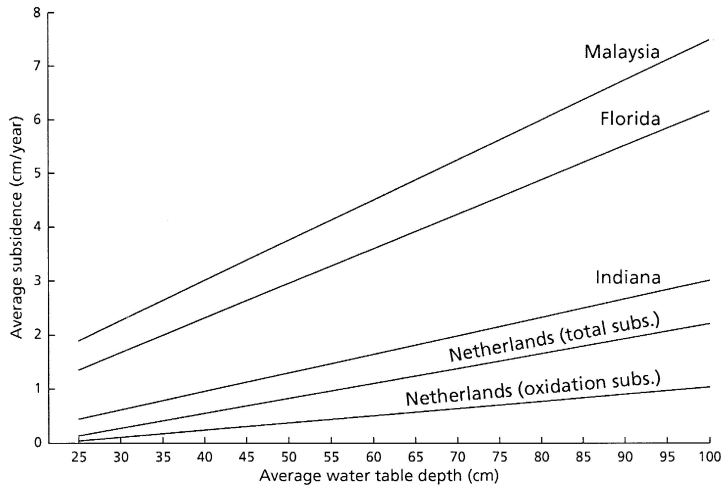


Figure 1.2: The relationships between average subsidence rates and groundwater levels for different countries in the world (Wösten et al., 1997)

in the rate of subsidence. Lifting up these lowlands or building dikes are common approaches to mitigating subsidence in peat lands. However, this is not a straightforward solution, because the significant stretches of dikes need to be continuously maintained or improved to avoid stability problems and accommodate for future water levels.

Groundwater lowering may also accelerate decomposition of organic matter. The products of decomposition, such as carbon dioxide and methane may be harmful to the environment and mankind. Carbon dioxide and Methane are known as green house gasses, and their emission stimulates global warming, which in turn leads to sea level rise. Other by-products of decomposition such as methane, soluble metals, increased acidity or suspended organic matter may deteriorate groundwater quality. Salinization of groundwater can also occur due to increased seepage, particularly in peatland close to sea. A decrease in water level may result in an upward hydraulic gradient, stimulating seepage of anaerobic and potentially saline groundwater, which may contaminate surface or drinking water.

For geotechnical engineers, building on peat or organic soils is a real challenge. Organic soils behave differently than other inorganic (mineral) soils such as silt and clay, as they are often heterogeneous, very weak and highly compressible. The common tradition to deal with this type soil in construction is to avoid building on it or to excavate and remove it, as this soil does not provide sufficient support for buildings in its natural condition (Huat et al., 2014). However, as the world population increases building on this problematic soil can no longer be avoided. In some countries, shortage of land resulted in land reclamation or water extraction of these waterlogged soils to increase the available land area for building or agriculture. To enable construction on soft soils ground improvement methods are required. The aims of the ground improvements are basically to reduce the compressibility, reduce permeability, increase the rate of settlement by reducing the consolidation time or avoid compression by transferring the load

to deeper layers (Kazemian & Huat, 2010). The most common methods of ground improvements are soil replacement, preloading and drainage through staged construction, stone columns, piles, thermal precompression and preload piers, or by reducing driving forces by light-weight fill; and chemical admixture such as cement and lime (Kazemian et al., 2011a; Huat et al., 2014). However, for larger areas or roads, soil mixing and piled foundations may not be economically feasible and pre-loading and drainage are the only viable option to avoid residual settlement after construction. However, preloading and drainage is difficult to apply under or near existing structures and still requires significant amount of borrow materials to compensate for the induced surface settlements.

When it comes to construction in peatlands, settlement is seen as the main problem. Whereas, regional settlements may affect the performance of infrastructure, such as pipelines, waterways or dikes and embankments, small scale differential settlements can cause collapse of structures and infrastructure during service life. Settlement as a result of a reduction in soil volume or soil compression due to an increase in load is defined as consolidation.

According to Skempton & Bjerrum (1957), soil compression can be divided into three stages which are initial compression, primary consolidation and secondary compression. Initial compression is the volume reduction of soil, which occurs immediately after load application without any expulsion of water, which is mainly attributed to elasticity of the soil structure and expulsion and compression of gas in soil voids. Considering, water is relatively incompressible, a load increase on a saturated soil will initially be mostly carried by the water and cause an increase in excess pore pressure. Primary consolidation is reduction in volume that involves drainage of water and dissipation of these excess pore water pressures. Simultaneously the load is transferred from the pore water to the soil skeleton, causing the soil structure to deform. Secondary compression is further volume change that occurs after primary consolidation has been completed, which is attributed to continuous adjustment of the soil structure under constant load conditions, which is also referred to as creep.

Peat and organic soils show different compressive behaviour than other types of soils. Peat soils typically show very high compression, rapid primary consolidation and large amount and relatively fast secondary compression (creep). In some cases the rate of secondary compression in peat does appear to decrease in time, and the term tertiary compression is introduced to describe the observed behaviour (Kazemian et al., 2011a). This behaviour differs from the established theory to describe compression behaviour, which indicates that after primary consolidation only secondary compression occurs and that the rate of secondary compression typically decreases in time and can be described using a log-linear relationship Whitlow (2004).

Common settlement analysis usually involves determining the amount of settlement and the rate of settlement (Sridharan & Prakash, 1998). In many cases, primary consolidation is considered as the only contributing factor in settlement analysis, as it is assumed that minimal or no settlement will take place after the completion of primary consolidation. However, as many structures are built to have a relatively long live span, long term settlement of soil is an important issue to be considered in foundation and structure design and for that reason, design should include primary and secondary compression. Currently, secondary compression is seen as a complex process, which is less

well understood among engineers. Several researchers investigate the effect of secondary compression in soft soils (Sridharan & Rao, 1982; Fatahi et al., 2013; Le et al., 2012; Takeda et al., 2012). The causes of secondary compression in soft soils are attributed to five different mechanisms, namely (a) breakdown of the inter-particle bonds, (b) sliding between soil particles, (c) water flow from micro-pores to macro-pores, (d) deformation due to structural viscosity and (e) deformation due to jumping bonds (Le et al., 2012).

For peat and organic soils, the secondary compression has been attributed to the water flow from micro to macropores concept (Zhang & O'Kelly, 2013). Hobbs (1986), which describes that consolidation of peat involves expulsion of pore water accompanied by structural rearrangement of the solid particles. During primary consolidation, pore water is only expelled from the macropores, while during secondary compression stage, pore water is gradually expelled from the micro- into macropores (De Josselin de Jong, 1968). In the early stages the two processes of pore pressure dissipation and structural rearrangement occur simultaneously, while at the later stage the excess pore water pressure has declined to a very small value, at which further structural rearrangement causes additional expulsion of water from micro to macropores, which continues as a creep-like process. Where peats and organic soils differ from non-organic mineral soils is that additional secondary compression can occur from the decomposition of organic matter. This process is claimed to be slow in organic soils and typically not taken into account in geotechnical settlement design. However, considering the lifespan of structures may be extended and decomposition can be accelerated significantly by natural or anthropogenic factors, the rate of decomposition may become relevant and decomposition may contribute to unexpected settlement during service life of buildings.

Decomposition of organic matter is a biological process, which involves loss of organic matter either in gas or in solution, disappearance of physical structure or change of chemical state of organic matter (Hobbs, 1986; Huat et al., 2009; O'Kelly & Pichan, 2013). Microorganisms play a major role in this process as the metabolism and activity of microorganisms can catalyse the chemical conversions in the subsurface, which result in the formation of carbon dioxide, volatile acids, methane, water, new bacterial cells and decrease in organic solids content (Al-Khafaji & Andersland, 1981). Decomposition can influence the compressibility of peat, particularly secondary compression, in two ways: either by reducing the amount of dry solids associated with the microbial metabolism or by weakening the structural integrity of the organic matter (O'Kelly & Pichan, 2013). Organic content and structural fabric play important roles in the mechanical properties of peat where any changes of the two attributes as a result of on-going decomposition can potentially influence compressibility behaviour in organic soils (Al-Khafaji & Andersland, 1981). Hence, unexpected or uncontrolled decomposition of peat or organic soils may influence the long term performance of engineering works in peatlands.

Decomposition of organic material has been suggested as the cause for land subsidence. For example Drexler et al. (2009) reported that the subsidence of Sacramento-San Joaquin Delta of California, USA was caused by decomposition. Gambolati et al. (2003) also reported that the land subsidence induced by decomposition of organic matter affected the surrounding hydraulic infrastructure causing a bridge to malfunction. Pichan & O'Kelly (2012) mentioned that in grass covered peatlands, almost 0.5 m thickness of peat is oxidised 100 years, whereas a peat bog complex in Sweden showed at least

150 mm of subsidence over more than 35 years, equivalent to approximately 4.3 mm per year. They mentioned that the main contributor to subsidence was decomposition, which is governed by several factors such as climate change, hydrology and nutrient supply. Andersland & Al-Khafaji (1984) reported that one of the factors that influence the continuous settlement of the fibrous peat with subsequent levee failure was attributed to peat decomposition, resulting in subsidence rates of 3 inches per year. Schothorst (1977) concluded that on average 65 % of the total subsidence of low moor peat in The Netherlands was due to oxidation of organic matter and shrinkage in the layer above groundwater table while 35 % attributed to compression in the layer below the groundwater table. van den Akker et al. (2008) used an empirical equation to predict the amount of carbon dioxide emissions by decomposition of organic matter in peatlands, for which they assumed that all subsidence in peatlands in the western part of the Netherlands was attributed to the oxidation of organic matter. They observed a cyclic seasonal pattern in subsidence rates, where most subsidence took place during dry summers, in which ground water level went below surface water level as a result of evapotranspiration allowing oxygen to penetrate further into the soil and oxidise deeper soil layers. In order to reduce the amount of surface subsidence they suggested to install infiltration drains to maintain groundwater level constant during dry periods.

1.2. SCIENTIFIC GAP

There is currently no consensus about the dominant mechanism causing land subsidence in peatlands. That rate and degree of decomposition may vary as it depends on the material properties (composition, fabric, texture and state of decomposition) and environmental conditions (availability of oxidising compounds, pH), and it may be accelerated by human influence, such as groundwater lowering or fertilizing. As decomposition significantly affects the compressibility of organic soils, the compressibility properties will be variable too and will change with time, which makes this material more complex to deal with and makes it difficult to predict the volume change as a result of secondary compression. Various approaches have been adopted in the field of geotechnical engineering to deal with subsidence and residual settlement of constructions on soft soils. As these measures typically aim to minimize secondary compression after construction, they typically ignore decomposition as the general consensus in geotechnical practice is that the decomposition rate in peat is slow in absence of oxygen and hence does not cause significant effects over the design life of engineering works. This brings the perspective that secondary compression problem is not severe and less attention is put into it (Hobbs, 1986; O'Kelly & Pichan, 2013).

However, the settlement rate can increase tremendously, particularly for secondary compression, when this soil is exposed to an environment which stimulates decomposition for example oxygen which may be significant during service life of buildings as a result of natural or anthropogenic activities such as groundwater table fluctuation or the construction of land drainage schemes.

1.3. PROPOSED SOLUTION

In order to improve current settlement predictions, a simple model should be developed, which incorporates both effects of mechanical loading and decomposition of organic matter. Before any method is established to mitigate or control secondary compression in peat and organic soil, understanding of the development of secondary compression by decomposition and mechanical stress in this soil is deemed necessary. The soil behaviour under influence of on-going decomposition needs to be understood and quantified to avoid any future failure in engineering works. Studies on the effect of decomposition on engineering properties of organic soils and peat have been performed (Al-Khafaji & Andersland, 1981; Wardwell & Nelson, 1981; Pichan & O’Kelly, 2012; O’Kelly & Pichan, 2013). However, the reported information, which describes the amount and rate of settlement as a result of on-going decomposition, is still limited. There are various questions that still need to be addressed and solved pertaining to secondary compression as a result of decomposition. For instance, the extent to which decomposition takes place and how it influences the development of secondary compression is yet to be known. Also, there is no established method available to capture the potential settlement which is governed by decomposition of peat or organic soils (O’Kelly & Pichan, 2013). It is claimed in the literature that secondary and tertiary compression are expected to reduce in peats that having higher degree of decomposition. Nevertheless, further laboratory and field studies are necessary in order to understand this concept better (O’Kelly & Pichan, 2013).

1.4. MAIN QUESTION

Therefore, the aim of this dissertation is to investigate the effect of decomposition on the compressibility behaviour of organic soil. The main questions to be answered include:

- What is the effect of decomposition on the compressibility of organic soils?
- What is the effect of decomposition on the rate of consolidation?
- What are the expected or potential rates of decomposition in the field?
- How to relate surface subsidence with carbon dioxide emissions?
- What is the effect of decomposition on soil shrinkage and water retention characteristics?

Answering these questions will help to identify the relative contribution of each of the three mechanisms to the total amount of subsidence, will enable to evaluate the potential of different subsidence mitigation measures and improve the ability to predict long term settlements for geotechnical engineering design.

1.5. METHODS

This research is carried out by performing a range of experiments. The organic soil used in this study is collected from a peatland site in The Netherlands, Wormer & Jisperveld.

Organic sediments were dredged from the bottom of lakes and ditches and deposited in a pond, from which they were sampled. Decomposition of the organic soils was accelerated by oxidising the sample using the chemical oxidant Hydrogen Peroxide. One Dimensional Consolidation tests were performed on samples, which were either non-oxidised, pre-oxidised prior to loading or oxidised inside the consolidation set-up at different levels of vertical confinement. The rate of decomposition was analysed during the one dimensional consolidation tests and in experiments using a bioreactor in which suspended organic sediments were oxidised using oxygen or hydrogen peroxide. The effect of decomposition on the shrinkage and water retention characteristics was determined by combining Hyprop tests with X-ray CT scanning.

1.6. THESIS OUTLINE

This dissertation consists of 6 Chapters. The outline of the dissertation is presented as follows;

Chapter 2 explains the background of organic soils and peat covering the formation, classification and physical and engineering properties. This chapter also provides an overview of the effect of different decomposition state on the physical and engineering properties of organic soils and peat which are obtained from the literature. Then, a brief introduction of organic compound element and the its formation and related matter concerning decomposition process is discussed.

Chapter 3 presents the laboratory results looking at the effect of in-situ oxidation on the compression behaviour of dredged organic sediments. Test samples are oxidised under varying effective vertical pressures using a type of chemical oxidant known as Hydrogen Peroxide. The results obtained are compared with non-oxidised samples which undergo the same test series.

Chapter 4 discusses the effect of oxidation on the time-dependent behaviour of consolidation and creep of organic samples. The results obtained from the same laboratory works obtained in Chapter 3 is further exploit by comparing the primary consolidation and secondary compression parameters for oxidised and non-oxidised samples.

Chapter 5 provides an additional new test series looking at the kinetics of oxidation in organic samples. Different ways to describe the kinetics of oxidation under different oxidising conditions are investigated and the results are compared.

Chapter 6 presents the effect of oxidation on shrinkage and water retention behaviour of organic soils. The effect of organic matter on gas formation during desiccation process is also investigated and discussed.

Chapter 7 presents the conclusions obtained from this study and several recommendations for future research are proposed.

Note that there may be some repetition in the chapters, particularly in the introductory part, as each chapter is prepared to be submitted independently for publication.

2

ORGANIC SOILS AND PEAT

*Organic soils and peats,
consists of remains of dead vegetation
in various stages of decomposition.*

Hobbs

*Degree of decomposition
is divided into
fibric, hemic and sapric.*

Astm

2.1. DEFINITION AND ORGANIC CONTENT CLASSIFICATION

ORGANIC soils and peat are very unique materials and having more complex definition compared to other inorganic soils. Until today, there is different school of thoughts used to describe these soils which based upon disciplines. However, the important thing to highlight here is that organic soils and peat have one common attribute in general that they contain carbon compound that is recently derived from fresh plant remains. This means that other carbon compounds which are not originally formed from plant remains such as calcium carbonate (calcite) which presence in sand is not considered as organic material (Huat et al., 2014).

The definition of organic soils and peat varies according to the discipline from which they are approached, either from soil science or engineering. In soil science, peat is defined as possessing more than 35 % organic content, while in geotechnical engineering, peat is defined as having more than 75 % organic content (Huat et al., 2014). However, for geotechnical engineers, organic soils are defined as containing at least 20 % organic matter, as this is the minimum amount that will change the mechanical properties of soil (Huat et al., 2014). In other words, they are no longer behaving like inorganic or fine mineral soils, such as silt and clay, and also their behaviour are difficult to predict which is beyond the norm. As this dissertation concern on the engineering behaviour of organic soils, the classification adopted in this study is based on engineering classification precisely.

The formation of peat involves biochemical process or decomposition of plant fibres carried out by aerobic microbial activities in the surface layers of the deposits subjected to groundwater table drawdown. Decomposition process is limited in deeper peat layers due to limiting oxygen condition where the rate of accumulation at this zone is high. The partly decomposed biomass is preserved and relatively little changes with times since the rate of accumulation is greater than rate of decay under anaerobic condition. As peat is formed with limiting decomposition with higher rate of accumulation in the sub-surface, it may develops three different zones which are non-decomposed (fibric), partly decomposed (hemic) and highly decomposed peat (sapric). The structure of each zone is represented in Figure 2.1 which corresponds to the composition of fibre content.

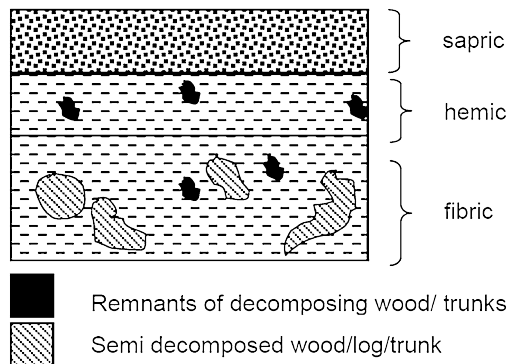


Figure 2.1: The different zones of saturated peat structure (Zulkifley et al., 2013)

Although the cut off value for classifying organic soils and peat varies throughout the world, one common way is based on amount of the organic content. This property can further classify whether a soil is considered as slightly organic 3 % to 20 %, organic 20 % to 75 % or highly organic (more than 75 %) (Zulkifley et al., 2013). In order to simplify the definition, Tables 2.1 and 2.2 summarised the different types of organic soils that are normally encountered ranging from high to low. The organic content can be determined by combusting the soils at high temperature oven (ASTM, 2007a).

Table 2.1: Different percentage of organic content (Huat et al., 2014)

Basic soil type	Description	Organic content (%)
Clay or silt or sand	Slightly organic	2 to 20
Organic soil		25 to 5
Peat		>75

Table 2.2: Classification of organic soils with varying organic content (Huat et al., 2014)

Basic soil type	Description	Symbol	Organic content (%)
Clay or silt or sand	Slightly organic	O	2 to 20
Organic soil		O	25 to 75
Peat		Pt	>75

A comparison of definition of peat in some countries has been discussed by Hobbs (1986) which primarily based upon the amount of organic content as below:

- Russian geotechnical engineers describe peat as a soil containing more than 50 % particle weight of vegetable origin (organic matters), while peaty soil contains 10 % to 50 % particles of vegetable origin.
- American Standard Testing Material suggests that peat contains more than 75 % organic matter.
- Hobbs (1986) looking at some British peats proposes peat for having at least 27.5 % organic matter.

Slightly organic silts or clays for instance have inorganic fine-grained texture and normally black to dark brown in colour with an organic odour with traces of organic remains. Peat is easily to recognise as it has visible undecomposed fibre and roots, strong odour with black to dark brown in colour and low density material. However, for organic soils, it is more difficult to make a distinction because of different cut-off values to separate these two soils as proposed by different classification systems.

Different soil classification systems have been developed in order to improve the characterisation of organic soils and peat. Unified Soil Classification System (USCS) for instance, distinguish the organic soils with inorganic soils when passing sieve size 75 µm (No. 200 sieve) and also based on the ratio of plastic limit before drying to plastic limit after drying which should be less than 75 % as stated in the standard. However, until today

there is no specific guidelines to separate the organic soils and peat. Figure 2.2 presents the summary of the system which assists the classification of organic soils.

Criteria for Assigning Group Symbols and Group Names Using Laboratory Tests ^A				Soil Classification		
				Group Symbol	Group Name ^B	
COARSE-GRAINED SOILS	Gravels (More than 50 % of coarse fraction retained on No. 4 sieve)	Clean Gravels (Less than 5 % fines ^C)	$Cu \geq 4$ and $1 \leq Cc \leq 3^D$	GW	Well-graded gravel ^E	
		Gravels with Fines (More than 12 % fines ^C)	$Cu < 4$ and/or $[Cc < 1 \text{ or } Cc > 3]^D$	GP	Poorly graded gravel ^E	
More than 50 % retained on No. 200 sieve	Sands (50 % or more of coarse fraction passes No. 4 sieve)	Clean Sands (Less than 5 % fines ^H)	$Cu \geq 6$ and $1 \leq Cc \leq 3^D$	SW	Well-graded sand ^I	
			$Cu < 6$ and/or $[Cc < 1 \text{ or } Cc > 3]^D$	SP	Poorly graded sand ^I	
		Sands with Fines (More than 12 % fines ^H)	Fines classify as ML or MH	SM	Silty sand ^{F,G,I}	
			Fines classify as CL or CH	SC	Clayey sand ^{F,G,I}	
FINE-GRAINED SOILS	Silts and Clays	inorganic	$PI > 7$ and plots on or above "A" line ^J	CL	Lean clay ^{K,L,M}	
		organic	$\frac{\text{Liquid limit} - \text{oven dried}}{\text{Liquid limit} - \text{not dried}} < 0.75$	ML	Silt ^{K,L,M}	
	50 % or more passes the No. 200 sieve	Silts and Clays	inorganic	PI plots on or above "A" line	CH	Fat clay ^{K,L,M}
			organic	PI plots below "A" line	MH	Elastic silt ^{K,L,M}
		organic	$\frac{\text{Liquid limit} - \text{oven dried}}{\text{Liquid limit} - \text{not dried}} < 0.75$	OH	Organic clay ^{K,L,M,P} Organic silt ^{K,L,M,G}	
HIGHLY ORGANIC SOILS	Primarily organic matter, dark in color, and organic odor			PT	Peat	

Figure 2.2: Unified soil classification system (ASTM, 2011)

An improved classification system is established by LPC (France) as shown in Figure 2.3 to separate organic soils and peat based on the amount of organic matter which is in this case is 30 %. The soil type is further linked with von Post scale index which describes the state of decomposition in a particular soil. For this classification, the organic soils contains at least 10 %. Besides, different classification systems are also discussed by Andrejko et al. (1983). It is observed in Figure 2.4 that the cut-off percentage for peat is highly different depending on the system used.

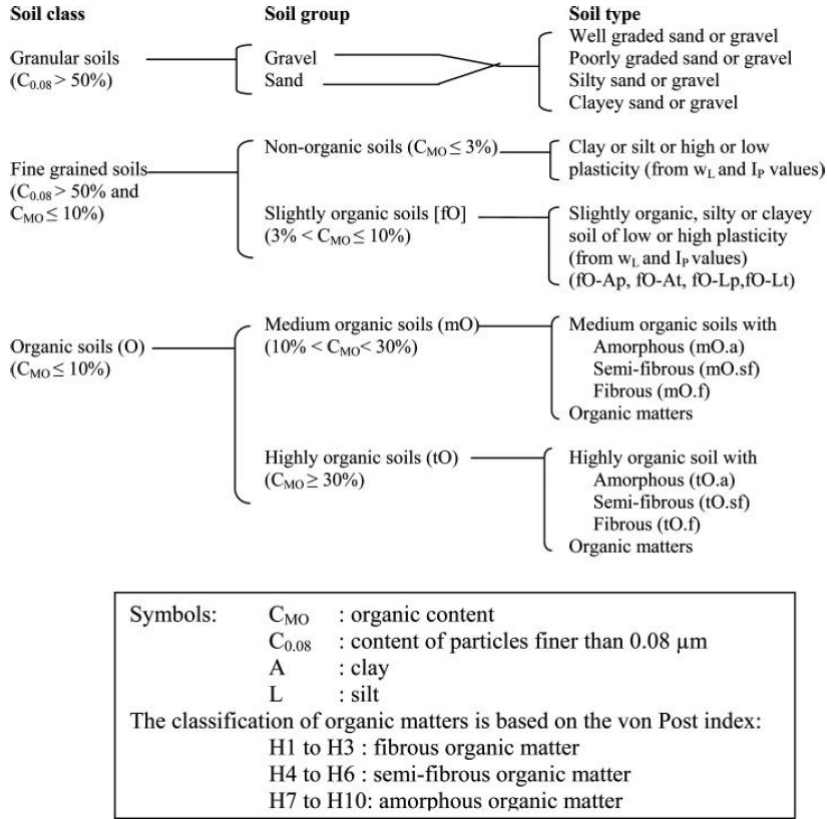


Figure 2.3: LPC classification of organic soils (Huat et al., 2014)

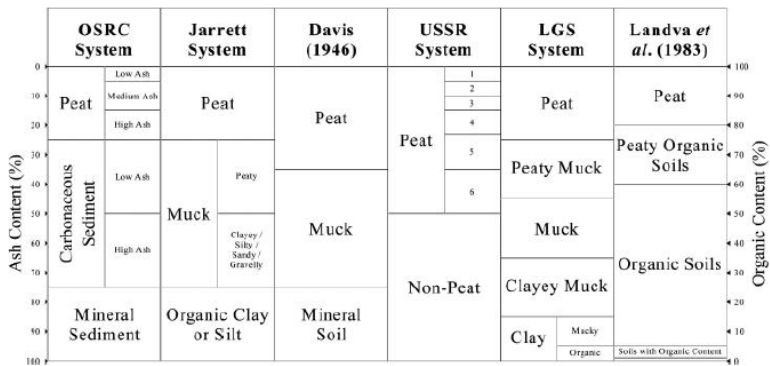


Figure 2.4: Comparison of classification systems used for peat and organic soils (Andrejko et al., 1983)

2.2. BOTANICAL CLASSIFICATION

Organic content determination is one of the preliminary way to identify organic soils. However, the classification alone is not sufficient as the material texture and composition are evolving with time due to decomposition process. In order to take account the changes resulting from this process, another useful method to characterise organic soils and peat is proposed which are based on degree of decomposition or humification. It involves visual examination of a sample by hand. There are several ways to examine the degree of humification. However, the most established botanical classification systems are : (a) Radforth classification system and (b) von Post Classification System. Both systems taking account the aspects of vegetation and depending on how detailed the botanical classification can be. For geologists, the characterisation is more detailed as their concern are mainly recognition of the material itself. Meanwhile, for geotechnical engineers, a simpler version of botanical classification is sufficient as they are more interested on the physical properties such as water content, density, specific gravity and others and how these properties influence the mechanical behaviour of the soils such as compressibility and strength. According to Landva et al. (1983), the key difference between the two systems is that von Post system is applied to all organic soils that support plant growth while Radforth classification is developed for the usage of engineers where there is limited knowledge of botanical is implicated in the system (Huang et al., 2009).

2.2.1. VON POST CLASSIFICATION SYSTEM

The von Post classification system was developed in the early 1920s in Sweden and is related to vegetation of the soil. This system is a quick identification of organic material at the field which requires the soil to be squeezed and the passing material which come out between two fingers is observed. The properties determined include botanical composition, water content, content of fine and coarse fibers and content of wood remnants. The original von Post system is then modified by Landva & Pheeney (1980) with the same concept and information but different way of presentation and it later extended by Hobbs (1986) by providing additional information such as organic content, tensile strength, odour, plasticity and acidity. The Dutch guidelines for classifying peat adopting the similar system (den Haan & Kruse, 2007). Following details below are the important characteristics that should be included when using the von Post classification system:

- **Humification (H):** The degree of humification is graded on a scale from 1 to 10 and designated H_1 to H_{10} . The various degrees of humification which was modified by Landva & Pheeney (1980) is shown in Table 2.4.
- **Water content (B):** In the field, the water content of peat is estimated on a scale from 1 (dry) to 5 (very high), designated B_1 to B_5 . In terms of actual water contents the following ranges are suggested: B_2 less than 500 %; B_3 500 % to 1000 %; B_4 1000 % to 2000 %; and B_5 greater than 2000 %.
- **Fine fibres (F):** Fine fibres are defined as fibres and stems smaller than 1 mm in diameter or width. They are often the Eriophorum species, but Hypnum or Sphagnum stems may also be included if properly specified, e.g. F(H) or F(S). Shrub

rootlets may also be included, specified as F(N). No special designation is indicated for plant roots hairs, rhizoids, or other fibres. The content of fine fibres is graded on a scale from 0 to 3 as follows: F_0 nil; F_1 low content; F_2 moderate content; and F_3 high content.

- **Coarse fibres (R):** Coarse fibres are defined as fibres, stems and rootlets greater than 1 mm in diameter or width. They are often of the *Carex* genus, but Hypnum and Sphagnum stems may also be included if properly specified, e.g. R(H) or R(S). Shrub (N) rootlets are specified as R(N). The content of coarse fibres is graded on a scale from 0 to 3 as follows: R_0 nil; R_1 low content; R_2 moderate content and R_3 high content.
- **Wood remnants (W):** The content of wood remnants was given by the symbol V_3 , V_2 , V_1 and V_0 . Landva & Pheeny (1980) suggests a division of V symbol into W for wood remnants and N for shrub remnants. Wood and shrub content are graded on a scale from 0 to 3 as follows: W_0 nil; W_1 low content; W_2 moderate content; and W_3 high content.
- **Designation:** The plant types suggested by Landva & Pheeny (1980) are described in Table 2.3. With few exceptions, natural peats consists of a mixture of two or more plant types. The designation adopted is to list the plant types in descending order of content, for example, a peat classified as *ErCS* consists mainly of Eriophorum remnants, while the content of *Carex* remnants would be lower and that of Sphagnum remnants relatively low. The designation is omitted when plant types cannot be identified.

Table 2.3: Plant types found in peat (Hobbs, 1986)

Plant types	Designation
Bryales (moss)	B
Carex (sedge)	C
Equisetum (horse tail)	Eq
Eriophorum (cotton grass)	Er
Hypnum (moss)	H
Lignidi (wood)	W
Nanolignidi (shrubs)	N
Phragmites	Ph
Scheuchzeria (aquatic herbs)	Sch
Sphagnum (moss)	S

Hobbs (1986) propose extending the von Post classification developed by Landva & Pheeny (1980) by adding additional information such as organic content, structural anisotropy, smell, plasticity and acidity as below:

- **Organic content (N):** It is not possible to estimate the organic content unless the peat is obviously clayey when the von Post humification test would not be realistic. Following ignition loss determinations the organic content may be graded as

follows: N_5 greater than 95% organic matter; N_4 95 % to 80 %; N_3 80 % to 60 %; N_2 60 % to 40 %; N_1 40 % to 20 %.

- **Tensile strength (TV and TH):** The tensile strength is the vertical and horizontal directions may be judged by pulling specimens apart in these directions. The following scale may be used: T_0 zero strength; T_1 low, say less than 2 kN/m²; T_2 moderate, say 2 kN/m² to 10 kN/m²; and T_3 high or greater than 10 kN/m².
- **Smell (A):** The smell which is an indication of fermentation under anaerobic conditions may be scaled as follows: A_0 no smell; A_1 slight; A_2 moderate; A_3 strong. Note, methane, CH_4 , the main indicator of anaerobic activity has no smell. If specially detected should be reported.
- **Plasticity (P):** Plastic limit test possible P_1 , not possible P_0 .
- **Acidity (pH):** Acid Ph_L ; neutral Ph_0 ; alkaline Ph_H .

Example in the use of the extended von Post classification description in the field for: Dark brown, oxidising to black, moderately decomposed H_5 , mainly fine fibrous PEAT with some coarses fibres and amorphous material. Low vertical tensile strength, moderate horizontally. No smell. Plastic limit test possible. Genera not identified. Extended von Post Classification with ignition loss and pH determinations:

$H_5 B_2 F_3 R_1 W_0 N_3 TV_1 TH_2 A_0 P_1 Ph_0$

Table 2.4: von Post classification system (Landva & Pheaney, 1980)

Degree of humification	Decomposition	Plant structure	Content of amorphous material	Material extruded on squeezing (passing between fingers)	Nature of residue
H1	None	Easily identified	None	Clear, colourless water	
H2	Insignificant	Easily identified	None	Yellowish water	
H3	Very slight	Still identifiable	Slight	Brown, muddy water; no peat	Not pasty
H4	Slight	Not easily identified	Some	Dark brown, muddy water; no peat	Somewhat pasty
H5	Moderate	Recognisable, but vague	Considerable	Muddy water and some peat	Strongly pasty
H6	Moderately strong	Indistinct (more distinct after squeezing)	Considerable	About one third of peat squeezed out; water dark brown	
H7	Strong	Faintly recognizable	High	About one half of peat squeezed out; any water very dark brown	
H8	Very strong	Very indistinct	High	About two thirds of peat squeezed out; also some pasty water	H6 - H8: Fibres and roots more resistant to decomposition
H9	Nearly complete	Almost unrecognisable		Nearly all the peat squeezed out as a fairly uniform paste	
H10	Complete	Not discernible		All the peat passes between the fingers; no free water visible	

2.2.2. RADFORTH CLASSIFICATION SYSTEM

The Radforth classification system classifies peat in terms of structure rather than botanical origin (Radforth, 1969). This system is better in estimating the mechanical properties of peat soil rather than the purely botanical classification system. It divides peat into three different structures which are amorphous-granular, fine-fibres, and coarse fibrous. Amorphous-peat has the lowest shear strength and tensile strength while coarse-fibrous peats have the highest natural void ratio and compressibility among the three types of peats. The peat can be classified into 17 categories based on wood remnants as shown in Table 2.5 below:

Table 2.5: Radforth classification system (Radforth, 1969)

Predominant characteristic	Category	Name
Amorphous granular	1	Amorphous-granular peat
	2	Non-woody, fine-fibrous peat
	3	Amorphous-granular peat containing non-woody fine fibres
	4	Amorphous-granular peat containing woody fine fibres
	5	Peat, predominantly amorphous-granular containing non-woody fine fibres, held in a woody, fine fibrous frame work
	6	Peat, predominantly amorphous-granular containing woody fine fibres, held on a woody, coarse-fibrous framework
	7	Alternate layering of non-woody, fine fibrous peat and amorphous-granular peat containing non-woody fine fibres
Fine-fibrous	8	Non-woody, fine-fibrous peat containing a mound of coarse fibres
	9	Woody, fine fibrous peat held in a woody, coarse-fibrous framework
	10	Woody particles held in non-woody, fine fibrous peat
Coarse fibrous	11	Woody and non-woody particles held in fine-fibrous peat
	12	Woody, coarse-fibrous peat
	13	Coarse fibres criss-crossing fine-fibrous peat
	14	Non-woody and woody fine-fibrous peat held in a coarse-fibrous framework
	15	Woody mesh of fibres and particles enclosing amorphous-granular peat containing fine-fibres
	16	Woody, coarse-fibrous peat containing scattered woody chunks
	17	Mesh of closely applied logs and roots enclosing woody coarse-fibrous peat with woody chunks

However, in this system it is realised that it does not include properties such as colour, wetness, degree of humification or organic content and these characteristics should be added. For this reason, this system is generally not applicable even for large areas such as in Canada (Landva & Pheeney, 1980; Hobbs, 1986). Radforth also suggest that vegetal cover and topsoil above organic soil deposit should be classified in terms of structure than genesis. The vegetal cover is divided into nine categories as depicted in Table 2.6. Meanwhile, Table 2.7 shows how the peat cover is applicable for engineering application.

Table 2.6: Peat cover specification for different classes (Radforth, 1969)

Coverage type (class)	Woodiness vs. non-woodiness	Statute (approximate height)	Texture (where required)	Growth habitat
A	Woody	15 ft or over	-	Tree form
B	Woody	5-15 ft	-	Young of dwarf tree or bush
C	Non-woody	2-5 ft	-	Tall, grasslike
D	Woody	2-5 ft	-	Tall shrub or very dwarfed tree
E	Woody	Up to 2 ft	-	Low shrub
F	Non-Woody	Up to 2 ft	-	Mats, clumps, or patches, something touching
G	Non-woody	Up to 2 ft	-	Singly or loose association
H	Non-woody	Up to 4 ft	Leathery to crisp	Mostly continuous mats
I	Non-woody	Up to 4 ft	Soft or velvety	Often continuous mats, sometimes in hummocks

Table 2.7: Engineering significance of peat cover (Radforth, 1969)

Predominant class in formula	Engineering significance
A	<ol style="list-style-type: none"> (1) Presence of large woody erratics in the peat (2) The position of relatively shallow depths of peat for the landscape as a whole (3) Location of best drained peat (qualified by item (a) and (b) in text) (4) Location of best drained mineral soil sublayer (5) Presence of highly permeable peat (6) Vicinity of lowest summer temperatures in the peat (7) Location of the coarsest, most durable peat (8) Best conditions for static load (see, however, item (c) in text) and dynamic loading
B	Same as for A above, but less intensively represented
C	Predominance rare, except in tropical and subtropical locations (for example, Guyana, Brazil, Paraguay and Uruguay, and possibly Southern Rhodesia, Nigeria, Israel, Malaysia, etc)
D	<ol style="list-style-type: none"> (1) Linear drainage, often an open water course (2) Lag condition around a confined muskeg (bog) (3) Traps present (4) Good, but highly elastic, bearing conditions; difficult to consolidate and with marked patterned local differentials as to rate of consolidation (5) Features highly conducive to spring flooding (6) Silt in the mineral soil sublayers with highly mixed aggregate from outwash (7) Features conducive to differential settlement (often abrupt) under load
E	<p>Equally important as D above and is very common in temperate, arctic, and subarctic zones</p> <ol style="list-style-type: none"> (1) High order of homogeneity in peat, even in relation to micro-topography in which mounds, ridges and ice knolls are important (2) Peat difficult to re-wet once drained of gravitational water (3) Conditions accommodating to certain articulated wheeled vehicles (4) Good cohesion and tensility, moderate elasticity even when water shows at the surface in the field (5) Easily drainable conditions (for free water)
F	<p>Presence of highly critical conditions when prominent in the formula:</p> <ol style="list-style-type: none"> (1) Low points on drainage gradients (2) Muskeg with centres of extremely low bearing potential whether wet or relatively dry (3) Peat of low tensile strength and showing little elasticity unless the local water table is consistently high (small open pools the year round) (4) Sites where shear strength is lowest in muskeg at frequent intervals with water is not excessive,
G	Rarely predominates in the formula, is indicative of a highly fluctuating water table
H	<p>When predominant indicates presence of:</p> <ol style="list-style-type: none"> (1) Permafrost and late seasonal subsurface ice conditions of uneven contour (2) Maximum range of microtopographic amplitude (often abrupt) for all muskeg (3) Local impounding and highly irregular, dissected drainage gradients (4) Relatively locally degraded peat (structurally and mechanically disrupted)
I	<p>Unless class I is the only component comprising the cover formula (which is rare), it lacks prominence. When it is a single contributing factor in cover it is very local, usually no more than 4 or 5 m in area of coverage, and the following occur:</p> <ol style="list-style-type: none"> (1) Vehicle immobilization on the second pass of amphibious vehicles (2) The base of minor or major drainage gradients

2.2.3. FIBRE CONTENT AND DEGREE OF HUMIFICATION CLASSIFICATION

Another method of describing these soils is by quantifying the amount of fibre content in the soils. As the concept of degree of humification was adopted earlier by von Post which was based on visual examination, researchers are improving the scale by quantifying the amount of fibre content. Fibre content is determined from dry weight of fibres retained on 100-mesh sieve (> 0.15 mm opening size) as a percentage of oven-dried mass (ASTM, 2008). Fibres can be fine (woody or non-woody) or coarse (woody). Fibre is defined as a fragment or piece of plant tissue that retains a recognisable cellular structure and is large enough to be retained on a 100-mesh sieve (openings 150 µm. Plant materials larger than 20 mm in smallest dimension are not considered fibres.

The US Department of Agricultural's (USDA) developed three-point scale classification based on fibre content as describe in Table 2.8.

Table 2.8: USDA Classification System (Huat et al., 2014)

Type of peat	Fibre content (%)	von Post scale
Fibic peat	Over 66	H ₄ or less
Sapric peat	33 to 66	H ₅ or H ₆
Hemic peat	Less than 33	H ₇

Another three-way division of peat based on the von Post scale is described in Table 2.9 and explained as follows:

- Fibrous peat is low humified and has a distinct plant structure. It is brown to brownish yellow in colour. If a sample is squeezed in the hand, it gives brown to colourless, cloudy to clear water, but without any peat matter. The material remaining in the hand has a fibrous structure. Degree of decomposition on the von Post scale: (H₁-H₄).
- Pseudofibrous peat is moderately humified and has an indistinct to relatively distinct plant structure. It is usually brown. If a sample is squeezed in the hand, less than half of the peat mass passes between the fingers. The material remaining in the hand has a more or less mushy consistency, but with a distinct plant structure. Degree of decomposition on the von Post scale: (H₅-H₇).
- Amorphous peat is highly humified and the plant structure is very indistinct or invisible. It is brown to brown-black in colour. If a sample is squeezed in the hand, more than half of the peat mass passes between the fingers without any free water running out. When squeezing, only a few more solid components, such as root fibres and wood remnants, can be felt. These constitute any material remaining in the hand. Degree of decomposition on the von Post scale: (H₈- H₁₀)

The quantification of fibre content, ash content and acidity can be linked with von Post system as shown in Table 2.10. The amount of fibre content, ash content and acidity can be referred to ASTM standard. As organic soils and peat are a very complex soil, detailed classification is required compared to other inorganic soils. Although many classification systems have been established, there is no one agreed way to classify this ma-

Table 2.9: Classification of peat on the basis of von Post classification (Huat et al., 2014)

Designation	Group	Description
Fibrous peat	H ₁ -H ₄	Low degree of decomposition. Fibrous structure Easily recognised plant structure, primarily of white masses.
Pseudo-fibrous peat	H ₅ -H ₇	Intermediate degree of decomposition. Recognisable plant structure
Amorphous peat	H ₈ -H ₁₀	High degree of decomposition. No visible plant structure Mushy consistency.

terial. Generally, the level of classification depends on the objective of the user and how does the it applies to your field area.

Table 2.10: Classification of peat based on ASTM guidelines (Huat et al., 2014)

Peat Properties	Division	Description
Fibre content	Fibric	fibre more than 67 %
	Hemic	fibre between 33 % to 67 %
	Sapric	fibre less than 33 %
Ash content	Low	ash less than 5 %
	Medium	ash between 5 % to 15 %
	High	ash more than 15 %
Acidity	Highly acidic	pH less than 4.5
	Moderate acidic	pH between 4.5 - 5.5
	Slightly acidic	pH greater than 5.5 and less than 7
	Basic	pH equal of greater than 7

Some information is available for advancement of knowledge and might not be used in practice. In principle, a general description of peat soil should incorporate the following properties (Hobbs, 1986):

- (a) Colour, which indicates the state of peat.
- (b) Degree of humification which depends on the fibre content whether fibric, hemic or sapric.
- (c) Water content by drying in the oven at 105 °C.
- (d) Principle plant components, such as coarse fibre, fine fibre, amorphous.
- (e) Organic content as percentage of dry weight determined by loss on ignition test at 450 °C to 550 °C as percentage of oven-dried mass at 105 °C.

- (f) Liquid limit and plastic limit.
- (g) Fibre content determined from dry weight of fibre retained on 100 mesh-sieve (>0.15 mm) as percentage of oven-dried mass.

However, organic matter that is finer than 0.15 mm with no distinct fibre shape is considered as amorphous-granular material or also known as peat humus.

Besides determining the fibre content using the dry weight retained as prescribed in ASTM, the degree of humification can also be determined using chemical properties. This method suggested by Klavins *et al.* (2008) aims to determine the quantity of formed humic substances as a fraction of the total amount of organic matter. Another method was also proposed by Blackford & Chambers (1993) using chemical extraction of soluble material. The degree of decomposition is governed by hydrothermal conditions, pH values and resistance of dead plants to decomposition (Nie *et al.*, 2012).

2.3. DUTCH CLASSIFICATION SYSTEM

Dutch peat are formed in place known as sedentary peat which consists of reed and sedge peat, wood peat and moss peat (den Haan, 1997). The peat which has traces of plant which resulted from eroded and deposited organic material is called as “meermolm” (organic lake mud), “detritus” and “verslagen veen” (detrital peat). Organic material which is strongly decomposed is known as “Rottingsslijk” (sapropelium). Detrital fragments, sapropelium and sedentary remains occur as constituents of organic clay together with mineral constituents.

The system used for Dutch organic soil is based on 2 ternary diagrams in which zones discern between a main constituent (either peat, clay, silt or sand) and secondary constituents in varying degrees as shown in Figure 2.5. Capital letters indicate the main constituent and lower case letters give the secondary constituent followed by a number to indicate its relative importance. For example, V_k3 indicates very clayey peat and K_s2h₂ indicates moderately silty, moderately organic clay. The slanted lines in the first ternary diagram reflect a dominance of the clay fraction in the properties of the mixture. The borderline between peat and organic soil lies at 15 % to 25 % organic matter.

In the Netherlands, the classification developed by von Post, Landva and Pheeny, Hobbs and Dutch guideline have not been applied as they requires more effort to construct. Hence, more simplified approach of classification is adopted which are based on bulk density, water content, main botanical type and perhaps some indication of degree of humification (den Haan & Kruse, 2007). The estimate bulk density for each soil type is discussed by den Haan & Kruse (2007) as described in Table 2.11. The first column represents the geological classification code as introduced in section 3.1. The second column gives a description of the material according to this code. The third column (nr) gives the number of samples that were used. The last two columns give the mean and range of the bulk density.

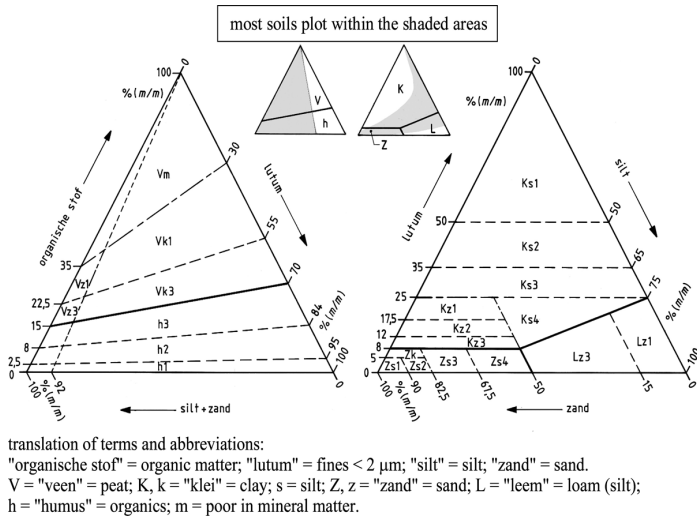


Figure 2.5: Ternary classification diagrams for soft soils (Reproduced from NEN-5104:1989 with permission of NEN, Delft)

Table 2.11: Indicative bulk density of Dutch organic soils (den Haan & Kruse, 2007)

Designation	Description	no. of samples used	Bulk density ρ (t/m^3)	
			Mean	Range
Vm	Peat, poor in mineral matter	98	1.06	0.95 - 1.13
VK1	Slightly clayey peat	21	1.11	1.02 - 1.17
Vk3	Very clayey peat	16	1.18	1.09 - 1.25
Kh3	Highly organic clay	13	1.27	1.20 - 1.35
Kh2	Mod. organic clay	30	1.37	1.26 - 1.51
Kh1	Slightly organic clay	60	1.45	1.30 - 1.60
Ks	Slightly to highly silty clay	89	1.51	1.40 - 1.60

2.4. SOIL FORMATIONS

Different terms are used depending on the process of peat formation such as peat lands, mires, bogs and fens. Before knowing the formation background into details, the usage of such terms should be defined. According to Huat et al. (2014) which based on Irish Environment and Heritage Service website, the definition of each term is defined as below:

- **Peat land:** An area with a naturally accumulated peat layer at the surface.
- **Mire:** A peat land where peat is currently forming and accumulating.
- **Bog:** A peat land which receives water solely from rain precipitation and / or snow falling on its surface. Raised bogs are found in lowland areas, generally below 150 m, such as river valleys, lake basins, and between drumlins. They are known as raised bogs because the bog surface is raised in the middle, like a dome. The

surface of a raised bog is a mixture of pools, raised mossy hummocks and flatter lawns, and is colonised by plants and animals adapted to the acidic conditions and low levels of nutrients found there. Blanket bogs usually form in upland areas above 200 m with heavy rainfall and low temperatures. The thickness of peat varies between 1 m to 6 m due to undulating nature of this ground. Like raised bogs, blanket bogs receive their nutrients from rainwater and the atmosphere, and also acidic.

- **Fen:** A peat land which receives water and nutrients from the soil, rock and ground-water as well as rain and /or snow. Fens generally form in natural basins that have been flooded and developed into lakes. Plants start to grow around the edges of these lakes and eventually extend over most of the surface, often with the only area of open water at the centre or deepest part. The fen peat forms as plants such as sedges, reeds and herbs, die and accumulate at the bottom of the lake.

The morphological differences between fen and bog depend on circumstances surrounding their formation and the plant types present in the soil. The differences extend to structure, fabric, humification and proportional of mineral material which have a significant influence on engineering properties such as plasticity, permeability, compressibility and strength. Limited studies are reported looking on the effects of morphology and structure of peat on the performance of engineering works (Hobbs, 1986). The morphology of some British peats with expected engineering properties are shown in Figure 2.6 and discussed by Hobbs (1986). Generally, there are three different morphological stages which are determined by the hydrological state of the mire.

- (a) Rheotrophic stage : This stage allows the colonization of vegetation by nutrients and sediments supply from surface run off. It develops in mobile water in lakes, basins and valleys under the control of ground water level. The landscape after the completion of this stage is mash-like and commonly known as fen or fen peat. Fen peat is underlain by very soft organic mud.
- (b) Transitional stage : Mire formed from rheotrophic stage growth upwards which allows more water is supplied by direct precipitation. The peat known as basin bog or transition peat and has a mixed and woody texture.
- (c) Ombrotrophic stage : Mire in the stage of growing beyond the maximum physical limits of the groundwater which means it is now depends on direct precipitation as water supply. The peat acts as a storage of water above ground water level. The water formed is normally acidic and it is generally termed as raised bog or bog.

STAGE and MIRE TYPE	MORPHOLOGY and simplified and diagrammatic	NUTRIENT		COMMON PLANT COMMUNITIES	CEA 4	pH of peat 5	Organic content %	Water Content %	Liquid limit %	Plastic limit test	K	Remarks
		Source	State									
THIRD STAGE Blanket or hill bog		Rainfall only	poor	Cleudberry ling Heather Purple moor grass Lotion sedge 2 Deer sedge 2 Sphagna 3 Bog asphodel	High in bog plant communities	4	>98%	2000 to 1000	1500 to 900	Not possible on pure bog peat		Bogs invaded by Pine & Birch under drier climatic conditions
THIRD STAGE Raised bog at bog		Umbra - oligo - trophic										
SECOND STAGE Basin bog		mixed		Willow Alder Sallow Fen mosses Spear-wort Meadow rue Purple loosestrife	Low in fen and transition plant communities	5	decreasing as conditions become more oligonous	1000 to 500	900 to 600	Generally possible on fen peats		Transition peats can be very variable Properties intermediate between fen & bog
SECOND STAGE Transition		Rainfall and run-off	meso - trophic									
SECOND STAGE Fen Carr		Ground Water run-off and rainfall	Rich	Sedges Common reed 1 Reedmaes Rushes			increasing with height above the substrate	500 to 200	600 to 200			Very Rich in species particularly under calcareous conditions pH > 6
FIRST STAGE Fen		Water run-off and rainfall	Eutrophic									Acid fens also occur Poorer in species pH < 5
FIRST STAGE Swamp		flowing water	ditto	Water lily Submerged plants								
FIRST STAGE Lake		Rainfall - trophic										

NOTES:
 1 The common reed (*Phragmites australis*) is actually a member of the grass family (Poaceae)
 2 More commonly known as cotton grass and deer grass, but are true sedges (Cyperaceae)
 3 The most prominent bog plant generally

Figure 2.6: Mire stages, morphology, flora and associated properties of some British peat (Hobbs, 1986)

2.5. STRUCTURAL ARRANGEMENT AND SOIL MODEL

Peats are formed by breakdown of plant and organic matter and are characterised for having high water content and void ratio. Peat is also defined as a mixture of fragmented organic materials formed in wetlands under appropriate climatic and topographic conditions and it is derived from vegetation that has been chemically changed and fossilised. At initial state, peat is porous and has low specific gravity but along the time, it is susceptible to bio-degradation. It is important to understand the structural arrangement of peat as its affect the mechanical behaviour of the soil. [Wong et al. \(2009\)](#) stated that the size, shape, fabric and packing of the soil particles influence the soil permeability, compressibility and shear strength. [Mitchell & Soga \(2005\)](#) mentioned that the size and shape of soil particles, arrangements and forces between them helps to understand the engineering properties such as strength, compressibility and permeability better.

The peat structure can be divided into two distinct levels which is macrostructure (microfabric) and microstructure (microfabric). Macrostructure is visible features that can be observed with naked eyes while microstructure involves much smaller features at the particle of fibre level. Overall, peat structure is based on two basic structure elements that is fibre and granules which are further categorised into three different groups: (1) coarse fibres (low degree of decomposition with visible plant remnants); (2) fine fibres (slightly decomposed with indistinct plant remnants) and (3) amorphous granular (highly decomposed with indistinct traces of plant structure; smaller organic granules/grains is observed). The fibres of peat consists of two-levels cellular structure involving macro and micro pores which located between and within fibres respectively ([Dhowian & Edil, 1980](#)). It is stated by that it is possible for soils having the same organic content but different in fibre content ([Colleselli et al., 2000](#)).

The physical model in peat is well described by [Wong et al. \(2009\)](#) by introducing the concept of multi-phase system which can be represented by a physical peat soil model as shown in Figure 2.7 below.

Organic bodies	Organic particles (solids)
	Water (inner voids)
Organic spaces	Water (outer voids)
	Soil particles (solids)

Figure 2.7: Physical model of peat ([Wong et al., 2009](#))

From this model, peat can be divided into two major components namely organic bodies and organic spaces. The organic bodies consist of organic particles with its inner voids filled with water whereas the organic spaces of the soil model comprises of soil particles with its outer voids filled with water. The soil model gives a clear indica-

tion that at its initial state, peat can hold a considerable amount of water due to hollow, spongy and coarse nature of the organic particles. Figure 2.8 shows a clear picture of organic fibrous peat with large pore spaces or porous structure with the ability to hold considerable amount of water when it is fully saturated. Normally at macroscopic level, large pore spaces between stems and leaves can be observed while at microscopic level is within the open and perforated structures (Huat et al., 2014). The fibre content of peat plays a major role in controlling soil behaviour. The terms fibre includes all other fibrous structures such as shrub, rootlets, plant root hairs, rhizoids (root like filaments and others (Landva & Pheeney, 1980). The stronger is the fibre and with greater amount make the soil more reinforced (Landva & Pheeney, 1980).

The network of fibrous elements and perforated hollow particles in horizontal direction show that individual fibres tend to rearrange themselves horizontally when consolidation pressure is applied on fibrous peat which results higher void spaces in the horizontal direction compared to vertical direction (Wong et al., 2009). This is well observed in Figure 2.9. The components of peat soil composition is shown in Figure 2.10 where peat soil consists of two different voids which is inner and outer voids. Inner void is within the organic coarse particles where water can trap in this micropore and outer void is the macropore normally fill with free water which consists of smaller organic grains. Approxiamtely, one third of the measured water content is due to the presence of water at an interparticle level (within the voids), with the remaining water existing at an intraparticle level (within the microstructures of the organics) (Nie et al., 2013).

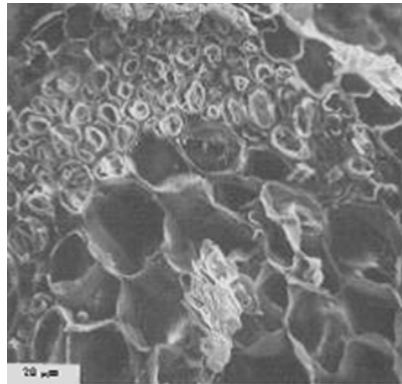


Figure 2.8: A photomicrograph of poriferous cellular plant particle (Terzaghi et al., 1996)

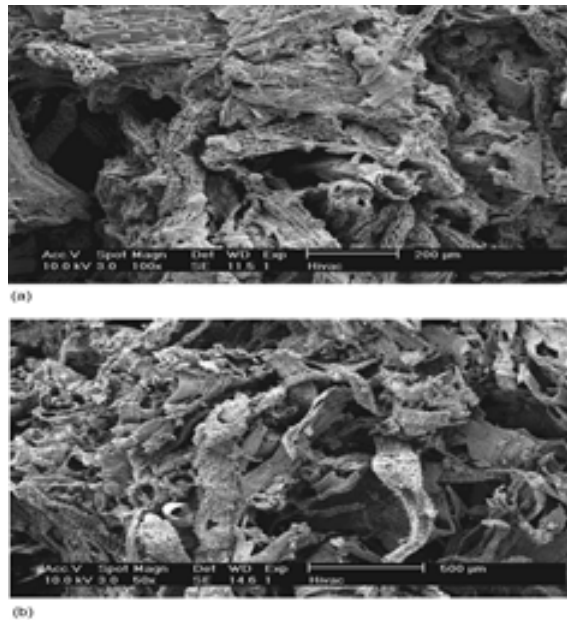


Figure 2.9: Scanning electron microphotograph of (a) vertical section; (b) horizontal section of peat showing network of fibrous elements and perforated hollow particles (Mesri & Ajlouni, 2007)

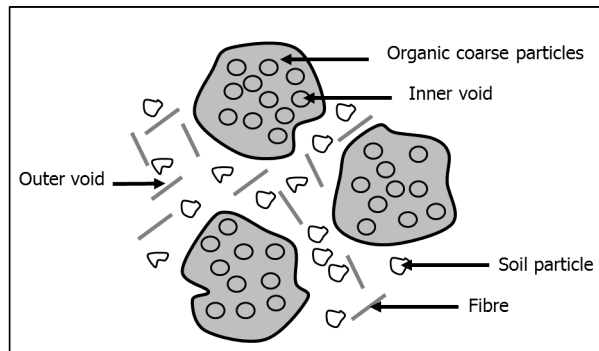


Figure 2.10: Schematic diagram illustrating composition of peat (Huang et al., 2009)

However, the fibrous structure will change with time due to decomposition process where at this state there is difficulties to identify if the material is derived from plant remnants although it has high organic content. High decomposed organic matter is generally difficult to distinguish as it has amorphous structure (Landva & Pheeney, 1980). This is clearly shown in Figures 2.11 and 2.12 for hemic and sapric peats when captured using Scanning Electron Microscopy (SEM) where they have a higher state of decomposition.

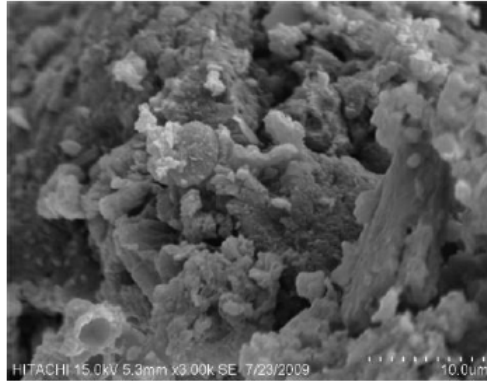


Figure 2.11: Example of hemic peat from Malaysia with von Post classification H6-H9 using SEM (Huat et al., 2014)

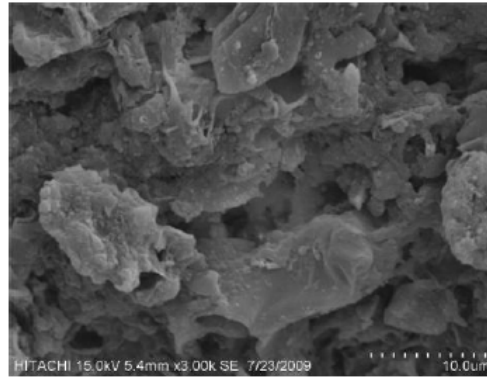


Figure 2.12: Example of sapric peat from Malaysia with von Post classification, H6-H9 using SEM (Huat et al., 2014)

In terms of soil mechanics, typical soil can be represented in a model which consists of three different phases that which is solid, liquid (water) and gas (air). However, for the case of organic soils and peat, the solid phase is divided into two separate components: organic matter and inorganic earth materials. The mineral component consists of clay minerals and sometimes non-clay minerals are also encountered. Clay mineral consists of small particles, typically less than 0.002 mm in diameter. The mineral constituent is incombustible and ash-forming while the organic matter is generally combustible carbonaceous matter. The relative proportion of organic and inorganic compositions is crucial to determine the physical and geotechnical properties of these soils (Huat et al., 2014). Figure 2.13 shows the three-phase diagram for these soils as suggested by Huat et al. (2014) and Al-Khafaji & Andersland (1981). From these phases, the weight-volume relationships are derived such as the formulation of moisture content, degree of saturation, void ratio, density, unit weight and specific gravity of soils.

The soil organic matter includes: (1) fresh plant and animal residues (decomposable), (2) humus (resistant) and (3) inert forms of elemental carbon (charcoal, coal or graphite). More details explanation of soil organic matter is described in Section 2.13

2

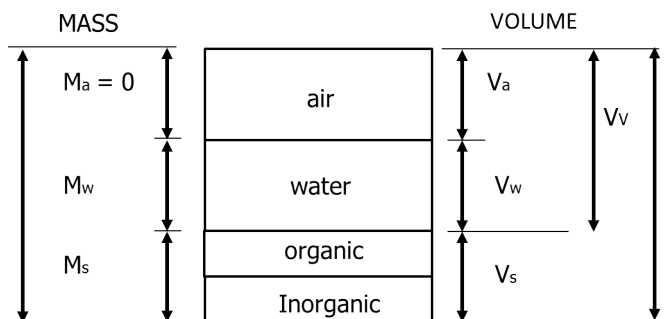


Figure 2.13: Soil phase diagram for organic soils and peat (Huat et al., 2014)

2.6. HUMIFICATION AND OXIDATION

Different terms are used to describe the physical and chemical change of peat for instance from fresh state (containing visible fibres structure) to decompose state (finer organic grains with invisible fibres structure). This change can either called as humification, decomposition or decay processes which can be used interchangeably. If the change of state of soil is accelerated, then oxidation term is used. Typically, the decomposition process includes: (a) loss of organic solid matter as gas or in solution (including leaching and by removal by small invertebrates), (b) loss of physical structure and (c) change of chemical state including changes mediated by micro-organisms (Hobbs, 1986). Two types of decomposition can occur depending on the environment whether aerobic (with the presence of oxygen) or anaerobic (limited supply of oxygen). It is reported that high pH (alkaline condition) and high temperature can stimulate decomposition process significantly.

In the beginning, the loss of organic matter is due to breakdown of plant remains as a result of earthworms and later supported by bacteria and fungi that stimulate biochemical oxidation. The product of biochemical oxidation is carbon dioxide and water. This loss is not only limited to the product of biochemical oxidation but also changes the chemical state of the fibrous plant by producing smaller organic grains containing humic substances. The organic grains also known as amorphous granular are the final product of decomposition containing gelatinous organic acids (humic substances) in the form of sponge-like solids (Landva & Pheeny, 1980; Hobbs, 1986; O'Kelly & Pichan, 2013).

In summary, if peat is fresh or undecomposed, there will be little or no granular looking material instead containing leaf, stem and root fibres light in colour whereas if peat is completely decomposed, there will be little or no residual fibre, dark in colour and spongy and gelatinous (Hobbs, 1986). The level of decomposition has been described earlier in Section 2.2.

Nie et al. (2012) reported that the organic content of peat soil gradually decreases

with time as a result of a complex conversion process of the organic matter which involves mineralization and humification, humus decomposition and the subsequent transformation into inorganic substances.

2.7. SOIL ORGANIC COLLOIDS

In soils, there is a chemically active fraction which is called as colloids. They are very small having the diameter of less than $2\ \mu\text{m}$. In term of structure, they can be crystalline (definite structure) or amorphous. Colloids can either be mineral clays or organic humus. They have the ability to impart chemical properties (the source of ions, source of electro-negativity and buffering capacity) and physical properties (the large surface area per unit of mass and the plasticity) to soils. The type of soil colloids are crystalline silicate clays, non-crystalline silicate clays, iron or aluminium oxide and organic material (humus) (Huat et al., 2014).

2.8. PHYSICAL PROPERTIES

Defining the properties of soil is very important in order to classify the soil accurately and also to understand soil behaviour better. In engineering design, determining properties of soil should be taken seriously in order to avoid any potential failures when building engineering structures. For organic soils, properties of soils can be divided into three different categories that are physical, chemical and engineering properties. Physical properties is described as the general classification of soil which are influenced by the changes soil phase components either solid part (organic or inorganic), air or water. The changes of these components are closely related to pore size distribution in the soil that depends on the degree of humification. For example, higher state of decomposition result to finer particles due to breakdown of organic matter while lower state of decomposition may produce coarser particles with visible plant remains. Hence, more dry material is obtained per unit volume and smaller pores. Huat et al. (2014) claimed that the degree of humification affects the pore size distribution and controlled by both particle size and structure of peat. Water content, density, specific gravity, organic content, density, void ratio are among the relevant physical properties mentioned and will be explained in details in the following section.

It is reported that organic matter affects the geomechanical behaviour of soils by modifying some properties significantly. Organic matter gives the soil aggregated structure by molecular complexation involving metallic, organic and clay molecules which contributes to increasing compressibility and also organic matter increases the liquid limit and plastic limit of soils (Tremblay et al., 2002). Listed below is the important physical properties that normally considered for geotechnical engineers. Any changes of these properties will have a great influence on the engineering properties such as compressibility and strength behaviour.

2.8.1. WATER CONTENT

Peat soil has high water content due to its natural ability to hold a considerable amount of water. The particles have a hollow cellular structure largely full of water; one third of

water content of fibrous peats is within the particles (Mesri & Ajlouni, 2007). The value of water content depend on origin, degree of decomposition, chemical composition and proportion of organic and inorganic materials. Peat has high water content due to low bulk density and low bearing capacity as a result of high buoyancy and high pore volume (Huat et al., 2011). Gravimetric water content of peat ranges from 200 % to 2000 % unlike silt and clay soil that are seldom reach 200 %. In West of Malaysia, peat has water content in the range of 200 % to 700 % (Huat et al., 2011). Figure 2.12 shows the water content for Dutch and international peats (Venmans, 2004). It is also reported that the natural content of tropical peat is in the range of 150 % to 700 % with organic content 50 % to 95 % and it increases with increase in organic content (Huat et al., 2009). The natural water content for peats is in the range of 200 % to 2000 % which higher than marine clay having value in the range of 50 % to 93 % (Zainorabidin & Wijeyesekera, 2007). This high natural moisture content is due to the water that is held in organic matter and cells of the plan which is higher for fibrous peat that other peats. Terzaghi et al. (1996) stated that natural content of peat ranges from 610 % to 830 % with its void ratio ranging from 11.1 to 14.2. The initial water content and void ratio are depend on the type of peat and amorphous granular peat can have initial moisture content and void ratio as low as 500 % and 9 respectively whereas for fibrous peat, the initial moisture content and void ratio can be as high as 3000 % and 25 respectively (Bell, 2000). Three states of water can present in organic soils:

- free water in large cavities of the peat (intracellular water).
- capillary water in the narrower cavities (interparticle water).
- water bound physically (absorbed), chemically, colloiddally and osmotically.

The water content of organic soils and peat can be determined by drying at 105 °C although some concern that this temperature will lead to charring of organic components in peat, hence producing large figures for water content. Lower temperatures between 50 °C to 95 °C are recommended. However, Skempton & Petley (1970) investigated these effects and concluded that the loss of organic matter at 105 °C is not significant, while drying at lower temperatures retains small amount of free water. The water content is calculated using equation below where, w = water content, M_w = mass of water and M_s = mass of dry solids.

$$w = \frac{M_w}{M_s} \times 100 \quad (2.1)$$

Table 2.12: Water content and organic content of different types of peats (Venmans, 2004)

Source of water	Amount of nutrients	Plants	water content (%)	Organic content (%)
river, lakes, groundwater	large: eutrophic	reeds, sedges, alder, willow, oak, UK: fen peat NL: laagveen	100 - 500	20 - 70
groundwater, rain	medium: mesotrophic	pine, birch, moss UK: transitional peat NL: overgangsveen	500 - 1000	70 - 95
rain only	low: oligotrophic / ombrotrophic	moss, cottongrass, heather UK: raised bog peat NL: hoogveen	1000 - 2000	>95

2.8.2. ORGANIC CONTENT

According to [Hobbs \(1986\)](#), organic content is defined as soil containing pure, ash free, vegetable matter (leaves, stems, roots or twigs), possible organic animal remains and any residual organic compounds from the humification process. The organic content depends on the water content of organic soils. Higher water content will result to higher organic content and this which also depends on the degree of humification. For example, fibrous peat has higher organic content due to its higher water holding capacity compared to degraded peat.

The organic content can be determined from loss ignition test described in [ASTM \(2007a\)](#). The accepted method to determine the organic content in soils is to burn off the organic matter at high temperature after drying the specimen at 105 °C. Different high temperatures were compared at 550 °C, 700 °C, 800 °C and 950 °C by [Skempton & Petley \(1970\)](#). However, [Skempton & Petley \(1970\)](#) found the effect of varying the ignition temperatures is less significant on high organic content Sphagnum peat. Various ignition temperatures has been used in Netherlands in the past: 500 °C, 550 °C, 800 °C and 950 °C ([den Haan & Kruse, 2007](#)). Overestimate of mass loss is necessary to be corrected due to evaporation and decomposition of non-organic constituents such as bound water in clay and CO₂ from calcium carbonates. Oxidation of FeS₂ in poorly aerated soil can result in a mass increase ([den Haan & Kruse, 2007](#)).

The ash content (A) and the organic content (OC) can be calculated from the loss on ignition (N) according to equations below as proposed by [Skempton & Petley \(1970\)](#) where (C) is the correction factor. For a temperature of 450 °C, C = 1.0 ([Arman, 1970](#)). In Europe, a higher temperature of 550 °C is used for combustion of peat, and C = 1.04 is then applied as the correction. However, the difference is usually small and hence not significant for practical considerations ([Huat et al., 2014](#))

$$OC = 100 - C(100 - N) \quad (2.2)$$

$$A = 1.04 \times (100 - N) \quad (2.3)$$

[ASTM \(2007a\)](#) proposed burning the oven dried sample from water content determination at 450 °C for 5 hours and the ash content (A) and organic content (OC) are calculated based on equation below where C = mass of ash after burning, B = oven-dried specimen after water content determination.

$$A = \frac{C}{B} \times 100 \quad (2.4)$$

$$OC = 100 - A \quad (2.5)$$

2.8.3. SPECIFIC GRAVITY

Peat has lower specific gravity than other mineral soils due to its composition and percentage of inorganic component. The cellulose and lignin content in peat has approximated specific gravity of 1.58 and 1.4 respectively unlike mineral soils in the range of 2.65

to 2.75 (den Haan & Kruse, 2007). These low values would reduce the compounded specific gravity in organic soils (Duraisamy et al., 2007). Higher specific gravity are for peats with higher degree of decomposition and higher mineral content. Peat contains 75 % organic content or more has specific gravity in the range of 1.3 to 1.8 with an average of 1.5 (Huat et al., 2011). For peats containing water content more than 600 %, the water content and specific gravity has little effect on bulk density compared to degree of saturation or gas content as shown in Figure 2.14. Peat is rarely in saturated condition due to the presence of gas that make it buoyant under water. However at low water content (less than 500 %) with high mineral content, the average bulk density is slightly lower than water (Huat et al., 2011). Authors such as Edil (1997); Hobbs (1986); den Haan (1997) reported values in the range of 1.1 to 1.9 (Zainorabidin & Wijeyesekera, 2007). Huat et al. (2009) reported that specific gravity tropical peats is in the range of 1.05 to 1.09 and this value decrease with increase in organic content. The specific gravity of tropical peats fall in the range of 1.07 to 1.7 and an average of 1.4 (Duraisamy et al., 2007). Bell (2000) stated that specific gravity is between 1.1 and 1.8. Skempton & Petley (1970) produced a correlation between specific gravity of organic soils and peats and their ignition loss as below:

$$\frac{1}{\rho_s} = \frac{1 - 1.04(1 - N)}{1.4} + \frac{1.04(1 - N)}{2.7} \quad (2.6)$$

den Haan (1997) presented results of specific gravity on Dutch organic soils and peats directly to ignition loss as shown in Figure 2.14 below and produced correlation equation. The correlations between specific gravity and ignition loss is very close thus specific gravity can therefore be obtained from ignition loss with confidence. It is important that both characteristics be measured on the same piece of material for correlations establishment.

$$\frac{1}{\rho_s} = \frac{N}{1.354} + \frac{1 - N}{2.746} \quad (2.7)$$

2.8.4. VOID RATIO

According to unit solid volume model, it usually divides soil in three different phase that is solid, water and air. An important parameter to describe the distribution of these three components is the porosity or void ratio. However, void ratio (e) is normally preferred as it describes the ratio of the volume of the voids with respect to a fixed volume of solid compared total volume which is always changing. The void ratio of peat is very high compared to inorganic soils ranges from 5 to 15 and can even reach 25 for fibrous peat (Huat et al., 2014). When peat gets dry, it can shrink and shrinkage can reach 50 % of the initial volume. When dried peat is re-saturated with water, it unable to absorb water as much as initial condition. Only 33 % to 55 % can be absorbed.

A graph showing a relationship between natural water content and void ratio of Dutch peat is plotted as shown in Figure 2.15. From the graph, it is well depicted that the linear onset of the correlation near the origin corresponds to a solids density of approximately

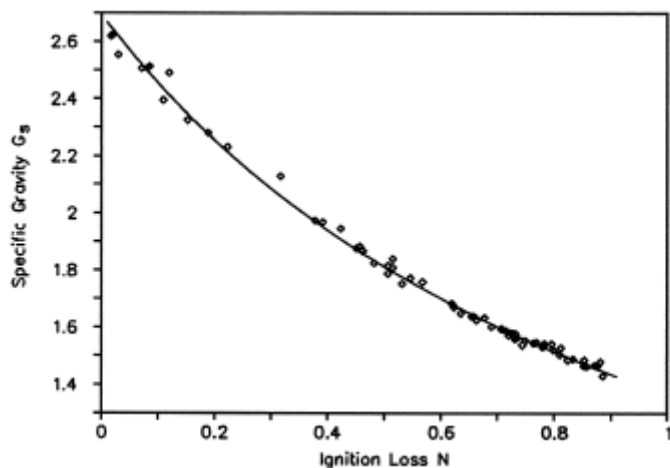


Figure 2.14: Correlations of specific gravity and ignition loss for Dutch organic soils (den Haan, 1997)

2.75. At higher water content, the void ratio increases which results to lower solid density.

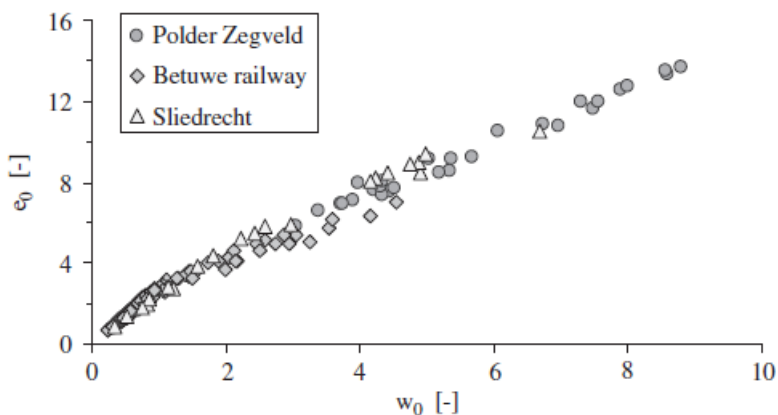


Figure 2.15: Correlations of natural water content and void ratio (den Haan & Kruse, 2007)

2.8.5. BULK DENSITY

Bulk density is defined as total mass of the material per total volume. The total mass is a summation of mass of water, solid and gas phase but under saturated condition, there is absence of gas in the system. Bulk density of peat is usually smaller than mineral soils due the higher water holding capacity and presence of gas and also low specific gravity of the solids material. The bulk density is depend on degree of decomposition and and

structure of peat. The average bulk density of fibrous peat is around the unit weight of water, 9.81 kN/m^3 (Huat et al., 2011). However, fibrous peat located in Peninsular Malaysia has unit weight in the range of 8.3 kN/m^3 to 11.5 kN/m^3 (Huat et al., 2011). Unit weight of peat is affected by the amount of water as the water content increases, the unit weight will decrease. For peat with water content 500 %, the unit weight ranges from 10 kN/m^3 to 13 kN/m^3 (Huat et al., 2011). When peat is dried, it reduces in volume significantly thus in order to represent the bulk density on field, it must be calculated on the basis of the wet bulk volume. Huat et al. (2009) reported that the bulk density of tropical peats is in the range of 0.8 Mg/m^3 to 1.2 Mg/m^3 compared to mineral soil in the range of 1.8 Mg/m^3 to 2.0 Mg/m^3 and bulk density decreases with increase in organic content. This is due the lower specific gravity of the particles and higher water holding capacity in peat compared to mineral soil. Bell (2000) claimed that the bulk density of amorphous peat is higher than fibrous peat which can reach up to 1.2 Mg/m^3 while for woody fibrous peat maybe up to half to that of amorphous peat. Wet bulk density of Dutch organic soils has been reported by den Haan & Kruse (2007). The wet bulk density is given by

$$\rho = \frac{(1 + w)}{\left(\frac{1}{\rho_s} + \frac{w}{S}\right)} \quad (2.8)$$

2.8.6. DRY DENSITY

Dry density of peat from West Malaysia is in the range of 0.1 Mg/m^3 to 1.4 Mg/m^3 (Duraismy et al., 2007). Data for tropical peat was also plotted and Equation 2.9 for dry density was obtained. Different correlations of dry density and water content were also reported by den Haan (1997) for temperate soils in the district of central Netherlands as shown in Equation 2.10. The data was taken from a railway stretch in "Betuwe" region between the Rotterdam harbour and the German hinterland while another data is from a single boring in Polder Zegveld in a 7 m thick peat deposit as shown in Figure 2.16

$$\rho_d = 22.422(w)^{-0.804} \quad (2.9)$$

Surprisingly, correlation proposed by den Haan (1997) for Dutch peats give almost similar results for Hungarian and California peats (den Haan & Kruse, 2007)

$$\rho_d = 0.872(w + 0.317)^{-0.982} \quad (2.10)$$

2.8.7. LIQUID LIMIT

Liquid limit is defined as the lowest water content which soil still behaves like liquid. This test is normally conducted for fine cohesive soils (silts and clays). There are two methods normally used which are Casagrande method and cone penetrometer ASTM D 4318 (ASTM, 2010b). For peat soil, the determination of liquid limit is rather difficult due to the presence of fibre. Skempton & Petley (1970) put a limitation for determining the liquid limit for samples at least H3 according to von Post degree of humification. Meanwhile, the liquid limit determination for fibrous peat is impossible. Authors like

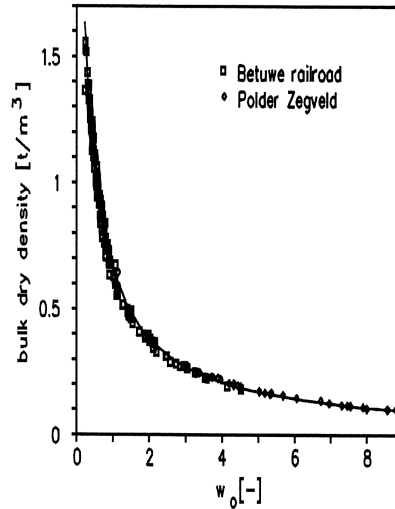


Figure 2.16: Correlations of natural water content and dry density of Dutch peats and organic soils (den Haan, 1997)

Hobbs (1986) stated that liquid limit depends on the type of plant detritus, degree of humification and clay content. Higher organic content results to higher cation exchange ability which contribute to higher liquid limit (Hobbs, 1986).

Huat et al. (2009) reported that for tropical peat the liquid limit increases with increase in organic content (Huat et al., 2009; Duraisamy et al., 2007). Zainorabidin & Wijeyesekera (2007) mentioned that liquid limit of peat is in the range of 190 % to 550 %. According to Skempton & Petley (1970) the liquid limit of peat can be as high as 500%. The liquid limit for fen peats is 200 % to 600 % and for bog peats is 800 % to 1500 % (Hobbs, 1986). This is clearly shown in Figure 2.17 which describing the variation of liquid limit with water content and ignition loss.

Hobbs (1986) also produced a correlation of liquid limit with ignition loss where LL = liquid limit and N = ignition loss as shown below:

$$LL = 5N + 50 \quad (2.11)$$

The results of liquid limit are sensitive to the chemistry of water for instance a significant drop of liquid limit is observed using tap water compared to distilled water.

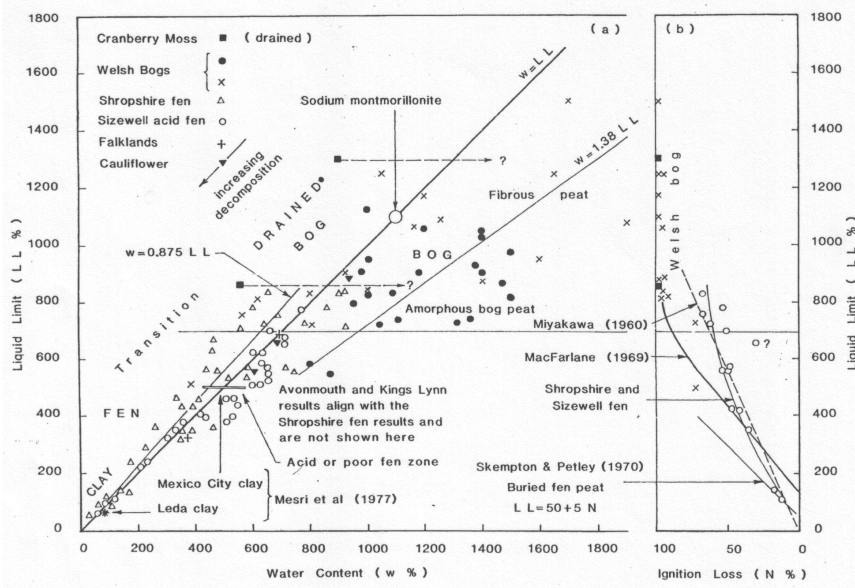


Figure 2.17: Liquid limit values against ignition loss and water content (Hobbs, 1986)

2.8.8. PLASTIC LIMIT AND PLASTICITY INDEX

Plastic limit is defined as the water content which thread 3 mm starts to break upon rolling. It is impossible to determine the plastic limit of peat soil due to the presence of fibres (Zainorabidin & Wijeyesekera, 2007). This is supported by Hobbs (1986), highlighting that it is impossible to carry out plastic limit test on pure bog peats and peat having water liquid limit exceeding 1000%. Nevertheless, this test is possible if there is some quantity of clay presence in peat soils which results closer the plasticity index to the A-line of the plasticity chart. The amount clay to make this test possible decreases as humification degree increases (Hobbs, 1986). Even the peats are highly humified, there was little point in performing plastic limit testing on peat soils since the deduced plasticity index give little indication of their character. Skempton & Petley (1970) suggested a limitation for determining the plastic limit for peats to be at least H_5 according to von Post degree of humification. Results of plastic limit for different types of peat is shown in figure 2.18.

2.9. CHEMICAL PROPERTIES

Chemical properties of peat include elemental composition, organic components and ash (Jinming & Xuehui, 1998) The common chemical compositions encountered are carbon (C), hydrogen (H), oxygen (O), nitrogen (N) and sulphur (S). The composition of each component is different from one type of soil to another depending on the environment of location of soil formation. Some locations have higher temperature which accelerate the decomposition of peat and subsequently contribute to low carbon content, pH and

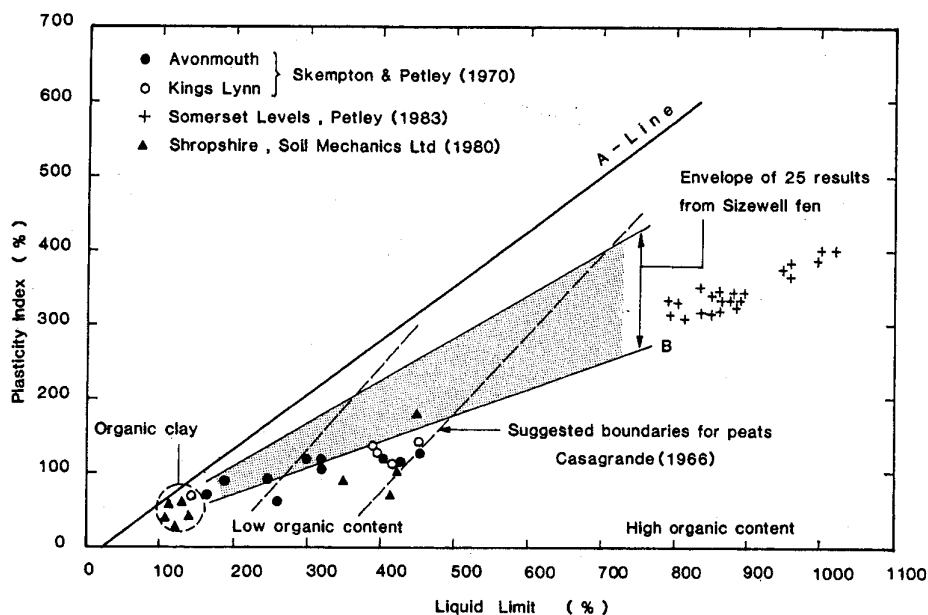


Figure 2.18: Plasticity index vs. liquid limit of some UK peats (Hobbs, 1986)

CEC among the important chemical properties that will be discussed.

2.9.1. ACIDITY

The pH of peat is decreasing with depth and the decrease may be large near the bottom layer depending on the type of the underlying soil. Peats are normally in acidic condition can have pH in the range of 4 to 7 (Huat et al., 2011). However, Bell (2000) claimed that in acidic condition, pH values ranging from 5.5 to 6.5. West Malaysia peats have very low pH values ranging from 3.0 to 4.5, in some cases where sulphide can be found within the profile, pH can be below 3.0. pH of peat is normally in the range of 2 to 6 but in some conditions where there is an infiltration of brackish water or it contains pyritic material, pH can be as high as 7.8 or less than 2 respectively (Kazemian et al., 2011b). The pH of organic soil depends on the presence of organic compounds, the exchangeable hydrogen and aluminium, iron sulphide and other oxidisable sulphur compound (Fao, 2015). In temperate regions, bog peat (blanket and raised bogs) is generally acidic with pH values in the range of 3 to 4. Fen peat is generally neutral or slightly alkaline. Bog peat has fibrous structure compared to fen peat. In tropical region, acidic peat is obtained with pH values in the range of 3 to 4.5 (Huat et al., 2014).

Figure 2.19 shows the compilation of physical and chemical properties of peats from all over the world.

Peat type	Natural water content (w, %)	Bulk density (Mg/m ³)	Specific gravity (G _s)	Acidity (pH)	Ash content (%)	Reference
Fibrous-woody	484-909	-	-	-	17	Colley (1950)
Fibrous	850	0.95-1.03	1.1-1.8	-	-	Hanrahan (1954), Asadi et al., 2009, 2010
Peat	520	-	-	-	-	Lewis (1956)
Amorphous and fibrous	500-1500	0.88-1.22	1.5-1.6	-	-	Lea and Browner (1963)
	200-600	-	1.62	4.8-6.3	12.2-22.5	Adams (1965)
	355-425	-	1.73	6.7	15.9	
Amorphous to fibrous	850	-	1.5	-	14	Keene and Zawodniak (1968)
Fibrous	605-1290	0.87-1.04	1.41-1.7	-	4.6-15.8	Samson and LaRochell (1972), Moayedi et al.(2011a, b)
Coarse fibrous	613-886	1.04	1.5	4.1	9.4	Berry and Vickers (1975)
Fibrous sedge	350	-	-	4.3	4.8	Levesque et al. (1980)
Fibrous sphagnum	778	-	-	3.3	1	
Coarse fibrous	202-1159	1.05	1.5	4.17	14.3	Berry (1983)
Fine fibrous	660	1.05	1.58	6.9	23.9	
Fine fibrous	418	1.05	1.73	6.9	9.4	NG and Eischen (1983)
Amorphous granular	336	1.05	1.72	7.3	19.5	
Peat portage	600	0.96	1.72	7.3	19.5	
Peat waupaca	460	0.96	1.68	6.2	15	
Fibrous peat (Middleton)	510	0.91	1.41	7	12	Edli and Mochtar (1984)
Fibrous peat (Noblesville)	173-757	0.84	1.56	6.4	6.9-8.4	
Fibrous	660-1590	-	1.53-1.68	-	0.1-32.0	Lefebvre et al. (1984)
Fibrous peat	660-890	0.94-1.15	-	-	-	Olson and Mesri (1970)
Amorphous peat	200-875	1.04-1.23	-	-	-	
Peat	125-375	0	1.55-1.63	5-7	22-45	Yamaguchi et al. (1985)
Peat	419	1	1.61	-	22-45	Jones et al. (1986)
Peat	490-1250	-	1.45	-	20-33	Yamaguchi et al. (1987)
Peat	630-1200	-	1.58-1.71	-	22-35	Nakayama et al. (1990)
Peat	400-1100	0.99-1.1	1.47	4.2	5-15	Yamaguchi 1990
Fibrous	700-800	~1.00	-	-	-	Hansbo (1991)
Peat (Netherlands)	669	0.97	1.52	-	20.8	Termatt and Topolnicki (1994)
Fibrous (Middleton)	510-850	0.99-1.1	1.47-1.64	4.2	5-7	Ajlouni (2000)
Fibrous (James Bay)	1000-1340	0.85-1.02	1.37-1.55	5.3	4.1	

Figure 2.19: Physical and chemical properties of peats (Kazemian et al., 2011a)

2.9.2. CATION EXCHANGE CAPACITY

Cation Exchange Capacity (CEC) is a number that describes the ability of soil to hold cations at a given pH value. Clay and organic matter for example, have a negative charge on their surface which allow them hold cations from soil water solution due to the attraction of charges. Soils with high clay or organic matter content will have a higher CEC. Sandy soils tend to have a lower CEC. For organic soils and peats, the CEC values are very high and the main exchangeable sites are the functional acid groups which is named humic acids. The most common exchangeable cations in peats are Ca^{2+} , Mg^{3+} , Al^{3+} , K^+ , Na^+ , NH_4^+ . It is reported that the CEC value is high when pH and exchangeable cation concentration are high as well (Huat et al., 2011). The CEC value able to give an indication of the amount of total negative charge available on soil surface. The CEC of organic and peat soils increases with increasing organic content. The water adsorption potential of organic soil increases with increasing CEC. Figure 2.20 shows the relationship of CEC and degree of humification of organic soils. It depicts that CEC values increase as degree of humification is increasing.

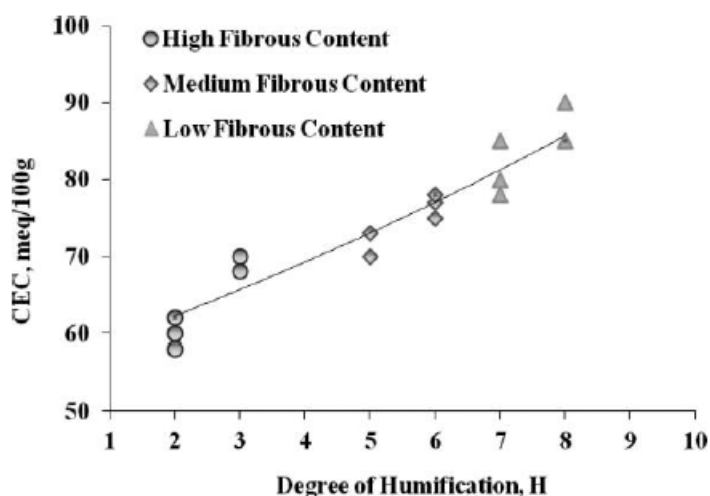


Figure 2.20: Relationship of CEC and degree of humification for organic soils and peat (Huat et al., 2014)

2.10. ENGINEERING PROPERTIES

The engineering properties are the most important aspects that need to be considered for geotechnical engineers. These properties include design parameters that directly affect the geo-mechanical behaviour of organic soils. In geotechnical design, soils are analysed in terms of compressibility and strength in order to overcome any design failure. Basically, compressibility and strength parameters are obtained by performing proper laboratory works which later will be used for design. In this dissertation, compressibility behaviour is the topic of discussion hence the following section will focus on the parameters that relate to it explicitly.

Generally, the compressibility of soil can be divided into three separate stages namely initial compression, primary consolidation and secondary compression. Initial or immediate compression is described as the instantaneous compression which occurs immediately after the application of load but before dissipation of drainage. This initial compression is due to the expulsion and compression of small pockets of gas within the pore spaces. Primary consolidation is a time dependent compression resulting from dissipation of excess pore water pressures as a result of increase in effective stress. Secondary compression is additional compression which continues after completion of dissipation of excess pore water pressures which occurs under constant effective vertical stress.

The required time to dissipate excess pore water pressures is greatly depends on permeability of soil. In granular soil for example, the permeability is very high due to bigger pore size hence the dissipation process is very fast. However, in clay soil, the process is very slow due smaller to void ratio between particles. In peat, primary consolidation is very rapid and secondary compression normally takes a significant part of compression. Even, tertiary compression is also sometimes observed (Kazemian et al., 2011a).

2.10.1. PRIMARY CONSOLIDATION

The compressibility of soil is determined by performing consolidation test using an apparatus known as Oedometer as shown in Figure 2.22.

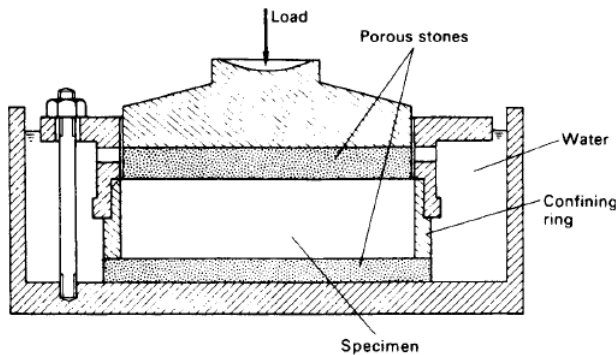


Figure 2.21: The oedometer cell (Craig, 2004)

A soil specimen in the form of disc usually of diameter 75 mm and thickness 15 mm to 20 mm is held inside a metal ring and lying between two porous stone. The assembly is placed in the cell and held in place by a clamping ring. A vertical static load is then applied through a lever system and the cell is saturated with water. Changes of thickness of soil specimen is recorded using a displacement dial gauge or transducer. Each pressure applied will take about 24 to 48 hours typically. Further increments of load are then applied, each being double the previous increment and the readings are recorded again. At the end of increment period, when the excess pore pressure has completely dissipated, the applied pressure equals to the effective vertical stress of specimen. The final load is

then removed either in one or in several stages and the sample is allowed to swell. The swelling enables the specimen to stabilise before the final water content and thickness are determined ; otherwise swelling might occur when specimen is removed from the oedometer which leads to error. The results are normally plotted in terms of thickness or void ratio at the end of pressure increment for each stage against the corresponding effective stress. The void can be calculated from the dial gauge readings and either the final water content or dry weight of the test specimen. The detailed procedure about this test can be referred to BS1377 The final void ratio can be calculated using either one of the two approaches below which based on the phase diagram shown in Figure 2.22

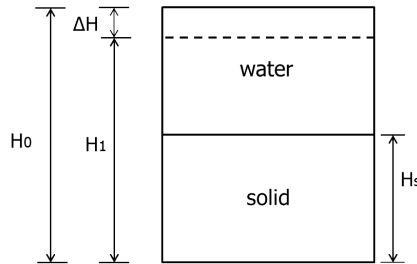


Figure 2.22: Soil phase diagram (Craig, 2004)

Method 1

Water content measured at the end of test : w_1

Void ratio at the end of test: $e_1 = w_1 G_s$ (assuming $S_r = 100\%$)

Thickness of specimen at start of test = H_0

Change in thickness during test = ΔH

Void ratio at start of test = $e_0 = e_1 + \Delta e$

where,

$$\frac{\Delta e}{\Delta H} = \frac{1 + e_0}{H_0} \quad (2.12)$$

In the same way, Δe can be calculated up to the end of any increment period.

Method 2

Mass of solid measured at the end of test: M_s

Thickness at end of any increment period: H_1

Area of specimen: A

Equivalent thickness of solids: $H_s : M_s / AG_s \rho_w$

Void ratio:

$$e_1 = \frac{H_1 - H_s}{H_s} \quad (2.13)$$

The theory of consolidation is developed by Terzaghi in 1925 by incorporating the following assumptions:

- (a) The soil is fully saturated and homogeneous.
- (b) Both the water and the soil particles are incompressible. Darcy's law of water flows applies.
- (c) The change in volume is one-dimensional in the direction of the applied stress.
- (d) The coefficient of permeability and volume of compressibility remain constant.
- (e) The change in volume corresponds to the change in void ratio and $(\frac{\partial e}{\partial \sigma'})$ remains constant.

The compressibility characteristics of soils can be expressed in terms of consolidation parameters such as coefficient of volume compressibility m_v , compression index C_c , coefficient of consolidation c_v and preconsolidation stress σ'_c where each parameter has their own definition as described below.

Coefficient of volume compressibility m_v , is described as the amount of change in unit volume due to a unit increase in effective stress. The value of m_v is not constant for a given soil, but varies with the level of effective stress; oedometer results can be used to obtain a range of values. The volume change can be expressed in terms of void ratio or sample thickness. If an increase in effective stress from σ'_0 to σ'_1 causing a decrease in void ratio from e_0 to e_1 , then m_v calculated based on sample thickness is,

$$m_v = \frac{\Delta H}{H \Delta \sigma'} \quad (2.14)$$

$$m_v = \frac{1}{H_0} \left(\frac{H_0 - H_1}{\sigma'_1 - \sigma'_0} \right) \quad (2.15)$$

If m_v is calculated based on void ratio, the equation can be derived as below where Equation ?? is originally based on the volumetric strain equation.

$$\frac{\Delta H}{H} = \frac{\Delta e}{1 + e_0} \quad (2.16)$$

$$m_v = \frac{\Delta e}{1 + e_0} \left(\frac{1}{\Delta \sigma'} \right) \quad (2.17)$$

$$m_v = \frac{e_0 - e_1}{1 + e_0} \left(\frac{1}{\sigma'_1 - \sigma'_0} \right) \quad (2.18)$$

Compression index C_c is the slope of linear portion of the e - $\log \sigma'$ plot or the slope of normal compression line (NCL) and is dimensionless. This slope is obtained from any two points from the loading line which is based on below :

$$C_c = \frac{e_0 - e_1}{\log \left(\frac{\sigma'_1}{\sigma'_0} \right)} \quad (2.19)$$

The swelling index/recompression index can also be obtained from the slope of any two points at the unloading stage. Figure 2.23 shows the detail description of each parameters from the e -log σ' plot.

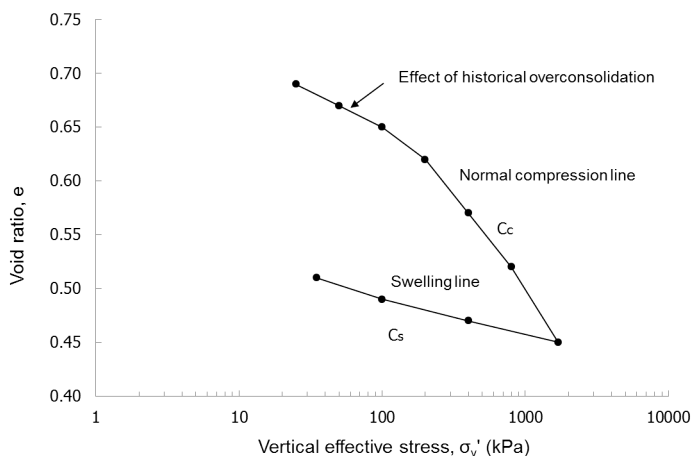


Figure 2.23: Plot of void ratio, e versus log effective stress, σ'

Coefficient of consolidation c_v , is the coefficient of consolidation for a particular pressure increment in oedometer test that can be determined by curve fitting methods. There are two methods normally used in order to estimate c_v values which are (a) logarithmic time (Casagrande's) and square root time method (Taylor's method). These empirical procedures were developed to fit approximately laboratory test data and Terzaghi's theoretical consolidation curve.

Logarithmic time method (Casagrande)

This method requires a plot of dial gauge readings in oedometer test versus the logarithm of time in minutes. It needs to follow certain procedure in order to determine the time at 50% consolidation. The procedure is described in detail as below which based on Figure 2.24.

- (a) Plot a graph of dial gauge reading (mm) versus log time (min).
- (b) Select two points on the curve where point A = t_1 and point B = $4t_1$. The difference in dial gauge between these two points is x .
- (c) Locate point C where it is located above point A at equal distance x . This point corresponds to degree of consolidation, $U = 0\%$.
- (d) Determine point D where it locates between the intersection of middle straight portion (primary consolidation line) and final straight portion (secondary compression line). This corresponds to 100% degree of consolidation ($U = 100\%$).

- (e) The distance between D_0 and D_{100} is the total amount of primary compression. In order to determine the time at 50% consolidation (t_{50}), the middle point of the total length between D_0 and D_{100} is located which equals to 50% consolidation.
- (f) Finally, the coefficient of consolidation can be calculated using the Equation 2.20 below where T_v is 0.196 and D is the half the thickness of specimen for a particular pressure increment.

$$c_v = \frac{T_v D^2}{t_{50}} \tag{2.20}$$

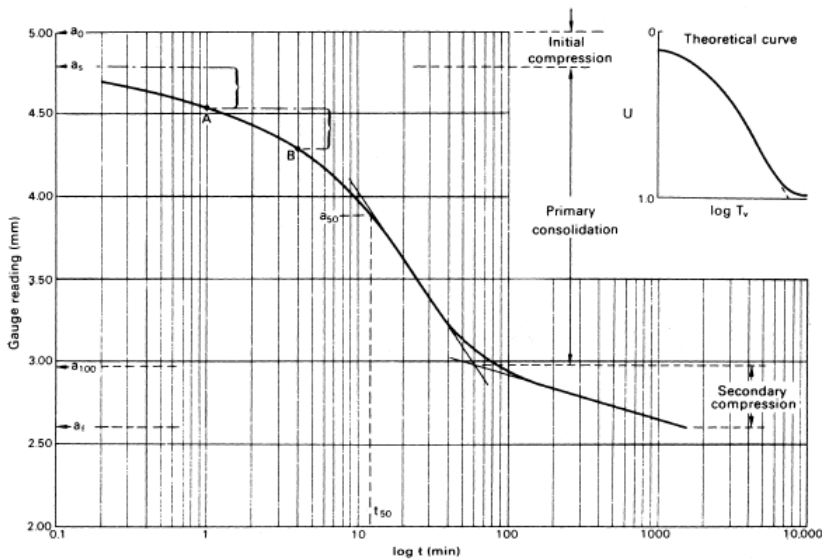


Figure 2.24: Determination of c_v by Casagrande method (Craig, 2004)

Square root of time method (Taylor) The square root time method (Taylor’s method) requires the plot of sample thickness versus square root of time as shown in Figure 2.25. The laboratory curve consists of three parts: initial compression, primary compression and secondary compression. The plot requires the time determination at 90% consolidation. The following procedure is recommended to determine the time at 90% consolidation.

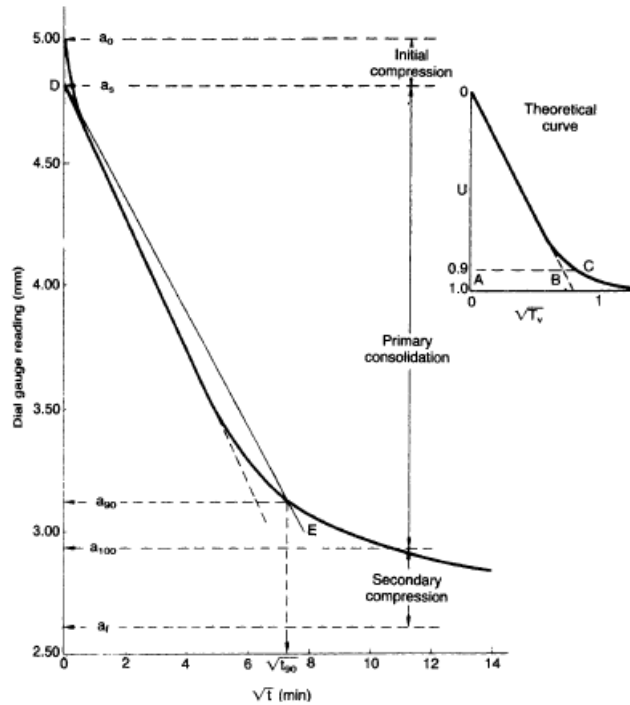


Figure 2.25: Determination of c_v by square root time method (Craig, 2004)

- Plot a graph of dial gauge reading (mm) versus log time (min).
- Extend the linear part of the curve and meet at Point D where this point is equivalent to 0% degree of consolidation ($U = 0\%$) and corresponds to initial reading D.
- Measure the distance of abscissae AB and plot another line intersecting Point D where the distance of AC = 1.15 AB.
- The intersection of line DE with the curve is called point E.
- Determine the time at point E which equivalent to square root time at 90% consolidation (t_{90}).
- Finally, the coefficient of consolidation can be calculated using the Equation 2.21 below where T_v is 0.848 and D is the half the thickness of specimen for a particular pressure increment.

$$c_v = \frac{T_v D^2}{t_{90}} \quad (2.21)$$

Preconsolidation stress (σ'_p) The preconsolidation stress is described as the highest historical stress experienced by the soil. An estimate of preconsolidation stress can be obtained from the oedometer test results. A graphical method is proposed to estimate the value of preconsolidation stress using the e - $\log \sigma'$ curve as shown in Figure 2.26 by adopting following steps:

- Locate point P where this point is located at the maximum curvature between A and B
- Draw a tangent line intersecting Point P and then draw line PQ which is parallel to the x-axis.
- Draw line PR where this line is half of the angle of QPT.
- Locate the intersection of line PR and line EC where line EC is the extension of straight portion BC.
- The intersection point which is point S is the relevant preconsolidation stress.

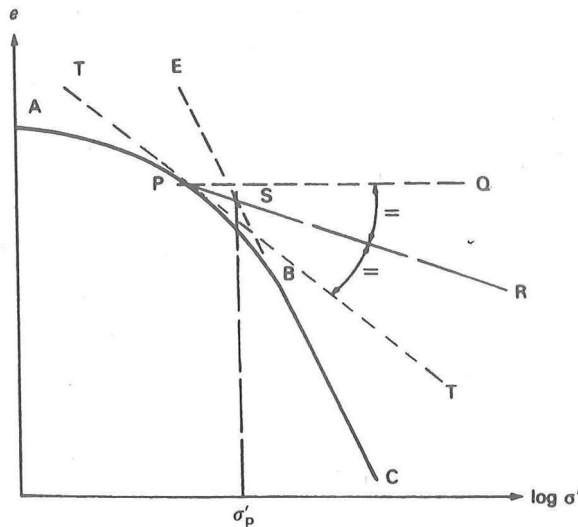


Figure 2.26: Determination of preconsolidation pressure (Whitlow, 2004)

Terzaghi theory of primary consolidation The process of consolidation involves gradual reduction of the volume of a fully saturated soil with time due to dissipation of excess pore pressures. Consider an element of soil in a consolidating layer as shown in Figure ???. The hydraulic gradient across the element given by Equation ??? where u is the excess pore pressure, A is the area flow path = $dxdy$.

$$i_z = \frac{\partial h}{\partial z} = \frac{1}{\gamma_w} \frac{\partial u}{\partial z} \quad (2.22)$$

According to Darcy's law:

$$Flow_{in} = q_{zin} = kiA = -\frac{k}{\gamma_w} \frac{\partial u}{\partial z} dx dy \quad (2.23)$$

$$Flow_{out} = q_{zout} = -\frac{k}{\gamma_w} \frac{\partial u}{\partial z} dx dy + \frac{k}{\gamma_w} \frac{\partial}{\partial z} \left(\frac{\partial u}{\partial z} \right) dx dy dz \quad (2.24)$$

The net rate of flow out of the element is therefore:

$$-\frac{\partial k}{\gamma_w} \frac{\partial}{\partial z} \left(\frac{\partial u}{\partial z} \right) dx dy dz \quad (2.25)$$

For continuity, the net rate of flow out must equal the rate of change of volume (V), i.e. dV/dt . Also, volume change is related to effective stress: $\Delta V = m_v \Delta \sigma' dy dx dz$. As the excess pore pressure dissipates, the effective stress on the soil fabric increases so that $\partial \sigma' = \partial u$

Then,

$$\frac{dV}{dt} = -m_v \frac{\partial u}{\partial t} dx dy dz \quad (2.26)$$

Equating Equations 2.25 and 2.26,

$$m_v \frac{\partial u}{\partial t} = \frac{k}{\gamma_w} \frac{\partial^2 u}{\partial z^2} \quad (2.27)$$

and defining the coefficient of consolidation either in unit $m^2/year$ or mm^2/min , etc.

$$c_v = \frac{k}{m_v \gamma_w} \quad (2.28)$$

Hence, the differential equation for one-dimensional consolidation is:

$$c_v \frac{\partial^2 u}{\partial z^2} = \frac{\partial u}{\partial t} \quad (2.29)$$

2.10.2. SECONDARY COMPRESSION BEHAVIOUR

The secondary compression or also called as creep in organic soils still developing even the excess pore water pressure has completely dissipated but continues at a gradually decreasing rate under constant effective stress. However, some researchers even reported that there is increase of strain rate during the secondary compression which is called as tertiary compression (Colleselli et al., 2000; Gokhan & Ahmet, 2003; Szymański et al., 2004; Boso & Grabe, 2013). Previous studies have shown that both primary and secondary compression can take place simultaneously. However, some researchers believed that the secondary compression is negligible during primary compression and is considered after primary consolidation is completed. This leads to two philosophies

called Hypothesis A and B. Hypotheses A separates strains induced from the dissipation of excess pore water pressures and creep and predicts that the relationship between end-of-primary (EOP) void ratio and effective stress is the same for both laboratory and field conditions. Hypothesis B assumes that creep occurs during both primary and secondary phases. Figure 2.27 shows the concept for both hypothesis in terms of vertical strain versus log time plot.

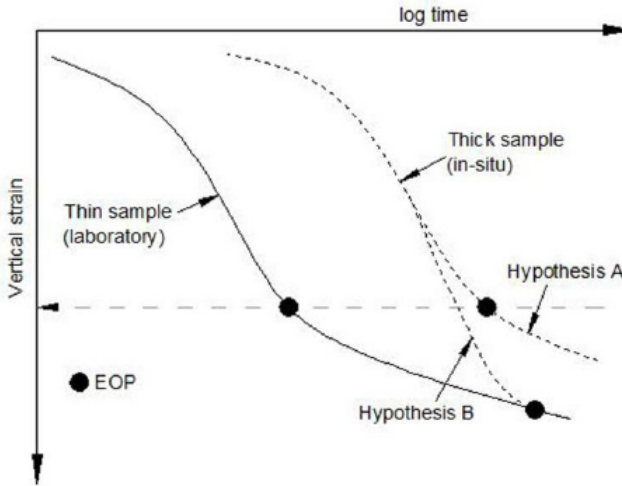


Figure 2.27: Effect of sample thickness with respect to creep hypothesis A and B (Zhang & O'Kelly, 2013)

The estimation of creep in organic soils is rather complex and there is lack of consensus on which is the best approach (Huat et al., 2014). However, in practice, the most common way to estimate the rate of secondary compression in oedometer test is based on the final part of the void ratio versus log time curve as shown in Figure 2.28. Equation 2.30 is used to estimate secondary compression in organic soils which is defined as the ratio of change on the void ratio to the change on the logarithmic of time.

$$C_{\alpha} = \frac{\Delta e}{\Delta \log t} \quad (2.30)$$

Other definitions in estimating secondary compression are also proposed in terms of linear strain (vertical strain) where

$$C_{\alpha \varepsilon} = \frac{C_{\alpha}}{1 + e_0} \quad (2.31)$$

THE SHAPE OF COMPRESSION VERSUS LOGARITHMIC OF TIME CURVE FOR ORGANIC SOILS

The compression versus logarithmic of time curves could be divided into three distinct shapes. These shapes are classified as type 1, type 2 and type 3 curves (Leonards & Girault, 1961; Gofar & Sutejo, 2007). Type 1 curve is the typical curve obtain from consoli-

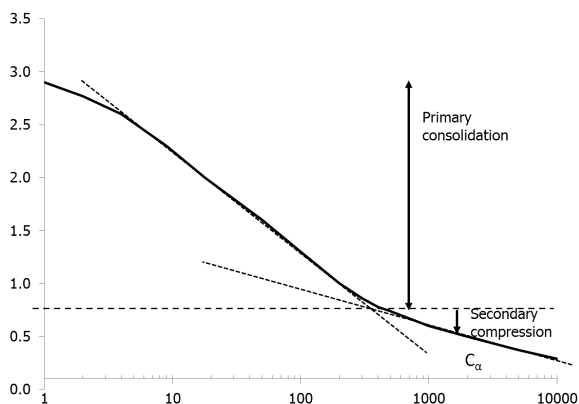


Figure 2.28: The void ratio versus log time plot for the determination of coefficient of rate of secondary compression

dation test with distinct S' shape curve and clear indication of end of primary consolidation. The secondary compression decreases linearly until soil reaching the final ultimate settlement. Type 2 curve is developed when rapid primary consolidation is occurred and secondary compression does not vary linearly with logarithmic of time. While, type 3 curve is described when there is no clear inflection point or no obvious point indicating the end of primary consolidation. The plot showing the three curves is shown in Figure 2.29.

FACTORS CONTROLLING SECONDARY COMPRESSION

(a) Consolidation Pressure

Based on previous literature, there is no exact trend when looking at the effect of consolidation pressure on secondary compression curve. Some authors reported that there is an increase or decrease in slope of the secondary compression curve. The effect of consolidation pressure on secondary compression was first reported by [Newland & Allely \(1960\)](#). They found out that C_α was almost independent of the consolidation pressure except near the preconsolidation stress where values of C_α were slightly higher. For both undisturbed and remolded organic silt, [Wahls \(1962\)](#) discovered that as the consolidation pressure increased, C_α increased rapidly to a maximum and then decreased slowly with further increase in stress. [Jonas \(1964\)](#) agreed that C_α increased with increasing consolidation pressure up to the preconsolidation stress but was constant thereafter. However, [Goldberg \(1965\)](#) proposed that after the preconsolidation pressure was reached, C_α increased almost linearly with increasing effective pressure. C_α was also found to be independent of the consolidation pressure ([Barden, 1969](#)).

[Olson \(1989\)](#) reported that C_α was maximum at a stress just after the maximum preconsolidation stress. However, lower value of C_α was obtained when applied stress was lower than the preconsolidation stress and be essentially zero for soils that were cemented. When soil is normally consolidated, C_α decreased with in-

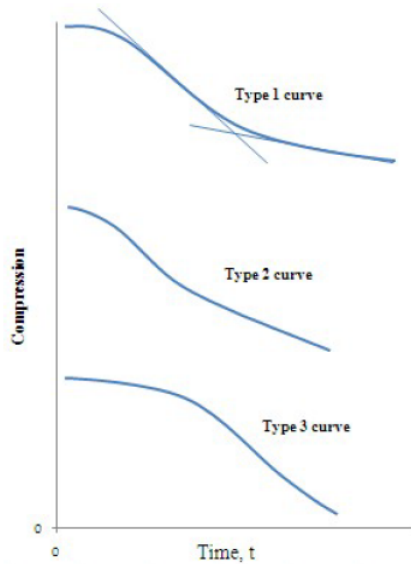


Figure 2.29: Different shapes of compression versus logarithmic of time curves derived from consolidation test (Leonards & Girault, 1961)

creasing consolidation pressure. Sensitivity of soil is also influenced the value of C_α . Quick clays for example, the C_α was very large at the point where the soil structure undergoes maximum breakdown under the applied stresses or when the state where soil has the highest compressibility as shown in Figure 2.30.

(b) Load-increment ratio

Load increment ratio (LIR) or $(\Delta P/P)$ is defined as the ratio of the difference of effective stress applied and previous effective stress over effective stress applied. In a report presented by Green (1969), several researchers reported that C_α is independent of $(\Delta P/P)$ (Newland & Allely, 1960; Leonards & Girault, 1961; Wahls, 1962) However, Leonards & Altschaeffl (1964) in Green (1969) mentioned that C_α decreases for extremely small load increment ratios. The reason for this type of behaviour was related to viscosity parameter, b as suggested by Barden (1968). He explained that b 's thixotropic nature was responsible for different amounts of secondary consolidation which dependent upon the viscosity of the pore fluid which may increase because with time dipolar water will orientate itself with the clay platelets. Small load increment may influence secondary effect significantly because of viscous effects rather than pore pressures. Meanwhile, Olson (1989) claimed that there was no apparent primary consolidation under the current load if the amount of secondary compression under the previous load exceeding the amount of primary compression in the next load (current load) or in other words, if the amount of secondary compression in the previous load become the major part of the primary compression under the next load. If there is a situation where soil experienced a major secondary compression at a certain load, the following

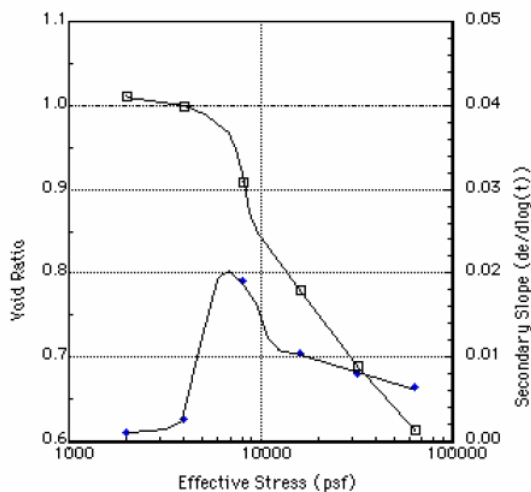


Figure 2.30: void ratios (top curve) and secondary slopes (bottom curve) for highly sensitive Leda clay from Canada (Olson, 1989)

settlement versus square root time ($S-\sqrt{t}$) curve in the next loading started out relatively flat and then slowly turned downwards into the usual linear portion. Larger amount of secondary compression in the current load also caused settlement versus square root time ($S-\sqrt{t}$) curve have a similar shape to a typical curve of settlement versus log time ($S-\log t$) curve .

(c) Temperature

There is general consensus saying that temperature rises caused increase in C_α (Gray, 1936; Lo, 1961; Hanrahan, 1954). A large change of C_α occurred when there were a slight change of temperature (Schiffman et al., 1966). The main reason for such response was due to reduction in the apparent viscosity of the contacts between particles (Green, 1969). However, Paaswell (1967) indicated that there was increase in strain in the sample which induced by temperature gradient due to the effect of movement of bulk water and not rearrangement of the internal structure. Hence, this movement is related to primary and not secondary compression. Similar conclusion was obtained from Campanella & Mitchell (1968) that the increase in temperature caused additional primary consolidation and did not affect C_α which result from increased of pore water pressures and upset the balance between structure and temperature at a particular stress level. Besides, results were obtained from Plum & Esrig (1969) which concluded that C_α changed slightly due to a change in temperature.

As most of the data reported were performed on normal consolidation cells, the temperature changes also influenced the consolidation ring as reported by Green (1969). The increase in temperature may caused extraneous effects to the consolidation ring for instance expansion of the ring which reduced the normal stress

applied stress applied on the top and between the soil and the ring) which leads to reduction in ring friction that increase the applied consolidation pressure in the soil that enhance consolidation process. Meanwhile, decreased in temperature contributed to increase ring friction and reduced the apparent rate of secondary compression.

(d) Thickness of sample

Some researchers even claimed that thickness of the sample did not influence the C_α (Newland & Allely, 1960; Barden, 1969). However, in-depth is necessary to justify this findings (Barden, 1969).

(e) Remolding

According to Gray (1936) and Taylor (1942), remolded soils showed lower value of C_α compared to undisturbed soils. Besides, remolded samples showed relatively independent of the consolidation pressure and to be less than the peak value of preconsolidation stress of undisturbed sample (Green, 1969). Figure 2.31 shows the comparison of C_α values for both undisturbed and remolded samples.

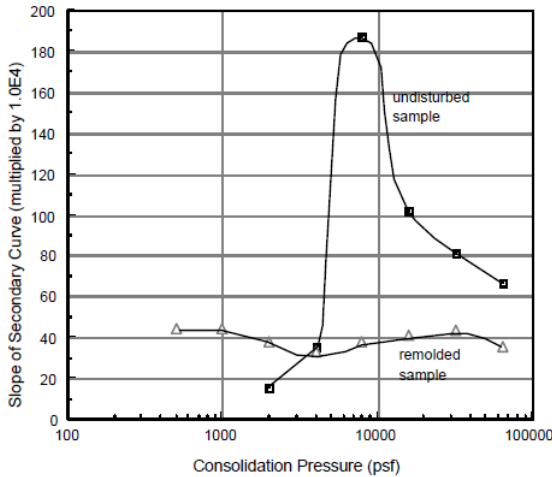


Figure 2.31: The comparison of slope of secondary compression curves for undisturbed and remolded samples at different consolidation pressures (Green, 1969)

(f) Organic matter

It has been substantiated that the presence of organic matter in the soil caused increased in C_α (Hanrahan, 1954; Barden, 1968; Schmidt, 1964; Olson, 1989). Schmidt (1964) suggested that C_α varied approximately linearly with the organic content.

(g) Disturbance

Any disturbance imposed to soil such as sudden vibration caused consolidation curve to move downwards but C_α remained constant. Some researchers even

claimed that a small amplitude of vibration in soil and repeated loading and unloading of cohesive soil increased secondary compression (Hardin & Black, 1968; Humphries & Wahls, 1968).

(h) State of stress

According to Olson (1989), C_α is lower for samples which are subjected to isotropic stresses compared to one-dimensional state of stress.

SOIL CREEP MECHANISMS

According to Taylor & Merchant (1940) and Bjerrum (1967), secondary compression or creep is defined as deformation under a constant effective stress. Until today, there are no clear consensus explaining the mechanism of creep deformation and also to predict soil settlement. Based on existing literature, the soil creep mechanisms for fine and coarsed grained soils were reported in Le et al. (2012). They described four theories justifying this mechanisms that were (a) the breakdown of interparticle bonds, (b) the jumping of bonds of molecule structures, (c) the sliding between particles, (d) water drainage from micropores to macropores and (e) the structural viscosity. Each of the mechanism is explained as follows:

(a) Creep due to breakdown of interparticle bonds

This mechanism is described based on saturated heterogeneous soil which consists of coarse grain, clayey particles (fine grain) and water. Water for this case is defined as free water which flows due to the hydraulic gradient. The secondary settlement is explained based on the transfer of stress and arrangement of soil particles which increases the effective vertical stress or contacts between particles. This effective stress is develop when total stress from porewater is transferred to the contact between particles once water flows out from the soil element due to primary consolidation. At the contact of clay particles, different types of bonding and interparticles forces are presence such as primary valence bonds between particles, van der Waals forces, hydrogen bonds, bonds by sorbed cations, attraction forces between particles with different charge, and cementation bonds. These bonds develop additional compression which are caused by creep is due to breakdown of interparticle bonds as soil shows increase in effective stress. Once the bonds are destroyed, soil particles may cause further rearrangement resulting further settlement or compression. This concept is proposed by Taylor & Merchant (1940); Terzaghi (1941); Gibson & Lo (1961); Mesri (1973, 2003); Mesri & Godlewski (1977) and Crooks et al. (1984). Some researchers even suggested that the breakdown were caused by relative movements of particles with respect to each other due to the shear displacement or change in particle spacings induced by the change in the net particle forces (Mesri, 1973).

(b) Creep due to jumping of molecule bonds

Creep mechanism is based on theory of rate process as proposed by Murayama & Shibata (1961); Mitchell (1964); Christensen & Wu (1964). This theory explains that the flow unit which referring to movement of atoms and particles, is resisted

virtual energy barriers and hence, a sufficient activated energy is required to conquer the barrier. The movement of atoms and molecules to a new equilibrium position under constant stress results to creep deformation. The flow unit in clay is the displacement of oxygen atoms within the contact surface between clay mineral particles (Kuhn & Mitchell, 1993). Low (1962) explained the concept of activation energy based on the influenced of absorbed water on the exchangeable ions (cations) movement. For example an ion (grey filled circles) is surrounded by water molecules (white filled circles) as shown in Figure 2.32 In order to move from a to b, it needs to break the bonds with all adjacent molecules in order to enable to move from one position to another. The energy requires to break the bond is known as activation energy, E_a which defined as a summation of different energies for different bonds. The creep deformation is evaluated based on the activation energy and the number of inter-particle bonds per unit area (Mitchell & Campanella, 1968)

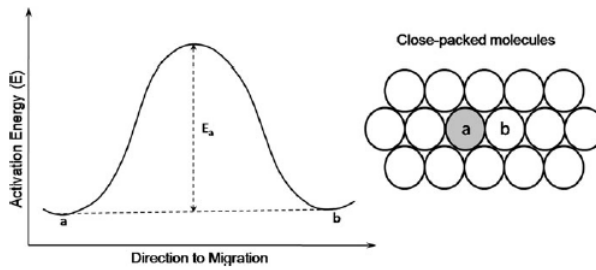


Figure 2.32: An ion surrounded by water molecules and a plot of activation energy required to move from a to b (Green, 1969)

(c) Creep due to sliding among particles

Creep was also believed due to slipping between soil grains after primary consolidation (Grim, 1962). When water content reduced during primary consolidation, the bonding forces between particles increased with the decrease in spacing between particles. The increased in bonding forces caused the increased in the frictional resistance against slipping relative to each other. Gupta (1964) described that creep was caused by the relative sliding movement of clay particles under an external pressure. However, the relative movement between the clay particles was delayed by the bonds of water molecules existing in adsorbed water layer of clay and can gradually caused the change in the orientation of soil particles.

Another concept was proposed by Kuhn & Mitchell (1993) which explained the soil creep under the effects of shear stress and temperatures. The creep compression was due to sliding movement between particles where the sliding movement was caused by the tangential component if the contact forces between soil particles, f_t . The deformation was proposed by having the relationship between sliding velocity (\dot{s}), sliding force and normal force (f_t / f_n) where f_t is the tangential component of the contact forces between particles f_n and f_n is normal force which relate to the

concept of rate process described by (Mitchell & Campanella, 1968).

- (d) Creep due to water flows in a double pore system (The double porosity)
 Another theory of creep was developed based on double porosity as suggested by De Jong & Verruijt (1965); Berry & Poskitt (1972); Zeevaart (1986); Navarro & Alonso (2001); Mitchell & Soga (2005) and Wang & Xu (2006). This theory assumes that soil structure consists of two levels structure including micro-pores and macropores. Creep is developed when there is a transfer of pore water from microstructure to macrostructure. Microstructure unit of clay consists of several single particles packed together by interparticle forces and bonds. The amount of pores produced in a microstructure as a result of an arrangement of several single particles is called micropores. Meanwhile, macrostructure of clay is formed by the aggregation of several microstructure units, and the pores between microstructure units are called macropores (Yong et al., 2010).

Different soil structure was described by Zeevaart (1986) that consists of primary and secondary structure as shown in Figure 2.33. Primary structure is consists of a continuous skeleton formed by coarsed grains and large pores of gravitational water while the secondary structure is formed by clay clusters aggregated around the primary structure. Micropores are the pores existing within clay clusters and water inside micropores which is formed by double layer water has different viscosity from water in pores within the primary structure. Creep compression is the reduction in micropore water and the relative reduction in pores in the microstructure.

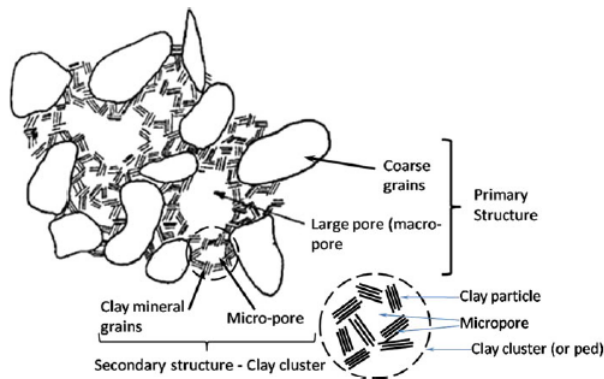


Figure 2.33: The clay structure concept diagram (Zeevaart, 1986)

The transfer of water from micropores to macropores is induced to the difference of chemical potential of water between microstructural and macrostructural water causes the mass transfer in order to reach the equilibrium state (Navarro & Alonso, 2001). Akagi (1994) suggested that the primary consolidation is based on the drainage of pore fluid in the macropores between the grains of clay particles (called 'peds'), and the creep is the due to delayed deformation of micropores within the clay particles induced by viscous flow of pore fluid existing in the

micropores.

(e) Creep due to structural viscosity

Viscosity is defined as the resistance of fluid to flow or deform under the applied pressure (Le et al., 2012). Structural viscosity of soil is defined as plastic structural resistance against compression within clay structure due to double layer surrounding the surface of clay particles (Taylor, 1942). In clay mineral particles, the internal structure contains adsorbed water that exhibit viscosity. This adsorbed water layer may induce plastic resistance against the relative movement between clay particles. The electrochemical of adsorbed water is different than normal pore water of free flowing water as it contains different cations and anions. According to Guven (1993), the microstructure of clay is formed by three types of absorbed water: (1) the water adsorbed on the internal surfaces of clay mineral, (2) the water layer held between clay minerals (double layer water) and (3) the capillary water held in pores between the clay particles. Figure 2.34 shows the schematic diagram of clay-water system explaining different types of absorbed water.

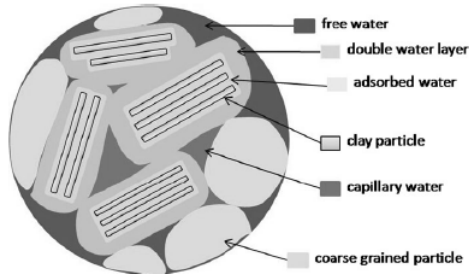


Figure 2.34: A schematic diagram showing the clay-water system (Le et al., 2012)

Creep compression is also thought as the movement of viscous water which results to deformation of clay clusters or microstructures (Le et al., 2012). The viscosity of water causing a delay in the pore water pressures dissipation that leads to delayed compression. Bjerrum (1967) used the term instant and delayed compression instead of primary and secondary compression. It was believed that the electrochemical distribution near clay particles within double layer cannot influence creep deformation. However, the physico-chemical property of pore fluid affects the creep deformation (Leonards & Girault, 1961).

Yin et al. (2002) described that creep is a combination of two different processes that are (a) viscous flow of adsorbed water in double layers on clay particles and (b) viscous adjustment of clay structure (plate structure) to reach a new equilibrium to balance with the external effective stresses. Hence, creep is mainly due to effective stress rather than free pore water flow that is controlled by hydraulic gradient. The summary of different creep mechanisms is shown in Table 2.13. Some of the mechanisms can be applied to granular and fine grained soil that focus more into clay soil.

Table 2.13: Summary of different types of creep mechanism (Le et al., 2012)

Mechanism	Main factor / focus	Published or supported by
Breakdown of interparticle bonds	Relative movement of particles, soil structure rearrangement	Taylor & Merchant (1940), Terzaghi (1941), Gibson & Lo (1961), Mesri (1973), Crooks et al. (1984)
Jumping of molecule bonds	Activate energy, temperature and deviatoric stress	Murayama & Shibata (1961), Christensen & Wu (1964), Mitchell (1964), Kwok & Bolton (2010)
Sliding particles	Activate energy, contact forces	Grim (1962), Gupta (1964), Kuhn & Mitchell (1993)
Water flows with two drainage structures (Macro-micro structures)	Two levels of soil structures, water flows in two pore structures and deformation of pores	De Jong & Verruijt (1965), Berry & Poskitt (1972), Zeevaert (1986), Navarro & Alonso (2001), Mitchell & Soga (2005), Wang & Xu (2006)
Structural viscosity	Different viscosity of absorbed water system, clay mineral-water interaction	Terzaghi (1941), Barden (1969), Bjerrum (1967) Garlanger (1972), Christie & Tonks (1985), Graham & Yin (2001)

CONCEPT C_α/C_c DURING SECONDARY COMPRESSION

Another parameters known as C_α/C_c was developed for analysis of secondary settlement. The details procedure to obtain this parameter was described in [Mesri & Castro \(1987\)](#). This concept states that the magnitude and behaviour of C_α with time is directly related to the magnitude and behaviour of C_c with effective vertical stress, σ'_v . In general, C_α remains constant, decreases or increases with time, in the range of σ'_v at which C_c remains constant, decreases or increases with σ'_v , respectively. This concept also suggests that for any given type of soil, the C_α/C_c is constant for any time, effective stress and void ratio ([Mesri & Castro, 1987](#)).

In order to explain clearly this concept, the void ratios at the end of primary consolidation (EOP) and at the end of pressure increment duration for each test stage is plotted against logarithm vertical effective stresses (e-log σ'_v). It is suggested that the C_α and C_c are evaluated graphically using the following equations:

$$C_\alpha = \frac{\Delta e}{\Delta \log t} \quad (2.32)$$

$$C_c = \frac{\Delta e}{\Delta \log \sigma'_v} \quad (2.33)$$

Based on Figure 2.35, compression curves for three different vertical effective stresses are plotted on (e-log σ'_v) chart. Besides, the void ratio versus logarithm of time, (e-log t) for each vertical effective stress is also plotted accordingly. The value of C_α at each σ'_v is obtained from the linear segment of the (e-log t) which equals to the slope of eop point to the end of secondary compression. The corresponding value of C_c at the same σ'_v is obtained from the slope passing through EOP point in the virgin loading range on (e-log σ'_v) curve. The relevant segments of C_α and C_c for each effective stress are marked with thick black line. It is well observed that, C_α increases, remains constant and decreases with time at the first, second and third σ'_v respectively. The procedure describing the selection of C_α and C_c has been described by [Graham et al. \(1983\)](#).

According to literature published, the C_α/C_c values have been obtained for soils ranging from peats, organic silts, highly sensitive clays, shales as well as granular materials. Some examples of different soils with the relevant C_α/C_c are shown in Figure 2.36. Three of four pairs of C_α and C_c values are generally sufficient to evaluate the C_α/C_c for any type of soil. Then, the relevant data pairs C_α and C_c for each effective stress are plotted in a C_α versus C_c diagram and the slope of the best fit line passing through the origin defines C_α/C_c .

Some authors have adopted this concept in their laboratory results for example [Badv & Sayadian \(2012\)](#) as deduced in Figure 2.37. The result of void ratio at eop consolidation and final void ratio for each vertical effective stress was plotted. As can be seen, the first pressure increment (25 kPa) ended near the pre-consolidation pressure. The slope of this point C_c and the corresponding C_α were determined. The secondary compression during the first effective vertical stress developed a pre-consolidation pressure where when further loading, soil developed a recompression to compression response. The final void ratio for the second increment ended near the developed pre-consolidation pressure. C_c was also increased with the increased of σ'_v . As the C_α/C_c is constant according to the

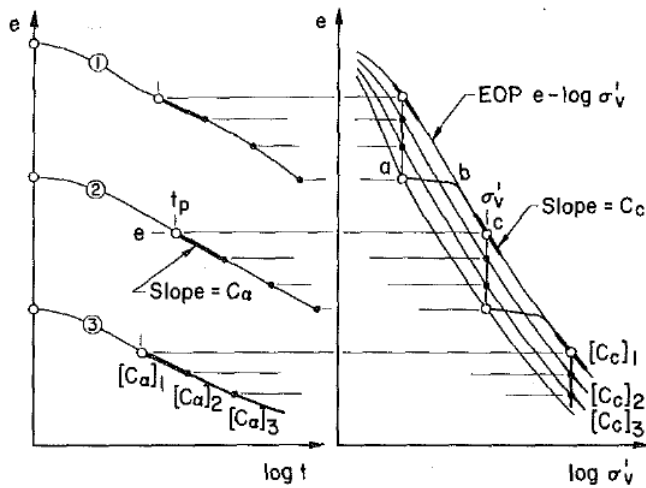


Figure 2.35: The corresponding values of C_a and C_c at three different vertical effective stresses (Mesri & Castro, 1987)

concept, C_a is also expected to increase with time. However, the two pressure increments showed different behaviour where despite the developed pre-consolidation pressure in the previous loading (100 kPa), the final void ratio at 200 kPa ended almost in the compression range where the change of C_c with σ'_v was negligible. Hence, the expected C_a is to be constant with time.

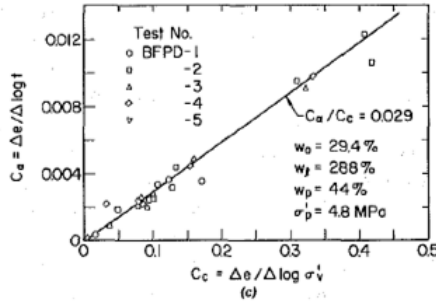
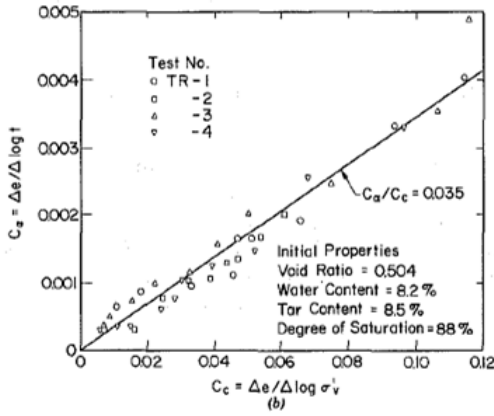
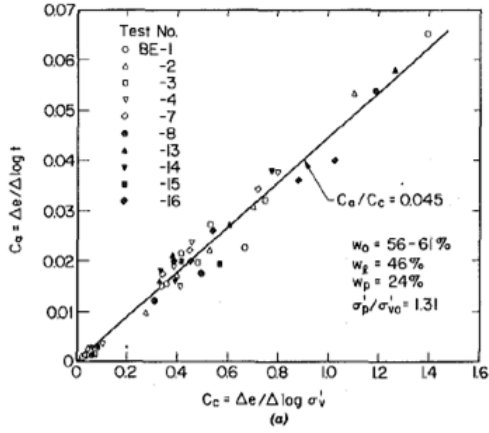


Figure 2.36: Different plots of C_α versus C_c values for different geotechnical materials (Mesri & Castro, 1987)

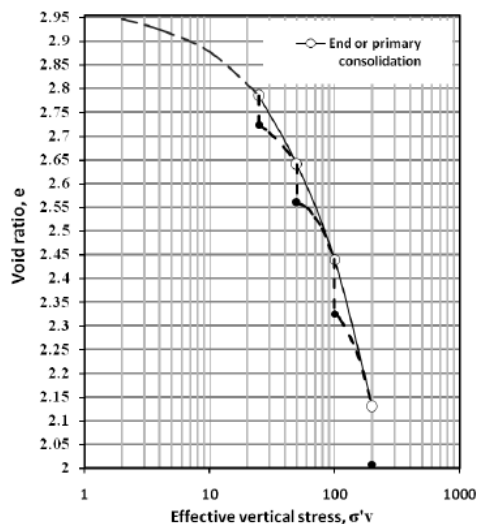


Figure 2.37: Laboratory results using the concept of C_{α}/C_c for organic soil (Badv & Sayadian, 2012)

2.10.3. TERTIARY COMPRESSION

Although it is assumed that the rate of secondary compression is constant with logarithmic of time, this is not the case for some organic soils. There is some published data regarding the increase coefficient of secondary compression (C_{α}) even in clays (Mesri & Godlewski, 1977). Tertiary compression is defined as the slope of the ε -log t after the secondary compression phase. This compression firstly reported by Dhowian & Edil (1980) on fibrous and hemic peat and later was reported extensively in Szymański et al. (2004). The tertiary compression rate uses new parameter C_{β} which introduced by Chandler & Chartress (1988). The tertiary compression rate can increase, constant or decreasing which is well defined in Figure 2.38 in terms of logarithmic strain rate versus log time scale. Tertiary compression is where the slope m decreases after the secondary phase (after constant stretch $m = 1$) in a plot of log strain rate versus log time. Tertiary compression may be related to viscous component of the soil structure which continues to deform at a constant rate (Szymański et al., 2004).

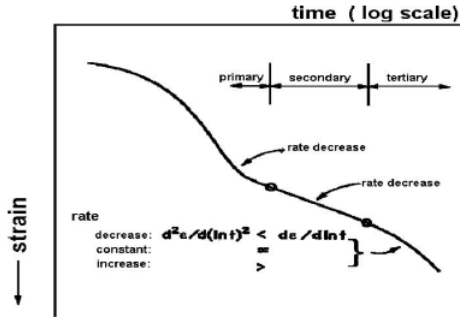


Figure 5.24 Primary, secondary and tertiary phases in oedometer compression.

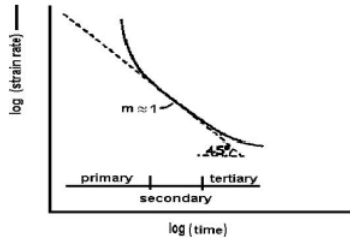


Figure 2.38: Primary, secondary and tertiary phases in oedometer compression (Huat et al., 2014)

2.11. INFLUENCE OF ORGANIC CONTENT AND DECOMPOSITION DEGREE ON PHYSICAL AND ENGINEERING PROPERTIES OF ORGANIC SOILS AND PEAT.

Organic soils and peat properties are continuously evolving as a result of decomposition of organic matter. The content of organic matter is reducing with time due to the effect of decomposition which subsequently increase the difficulties to predict the behaviour of this material. Several authors have studied the changes of physical and engineering properties of natural and reconstituted organic soils with regards to different organic content and state decomposition (Al-Khafaji, 1979; Wardwell & Nelson, 1981; Farrell et al., 1994; Nie et al., 2012; Koti Reddy et al., 2014). This section compiles the changes of organic soil selected parameters after decomposition occurs.

Nie et al. (2013) conducted various laboratory test in order to study the influence of organic content on the characteristics of peat. Different regression results were obtained for each physical properties such as density, particle density, moisture content and initial void ratio. The results are shown in Figure 2.39. The density and particle density showed almost similar trend where both properties decreased linearly with increasing organic content. Higher organic content implies that soil consists a large number of undecomposed organic material and less inorganic particles. This also closely related to specific gravity of the material (Macfarlane, 1969). Higher organic content also results to higher moisture content due fibrous open cellular structure which able to retain more water (Bell, 2000). Nie et al. (2013) mentioned that 1 % increase in organic content was equiv-

alent to an 1.5% increase in the clay content. Meanwhile, the void ratio also increase with increasing organic content due to its perforated cellular structure and a network of fibrous elements in peat soil.

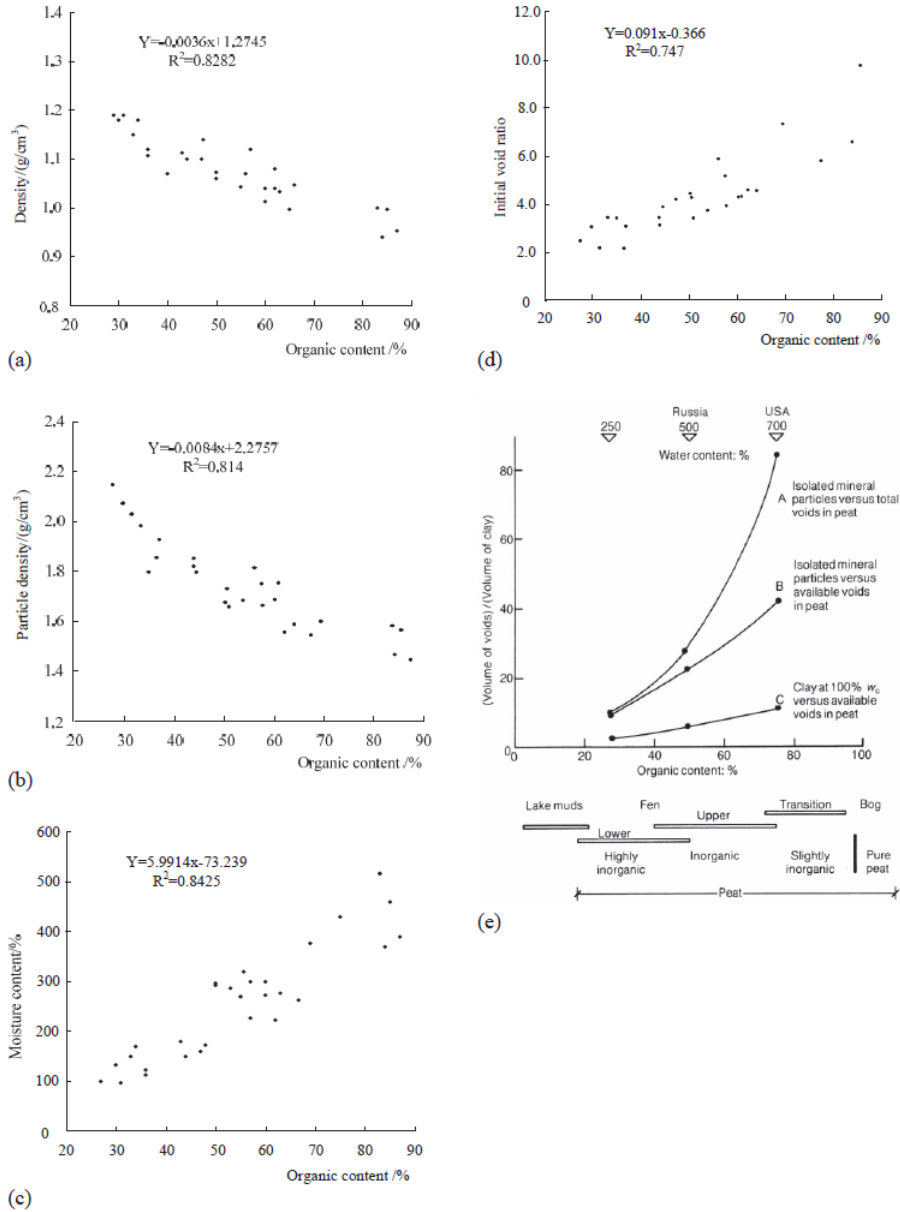


Figure 2.39: Relationships between organic content and physical properties of peat soil : (a) Density-organic content relationship, (b) Soil particle density-organic content relationship, (c) Moisture content-organic content relationship, (d) Initial void ratio-organic content relationship and (e) Void ratio-organic content for some worldwide peats (Hobbs, 1987; Nie et al., 2012)

Most plants are tabular or half-tabular shaped with a large amount of connected voids. Most of the case, stems have a 200 mm to 500 mm diameter and leaves have a

thickness of 10 mm to 15 mm and a width and length of 100 mm to 1200 mm respectively (Landva & Pheaney, 1980; Landva et al., 1983). Different organic soils and peat from different location showed that increase in organic content mostly contribute to higher void ratio and water content. Similar climatic, geographical and geomorphological conditions have the tendency for organic soils to have similar properties (Nie et al., 2012).

Oedometer tests were conducted to study the effect of organic content on the compressibility behaviour of peat soil (Nie et al., 2012). The results are tabulated in Table 2.15. The results deduced that increased in organic content contributed to higher compressibility coefficient, m_v . However, the consolidation coefficient, c_v and density decreased with increasing organic content while the compression index and rebound index showed increasing values as organic content increased.

Table 2.14: Physical properties of peat samples consisting different organic content (Nie et al., 2012)

Sample number	Organic content (%)	Fibre content (%)	Degree of decomposition	pH	Density (g/cm ³)	Moisture content (%)	Particle density (g/cm ³)	Void ratio
1	36.34	54.43	H ₅	5.81	1.122	117.01	1.924	2.17
2	43.65	63.98	H ₄	5.75	1.145	142.65	1.920	3.46
3	55.99	56.77	H ₅	5.33	1.045	272.24	1.887	5.91
4	69.29	59.10	H ₅	5.56	1.010	385.00	1.690	7.36
5	85.36	49.51	H ₆	5.30	0.944	467.55	1.658	9.82

Table 2.15: Consolidation properties of peat samples consisting different organic content (Nie et al., 2012)

sample number	Settlement (mm)	Initial void ratio	Final void ratio	Compressibility coefficient, m_v (M/Pa)	Consolidation coefficient, c_v 10 ⁻⁵ cm ² s ⁻¹	Compressibility index, C_c	Rebound index, C_r
1	84	2.17	1.19	1.91	2.45	0.59	0.12
2	102	3.08	1.51	5.71	2.00	1.24	0.18
3	125	5.91	2.89	7.74	1.58	1.48	0.19
4	149	7.36	6.44	10.90	1.07	2.01	0.32
5	170	9.82	5.43	15.65	0.98	2.61	0.31

The vertical and horizontal permeabilities results are plotted as shown in Figure 2.40 for the same peat samples with varying organic contents. The results showed an increase in permeability values with increasing organic content. Furthermore, higher consolidation pressures resulted to lower permeability values. Under microscopic view, small size of organic particles was produced compared with other clay mineral particles. With rounded shape and loose molecule structure (flocculent structure), micropores were developed with chain-linked aggregates. When the organic content increased, the organic matter accumulated and bonded around soil particles. This, to some extent, blocked the flow of moisture between soil particles and subsequently affected the permeability of the peat soil (Nie et al., 2012). However, increase in humification degree contributes to lower permeability. The hydraulic anisotropy was also studied by Nie et al. (2012) where the results showed that the horizontal component had higher permeability compared to vertical component. However, Macfarlane (1969) indicated that for the same organic content, the horizontal component of the permeability was less than vertical component. This was due to the orientation of the plant cellulose in the peat soil in its formation process.

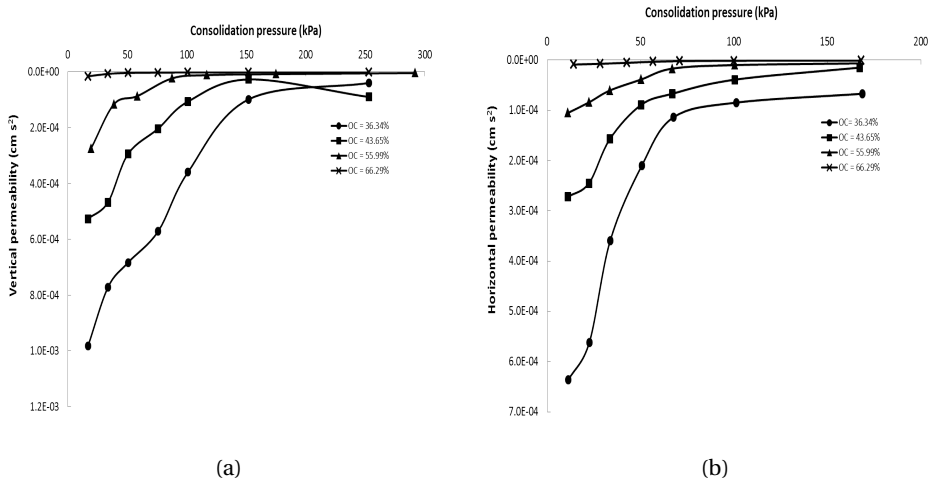


Figure 2.40: Relationships of a)vertical permeability and b)horizontal permeability coefficients and organic content of peat soils (Nie et al., 2013)

Consolidation properties of organic soils from different studies are tabulated by [Koti Reddy et al. \(2014\)](#) as shown in Table 2.16. From the data, it was observed that the void ratio, compression index (C_c) and C_α/C_c values increased with increasing organic content. These parameters were also compared with other types of soil.

Table 2.16: Summary of consolidation parameters at different amount of organic content in comparison with other typical soils (Koti Reddy et al., 2014)

Type of soil	OC (%)	Void ratio	C_c	C_a/C_c	c_v	k_v	Reference
Celery bog (highly organic soil)	40 to 60	4.30 to 5.50	2.00 to 2.50	0.095	9.20×10^{-5} to 5.00×10^{-8}	2.10×10^{-7} to 6.66×10^{-11}	Santagata et al. (2008)
Howrah (OH/organic soil)	25 to 28	2.00 to 2.10	0.85 to 0.91	0.051	2.17×10^{-7} to 5.96×10^{-8}	1.82×10^{-9} to 6.17×10^{-11}	Present study
Jadavpur (CH/mineral soil with organics)	12 to 14	1.24 to 1.41	0.62 to 0.65	0.038	1.78×10^{-7} to 2.50×10^{-8}	8.18×10^{-10} to 3.23×10^{-11}	Present study
Boston blue clay (mineral soil)	0	1.15 to 1.20	0.30 to 0.35	0.030	1.20×10^{-7} to 2.50×10^{-8}	2.50×10^{-10} to 5.50×10^{-10}	Force (1998)
General range of consolidation parameters							
Mineral soil	-	-	0.10 to 0.50	0.03 to 0.05	10^{-8} to 10^{-7}	10^{-12} to 10^{-8}	
Soft clay	-	-	0.20 to 0.90	0.04 to 0.06	10^{-9} to 10^{-5}	10^{-11} to 10^{-5}	
Peat	-	-	0.80 to 1.50	0.065 to 0.10	10^{-6} to 10^{-4}	10^{-8} to 10^{-5}	

Another study was also performed by Farrell et al. (1994) looking at the changes in mechanical properties of soils with variation in organic content. The soils tested were predominantly from Fen type bogs. The organic content values were plotted on a organic content versus liquid limit chart as shown in Figure 2.41. The results showed that most organic content had strong correlations with correlation proposed by Miyakawa (1960). The coefficient of consolidation, c_v versus effective stress, σ' plot for soils at different organic content produced by McGeever (1987) and reported by Farrell et al. (1994) is shown in Figure 2.42. There was a significant decrease in the c_v of the undisturbed sample with an increase in effective stress above the apparent preconsolidation pressure, ρ'_c which was obvious for sample that had high organic content. The c_v values were obtained using square root method as the log time method unable to give a clear S shape curve.

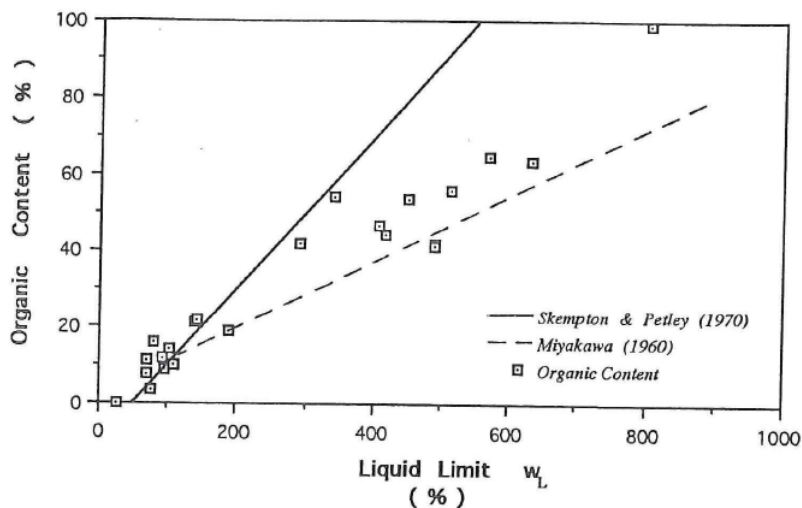


Figure 2.41: Organic content versus liquid limit chart (Farrell et al., 1994)

Another plot showing c_v versus organic content was also reported by Farrell et al. (1994) for undisturbed and disturbed samples where undisturbed sample showed an increase in c_v with increasing in organic content while artificial sample showed the opposite trend. This was pertaining to structure, gas content and other natural factors that was lost during remoulding. Badv & Sayadian (2012) performed a study on peat samples having organic content ranging from 25 % to 77 %. A plot showing different percentage of organic content versus specific gravity was plotted and the results were compared with other published data as shown in Figure 2.43 respectively. The result showed that specific gravity increased with increasing organic content. A correlation was proposed by Badv & Sayadian (2012) as shown in Equation 2.34 to estimate the amount of organic matter.

$$OC = (290.8/G_s) - 107.7 \quad (2.34)$$

Figure 2.44 shows the relationship between initial void ratio and organic content for different peats obtained from Badv & Sayadian (2012); Long (2005); Mesri & Ajlouni (2007); Mesri et al. (1997); Fox et al. (1992). There is a wide scattered data obtained from previous literature although peats have the same organic content. Badv & Sayadian (2012) showed that peats having identical organic content can have different initial void ratio as a result of different preconsolidation pressures and durations (Badv & Sayadian, 2012).

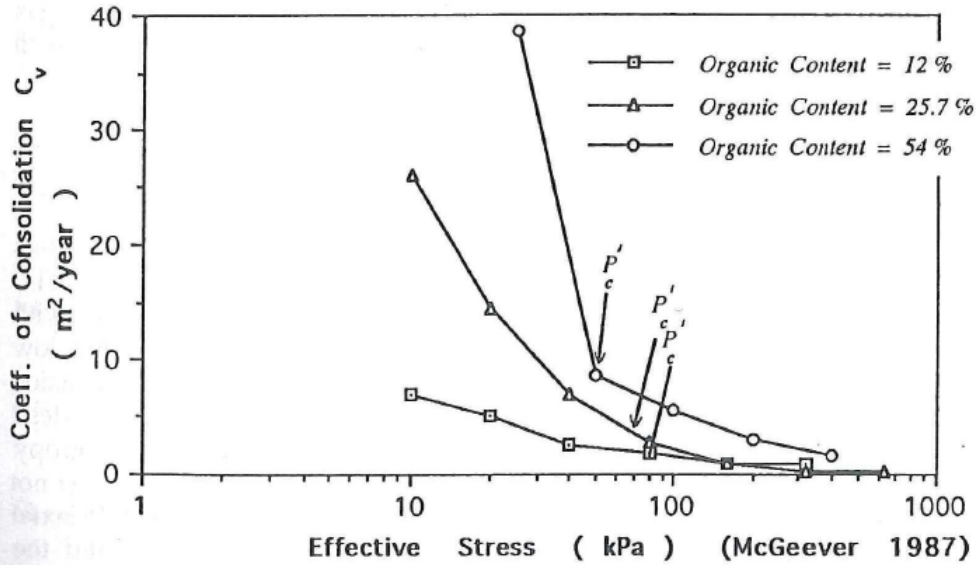


Figure 2.42: Coefficient of consolidation versus organic content for undisturbed and artificial samples (Farrell et al., 1994)

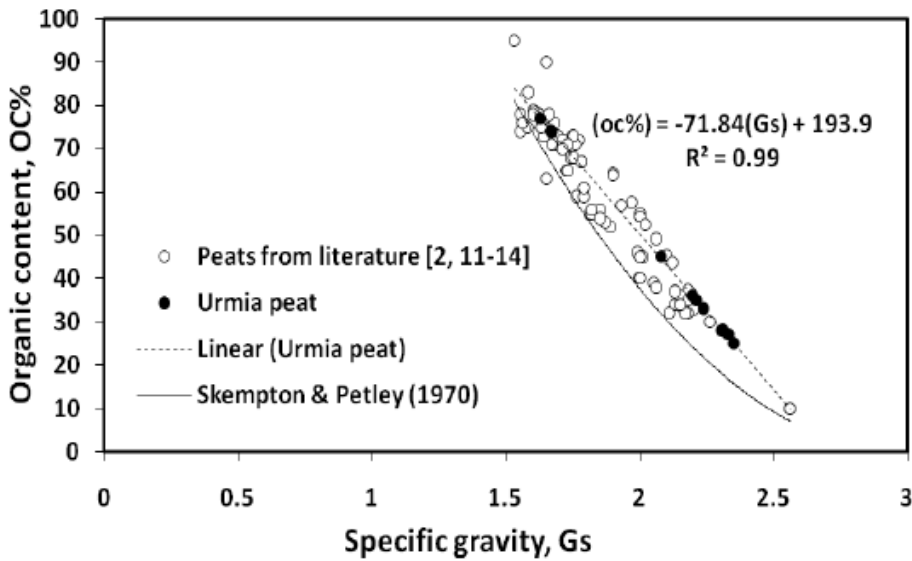


Figure 2.43: The change of organic content and specific gravity from different types of peat (Badv & Sayadian, 2012)

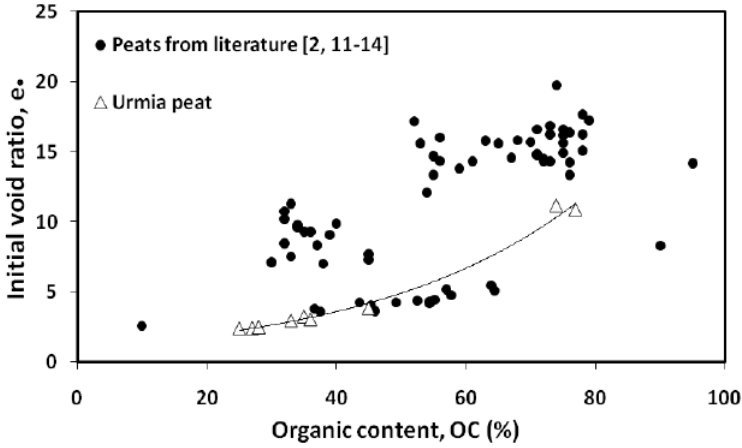


Figure 2.44: Different values of initial void ratio plotted against varying organic content (Badv & Sayadian, 2012)

The results were also plotted in terms of coefficient of consolidation c_v and coefficient of volume compressibility m_v with respect to vertical effective stress. They suggested that higher c_v value observed at low effective vertical stress was from preconsolidated sample whereas m_v values increased with increasing organic content. Significant decreased in m_v values with increasing effective vertical stress were observed for sample having the highest organic content. The findings are presented in Figure 2.45.

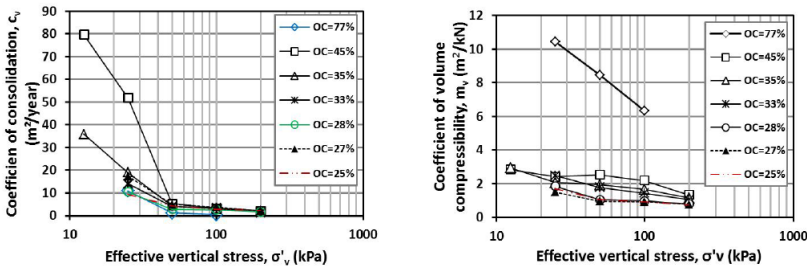


Figure 2.45: The influence of organic content towards coefficient of consolidation and coefficient of volume compressibility with vertical effective stress (Badv & Sayadian, 2012)

The average value of coefficient of vertical permeability, k_v for each vertical effective stress and its relation with average void ratio for the particular step is shown in Figure 2.46. It can be substantiated that the k_v values for all tested samples decreased significantly (less permeable) when the applied pressure increased from 25 kPa to 200 kPa (for peat having OC = 77 %, pressure was from 25 kPa to 100 kPa). A new parameter known as permeability change index, C_k was used to describe the decrease in permeability with the decrease in void ratio. It was based on the slope of e -log k_v curve. The results showed that the C_k increased with increasing organic content.

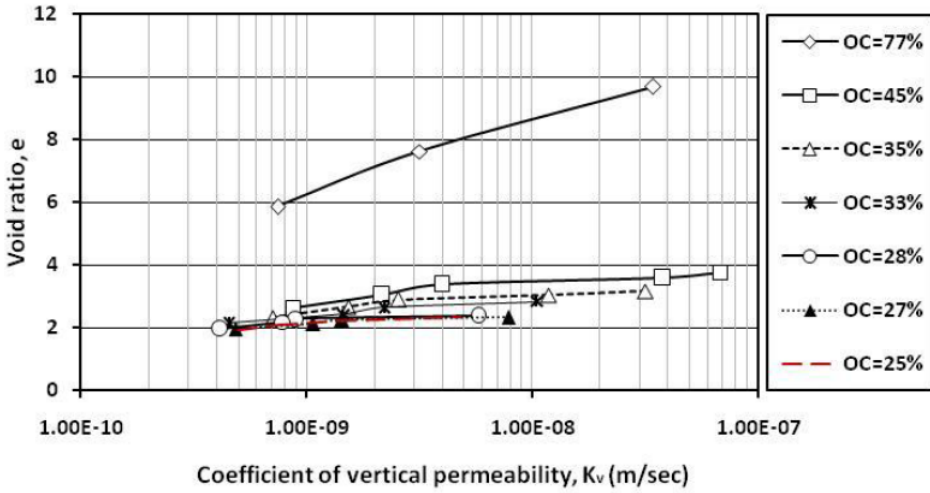


Figure 2.46: Relationship between void ratio and coefficient of vertical permeability for different peat sample having different organic content (Badv & Sayadian, 2012)

The value of compression index, C_c in the normal consolidation region and swelling index, C_s in the swelling region were also obtained from the slopes of the compression and swelling curves of $e - \log \sigma'_v$ as shown in Figure 2.48. Two types of plot were produced where figure on the (left) used the final void ratio for each loading step while figure on the (right) used the final void ratio at end of primary consolidation (eop) that was determined by log time method. It was observed that the slope the C_c and C_s values increased with increasing organic content and the value of C_c obtained from the figure (right) was slightly higher. Higher value of C_c is more conservative and is normally used in correlations (Mesri et al., 1997; Badv & Sayadian, 2012).

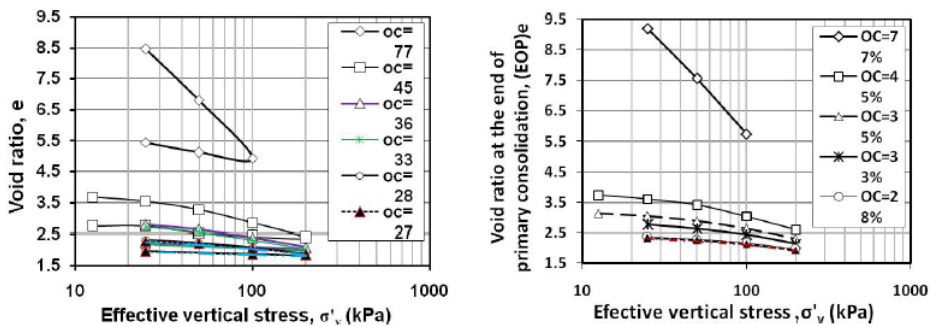


Figure 2.47: Changes of void ratio with vertical effective stress during compression and swelling (left) and changes of void ratio at the end of primary consolidation versus vertical effective stress(right) for peat having different organic contents (Badv & Sayadian, 2012)

The variation of secondary compression index, C_α immediately beyond the transition from primary to secondary compression against the vertical effective vertical stress is shown in Figure 2.48. For a constant value of σ'_v , the value of C_α increased with σ'_v and the slope of the curve increased with increasing amount of organic content (Badv & Sayadian, 2012).

A review on the effect of degree of decomposition on the changes of compressibility behaviour of peat at different organic content was also reported by O'Kelly & Pichan (2013). It was believed that the the compressibility of peat reduces with increasing degree of decomposition (Hobbs, 1986; Price et al., 2005). Figure 2.49 shows the relationship between the change of volume compressibility coefficient against degree of humification (von Post number). Stiffer response (drop value of m_v) was observed with increasing von Post number. This was significant from H_1 to H_4 .

Another plot in Figure 2.50 shows the void ratio versus effective vertical stress for different soils having high degree of decomposition(amorphous) and low degree of decomposition(fibrous). The reduction of void ratio for a given effective stress level(creep) is significantly lower for amorphous peat compared to fibrous peat. Meanwhile Figure 2.51 shows the initial void ratio versus compression index for three types of peat that are fen, transitional and bog peats. Fen peat is alkaline is more likely to decompose which gives lower initial void ratio and compression index compared to least decomposed acidic peats.

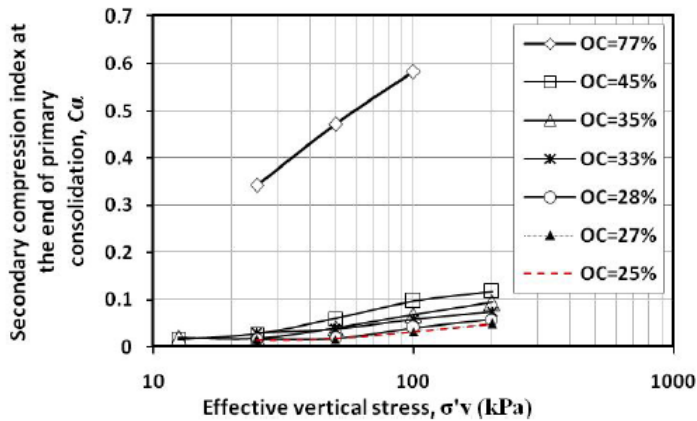


Figure 2.48: Changes of secondary compression index, C_α values with vertical effective stress, σ'_v for peat having different organic contents (Badv & Sayadian, 2012)

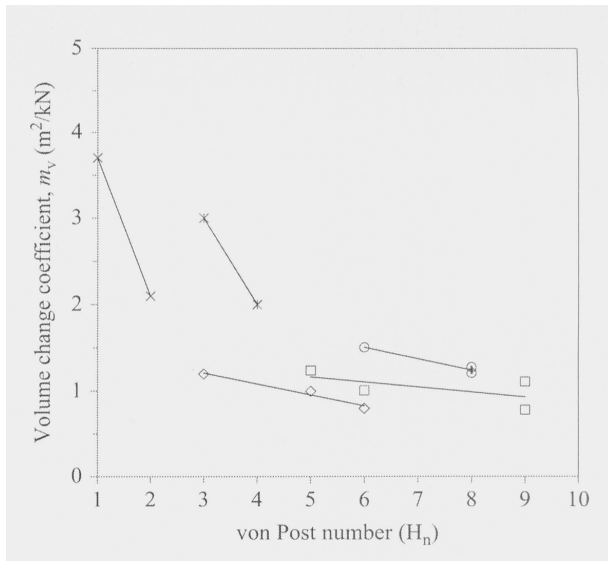


Figure 2.49: Compressibility of peats at different degree of decomposition (O’Kelly & Pichan, 2013)

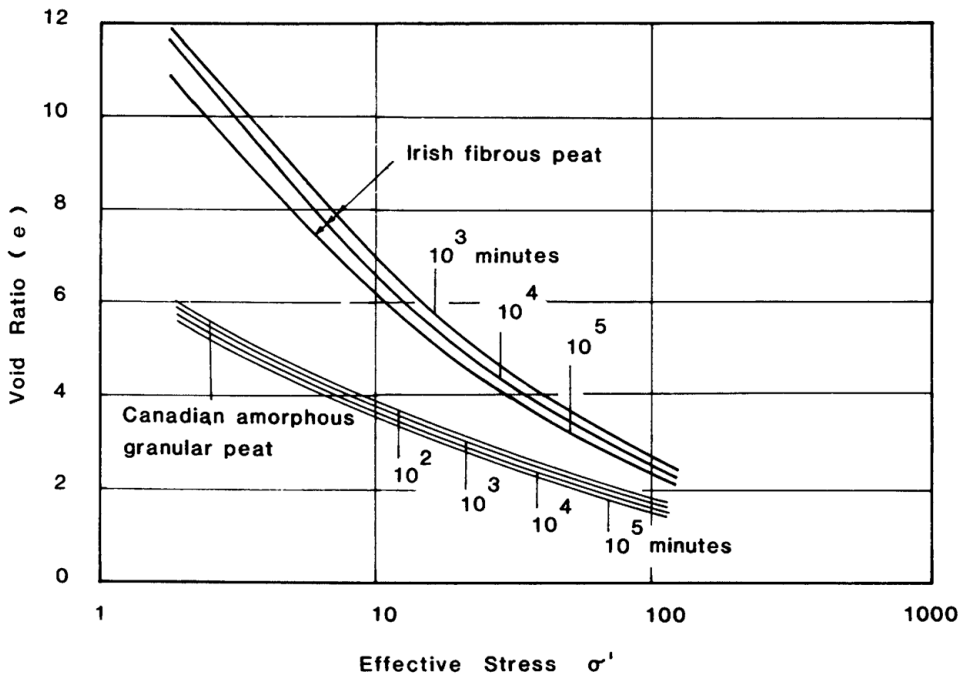


Figure 2.50: Void ratio-effective stress relationships for fibrous and amorphous peat (O’Kelly & Pichan, 2013)

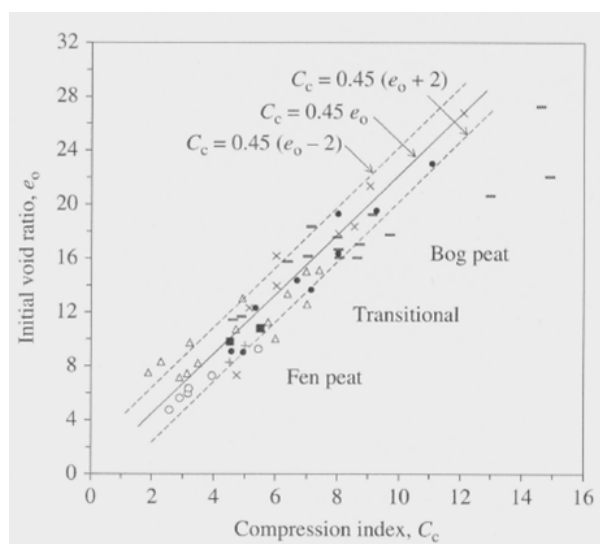


Figure 2.51: Void ratio against compression index for peats of different origin (O'Kelly & Pichan, 2013)

This is supported by the findings by Duraisamy et al. (2007) where they compared the compressibility parameters for tropical peat at different states of decomposition as shown in Table 2.17. The results showed that decreasing values of compression index, compression ratio, coefficient of secondary compression and settlement were observed from fibric to sapric peat using both oedometer and Rowe cell consolidation apparatus. However, the C_a/C_c values determined by oedometer were the same for all the samples but using Rowe cell, the C_a/C_c values were lower which was outside the typical range.

Table 2.17: Summary of consolidation results for tropical peat at different degree of decomposition (Duraisamy et al., 2007)

Type	Test Type	Compression index C_c	Compression ratio $C_c/1+e_0$	Coefficient of secondary compression C_a	Law of compressibility C_a/C_c	Predicted consolidation settlements (m)
Fibric	Rowe Cell	2.752	0.422	0.0608	0.0283	2.32
Hemic	Rowe cell	2.165	0.253	0.0585	0.0356	1.82
Sapric	Rowe cell	1.935	0.217	0.0544	0.038	1.63
Fibric	Oedometer	2.332	0.358	0.0637	0.027	1.97
Hemic	Oedometer	2.035	0.238	0.0553	0.027	1.72

Physical properties of the same peat are shown in Table 2.18. Generally, fibric peat has higher water content, void ratio, fibre content and liquid limit followed by hemic and sapric. However, reducing values of specific gravity, dry density and bulk density are observed from fibric to sapric peat. Although the fibre content is reduced due to decomposition, the organic content does not directly affect the organic content. It is stated that peats having the same organic content can possibly have different fibre content in nature (Colleselli et al., 2000). This is clearly shown by the settlement against time plot for Adria-1, Andria-2 and Correzzola peats with respective organic and fibre contents as shown in Figure 2.52. The results showed that peat with higher fibre content (Andria-2) had greater tertiary compression after $\times 10^4$ minutes compared to Adria-1 although the

both soils had the same organic content. However, Andria-1 and Correzzola samples showed a curve with clear primary consolidation and secondary compression components. It is expected that higher degree of decomposition will reduce the secondary and tertiary compression (Colleselli et al., 2000).

Table 2.18: Summary of physical properties results for tropical peat at different degree of decomposition (Duraismy et al., 2007)

Peat type	Water content (%)	Liquid limit (%)	Organic content (%)	von Post scale	Fibre content (%)	Specific gravity	Void ratio	Dry density (Mg/m ³)	Bulk density (Mg/m ³)
Fibric	330	350	84	H_4	75	1.45	9.535	0.147	0.834
Fibric	350	398	88	H_4	77	1.42	10.48	0.136	0.811
Fibric	286	310	77	H_5	68	1.51	7.895	0.17	0.956
Hemic	266	285	76	H_5	65	1.52	7.541	0.17	0.922
Hemic	181	250	73	H_7	55	1.55	5.522	0.238	1.008
Hemic	241	275	75	H_6	58	1.53	6.536	0.192	0.856
Sapric	140	240	70	H_6	32	1.56	4.125	0.283	1.019
Sapric	300	330	80	H_6	31	1.49	4.824	0.249	0.996

The influence of peat types on consolidation behaviour was also investigated (Dhowian & Edil, 1980). Different peat samples at different degree of decomposition were subjected to consolidation pressures ranging from 25-400 kPa where each pressure was allowed to compress the soil for 20 days. The results of instantaneous and primary strains, rate of secondary and tertiary compression were plotted in terms of consolidation pressure as illustrated in Figure 2.53. The results indicated that both strains ($\epsilon_i + \epsilon_p$) were high at the beginning of consolidation pressure and subsequently dropped to an average strain of 2.2%. The rate of secondary compression α_1 was higher for fibrous peat compared to amorphous peat

Meanwhile, the rate of tertiary compression, α_2 decreased linearly for fibrous peats with increasing consolidation pressure but for amorphous peat, constant value of α_2 was obtained. Besides, the α_2 value at a certain consolidation pressure was obviously higher for fibrous peat compared to amorphous peat but later, both samples had equal α_2 values when reaching 400 kPa consolidation pressure. Lower magnitude and rate of compression was expected for amorphous peat. The change of void ratio was more influential factor controlling the rate of compression in fibrous peat compared to the difference in fibre content. The results are shown in Figure 2.54 which indicated that a linear increase in α_1 with increasing void ratio. The rate of tertiary compression, α_2 versus void ratio at the beginning of each pressure increment is shown in Figure 2.55. Fibrous peats showed a linear increase in α_2 as a function of void ratio, whereas α_2 does not vary with void ratio for amorphous granular peats.

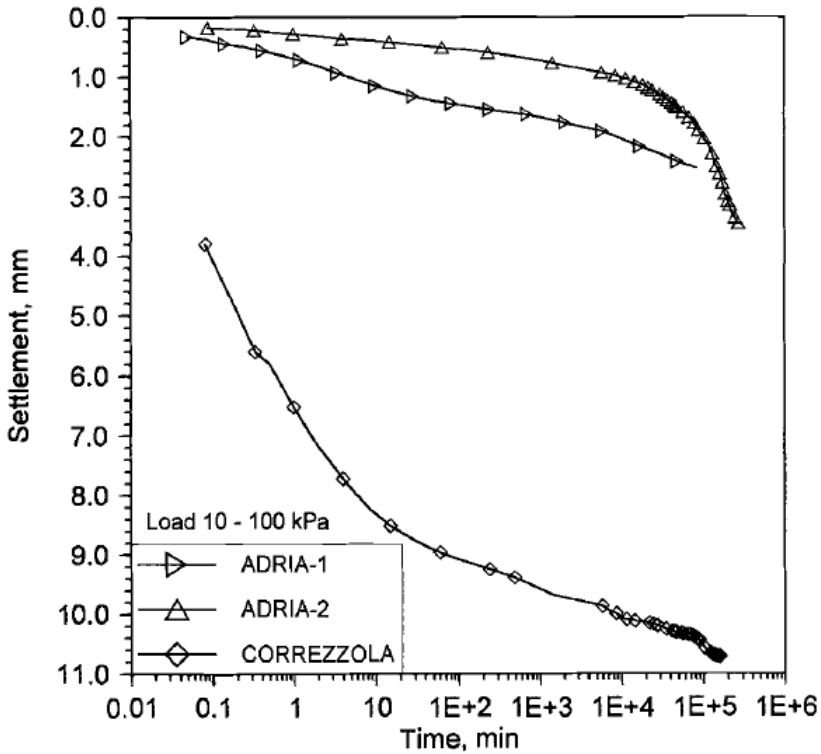


Figure 2.52: Settlement against time response for three Italian peats having different degree of decomposition (Colleselli et al., 2000)

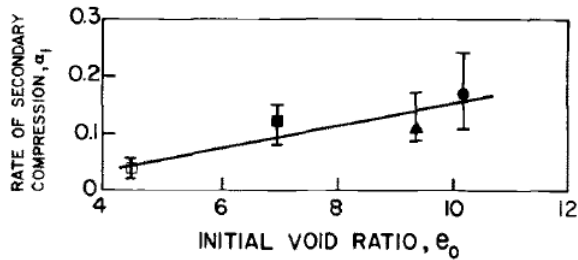


Figure 2.54: Rate of secondary compression versus initial void ratio for four different peats at different degree of decomposition (Dhowian & Edil, 1980)

The beginning time of tertiary compression t_k with consolidation pressure are shown in Figure 2.56 where it can be concluded that the variation of t_k with respect to type of peats and the initial void ratio (or water content) seemed insignificant and without any consistent trend after the first stress increment.

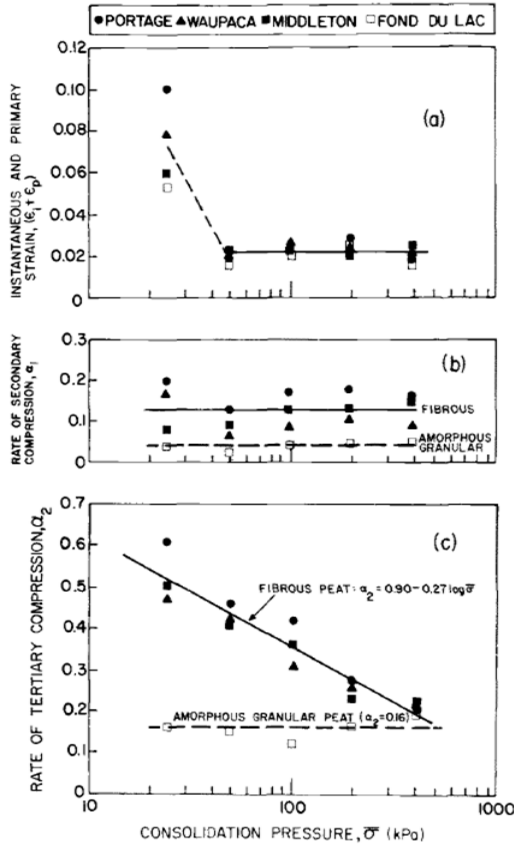


Figure 2.53: Compression parameters versus consolidation stress for four different peats at different degree of decomposition (Dhowian & Edil, 1980)

The compression characteristics of the four peat samples are compared in Figure 2.57 in terms of void ratio versus logarithm of stress e - $\log \sigma'_v$ curves. The fibrous peats had high compression indices as well as two-segments virgin compression curves. Meanwhile, amorphous granular peat was distinctly different in its e - $\log \sigma'_v$ response than the fibrous peats in terms of initial void ratio as well as its compression index being much lower than those of the fibrous peats. Furthermore, the virgin curve obtained consisted of a single straight line similar to the ones observed in inorganic soils.

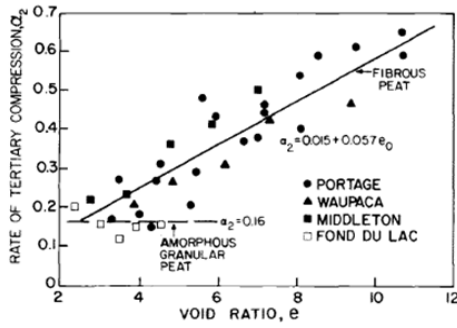


Figure 2.55: Rate of tertiary compression versus void ratio for four different peats at different degree of decomposition (Dhowian & Edil, 1980)

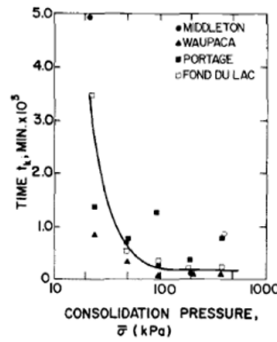


Figure 2.56: Tertiary compression starting time versus consolidation pressure for four different peats at different degree of decomposition (Dhowian & Edil, 1980)

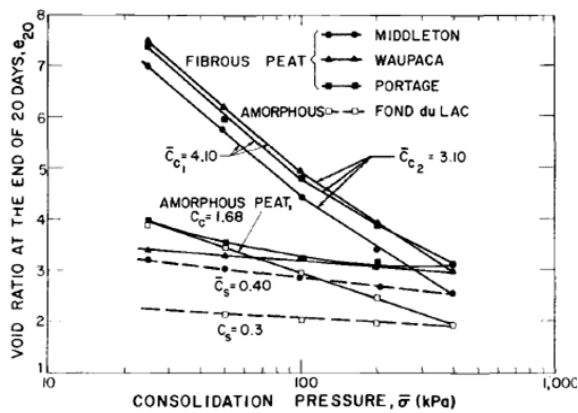


Figure 2.57: Void ratio versus logarithm of stress curves for four different peats at different degree of decomposition (Dhowian & Edil, 1980)

2.12. LITERATURE REVIEW ON STIMULATED DECOMPOSITION ON PHYSICAL AND ENGINEERING PROPERTIES

The effect of decomposition process on physical and engineering properties of organic soils and peats are not widely understood by engineers. There are limited data discussing the changes of engineering design parameters once decomposition occurred in these soils. Understanding this issues is of great importance as accelerated decomposition may cause unexpected settlement in building structures and foundation. A review on how this process influences the properties of organic soils and peat will be discussed explicitly. Currently, there are several studies discussing the engineering properties of these soils at different state of decomposition. However, the engineering properties that will be incorporated here is the compressibility properties and not strength properties under the influence of decomposition. For this reason, the changes on strength parameters will not be reviewed. An overview of the state of art of this research is discussed in this Section.

The research on decomposition and compressibility in organic soils and peat has been investigated by several authors (Khattak, 1978; Al-Khafaji & Andersland, 1981; Wardwell et al., 1983; Elsayed et al., 2011; Pichan & O'Kelly, 2012; McDougall et al., 2004; Wardwell & Nelson, 1981). The first study was conducted by Khattak (1978) on fibrous organic soils which was part of his unpublished PhD thesis and later, Al-Khafaji (1979) extended the work of Khattak (1978) looking at decomposition effects on engineering properties of fibrous organic soils. This was also part of his unpublished PhD thesis. Then, Al-Khafaji & Andersland (1981) published his work using some results obtained from Khattak (1978) and Al-Khafaji (1979) looking at artificially fibre clay soils which were prepared at different proportions of kaolinite and pulp fibre content. The decomposition was stimulated or accelerated by adding carbon source (pulp fibre), nitrogen source (ammonium chloride) and 1 % of a municipal sludge as seed sources to promote anaerobic decomposition. The amount of nutrients added were based on empirical formulation $C_5H_7O_2N$. One Dimensional(1-D) compression tests were performed on samples without nutrients with pressure ranging from 122 kN/m^2 to 35 MN/m^2 and for samples with nutrients, smaller consolidation loads were applied starting from 0.47, 1.14, 2.28 and 3.42 kN/m^2 . Anaerobic decomposition was stimulated by adding ammonium chloride to reach optimum condition of C:N and stored about 35°C before each series of consolidation testing. All decomposed samples were stored for 1, 3 and 5 weeks respectively. Results obtained from the studies of Khattak (1978) and Al-Khafaji (1979) that were published in Al-Khafaji & Andersland (1981) showed that the settlement of fibrous organic soils decreased with increasing decomposition under constant loading of 3.42 kN/m^2 . The same trend was observed for all the samples having different initial organic fraction. This is clearly shown in Figure 2.58.

Meanwhile, the coefficient of consolidation, c_v for original sample (no decomposition) at different initial organic content is plotted in Figure 2.59. It was observed that the c_v increased as organic content increases. However, c_v values decreased when consolidation pressures increased. At low organic content, the influence of consolidation pressures on c_v values was less significant. At high organic content, consolidation pressures influenced the c_v values significantly. They concluded that higher c_v values corre-

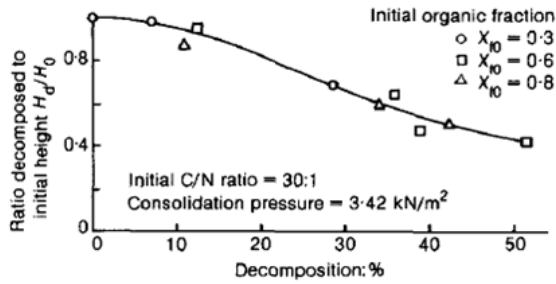


Figure 2.58: Ratio of decomposed sample height to initial sample height against percentage of decomposition (Al-Khafaji & Andersland, 1981)

sponded to larger fibre(organic) contents and to lower stress levels (Al-Khafaji & Andersland, 1981).

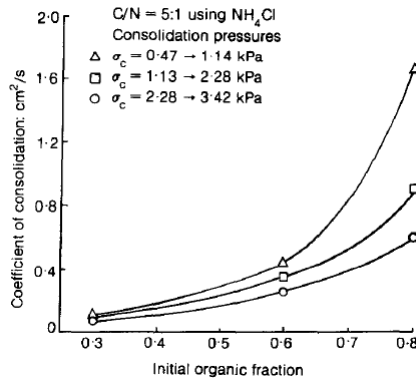


Figure 2.59: Coefficient of consolidation for original sample without decomposition at different organic content which subjected to different consolidation pressures (Al-Khafaji & Andersland, 1981)

As samples was allowed to decomposed anaerobically at different incubation periods. Al-Khafaji & Andersland (1981) presented the the results of c_v values for each duration for one of the samples having initial organic fraction 60 %. The results are shown in Figure 2.60. It was observed that the c_v values decreased as decomposition occurred for both consolidation pressures. Higher consolidation pressures resulted to lower c_v values.

The relationship between the organic fraction, void ratio and consolidation pressures for reconstituted soil samples were also plotted by Al-Khafaji & Andersland (1981) as shown in Figure 2.61. From the plot, it was observed that as organic content increased, the void ratio increased as well. Meanwhile, the void ratio reduced as consolidation pressures increased. He also claimed that the influence of organic content was decreased with higher pressure levels and became very small for pressure greater than 8 kN/m².

The results obtained from Khattak (1978) were also published in Andersland et al.

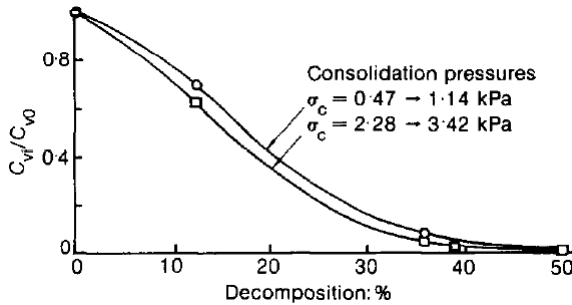


Figure 2.60: Anaerobic decomposition effects on the coefficient of consolidation for fibre-clay soils for sample with sample having 60% initial organic content (Al-Khafaji & Andersland, 1981)

(1980) as shown in Figure 2.62. It described the void ratio versus pressure for several model organic soils. Andersland et al. (1980) suggested that the compression index, C_c was not constant but will decrease with an increase in pressure and if any decomposition occurred, the void ratio-logarithm pressure curves were shifted downward.

Wardwell & Nelson (1981) investigated the effect of fibre decomposition on sludge landfills on the long term secondary compression. A man made organic materials which contained of kaolin clay, cellulose fibre and water were mixed at different proportion. Soils were decomposed by adding sufficient nutrients and then put under load (48 kNm^2) for six months. Settlement behaviour was compared with undecomposed sample and the results obtained were presented in Figure 2.63. They claimed that the increase in the rate of secondary compression for decomposed sample was related to constant gas production rates which related to linear microbial activity and not necessarily related to instantaneous structural breakdown. Besides, the additional strain increased with increasing organic content due to higher percentage of decomposition at the higher organic levels as shown in Figure 2.64.

Wardwell et al. (1983) developed a laboratory procedure in order to determine possible environmental factors which influenced anaerobic microbial breakdown of organic soils. Clays with various percentage of organic substrate were prepared. To activate decomposers activity, nutrients were added at different proportions on prepared samples to encourage organic breakdown. Soil samples were evaluated for critical parameters such as organic content, nitrogen, temperature and pH as these factors influencing the resulting decomposition. The anaerobic activity in the soil was monitored by collecting and analysing the gas production during decomposition process. The type of biological activity taking place was determined by measuring the rates of gas production, the total amounts of gas produced, the component of the gas and the change in soil properties as a function of time. This research look at the changes in organic content to gas production and relate it to compressibility behaviour. The total settlement for soil with nutrient was more than 50 % greater than sample without nutrient. However, the engineering results were published elsewhere. Compressibility were influenced by decomposition in two ways: (1) volume loss associated with the microbial metabolism and (2) increase in organic matter compressibility as a organic structure loses its integrity.

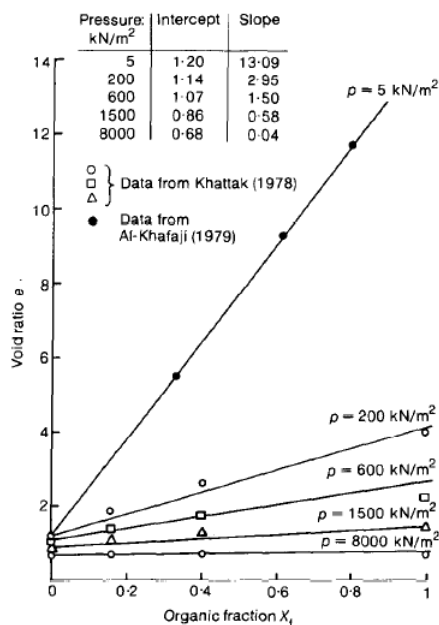


Figure 2.61: Relationship between organic fraction, void ratio and consolidation pressure for the reconstituted soil sample (Al-Khafaji & Andersland, 1981)

Meanwhile, the biodegradation effects on compressibility of over-consolidated fibrous peat were also reported by [Elsayed et al. \(2011\)](#). Different oriented sample directions particularly in vertical and horizontal directions were tested in Series 1 and Series 2 using conventional oedometer testing. The different series were indicated by the period of incubation in which Series 1 were samples stored for one month in cold humid place and submerged in groundwater from site whereas Series 2 were samples stored for 9 month as same procedure in Series 1 and submerged in water different than groundwater. It was found out that in Series 1, the coefficient of consolidation c_v in the horizontal direction was higher than the vertical direction due to high permeability in the horizontal direction which relates to fibre's orientation. No comparison of was made with c_v Series 2. Compression index C_c for series 2 in vertical direction was higher than series 1 due to the loss of structural integrity of cell walls as a result of biodegradation for 9 months and fibre orientation or soil anisotropy. The coefficient of secondary compression C_α and the coefficient of tertiary compression C_β increased for series 2 for both orientations. Besides, the coefficient of volume of compressibility m_v in horizontal direction was higher compared to vertical direction due to fibres orientation was mainly in horizontal direction in Series 1. m_v was dependent on stress level where m_v decreased with increasing consolidation stress for both horizontal and vertical directions in Series 1. The permeability also decreased during compression for both orientations.

[Pichan & O'Kelly \(2012\)](#) also conducted a review on the effect of decomposition on compressibility of fibrous peat and it was found out that the more decomposed the peat

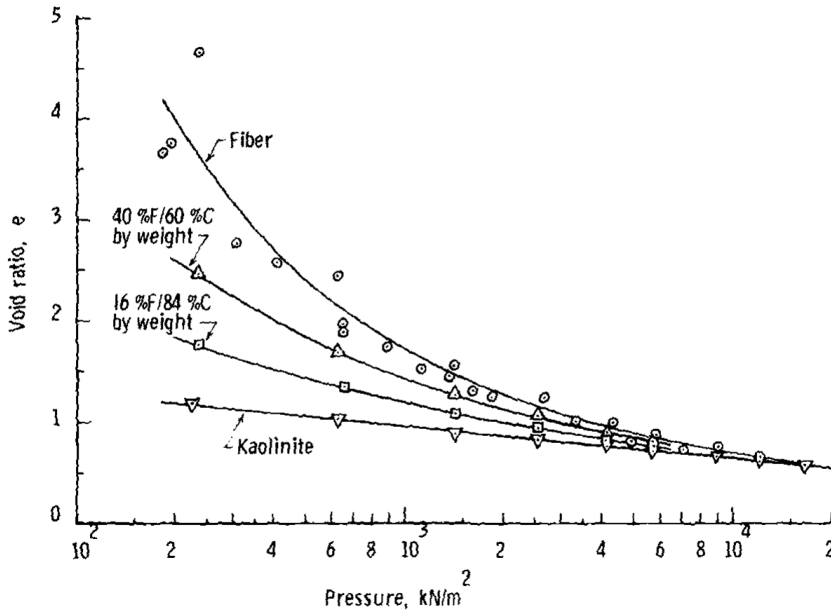


Figure 2.62: void ratio versus pressure for different model organic soils (Andersland et al., 1980)

material, the lower its compressibility. Besides that, a preliminary study was also conducted to investigate the potential for accelerated decomposition in fibrous peat by incubating two undisturbed in water bath from the site under submerged and partially submerged conditions at temperature 30 °C, for a period of 2 month without applying any confining stresses. The results showed that water content was greater than measured natural material due to swelling and some additional pore water generated within the incubated specimens. The organic content unchanged and liquid limit were lower than natural specimen due to reduction in water holding capacity of the incubated material. Besides that, the decomposition rate of partially submerged specimen was greater than submerged specimen due to exposure of oxygen at the top of specimen. This was indicated by the change of material colour and relative volume of biogas generated. This experiment only taking account the temperature and water level as control parameters but did not look other important limiting factor such as C:N ratio, pH and oxygen.

Pichan & O'Kelly (2013) stimulated decomposition process in fibrous peat by a kind of pre-treatment of the ground before building works are started. The decomposition process was stimulated by adjusting limiting factors such as pH and carbon:nitrogen ratio (C:N). Peat blends were prepared by adding sufficient amount of peat pulverised fly ash (PPFA) which was highly alkaline and nitrogenous material (urea) in order to achieve the optimum decomposition blend of C:N ratio (C:N = 25:1 to 30:1) and pH (pH = 7.0-7.5). The addition of PPFA resulted to reduction in water content and loss ignition and increased in pH and specific gravity. However, the addition of urea did not influence the pH, loss on ignition and specific gravity except causing a reduction in water content.

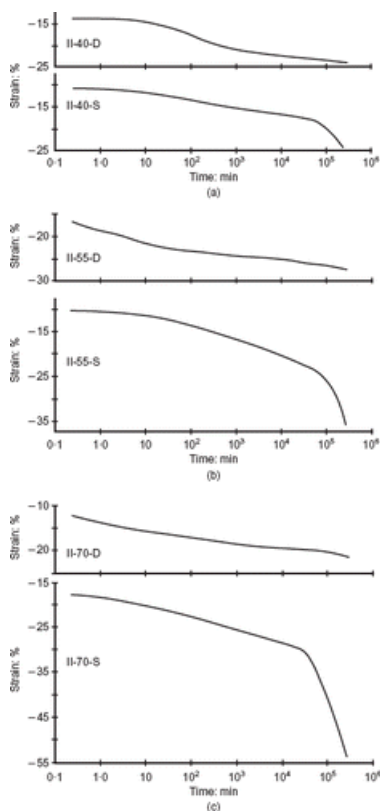


Figure 2.63: Secondary settlement with time for decomposed (D) sample and non-decomposed (S) samples (Wardwell & Nelson, 1981)

O'Kelly & Pichan (2014) performed a study looking on the effect of decomposition on the physical properties of fibrous peat. Natural peat and blended peat with sufficient amount of urea and PPFA were incubated under aerobic and anaerobic conditions at 30 °C. The results showed that decomposition rate was highly influenced by aeration and temperature and not carbon/nitrogen ratio. Properties such as water content, specific gravity of solid and volatile organic content were found to be independent of incubation period. However, the fibre content was approximately inversely proportional to incubation period which suggests that decomposition rate increase was due to increase in microbial population for blended material under aerobic condition. The loss of fibre content during one-dimensional compression loading and incubation treatment was claimed due to mechanical degradation and breakage and also structural rearrangement of the peat fibres occurring the large strains.

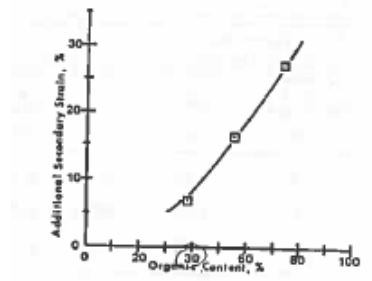


Figure 2.64: Effects of organic contents on additional secondary strains (Wardwell & Nelson, 1981)

2.13. ORGANIC MATTER

2.13.1. ORGANIC MATTER AND ORGANIC CARBON

UNDERSTANDING the common terminology used to describe organic soils is obviously important in order to better understand the composition of organic soils. Before going into detail, the definition of organic matter and organic carbon is firstly explained.

Organic matter (OM) is described as a large-pool carbon based molecule compounds containing all different elements not only carbon. It contains elements such as carbon (45-55 %), hydrogen (3-5 %), oxygen (35-45 %), nitrogen (1-4 %) and others. It is derived from remains of organisms such as plants and animals and their waste products in the environment (Wikipedia, 2016). Some organic matter can also be created by chemical reactions and does not naturally formed. Basic structure of organic matter is created from cellulose, tannin, cutin and lignin along with other various proteins, carbohydrates and lipids. An organic soil may contain a mixture of different types of organic matter.

Organic carbon is described as the amount of carbon found in an organic compound. Generally, organic carbon (OC) is used as an indicator to describe the chemical components of organic matter in a soil or sediments. The reason is because some authors claimed the complexity of measuring the organic matter in the laboratory accurately (Chesworth, 2008). According to Schumacher (2002) and Skempton & Petley (1970), a factor of 1.724 is used to convert organic carbon to organic matter. This is based on the assumption that organic matter contains 58% organic C. The equation for the conversion is shown below:

$$OM = OC \times 1.724 \quad (2.35)$$

However, this conversion factor is depending on the type of organic matter that present in the soil which can be as high as 2.5. A factor of 1.9 and 2.5 are also recommended for surface and subsurface soils respectively (Schumacher, 2002).

2.13.2. SOURCES AND FORMS OF CARBON

According to [Schumacher \(2002\)](#), there are three basic sources of carbon which contain in soils and sediments:

- (a) **Elemental carbon** are formed from incomplete combustion products of organic matter (for example: charcoal, graphite and soot), from geologic sources (for example: graphite and coal), or dispersion of these carbon forms during mining, processing, or combustion of these materials
- (b) **Inorganic carbon** is derived from minerals in the earth or from geological or soil parent material sources. This compound is non-organic material which means it is not derived from living matter. Inorganic carbon normally presents in soils and sediments as carbonates. Two most common carbonate minerals are calcite and dolomite depending on the formation and location of the soils and sediments
- (c) **Organic carbon** is derived from the decayed plants and animals. It contains carbon and it can be combined to form a structure of organic matter. Different organic carbon sources are available ranging from decomposable plant to highly decomposed plant such as humus.

As this dissertation is focussing on organic material, more attention is put on carbon which is derived organically.

2.13.3. TYPES AND CLASSIFICATION

Organic matter is a complex material containing different compounds originally from plant and animals that can have different state of decomposition. At one point where it decomposes until it becomes stable and resists further decomposition, it is called as humus. [Huat et al. \(2014\)](#) described that soil organic matter contains: (1) fresh plant animals residues (decomposable), (2) humus (resistant) and (3) inert forms of nearly elemental carbon (charcoal, coal or graphite). Carbon is considered as the main element of soil organic matter that is measured quantitatively by combustion (C is determined as CO₂ emitted). According to [Jinming & Xuehui \(1998\)](#), organic components in peat soil can be divided into 4 major groups which are :

- **Group 1:** bitumen (which can be extracted by organic solvents)
- **Group 2:** water soluble matter, easily hydrolyse matter and cellulose
- **Group 3:** humus which includes humic acid and fulvic acid
- **Group 4:** Lignin, cutin, suberin and other (which do not hydrolyse in water)

Meanwhile, Soil Science Society of America (SSSA) describes soil organic matter as below:

Meanwhile, [Tremblay et al. \(2002\)](#) described that organic matter in soils can be divided into non-humic and humic portions. Non-humic portion consists of vegetal, animal or microorganism remains including cellulose, hemicellulose, sucrose, starch, proteins, amino acids, fats, waxes, resins and organic acids. The activity of microbes will

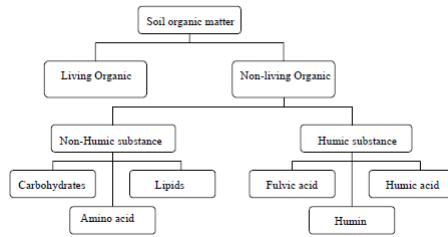


Figure 2.65: Classification of soil organic matter (Huang et al., 2009)

transform these compounds into polysaccharides and carbohydrates. The humic portion is comprised of alkanes, fatty acids, humic acids, fulvic acids and humins which are the products of the weathered or transformed non humic portion and lastly is organic contaminants which formed the third group of organic matter.

The organic matter when extracted can be fractionated into components have the characteristics of plant tissues and those based on humus. The first group (non-humic matter) includes fats, waxes, oils, resins, water soluble polysaccharides, hemicellulose, cellulose and protein. The second group includes the humus fraction consisting of basically humic and fulvic acids and humin and exists in both solid and liquid phases (Huat et al., 2014). Swift (1996) divided humic substances into three main fractions with the relevant properties as shown in Figure 2.66.

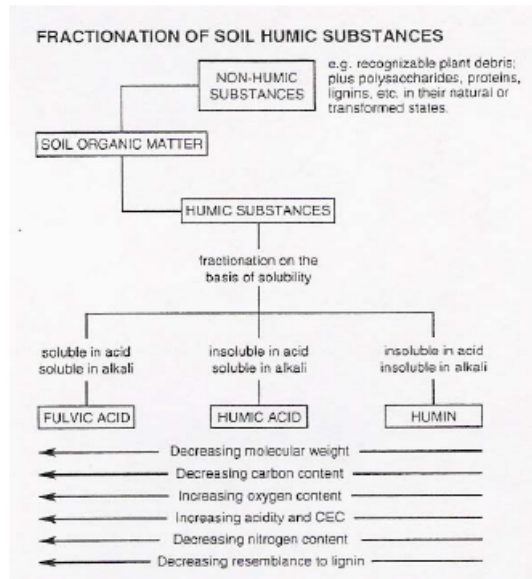


Figure 2.66: Fractionation of soil humic substances (Swift, 1996)

2.13.4. STRUCTURAL COMPOUNDS

Cellulose

Cellulose is the major structural component of the cell walls (Kogel-Knabner, 2002). It is made up of repeated units of glucose as monomers as shown in Figure 2.67 and are linked by β -(1-4)-glycosidic bonds. Glucose does not have any carboxyl ($-\text{COOH}$, carbonyl ($\text{C}=\text{O}$)) and phenolic group ($-\text{Arom-OH}$). The glycosidic bond is created when a water molecule is released and subsequently linking two glucose monomers during a dehydration reaction (Sleiderink, 2016). The chemical formula is $\text{C}_6\text{H}_{10}\text{O}_5$, where n is the repeating units of glucose monomers which results in the cellulose structure as shown in Figure 2.68. Due to glucose monomers as the building units, it is also called a polysaccharide.

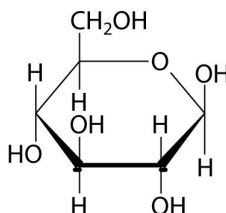


Figure 2.67: Glucose monomers

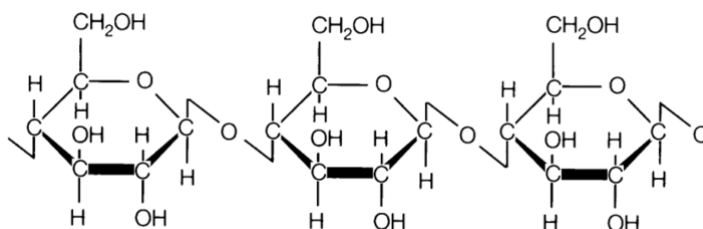


Figure 2.68: Structure of cellulose consists of glucose monomers

Hemicellulose

Hemicellulose or also known as polyoses is a non-cellulosic polysaccharide. It is the second most common polysaccharide after cellulose. Unlike cellulose, the composition of monomers is not only containing glucose but instead other types of sugar units such as pentoses, hexoses, hexuronic acids and desoxyhexoses. These units are bonded together with glycosidic linkages but have a lower degree of polymerization than cellulose. Polymerization means the process of converting a monomer or a mixture of monomers into a polymer. For example in Figure 2.69 shows that pentoses as sugar monomers of hemicellulose containing other similar chemical structures but different chemical formulas (isomers) as a result of different side chains and branching such as xylose, ribose, and arabinose. Isomers are defined as molecules with the same chemical formula but different chemical structures (side chains and branching).

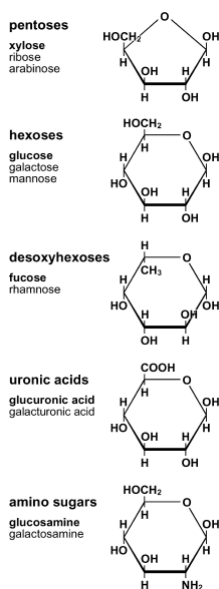


Figure 2.69: Basic structures of major sugar monomers in plant hemicellulose (Kogel-Knabner, 2002)

Lignin

Lignin provides structural rigidity to a plant. Lignin is not from polysaccharides polymer group unlike cellulose and hemicellulose. Lignin is a complex polymer consisting combination of any types of phenylpropane units which then creates a complex macromolecule. These phenylpropane units can be from different monomers such as cinnamyl alcohol, coniferyl alcohol, sinapyl alcohol and p-caoumaryl alcohol. The different structure of lignin monomers is shown in Figure 2.70. These monomer units are bonded in many ways either α or β ether linkages (Le et al., 2012). Some even creates C-C linkages. The arylglycerol- β -arylether (β -0-4) is most common linkage followed by biphenyl (5-5) and phenylcoumaran (β -5) as shown in Figure 2.71. Lignin is highly resistant to chemical, enzymatic and microbial hydrolysis due to extensive cross linking (Le et al., 2012).

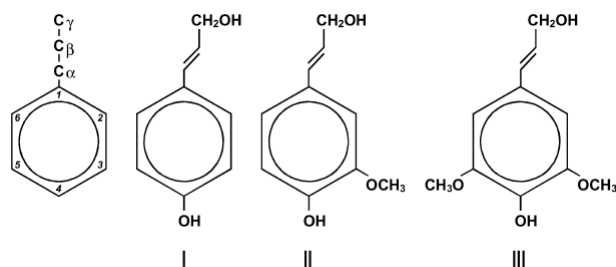


Figure 2.70: Different monomers in lignin: (I)coumaryl alcohol, (II)coniferyl alcohol, (III)sinapyl alcohol (Kogel-Knabner, 2002)

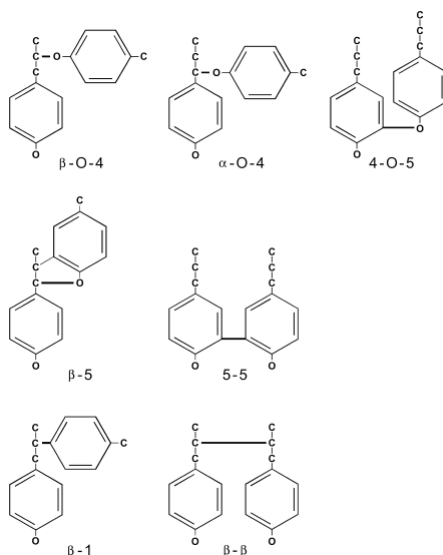


Figure 2.71: Structure showing different chemical bonding that can occur in lignin (Kogel-Knabner, 2002)

Tannins

Tannins are polyphenols occur in higher plants and they precipitate proteins from aqueous solution which called as tannic substances. Tannic substances can be divided into two groups which are hydrolyzable tannic and non-hydrolyzable (condensed) tannins. The condensed tannins are polyphenols from polyhydroxy-flavan-3-ol-units which are linked thorough C-C bonds between C-4 and C-8 and between C-4 and C-6 and not acid or base hydrolyzable. Hydrolyzable tannins have two basic units namely sugar (mostly D-glucose or similar polyoles) and phenolic acids.

2.13.5. LABORATORY METHODS

There are two direct methods to estimate the organic matter (organic content) in soils which are: (a) loss-on-ignition method and (b) Hydrogen peroxide digestion. These methods measure the quantity of organic matter removed by calculating the percentage of weight loss in dry condition or the organic content of the material.

The LOI method involves heating organic matter compound in soil or sediment at high temperature. An oven dried sample is firstly placed in a ceramic crucible and set in a well temperature-control furnace. The weight loss of the soil sample due to the oxidation of organic matter or called as LOI can obtained from the following equation:

$$LOI = \frac{M_{105^{\circ}C} - M_{440^{\circ}C}}{M_{105^{\circ}C}} \times 100 \quad (2.36)$$

where M = weight of the soil after oven-drying at 105 °C and M = weight after ignit-

ing sample at 440 °C for 5 hours. The proposed temperature and duration are based on ASTM D 294 Method C (ASTM, 2013). Different temperatures are proposed depending on soil standard as described in Chapter 1.

There is some concern regarding the mass loss produced when igniting organic soils at high temperature. This is due to overestimation of the mass loss produced which is not only from the organic matter but also loss of structural water present in some clay minerals. The structural water loss will contribute to overestimation of organic matter. An example of such mineral is gypsum ($\text{CaSO}_4 \cdot 2\text{H}_2\text{O}$) common mineral in soils from arid regions. At different temperatures gypsum releases different amount of water, for example, $1.5\text{H}_2\text{O}$ at 128 °C and the remaining H_2O at 163 °C. Apart from that, de-hydroxylation of aluminosilicates and decomposition of inorganic carbonates may also influence the additional mass loss (Huang et al., 2009). One way to avoid this problem is to pre-treatment of organic sample using HCl and HF acids to eliminate de-hydroxylation of aluminosilicate and decomposition of inorganic carbonates. However, this pre-treatment method may dissolve part of the organic matter which result underestimation of organic content.

Another method is known as Hydrogen Peroxide H_2O_2 digestion method which destroys the organic matter in soil by oxidation. This method requires the addition of concentrated H_2O_2 (30 % or 30 %) to a known weight of soil or sediment. H_2O_2 is continually added to the sample until bubbling ceases at which point the digestion is considered to be completed. The oxidised sample is then oven-dried at 105 °C and the total organic matter is estimated by loss of weight using equation below :

$$OM = \frac{Weight_{(loss)}}{Weight_{(original)}} \quad (2.37)$$

For indirect methods, the organic matter (organic content) is obtained by firstly determining the organic carbon in the soil and then multiplying a certain correction factor. This factor represent the ratio of the total weight of organic soil to the weight of the organic carbon. Dry combustion, wet combustion and dichromate oxidation are among the indirect methods available (Huang et al., 2009; Schumacher, 2002)

2.14. DECOMPOSITION PROCESS

DECOMPOSITION is a biological process which involves the production of digested organic matter or in other words, the transformation of the complex organic fraction into simpler forms of organic by-products. Micro-organisms decomposed dead organic material of plant and animal to a more stable material which is known as humus. The metabolism and activity of micro-organism result in the formation of carbon dioxide, volatile acids, methane, water, new bacterial cells and decrease in organic solids content. These products of decomposition can significantly influence the mechanical properties of the organic soil over period of time (Al-Khafaji & Andersland, 1981). Tremblay et al. (2002) claimed that the presence of organic matter can alter the geomechanical behaviour of soils by modifying some properties especially high compressibility due to an aggregated structure by molecular complexation involving metallic, organic and clay molecules.

In highly organic soil such as fibrous peat, cellulose forms the largest group of constituents in plant remains as fibrous peat contains fragment of plant tissue. The cellulose is decomposed by microorganism under anaerobic condition resulting increase in gaseous products (carbon dioxide and methane), water and organic acids. Meanwhile, lignins are more resistant to microorganism and difficult to decompose which consequently accumulate but under aerobic condition, the lignins undergo certain degree of decomposition compared to cellulose. Under deficiency of oxygen (anaerobic), the lignins are practically preserved while the celluloses are gradually decomposed (Waksman, 1930). Some general background of different mechanisms of aerobic and anaerobic decomposition are discussed as below:

Under aerobic condition: The land subsidence occurring in the upper aerated zone (aerobic condition) of temperate and tropical peatlands is resulted from microbial oxidation of the soil organic fraction. The complex carbohydrates is polysaccharides polymers which mainly composed of long chain of monomers that are linked together covalently by glycosidic linkages. For example, cellulose is the major polysaccharides found in plant which is responsible for structural roles. The conversion of monomers particularly glucose to fully mineralised products is rather simple because oxygen respiring bacteria (aerobic bacteria) can degrade monomers completely to carbon dioxide (Mego-nigal et al., 2004). The release of carbon dioxide causes a soil mass loss which turns into an apparent layer compaction with a significant land settlement. The reaction is controlled by temperature and the process is limited due to absence of oxygen. The reaction rate is high when having higher ambient temperature and lower degree of saturation.

Under anaerobic condition: The breakdown of monomers (glucose) to methane is following a series of steps. The first step is primary fermentation which breakdown glucose to low molecular weight products such as alcohol, volatile fatty acids, H_2 and CO_2 . This acidogenesis stage is performed by non-methanogenic bacteria that can be facultative or strictly anaerobic (Mer & Roger, 2001). These primary products are further mineralised to CO_2 and CH_4 or undergo secondary fermentation to acetate or smaller volatile fatty acids. The final step of anaerobic degradation are fermentation of acetate to CO_2 and CH_4 which are formed by methanogenic bacteria. Figure 2.72 shows the different stages involved in decomposition of organic soils under the presence and absence of oxygen

Decomposition process involves the breakdown of fresh plant material into finer detritus by the action of microorganisms which use the decaying organic matter as both an energy source and building material (Hobbs, 1986). Based on the Figure 2.72, the mechanisms of decomposition of organic matter is firstly explained by breakdown of cellular remains by earthworms in non-acidic soils and then further transformed by bacteria and fungi under two different conditions either aerobic or anaerobic. Under aerobic condition, acid forming bacteria hydrolyses complex carbohydrates (cellulose) into glucose. With the presence of oxygen, glucose is then used by aerobic bacteria for their metabolism and oxidised glucose to carbon dioxide and water. Meanwhile, under anaerobic conditions, two types of bacteria are involved to decompose organic matter which are non-methanogenic bacteria and methanogenic bacteria. Non-methanogenic bacteria involves transformation of cellulose to glucose by acid forming bacteria into low molecular weight fatty acids (volatile acids). The volatile acids is then used by methanogenic

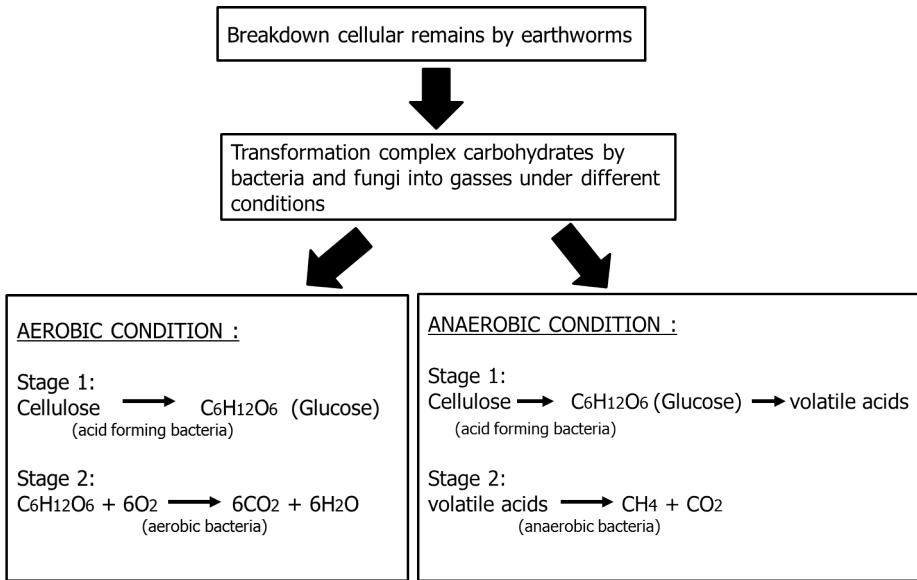


Figure 2.72: Summary of different processes of methane production under aerobic and anaerobic conditions

bacteria or anaerobic bacteria which eventually produce methane and carbon dioxide as their products.

From the previous explanation, we can conclude that decomposition process generally involves: (i) disappearance of physical structure; (ii) change in chemical state of organic matter / transformation of humic substances and (iii) loss of organic matter either in gas or solution (Hobbs, 1986; Huat et al., 2014; O’Kelly & Pichan, 2013). Disappearance of physical structure involves breakdown of plant structure such as soft inner cell walls, cellulose of the leaves, stems and roots into finer fibres and reduce in strength until it becomes amorphous structure which has more granular organic grains which are smaller and equi-dimensional in size after decomposition process takes place (Mesri & Ajlouni, 2007).

Changes of chemical state of organic matter involves transformation of organic matter into humic substances which can be divided into three major classes which are humic acids, fulvic acids and humin. All of these compounds are a complex series of relatively high molecular weight, yellow-black organic substances formed by secondary synthesis reactions in organic soils (Santagata et al., 2008). Fulvic acid is the most active fraction with lower molecular weight, higher acidity and higher oxygen content. Humic acids are the most recalcitrant fraction (Pichan & O’Kelly, 2012). The final stage of decomposition process is conversion of humic substances into humus, carbon dioxide and methane gasses or dissolved organic carbon and water which reduce the amount of organic content in peat. Decomposition causes changes in terms of physical properties which include reduction in total water content, increase in specific gravity, increase in compaction, decreases in the pore space and changes in colour towards dark brown and black Huat et al. (2014). The methane transport in organic soils is discussed in detailed

by (Couwenberg, 2009).

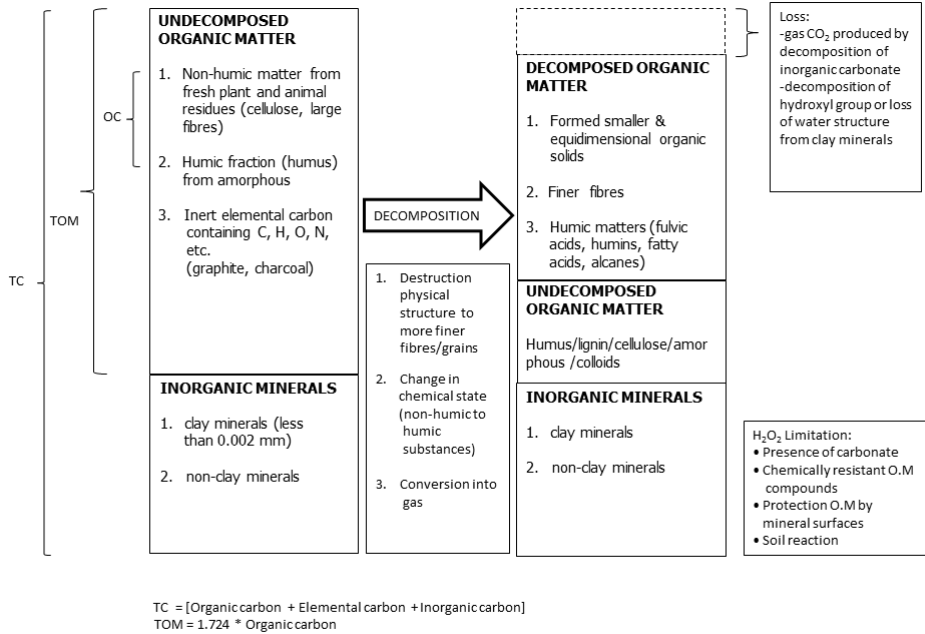


Figure 2.73: Summary of volume change due to decomposition process

2.15. FACTORS AFFECTING DECOMPOSITION PROCESSES

Decomposition rate is dependent on microbial activity in the soil. Submerged Peat will slow down the decomposition process due to limited microbial activity as consequent of lack of oxygen supply or specifically under anaerobic condition (Hobbs, 1986). The presence of oxygen is favourable condition to accelerate as groundwater fluctuations increasing the oxygen concentration in soil by as much as four orders of magnitude (Pichan & O'Kelly, 2012). Decomposition in peat involves the consortia of microorganism including bacteria and fungi which utilise carbon in soil for metabolism process to form cell components and produce energy in order to sustain life (Hobbs, 1986; Pankratov et al., 2011).

Nutrient is consider important as a source of energy for bacterial growth. Carbon, nitrogen, phosphorus and other types of minerals are important to form molecules in the cell and optimum growth (Wardwell et al., 1983; Mitchell & Soga, 2005). The available nutrients influence cellulose degradation in which the presence of nitrogen and carbon are the main nutrient that influence the decomposition process. Peat has made up of high percentage of carbon which comprises of 40 % to 60 % and little amount of nitrogen

with 0 % to 5 % content (Huat et al., 2011). The higher is the available nitrogen proportion in peat soil, the higher is the activity of decomposers bacteria (Hobbs, 1986). The amount of available nutrient in peat soil can be evaluated using the total carbon and nitrogen ratio which is expressed as C:N. (Wardwell et al., 1983) reported that the optimum C: N ratio for decomposition is in the range of 15 to 30.

The C: N ratio in peat soil is high due to high amount of carbon content and small amount of nitrogen. Example of C: N ratios of soil, sedge peat and young sphagnum peat in the U.K. are 10:1, 20:1 and 40:1, respectively (Bunt, 1988). There are limitations with the C:N ratio as not all C is available to microorganism and the available C:N ratio may be a more useful concept. Although a substrate may have similar C:N ratio or cellulose content, the rate of decomposition may be different due to the presence of higher lignin content. It can be concluded that the C:N ratio is not an appropriate indicator in decomposition for all types of media but it more useful for predicting N immobilisation (Thomas & Spurway, 1998).

Fog (1988) reviewed the influence of added nitrogen to the decomposition of organic matter and it was found out that the effect was dependent on the composition material. Easily decomposable material with low lignin content and C:N ratio (low cellulose content) will decompose much quickly if additional N is supplied. However, resistant material with high C:N ratio (high cellulose content) and lignin content often decompose more slowly following addition of nitrogen. This is due to the presence of added nitrogen which disturbed the balance competition between specific microorganism, blocking the production of ligninase enzymes, increasing the breakdown of easily available cellulose and the accumulation of recalcitrant lingo-cellulose and stimulating the formation of toxic substances.

The level of pH in peat soil is governed by lithology of the catchment supplying the mire, plant community(mire type or stage), oxygen supply and concentration of humic acids which have already formed (Hobbs, 1986). Pankratov et al. (2011), stated that pH level depends on the origin and chemistry of the water supply, bacterial activity and also the dominant species in mire. Vegetation growth may influence the acidity of the peat for example plant species such as Sphagnum mosses produce acidic peat and phenolic metabolites which is a type of antimicrobial properties resulting slow decomposition process (Pankratov et al., 2011). Decomposition process requires pH neutral to weakly alkaline environment (pH= 7.0-7.5) as the structure of plant is well preserve and microbial activity is inactive in acidic medium.

Temperature is another factor that can control the rate of decomposition or microbial activity whereby microorganism is active in high temperature compared to low temperature for their optimum growth. Mesophilic bacteria for instance is a type of anaerobic bacteria which is most active in temperatures varying from 15 °C to 45 °C and the microbial activity will increase a two to threefold for each 10 °C rise. The optimum temperature for cellulose degradation is around 35 °C to 40 °C (Hobbs, 1986).

The composition of organic matter also influences the rate of decomposition. Apart from cellulose for having the largest constituents in plant remains (Waksman, 1930), lignin is also a type of constituent that is largely found in the secondary cell wall (Wardwell et al., 1983). Cellulose will be degraded by microorganisms under anaerobic con-

dition predominant in peat bogs to form gaseous products such as methane (CH_4) and carbon dioxide (CO_2), water and organic acids. Lignin, on the other hand, is more resistant to decomposition and therefore accumulated. Therefore, it can be concluded that, the more lignified the plant, the slower is the decomposition process especially under anaerobic condition (Waksman, 1930; Wardwell et al., 1983). Under aerobic condition, lignin is not resistant and undergo a specific degree of decomposition to a much more limited extent than cellulose while under anaerobic decomposition for peat bogs, cellulose is the main constituent that take part in decomposition process but happening gradually as compared to lignin which is well preserved (Waksman, 1930). Thomas & Spurway (1998) reported that the rate of decomposition of organic matter is related to its cellulose, lignin and polyphenol content. Methods of predicting decomposition had been proposed by using a residue quality index which is a combination of C:N, lignin and polyphenol concentrations (Tien et al, 1995) or by calculating the amount of C available for microbial decomposition (Mtambanengwe and Kirchmann, 1995).

Particle size does influences decomposition because it relates directly to the surface area exposed to the surrounding environment and microbial attack. The smaller the particle, the greater area is exposed to potential decay. However in peats, decomposition is depending on chemical composition rather than their fine particle size (Thomas & Spurway, 1998). Wettability of soil also plays an important role in decomposition. For instance peat contains wax and suberin, both of which are water repellent and hence it stability of the soil. The water resistant substrate provide a poor substrate for microbial growth.

Al-Khafaji & Andersland (1981) described different requirements were needed for aerobic and anaerobic decomposition. The rate and degree of microbial activity which influence aerobic decomposition process in organic soil are depend on moisture content, temperature, nutrients, oxygen concentration, microorganism type and substrate composition. The optimum moisture content, 50 °C to 100 °C of the dry solid's weight and the need of oxygen were the limiting factor for decomposition above water table. Aerobic activity was limited to about 30 cm below waterlogged peat surface. The temperature controlled the type of microorganism in the soil for example cryophilic (5 °C to 10 °C), mesophilic (10 °C to 40 °C) and thermophilic (45 °C to 70 °C). Countries with colder temperature inhibit aerobic decomposition while woody plants decomposed slower than more succulent herbaceous species. The plant geometry specifically fragmented plants provide larger surface area and more sites for microbial activity to initiate decomposition process. The main player of this process is aerobic bacteria and fungi which have different pH levels tolerance to survive. Bacteria requires pH 6-7.5 and fungi pH 5.5-8. The acidity or alkalinity of peaty waters influence the potential for decomposition of the deposits. Peaty waters which are free from salts show pH values in the range of 4-7.

To enable decomposition process to continue there must a balance between acid and methane production. Acid forming micro-organisms can survive within a pH range of 5-8 whereas methane formers require a pH of about 6.2-7.2. If pH in organic soil below 6.0, methane formers cannot survive and the production of volatile acids keep growing and subsequently decrease the pH level in the soil. Acid conditions continues to increase until the process terminates due to unsuitable environment to proceed to another stage

which is methane production.

2.16. THE IDEAL GAS LAW

The ideal gas law is an equation of state of a gas, where the state of the gas is its condition at a given time. A particular state of a gas is described by its pressure, volume, temperature and number of moles. Knowledge of any three of these properties is enough to completely define the state of a gas as the fourth property can be defined from the equation for the ideal gas law. The equation is given as below where P is the pressure in atmospheres, V is the volume in litres, n is the number of moles present, R is the universal gas constant with the value of 0.08206 L.atm/K.mol and T is the temperature in Kelvin.

$$PV = nRT \quad (2.38)$$

The ideal gas law is normally used if the conditions of a problem are different from standard temperature and pressures (STP) at 0°C and 1 atm. However, if condition is at STP, the molar volume of an ideal gas is approximately 22.42 litres. In other words, a mole of any gas occupies a volume of approximately 22.4 Litre at STP.

Molar mass (molecular weight) of a gas can be calculated from its measured density. The relationship between gas density and molar mass is shown in Equation 2.39 where n represents the number of moles of a particular gas.

$$n = \frac{\text{grams of gas}}{\text{molar mass}} = \frac{\text{mass}}{\text{molar mass}} = \frac{m}{\text{molar mass}} \quad (2.39)$$

Substitute into the ideal gas equation gives

$$P = \frac{nRT}{V} = \frac{\left(\frac{m}{\text{molar mass}}\right)RT}{V} = \frac{m(RT)}{V(\text{molar mass})} \quad (2.40)$$

However, $\left(\frac{m}{V}\right)$ is the gas density d in grams per litre.

Hence,

$$P = \frac{dRT}{\text{molar mass}} \quad (2.41)$$

$$\text{molar mass} = \frac{dRT}{P} \quad (2.42)$$

2.17. DALTON'S LAW OF PARTIAL PRESSURES

For a mixture of gases in a container, the total pressure exerted is the sum of the pressures that each gas would exert if it were alone. This statement known as Dalton's law of partial pressure which is expressed as follows

$$P_{TOTAL} = P_1 + P_2 + P_3 + \dots \quad (2.43)$$

where the subscripts refer to the individual gases (gas 1, gas 2, etc.). The symbols P_1 , P_2, P_3 and so on represents each partial pressure. Partial pressure is described as the pressure that a particular gas would exert if it were alone in the container. The total pressure of any gas mixture assuming each gas behaves ideally is

$$P_{TOTAL} = P_1 + P_2 + P_3 + \dots \quad (2.44)$$

$$= \frac{n_1 RT}{V} + \frac{n_2 RT}{V} + \frac{n_3 RT}{V} + \dots \quad (2.45)$$

$$= (n_1 + n_2 + n_3 + \dots) \left(\frac{RT}{V} \right) \quad (2.46)$$

$$= n_{TOTAL} \left(\frac{RT}{V} \right) \quad (2.47)$$

where n_{TOTAL} is the sum of the numbers of moles of the various gases. Hence, for a mixture of ideal gas, is it the total number of moles of particles that is important not the identity or composition of the individual gas particles.

The mole fraction of a gas is described as the ratio of the number of moles of a given component in a mixture to the total number of moles in the mixture. For example, for a given component in a mixture, the mole fraction χ is

$$\chi = \frac{n_1}{n_{TOTAL}} \quad (2.48)$$

$$\frac{n_1}{n_1 + n_2 + n_3 + \dots} \quad (2.49)$$

Using the ideal gas equation, Equation 2.49 can be written as

$$= \frac{P_1 \left(\frac{V}{RT} \right)}{P_1 \left(\frac{V}{RT} \right) + P_2 \left(\frac{V}{RT} \right) + P_3 \left(\frac{V}{RT} \right)} \quad (2.50)$$

$$= \frac{P_1 \left(\frac{V}{RT} \right)}{\left(\frac{V}{RT} \right) (P_1 + P_2 + P_3 + \dots)} \quad (2.51)$$

$$\frac{P_1}{P_1 + P_2 + P_3 + \dots} \quad (2.52)$$

$$= \frac{P_1}{P_{TOTAL}} \quad (2.53)$$

The mole fraction of each component in a mixture of ideal gases is directly related to its partial pressure

$$= \chi_2 = \frac{n_2}{n_{TOTAL}} = \frac{P_2}{P_{TOTAL}} \quad (2.54)$$

2.18. CHEMICAL KINETICS

In chemistry, chemical kinetics or also known as reaction kinetics study the rate of chemical processes. The reaction rate of a chemical reaction is defined as the change of concentration of a reactant or product per unit time which is given by Equation 2.55. The rate can be measured from experimental data.

$$Rate = \frac{\Delta[A]}{\Delta t} \quad (2.55)$$

where A is the reactant or product being considered, t is time corresponding to selected time reaction, squared brackets $[\]$ indicate concentration in mol/L, symbol Δ indicates the change in a given quantity. Note that a change can be positive (increase) and negative (decrease), thus leading to positive or negative reaction rate. The rate of reaction in terms of reactant or product must firstly take account the coefficient of balanced equation because the stoichiometry determines the relative rates of consumption of reactants and generation of products. Reaction rate depends on concentration of reactants, temperature, physical state, presence of catalyst, mixing and pressure.

There are two type of rate law where

- The differential rate law or simply called as the rate law shows how a rate of reaction depends on concentrations.
- The integrated rate law shows how the concentrations of species in the reaction depend on time.

These laws only apply for reactions under conditions where the reverse reaction is unimportant, thus, the rate laws only involve concentrations of reactants. The types of rate law can be determined experimentally. The significant of knowing the rate law of reaction is important because we can infer the individual steps involve in the reaction from the specific form of the rate law.

2.18.1. RATE LAW

Rate law (rate equation) expresses the rate as a function of concentrations of reactant. The rate law is based on experiments. If chemical reactions are considered irreversible, the reaction rate will depend only on the concentration of the reactants and temperature and not the products. For a general reaction occurring at a fixed temperature, the reaction can be written as



The rate law is given by Equation 2.57

$$Rate = k[A]^m[B]^n \quad (2.57)$$

The term k is proportionality constant, called the rate constant that is specific for given temperature and does not change as the reaction proceeds. The exponent m and n known as reaction orders and both must be determined by experiment. The important key points to remember when using Equation reaction is that

- The balancing coefficients a and b in the reaction Equation 2.57 are not necessarily related in any way to the reaction orders m and n .
- The values exponent m and n must be determined by experiment; it cannot be written from the balanced equation.
- The concentrations of the products do not appear in the rate law because the reaction rate is being studied under conditions where the reverse reaction does not contribute to the overall rate.

2.18.2. INTEGRATED RATE LAW

As the previous rate law considering the rate of a reaction as a function of the reactant concentrations, integrated rate law expresses the reactant concentrations as a function of time. This law can be divided into three different cases where $n = 0$ (zero order), $n = 1$ (first order) and $n = 2$ (second order)

a) First-Order Rate Laws

Looking at a chemical reaction involving a single reactant



where the kinetics are first order in $[A]$, the rate law is

$$\text{Rate} = -\frac{\Delta[A]}{\Delta t} = k[A] \quad (2.59)$$

and the integrated first-order rate law is

$$\ln[A] = -kt + \ln[A]_0 \quad (2.60)$$

This equation shows how the concentration of A depends on time. If the initial concentration $[A]_0$ and the rate constant k are known, the concentration of A at any time can be calculated. Equation 2.60 can be plotted in the form of $y = mx + c$ where $y = \ln[A]$, $x = t$, $m = -k$ and $c = \ln[A]_0$

The reaction is considered to be a first order reaction in A if a plot of $\ln[A]$ versus t is a straight line given the slope as $-k$. If the plot is not a straight line, then the reaction is not a first order reaction.

The integrated rate law for first-order reaction can also be written in terms of ratio of $[A]$ and $[A]_0$ which is based on Equation 2.60 as below

$$\ln\left(\frac{[A]_0}{[A]}\right) = kt \quad (2.61)$$

Half life of a reaction is defined as the time required for a reactant to reach half its original concentration. A general formula for the half-life of a first order reaction can be derived.

By definition, when $t = t_{1/2}$,

$$[A] = \frac{[A]_0}{2} \quad (2.62)$$

Substituting Equation 2.62 in Equation 2.61, for $t = t_{1/2}$ the integrated first-order rate law becomes

$$\ln\left(\frac{[A]_0}{[A]_0/2}\right) = kt_{1/2} \quad (2.63)$$

or

$$\ln(2) = kt_{1/2} \quad (2.64)$$

Hence, the general equation for the half-life of a first-order reaction value $t_{1/2}$ gives

$$t_{1/2} = \frac{0.693}{k} \quad (2.65)$$

b) Second-Order Rate Laws

The second order rate law in [A] is given by

$$\text{Rate} = -\frac{\Delta[A]}{\Delta t} = k[A]^2 \quad (2.66)$$

and the integrated second-order rate law is

$$\frac{1}{[A]} = kt + \frac{1}{[A]_0} \quad (2.67)$$

This equation shows how [A] depends on time and can be used to calculate [A] at any time t , provided k and $[A]_0$ are known. For second-order reactions, a plot of $1/[A]$ versus t will produce a straight line with a slope equals to k .

When half life of the second-order reaction has reached at $t = t_{1/2}$, the definition is

$$[A] = \frac{[A]_0}{2} \quad (2.68)$$

Substituting Equation 2.68 in integrated second-order equation, a general formula for the half-life of a second order reaction is

$$\frac{1}{[A]_0/2} = kt_{1/2} + \frac{1}{[A]_0} \quad (2.69)$$

$$\frac{2}{[A]_0} - \frac{1}{[A]_0} = kt_{1/2} \quad (2.70)$$

$$\frac{1}{[A]_0} = kt_{1/2} \quad (2.71)$$

Hence, the general equation for the half-life of a first-order reaction value $t_{1/2}$ gives

$$t_{1/2} = \frac{1}{k[A]_0} \quad (2.72)$$

2

c) Zero-Order Rate Laws

The rate law for zero-order reaction is shown in Equation below. For a zero-order reaction, the rate is constant and does not change with concentration as it does for first-order or second-order reactions.

$$\text{Rate} = k[A]^0 = k(1) = k \quad (2.73)$$

The integrated rate law for a zero-order reaction is

$$[A] = -kt + [A]_0 \quad (2.74)$$

For zero-order reactions, a plot of $[A]$ versus t will produce a straight line with a slope equals to $-k$. The half-life of a zero order reaction is obtained from the integrated rate law. By definition, when $t = t_{1/2}$,

$$[A] = \frac{[A]_0}{2} \quad (2.75)$$

Substituting Equation 2.75 in Equation 2.74,

$$\frac{[A]_0}{2} = -kt_{1/2} + [A]_0 \quad (2.76)$$

or

$$kt_{1/2} = \frac{[A]_0}{2} \quad (2.77)$$

Hence, the general equation for the half-life of a first-order reaction value $t_{1/2}$ gives

$$t_{1/2} = \frac{[A]_0}{2k} \quad (2.78)$$

The summary of the rate laws corresponding to zero, first and second order kinetics of one-reactant reactions is given in Table 2.19 as shown below :

Table 2.19: Summary of the kinetics for reaction of the type $aA \rightarrow$ Products that are zero, first or second order in $[A]$

Order	Zero	First	Second
	Rate law	Rate = k	Rate = $k[A]$
Integrated rate law	$[A] = -kt + [A]_0$	$\ln[A] = -kt + \ln[A]_0$	$\frac{1}{[A]} = kt + \frac{1}{[A]_0}$
Relationship of rate constant to the slope of straight line	Slope = $-k$	Slope = $-k$	Slope = k
Half life $t_{1/2} = \frac{[A]_0}{2k}$	$t_{1/2} = \frac{0.693}{k}$	$t_{1/2} = \frac{1}{k}[A]_0$	

2.19. HENRY'S LAW

Henry's law states that at a constant temperature, the amount of gas dissolved in a solution is directly proportional to the partial pressure of the gas above the solution. Henry's law is applied for dissolved gas that does not dissociate in or react with the liquid. There are two different equations that can be used depending on Henry's constant formula and unit either $K_{H,pc}$ or $K_{H,cp}$ (Zumdahl & Zumdahl, 2007). Nevertheless, Henry's constant is depending on temperature changes. If Henry's constant $K_{H,pc}$ is used, the dissolved oxygen concentration in liquid becomes

$$C = \frac{P}{K_{H,pc}} \quad (2.79)$$

Meanwhile, if Henry's constant $K_{H,cp}$ is used, the dissolved oxygen concentration equation is

$$C = K_{H,cp} \cdot P \quad (2.80)$$

where;

C = concentration of dissolved gas (mol/L)

$K_{H,pc}$ = Henry's law constant (L.atm/mol)

$K_{H,cp}$ = Henry's law constant (mol/L.atm)

P = Partial pressure of gas above liquid (atm)

Fick's first law describes the amount of particles flowing through a unit cross section A in unit time t which known as flux J . In other words, this law describes how fast a high concentrated solute can diffuse through a surface area and later moves towards a low concentrated area.

In a steady state diffusion, the flux is proportional to concentration gradient as shown in Equation 5.11. Steady state means the state variable of the system is not changing in time

$$J = -D \frac{\Delta C}{\Delta x} \quad (2.81)$$

where;

J = diffusion flux equals to the amount of substance per unit area per unit time ($\text{mol m}^{-2} \text{s}^{-1}$)

D = diffusion coefficient ($\text{m}^2 \text{s}^{-1}$)

C = concentration of which the dimension is amount of substance per unit volume (mol m^{-3})

x = position (m^2)

2.20. BASIC PRINCIPLES OF GAS-LIQUID TRANSFER

Fick's law can be used to describe the transport of flux from simple system of oxygen dissolves in water which relates the transition from gas to liquid phase. Transport of

oxygen in liquid phase is influenced by aeration and agitation (stirring). In order to provide efficient oxygen transfer for aerobic degradation to occur, aeration and agitation are required in the system.

Consider a system where oxygen from air phase transports to liquid phase as shown in Figure 2.74. According to van der Lans (2009), there are several steps taking place which explains the transport of oxygen in microorganism to enable organic matter degradation takes place.

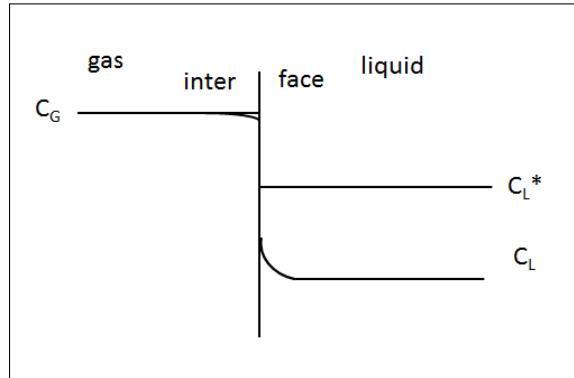


Figure 2.74: Oxygen concentration distribution at the interface between gas and liquid

When OTR is not 0, where there is an uptake of oxygen / in a well mixed liquid, biochemical reaction takes place is given by:

$$\frac{\Delta C}{\Delta t} = OTR - OUR \quad (2.82)$$

$$k_L a (C_L^* - C_L) - r \quad (2.83)$$

where;

k_L = mass transfer coefficient

a = specific surface area (A/V)

C_L^* = concentration at the interface based on Henry's law ($C = kP$)

C_L = concentration of bulk liquid

$k_L a$ = volumetric mass transfer coefficient

When OTR = 0 where there is no uptake of oxygen / in a non-mixed system / biochemical reaction takes place is given by:

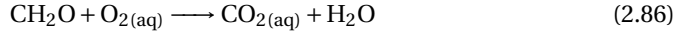
$$\frac{\Delta C}{\Delta t} = -OUR \quad (2.84)$$

$$\frac{\Delta C}{\Delta t} = -r \quad (2.85)$$

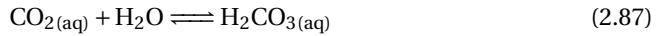
where r is the reaction rate obtained from the Michaelis-Menten kinetics equation which is described in 2.22.

2.21. INFLUENCE OF CARBON DIOXIDE PRODUCTION ON PH

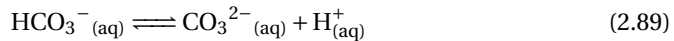
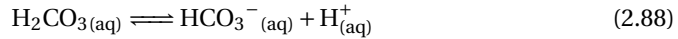
Organic matter consumed oxygen in water to form carbon dioxide CO_2 and water H_2O . The general equation for a simple biomass degradation under the presence of oxygen (aerobic condition) is



Carbon dioxide dissolves in water which denotes as $\text{CO}_{2(\text{aq})}$ combines with water molecule to form carbonic acid $\text{H}_2\text{CO}_{3(\text{aq})}$. One molecule of carbon dioxide in water forms one molecule of carbonic acid in aqueous phase as below

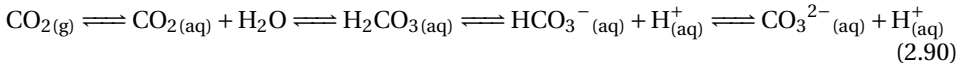


Dissolved carbonic acid then dissociates in water and forms two hydronium ions H^+ through bicarbonate HCO_3^- and carbonate CO_3^{2-} productions.



The presence of hydronium ions decreasing the pH of the solution and in contrast the absence of hydronium ions may increase the pH. The losing of hydronium ions occur when CO_2 from aqueous phase is transferred to gas phase which results to losing H^+ ions in solution and thus increasing the pH.

In general, the overall reaction can be summarised as follows



2.22. LAW OF REACTION RATE OF OXIDATION ORGANIC MATTER

The degradation of organic matter involves multiple enzymatic reactions which includes different organism, organic compounds and oxidants as well as intermediate compounds (Arndt et al., 2013). The overall reaction normally determined by the slowest step or known as rate limiting step. Normally, the prediction of a rate of reaction is approximate by the rate limiting step. For degradation organic matter, the breakdown of polymer (cellulose) to monomer (glucose) for instance is performed by hydrolysis reaction with the assistance of acid forming bacteria. Hydrolysis is a process of breakdown of chemical bonds by addition of water. Under aerobic condition, glucose will then be used by aerobic bacteria for their metabolism to form carbon dioxide and water. Organic matter degradation is usually described as a single-step overall reaction (Arndt et al., 2013).

The reaction rate is described by velocity v which explains how fast an enzyme converts substrate to product, the amount of substrate consumed or product formed per

unit time. The velocity can be obtained by measuring the product (or substrate) concentration with time. As degradation of organic matter involves many steps of complex enzymes, the slowest one will determine the rate of overall reaction. Michaelis-Menten kinetics equation is normally used to describe a large number of enzymes. Even, many complex reactions are believed to follow this equation when only one substrate is varied and at a time and the others are held constant. The Equation is as follows

$$v = \frac{V_{max}[S]}{K_m + [S]} \quad (2.91)$$

where V_{max} denotes the maximum reaction (or velocity) rate, K_m is Michaelis-Menten constant (when substrate concentration $v = 1/2 V_{max}$ and $[S]$ is substrate concentration).

Figure 2.75 shows the plot of describing the velocity of reaction with substrate concentration.

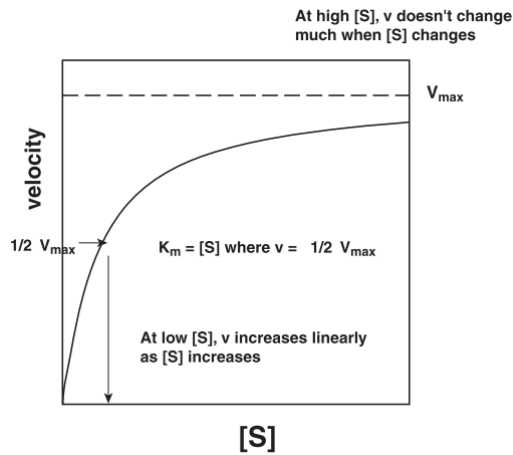


Figure 2.75: Velocity vs. substrate concentration

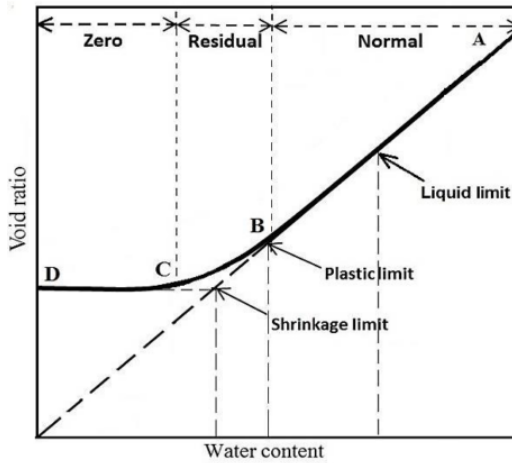


Figure 2.76: Shrinkage characteristics curve for an initially slurried clay (Fredlund et al., 2002)

2.23. SOIL SHRINKAGE

Soil shrinkage is defined as loss of moisture in soil due to drying which may lead to decrease in soil volume. The weight and volume of a soil decrease during drying (Oleszczuk et al., 2003). Soil shrinkage is also defined as the specific volume change of soil relative to its water content which can also induce settlement of soil (Stirk, 1954). The shrinkage property of a soil is usually presented as soil shrinkage characteristics curve (SSCC), which is represented as either the specific volume versus gravimetric water content or void ratio versus water content relationship. Generally, when a non-structured soil or clay slurry dries out, the shrinkage stages can be divided into several phases as shown in Figure 2.76 (Fredlund et al., 2012). Schindler et al. (2015) also introduces a soil shrinkage curve for loamy clay sample as shown in Figure 2.77 where structural shrinkage is present before normal/proportional shrinkage phase which does not include in Figure 2.76.

The definition for each shrinkage phase is described as below:

1. **Phase 1:** Structural shrinkage is when the loss of water due to draining of the macropores is larger than the volume changes, soil that the soil structure behaves stable. This phase is shown in Figure 2.77 which is not present in Figure 2.76.
2. **Phase 2:** Normal/Proportional shrinkage (A-B) where the volume change caused by shrinkage is proportional to the water loss or in other words, equal decrease in water volume to bulk soil volume with the intra-aggregate pores still being saturated. For non-structured clay paste, the SSCC in the normal shrinkage stage is a straight line and this line coincides with the line representing 100% saturation degree. At the end of normal shrinkage stage, air enters the soil at a point that is referred to as the general air entry value (AEV) point.
3. **Phase 3:** Residual shrinkage (B-C) where the curve deviates from 100% saturation

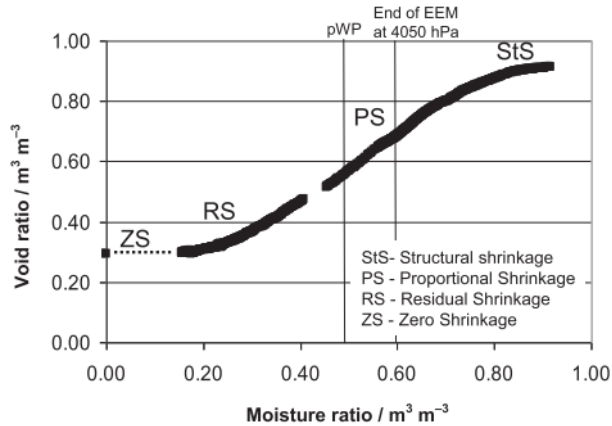


Figure 2.77: Soil shrinkage curve, loamy clay sample (Schindler et al., 2015)

line and the slope of the curve is decreasing. Air enters the intra-aggregate pores and a further loss of water volume is greater than the total decrease in sample's volume.

4. **Phase 4:** Zero shrinkage (C-D) where the sample's volume does not decrease any further and a small amount of water evaporates.

The pattern of shrinkage curve depends on particle size distribution and stress history and this curve can be used to determine the plastic limit and shrinkage limit of a soil (Fredlund et al., 2002). The real shrinkage limit is when the air entry water content is close to the plastic limit and the water content at the intersection between saturation line and the horizontal asymptote of the curve when water content tends towards zero (Fredlund et al., 2002).

2.24. SOIL WATER RETENTION CHARACTERISTICS

2.24.1. SOIL SUCTION

Soil suction is defined as the energy required for extracting unit volume of water from soil (Fredlund & Rahardjo, 1993). The major components of soil suction include matric suction (ψ_m) and osmotic suction (ψ_o). The sum of these two components is termed as total soil suction (ψ).

Matric suction is associated with the capillary action phenomenon resulting from surface tension. Above the ground water table, the soil is unsaturated and water moves upward in the soil through adhesion to the sides of the pores and is held there by surface tension forces and this process is called capillary rise. At the interface between the water and air, the contractile skin, imbalanced intermolecular forces result in a pressure difference of $u_a - u_w$, where u_a and u_w refer to pore air pressure and pore water pressure respectively. This pressure difference is known as matric suction. Since the pore air pressure is considered to be atmospheric, and takes a value of 0, the matric suction is

a negative pressure. Matric suction vary with time due to environmental changes. Any change in suction affecting the overall equilibrium of soil mass.

Higher capillary rise means higher negative pore water pressures which normally can be observed in smaller particles which has smaller voids. Initially, soil is saturated having positive pore pressure and as it starts drying, pulling force of water or tension pull is developed. If we apply this concept to a capillary phenomenon in a glass tube containing water, a pulling force is developed at the surface between air and water known as contractile skin in order to be in an equilibrium state. Once equilibrium state is achieved, surface tension is mobilised at the air-water boundary. Surface tension causes the contractile skin to behave like elastic membrane or sheet forming a meniscus with radius of curvature. The surface tension places a reaction force on the wall of the capillary tube. The vertical component of this reaction force produces compressive stresses on the wall of the tube. In other words, the weight of the water column is transferred to the tube through the contractile skin. The contractile skin results in an increased compression on the soil structure in the capillary zone. As a result, the presence of matric suction in an unsaturated soil produces a volume decrease and an increase in the shear strength of the soil. The radius of curvature of the contractile skin decreases as the matric suction of a soil increases (Fredlund et al., 2012).

The osmotic suction is more closely related to the diffuse double layer around the clay particles whereas matric suction is mainly associated with the air-water interface. Osmotic suction is related to the amount of salts dissolved in the free pore-water. The pore water in a soil normally contains dissolved salts and therefore it has lower vapor pressure compared to pure water (Fredlund & Rahardjo, 1993). Osmosis is the term used to describe the phenomenon by which a solvent (water) passes from a solution of lower solute (salt) concentration through a semi-permeable membrane into a solution of higher solute concentration. A membrane is described as semi-permeable if it allows the passage of solvent but not solute. If the flow of water is restricted, a pressure imbalance equal to the osmotic pressure difference between the two solutions needs to be present.

2.25. SOIL WATER RETENTION CURVE

The soil water retention curve (SWRC) or sometimes called as soil water characteristic curve (SWCC) defines the relationship between gravimetric water content (or volumetric water content, degree of saturation) and soil suction. As the water content decreases due to evaporation or drainage, the matric suction increases. When water infiltrates the soil, the reverse occurs where the water content increases and the matric suction decreases. However, when rewetting and drying cycles take place, different wetting and drying path may be distinguished, this is known as hysteresis (Chin A Moei, 2016).

The full range of SWRC can be divided into three stages which are the boundary effect stage, the transition stage and residual zone of desaturation. In the boundary effect stage, all of the pores are filled with water and the contact between water menisci and soil particles is continuous. However, the pore water is in tension and suction is present due to the action of capillary forces. As suction increases, the resistance offered by the capillary tension prevents the flow of water out of the soil up to a point where it is big enough to overcome the capillary forces, the air entry values (AEV), where air enters the

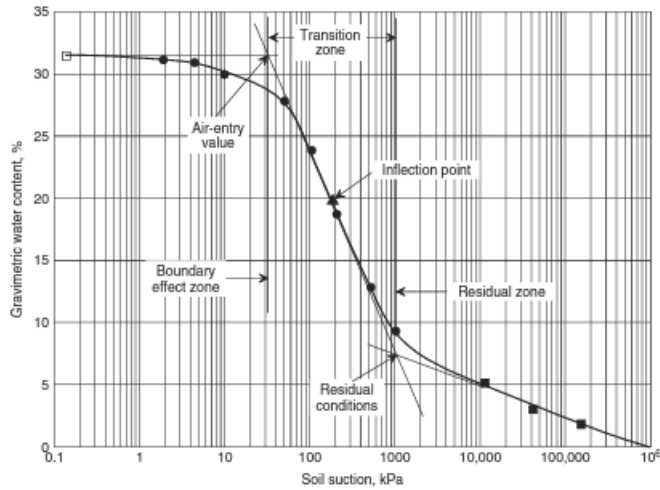


Figure 2.78: Definition of variables for SWRC (Fredlund et al., 2012)

largest pores in the soil and the soils begin to desaturate. In the transition stage, water content decreases with increasing suction and water menisci area in contact with soil particles is not continuous and reduces as air phase becomes more continuous. In the residual zone, the water phase is discontinuous and the air phase is continuous. There is very little water-soil particle contact and water leaving the soil occurs in vapour phase (Fredlund & Rahardjo, 1993).

Several parameters such as initial water content, initial void ratio and stress state affect the SWRC of a given soil. For the same soil but having different initial water content value, SWRC vary at lower matric suction values but they tend to converge at higher matric suction values. Soil with lower void ratio (dense soil) has higher high entry value (Heidarian, 2012).

2.26. HYSTERESIS

Figure 2.79 shows a typical SWRC for silt. The air-entry value of the soil is the matric suction where air starts to displace water in the largest pores in the soil. The residual water content is the water content where a larger suction change is required to remove additional water from the soil. Residual water content is remaining water content at high tension or matric suction.

The main curve shown in Figure 2.79 is a desorption (drying) curve. The adsorption (wetting) curve differs from desorption curve as a result of hysteresis related to wetting and drying. The end point of adsorption curve may differ from the starting point of desorption curve due to air entrapment in the soil.

When rewetting and drying cycles take place, different wetting and drying paths may be distinguished. As shown in Figure 2.80, when the soil is rewetted from the residual water content (rewetting) or drained from saturated (drying), the main wetting or drying

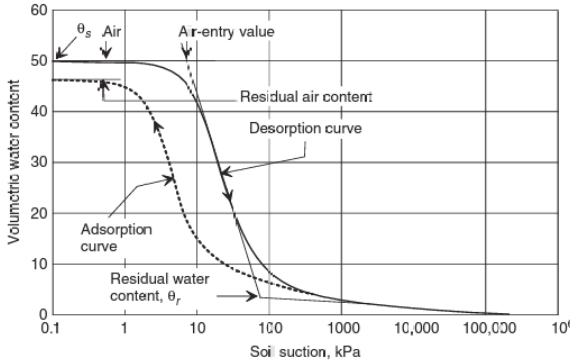


Figure 2.79: Typical SWRC for silt soil (Fredlund et al., 2012)

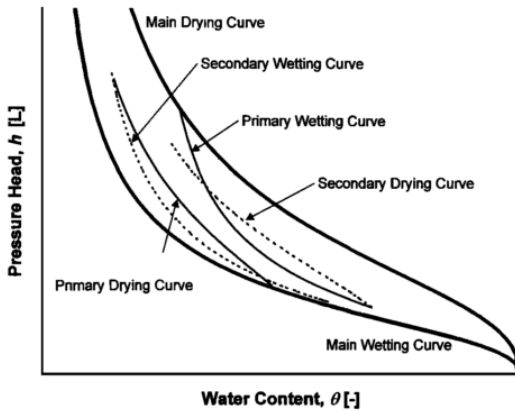


Figure 2.80: Idealised hysteretic soil-water characteristics curves showing main, primary and secondary wetting and drying curves (Šimůnek et al., 1999)

curves are followed respectively. When a wetting or drying process is reversed while following the main hysteresis curve, the retention curve follows a primary hysteresis curve. Secondary and higher order scanning curves are a result of additional reversals (Šimůnek et al., 1999; Yao, 2016)

2.27. VOLUME-MASS RELATION

The definitions of volumetric water content and gravimetric water content needs to be distinguished when plotting the SWRC. Early research related to SWRC which mostly in the area of soil physics and agriculture disciplines normally expressed amount of water in terms of volumetric water content. Hence, it is necessary for engineers to become familiar with both mass and volumetric definitions. Figure 2.81 shows the volume and mass designation for a soil model which comprises of air, water and solid.

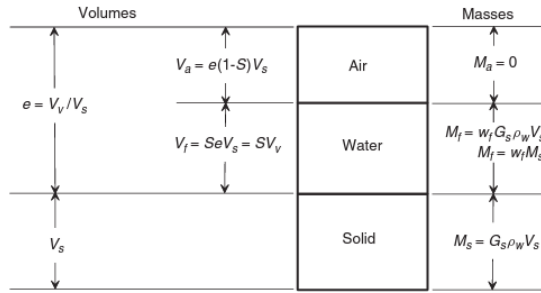


Figure 2.81: Three-phase soil model relating mass and volume (Fredlund et al., 2012)

2.27.1. POROSITY

Porosity, n is defined as the ratio of volume of voids V_v to the total volume of soil V_t .

$$n = \frac{V_v}{V_t} \quad (2.92)$$

2.27.2. VOID RATIO

Void ratio e is defined as the ratio of volume of voids V_v to the volume of solids V_s . This term is normally preferred as it expresses the volume of voids over a fixed volume of solids.

$$e = \frac{V_v}{V_s} \quad (2.93)$$

2.27.3. DEGREE OF SATURATION

The percentage of the void space that contains water is expressed as the degree of saturation S (%).

$$S = \frac{V_w}{V_v} \quad (2.94)$$

2.27.4. VOLUMETRIC WATER CONTENT

In engineering applications, volumetric water content can be described as the volume of water over the total volume or the volume of solids. Total volume is used in aggregate soils where the total volume does not vary as much. For this case, the soil being studied is highly organic and shrinkable, thus water volume will be expressed over a fixed volume of solids. Assuming no loss of organic material. Usually, the gravimetric water content is determined first and then converted to volumetric water content based on the water density ρ_w and soil particle density ρ_s or the specific gravity ($G_s = \frac{\rho_s}{\rho_w}$). This is done because mass relations are usually more easily available (Verruijt, 2001)

$$\theta = \frac{V_w}{V_s} = \frac{M_w}{M_s} \cdot \frac{\rho_s}{\rho_w} = w \cdot G_s \quad (2.95)$$

2.27.5. GRAVIMETRIC WATER CONTENT

The gravimetric water content is described as the mass of water over the mass of the dry solids.

$$w = \frac{M_w}{M_s} \quad (2.96)$$

This is normally used by geotechnical engineers to express the water content in soil. However, for SWRC it can be plotted in terms of gravimetric water content or volumetric water content. Hence, it is important to note that which reference is being made.

2.27.6. VOLUMETRIC GAS CONTENT

Similarly, the volumetric gas content (VGC) can be described as the volume of gas over the volume of solids.

$$VGC = \frac{V_g}{V_s} \quad (2.97)$$

3

OXIDATION EFFECT ON COMPRESSION BEHAVIOUR OF ORGANIC SOIL

*Decomposition involves,
changes in the physical soil structure,
changes in the chemical state,
and generation of biogas.*

Hobbs

3.1. ABSTRACT

Settlement due to decomposition of organic soils causes major problems during the service life of buildings and infrastructure. Decomposition is assumed to be a very slow natural process, however, it can be accelerated as a result of anthropogenic activities such as groundwater lowering or drying. The increased supply of oxygen in the partially saturated zone above the groundwater level leads to accelerated oxidation of organic matter. Previous studies have shown the consequences of decomposition of peat and organic soils on compression and subsidence. Field studies in The Netherlands have shown a correlation between settlement and oxidation rates, attributing the major part of subsidence in peat meadow areas to the oxidation of organic matter. Laboratory studies have investigated the effect of decomposition on the consolidation behaviour of highly organic soils. However, these studies do not replicate the field process to the extent that decomposition is induced before loading is applied. In this work, decomposition is accelerated on samples loaded in oedometer, to replicate the field conditions. Hydrogen Peroxide is used to oxidise the organic soil, and the compression behaviour of the oxidised samples under different constant vertical stress is compared to that of the non-oxidised sample. Besides the effect of ex-situ oxidation is also investigated and compared with non-oxidised sample.

The results show that ex-situ oxidation of organic soils results in lowering the Atterberg limits and, consequently, the compressibility under both loading and unloading stages. In-situ oxidation results in volumetric compression which is mainly due to decrease in the water content. Loss of solid matter is a minor part of the recorded volume change. Samples oxidised in-situ suffer an abrupt volume change at constant applied stress. Upon subsequent loading after oxidation, they show an increased apparent pre-consolidation stress and a stiffer response, until the normal compression line (NCL) of the non-oxidised sample is attained. Upon unloading, the in-situ oxidised samples have a similar low swelling capacity as the sample oxidised before loading. This study shows that the most relevant effect of chemical oxidation on the tested soil is to lower the water holding capacity. The total volume reduction due to decomposition increases at increasing applied stress. However, it never overpasses the volume reduction due to increasing stress.

Keywords: compressibility, decomposition, oxidation, organic soils, settlement

3.2. INTRODUCTION

Organic soils derive from the accumulation of incompletely decomposed plant materials that are preserved under wet anoxic conditions. They contain at least 20 % organic matter and are known as problematic soils for having high water content and high compressibility in nature. The physical and engineering properties of organic soils continuously changes over time, partly due to oxidation of the organic matter. In the current state of practice, on-going decomposition in organic soils is assumed to be very slow and it is not taken into account in settlement prediction models for the design of buildings and infrastructure. As a result, long-term settlement predictions can be highly inaccurate. In order to improve current prediction methods, rigorous research is required to

better understand the coupled oxidation and consolidation processes in organic soils.

Decomposition is described as a process which involves loss of solid organic matter by oxidation to either gas or dissolved compounds and changes in the physical structure and chemical state (Hobbs, 1986; Kazemian et al., 2011a; O'Kelly & Pichan, 2013). Several environmental factors can activate and accelerate this process significantly such as changes in temperature, aeration, pH and nutrients as a result of groundwater fluctuation or anthropogenic disturbances (O'Kelly & Pichan, 2013; Wardwell et al., 1983; Hobbs, 1986; Kazemian et al., 2011a). The physical and mechanical properties of organic soil are influenced by oxidation in two ways, either by losing actual solid mass due to chemical decomposition (that is often catalysed by micro-organisms present in the subsurface) or by changes in the original structural fabric (Al-Khafaji & Andersland, 1981; O'Kelly & Pichan, 2013).

Several studies have been carried out to study the effect decomposition on the compression behaviour of natural and reconstituted organic soils, both addressing primary compression, which is the volume change under a vertical stress change, and secondary compression which is typically described as a volume change occurring over time under constant effective stress (Al-Khafaji & Andersland, 1981; Wardwell & Nelson, 1981; Wardwell et al., 1983; O'Kelly, 2008; Elsayed et al., 2011; Pichan & O'Kelly, 2012, 2013). Al-Khafaji & Andersland (1981) investigated the compression behaviour of different fibre-clay mixtures. Slurry organic samples were seeded with optimum decomposition nutrients and allowed to degrade under low constant vertical effective stress (3.42 kPa). Their studies suggest that secondary compression increases as the degree of decomposition increases. Wardwell & Nelson (1981) performed similar studies but at higher constant effective vertical stress (48 kPa) for a period of six month and compared the secondary compressibility for samples with and without nutrients. They observed a similar trend, with settlement due to decomposition increasing with increasing organic content.

However, in most of the previous studies, decomposition was triggered by adding sufficient amounts of nutrients and oxygen, and by changing pH and temperature, to achieve optimum conditions for bacterial growth before loading the soil. Little information is given on the time needed for decomposition to fully develop. As a result, the total settlement recorded on subsequent loading could be affected by an unknown amount of change in volume still due to the ongoing biochemical process. Moreover, the influence of oxidation on compressibility was mostly studied in single load steps, while its consequences on increasing load were not studied. Lastly, most of the laboratory tests were performed starting decomposition on reconstituted unstresses samples, which do not replicate the state of the soil and the oxidation process in situ.

Schothorst (1977) claimed that 85 % of the total settlement in low moor peat in the western of Netherlands is due to oxidation of organic matter while the remaining 15 % is due to shrinkage. He also stated that 55 % of the volume change of Dutch peatland over a period of six years is from peat oxidation above the water table, 35 % is from compression below the water table and 10 % is due to shrinkage above the water table. These conclusions were based on field measurements, but they were not validated by replicating the oxidation processes in controlled laboratory tests.

From the literature review, it can be concluded that there is the necessity to investigate the missing link between field observation and material behaviour in the laboratory, to better understand the coupled compression and oxidation response of organic soils. In particular, there is a need for understanding the relevance of oxidation on settlement at constant load, which affects existing constructions, from the consequences of oxidation on the compressibility upon subsequent loading, which is of relevance for urban and infrastructure development.

This study wants to reduce the knowledge gaps on the coupled oxidation and compression behaviour of natural organic soils. The work is expected to answer three different research questions that are (1) to design a simple laboratory test able to properly capture the settlement response by replicating in-situ oxidation process occurring under load in the field, (2) to investigate the combined effects of loading and oxidation (in-situ and ex-situ) on the compression behaviour of organic soil and (3) to compare the compression behaviour of organic soils when oxidised in-situ under different constant loads.

3.3. MATERIALS AND METHODS

Organic sediments were dredged from the ditches and canals in the peat meadow area of Wormer & Jisperveld, the Netherlands. A series of classification tests was conducted according to the relevant standards (CEN, 2004a,b; ASTM, 2007b). The particle size distribution (PSD) of both the natural samples and the samples pre-treated with Hydrogen Peroxide, to remove the organic matter, were determined by wet sieving (CEN, 2004b). The grain size distribution of the fine fraction was analysed using the Hydrometer method (CEN, 2004b). The mineralogy and chemical composition were analysed using X-ray diffraction and X-ray Fluorescence and the samples were analysed using an Environmental Scanning Electron Microscope (Philips ESEM XL30) equipped with an EDAX X-ray microanalysis system. Water content was determined by drying the specimen for at least 24 hours in an oven at 105 °C (ASTM, 2007a). The water content, w , is defined here on a mass basis, as commonly done in geotechnical engineering, as:

$$w = \frac{A - B}{B} \times 100 \quad (3.1)$$

in which A is the mass of the wet specimen before drying [g] and B is the mass of the oven-dried specimen [g].

The Atterberg limits were determined for both oxidised and non-oxidised samples: The samples were first spread on a tray and partially dried at room temperature of 20 to 25 °C to reduce its water content. A very strong odour was produced during mixing and drying, indicating that the material was partly oxidising during the drying process. To accelerate the drying process of the material, a fan was used until enough water was evaporated. The soil was mixed occasionally in order to ensure uniform consistency and avoid excessive drying and crust formation. The liquid limit was determined using the fall-cone test while the plastic limit was determined by rolling-thread method. It is expected that the oxidised and non-oxidized specimens significantly differ in consistency. In order to compare the experimental results on different soil specimens, which can have quite different void ratios and different Atterberg limits at the same time, it

might be worthwhile normalising the the void ratio or moisture content by using the liquidity index (e.g., (Terzaghi et al., 1996)) according to:

$$I_L[\%] = \frac{w - w_{(PL)}}{w_{(LL)} - w_{(PL)}} \quad (3.2)$$

$$I_L[\%] = \frac{e - e_{(PL)}}{e_{(LL)} - e_{(PL)}} \quad (3.3)$$

The specific gravity of the solid particles was determined using gas-expansion pycnometer (ASTM, 2014). To analyse the organic matter several methods were employed. Firstly, a combustion method was used according to Dutch standards (R.A.W, 2005). The material which was oven-dried at 105 °C for 24 hours and cooled down in a desiccator. The dried samples were grinded and then placed in a muffle furnace at 500 °C for 4 hours and subsequently the mass of the ignited samples was measured. The mass loss due to combustion, i.e., Loss on Ignition (LOI) is defined as ASTM (2007a):

$$LOI[\%] = \frac{B - C}{B} \times 100 \quad (3.4)$$

in which C is the mass of ash [g] after combustion. The fibre content was determined on the original and oxidised samples according to ASTM (2008).

Preparation of oxidised ex-situ samples

To accelerate decomposition compared to the natural biochemical activity, Hydrogen Peroxide (H₂O₂) was used. Sufficient care was taken to reduce exposure to the gaseous products of the oxidation reaction. This solution is most commonly used to remove organic matter as pre-treatment of organic soils in sedimentation tests (CEN, 2004b). In this research, a 10% (w/w) solution of H₂O₂ was used to trigger oxidation of organic matter. In order to prepare ex-situ oxidised samples, 300 ml of H₂O₂ were mixed with 100 g of partially dried organic sample. The chosen amount of H₂O₂ was expected to be sufficient to oxidise all the organic matter. Oxidation was carried out in batches in order to ensure that complete oxidation took place. Using a glass rod, the mixed solution with organic material was stirred gradually from time to time so that all the organic materials were well suspended. Distilled water was added carefully to avoid excessive frothing and sample loss over the lip of the beaker. Once the froth subsided, the suspended solution was left overnight to allow complete reaction. H₂O₂ was added again the next day to confirm that the oxidation reaction was completed. Once no gas formation nor frothing could be visually observed any longer, it was assumed that all organic matter had been oxidised. The solid fraction was filtered, washed with distilled water and dried in the oven for 24 hours at 105 °C, cooled down in a desiccator and weighed (Schumacher, 2002). The mass loss due to chemical oxidation (LOCO) was calculated using

$$LOCO = \frac{B - D}{B} \times 100 \quad (3.5)$$

in which D is the mass of the oven-dried specimen after chemical oxidation. Next the oven-dried sample was combusted again according to R.A.W (2005) as described above

and the mass loss due to combustion was determined again. The latter can be quantified in two ways, either considering only the mass loss due to combustion $LOI = (D-E)/D \times 100$, or by referring to the original dry mass before chemical oxidation:

$$LOCO + LOI[\%] = \frac{B - E}{B} \times 100 \quad (3.6)$$

in which E is the mass of the ash [g] of the specimen which is chemically oxidised before combustion.

Compression tests

One-dimensional compression tests were performed using a conventional oedometer set-up (CEN, 2004c), in which the oxidation procedure and the initial consistency of the specimens were varied. The initial liquidity index of the samples was changed by reducing the natural water content to the target value by evaporation. Two test series were performed, first with a high initial I_L ranging between 2.42 and 2.46 and a second with low I_L ranging from 0.81 to 0.89. At these low consistencies the samples could be prepared by pouring them directly in the oedometer rings. Care was taken to avoid the inclusion of air bubbles and the top cap and loading frame, imposing an initial total axial stress of 0.5 kPa, were placed very carefully on top of the sample in order to prevent the material from squeezing out of the sample ring. During the first load step a large immediate displacement was observed, indicating that some squeezing took place. Consequently, the final thickness of the sample, after testing and dismounting, was used to back-calculate the sample strains throughout the test. Tests were performed on non-oxidised specimens and on specimens which were oxidised ex-situ using the procedure described above. To replicate the *in-situ* oxidation of organic soils, tests were performed on specimens which were chemically oxidised *inside* the oedometer cell under different levels of constant load. Oxidation was stimulated by replacing the water in the surrounding cell by a 10 wt% H_2O_2 solution. The amount and concentration of H_2O_2 was based on the amount of organic matter in the oedometer specimen.

Sequential load increments of 2, 5, 10, 20, 40, 80, 160 kPa and unloading steps of 40, 10, 2 kPa were applied. During each load step the samples were allowed to consolidate for 24 hours. Oxidation was started during the load steps at 5 and 20 kPa for the high liquidity samples and 5, 20 and 80 kPa for the low liquidity samples. The compression under constant load period was extended by another 9 days, after which the deformation rate of the samples had decreased enough to suggest that oxidation had been virtually completed. The non-oxidised and ex-situ pre-oxidised samples were also kept under constant load for the same time duration, in order to isolate the amount of deformation occurring due to oxidation from that occurring due to the natural secondary compression of the organic soil

The non-oxidised and ex-situ oxidised samples, were left in normal tap water at 5, 20 or 80 kPa, depending on the test, for 9 days. At the end of consolidation tests, the final thickness of all the consolidated samples was measured, and water content, loss on ignition and specific gravity were determined.

3.4. RESULTS AND ANALYSIS

Physical and Chemical Properties

The index properties of both the fresh and ex-situ oxidised specimens are shown in Table 3.1. The natural water content of the organic sample is about 1200 %. At such high water content the soil is considered a slurry for having water content exceeds the liquid limit. Dark black in colour with traces of thin plant fibres are observed. Based on the low fibre content, the sediments are classified as sapric/amorphous organic matter according to ASTM (2007b) which corresponds with von Post Scale H₇-H₁₀. ESEM analysis with EDAX showed that the inorganic fraction is still mostly biogenic, composed of siliceous diatom skeletons, some calcium carbonate (CaCO₃) and in situ formed pyrite framboids (FeS₂). There is only a very small fractions of clastic clay minerals observed (composed of Si, Al, K). Sieving analysis indicates that about 80 % of the solid particles (based on dry mass) passes the 63 µm, which indicates the sample mainly consists of fine particles. Both the fresh and oxidised sample show very high liquid and plastic limit. Compared with other organic soils as reported e.g., by Hobbs (1986) the dredged sediments from Wormer and Jisperveld correspond to other peat soils with similar loss on ignition, but the plasticity index is significantly higher. Hence, based on the consistency limits the soil plots closer to the A-line than other organic soils with similar liquid limit, probably because chemical decomposition of the particles is limited.

Table 3.1: Summary of selected properties for non-oxidised and oxidised ex-situ samples

Properties	Unit	Non-oxidised	Oxidised ex-situ
Water content	%	1200	940
Liquid limit	%	582	270
Plastic limit	%	228	127
Plasticity index	%	354	143
Specific gravity	[-]	1.80-1.82	1.86-2.03
Fibre content	%	15	7

The specific gravity (G_s) measured is 1.80 which is strongly influenced by the amount and type of organic constituent in the test sample (den Haan & Kruse, 2007; Hobbs, 1986). Organic compounds such as cellulose have a G_s value of approximately 1.58 and for lignin it is approximately 1.40. These compounds present in the organic soil and affects the compounded specific gravity (den Haan & Kruse, 2007). However, higher specific gravity is observed for oxidised material as a result of breakdown and mineralisation of organic matter. Generally, higher mineral content and (or) higher degree of decomposition will contribute to higher specific gravity values (Hobbs, 1986; Huat et al., 2011; O'Kelly & Pichan, 2013). Higher specific gravity is obtained after chemical oxidation not only due to oxidation of organic matter but also oxidation of minerals or metals which results to higher heavy compound due to presence of oxygen. The resulting specific gravity upon chemical oxidation is highly variable and strongly dependent on the concentration of solid mass in the hydrogen peroxide solution. Decomposition process leads to disappearance of the physical texture of the sample and also changing the complex organic

composition into simpler forms of organic by-products (Al-Khafaji & Andersland, 1981).

The Loss on ignition (N) of the original sample obtained is agreeable with the preliminary estimation of Loss on ignition (N) estimated using measured G_s proposed by Skempton & Petley (1970) as shown in Equation 3.7 where $G_{s,organic} = 1.4$, $G_{s,mineral} = 2.7$ and $C = 1.04$ respectively:

$$\frac{1}{G_s} = \frac{1 - C(1 - N)}{G_{s,organic}} + \frac{C(1 - N)}{G_{s,mineral}} \quad (3.7)$$

The soil is classified as organic soil for having organic content around 51 %.

A comparison is made to determine the organic content of oxidised samples by using different oxidation procedures as deduced in Table 3.2. Generally, combining chemical oxidation and ignition methods result to higher degree of mass loss 59 to 68 % compared to chemical oxidation or ignition method respectively. However, chemical oxidation is unable to oxidise the organic matter fully. This is indicated by the further amount of mass loss produced 31 to 36 % by ignition method after chemical oxidation is carried out. It is reported that, the decomposition of organic matter by H_2O_2 is incomplete probably due to soil reaction, presence of carbonate, chemical resistant organic compound and protected organic matter by mineral surfaces (Mikutta et al., 2005). The organic carbon is estimated from the organic matter content by using a conversion factor of 1.724 (Schumacher, 2002; Skempton & Petley, 1970). The factor is used based on the assumption that organic matter contains 58 % organic carbon which is recommended for higher degree of decomposition of peats ($H_4 - H_4$) while 53 % is particularly for less decomposed peats ($H_1 - H_3$) (Skempton & Petley, 1970). Besides, combustion at temperatures 500 °C is able to remove the decomposed (humified) organic matter only. While, higher temperature of at least 850 °C is required to remove non-humified organic matter such as fresh plant roots, cellulose, lignins, protein, fats and waxes (Landva et al., 1983).

Table 3.2: Changes in organic content composition as a result of different oxidation procedures

Sample	Solid mass concentration [g/L]	Mass loss			Specific gravity		
		LoI [%]	LoCO [%]	LoCO + I [%]	initial [-]	after CO [-]	After I [-]
non-oxidised	-	51.3	-	-	1.82	-	2.62
oxidised	33	-	52.5	68.1	1.82	1.91	2.56
	49	-	48.0	64.2	1.82	2.02	2.65
	54	-	50.4	66.6	1.82	1.99	2.6
	84	-	36.0	58.9	1.82	1.97	2.66

Compression behaviour

Figure 3.1 reports the compression curves of the non-oxidised sample and the ex-situ oxidised. The results are reported in a semi-log plot, where the void ratio is plotted as a function of the logarithm of the vertical stress. The points indicate the void ratio corresponding to the settlement measured after 24 hours consolidation time. As indicated previously, at 5 kPa and 20 kPa the samples were left creeping during 9 days, to provide the reference for the in-situ oxidised samples. The corresponding two points represent the void ratio corresponding to 24 hours consolidation and to that achieved after another

9 days secondary compression. In the same figure data from Al-Khafaji & Andersland (1981) are also plotted to the sake of comparison. The first evident effect of ex-situ pre-oxidation is to reduce the initial void ratio of the sample by a dramatic amount, which suggests that a huge amount of water is lost during oxidation, with a consequent rearrangement of the initial fabric. The two slurries then show an almost linear curve in the semi-log plot, which indicates that a unique average compression coefficient can be associated to each sample. However, besides decreasing the initial void ratio, oxidation dramatically decreases the compressibility of the soil, with the slope of the compression curve of the ex-situ oxidised sample becoming about one half of the slope of the non-oxidised sample. It is also clear that pre-oxidation reduces the amount of creep settlement which is eventually accumulated under constant load, which seems to suggest that oxidation and creep are inherently related. Upon further loading, after creep, all samples are initially stiffer, until the original compression curve is reached at the vertical stress corresponding to the original compression line for the current void ratio.

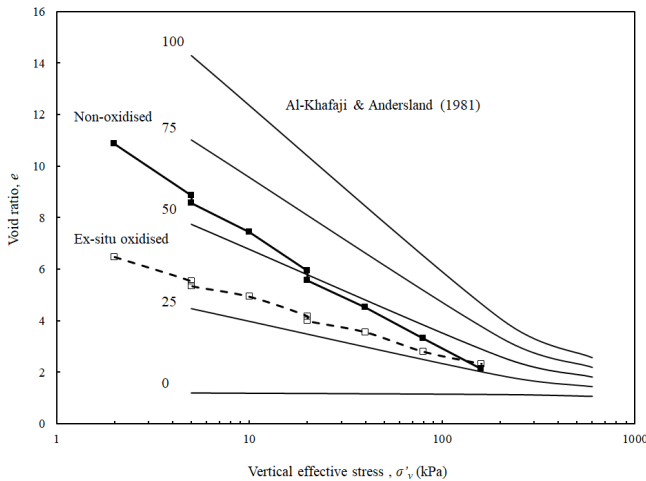
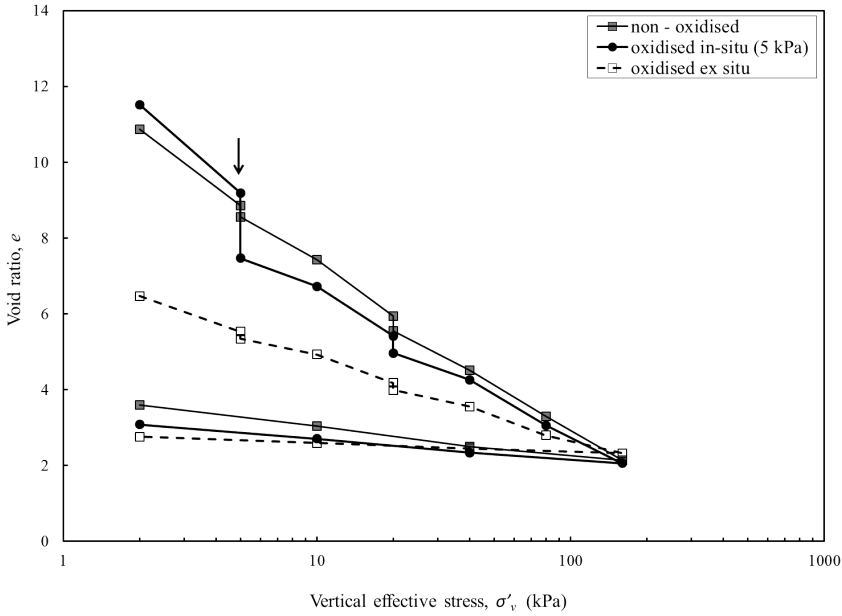


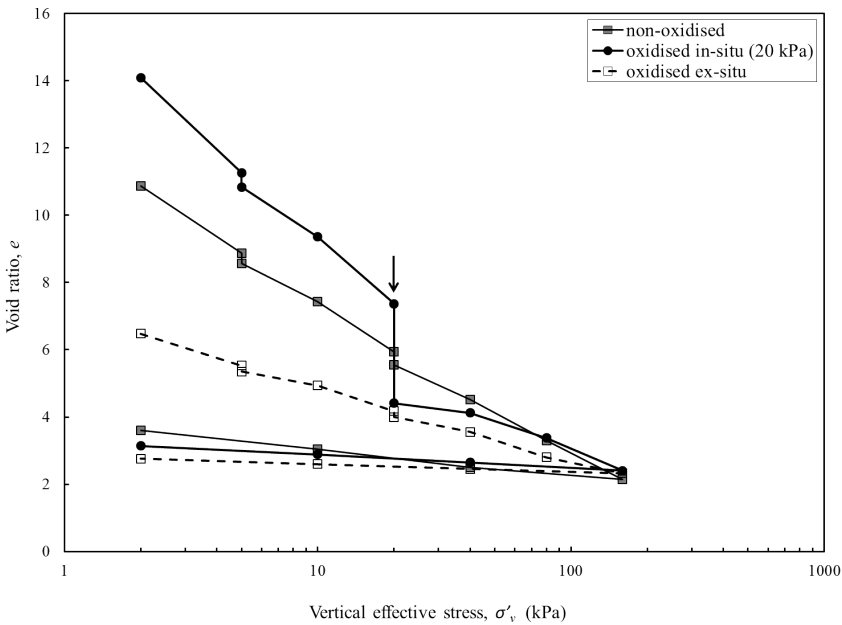
Figure 3.1: Compression curves for natural and ex-situ chemically oxidised organic soil in comparison with the results of Al-Khafaji & Andersland (1981). The numbers indicate the percentage of organic fibres in a kaolinite fibre mixtures

The shape of the two compression curves compare well to the curves coming from the tests performed by [Al-Khafaji & Andersland \(1981\)](#) on samples of kaolin mixed with different percentage of organic fibres. The higher the percentage of organic matter, the higher the compressibility, with similar linear curves in the semi-log plot, which tend to converge at high stresses. Eventually, at 160 kPa, the curves describing the compression of the non-oxidised and ex-situ pre-oxidised samples converge.

Figure 3.2 shows the results of the compression test on the soil samples, which were oxidised under constant load at 5 kPa (a) and 20 kPa (b), which better replicate oxidation in the field. Again, the void ratio is plotted versus the logarithm of effective vertical stress ($e - \log(\sigma'_v / \sigma'_{vref})$). It can be observed that the initial compressibility of the different samples is similar, just changing slightly with the initial void ratio. A huge drop of void ratio is observed when the samples are exposed to H_2O_2 during 9 days. The creep settlement of the natural sample during the same period is minimal compared to the one of the sample experiencing oxidation. This shows that oxidation causes a collapse of the original metastable soil fabric, with substantial rearrangement of the soil particles fabric leading to a dramatic soil volume change. However, in spite of the volume reduction, the void ratio of the in-situ oxidised samples does not reach the same void ratio of the ex-situ pre-oxidised sample at the same vertical stress. This result suggests that the sequence of loading and oxidation is of relevance on the amount of deformation of the sample, and that the net effects of oxidation may be different depending on the applied effective stress. The equilibrium void ratio reached is governed by composition, pressure, temperature and chemical environment ([Al-Khafaji & Andersland, 1981](#)).



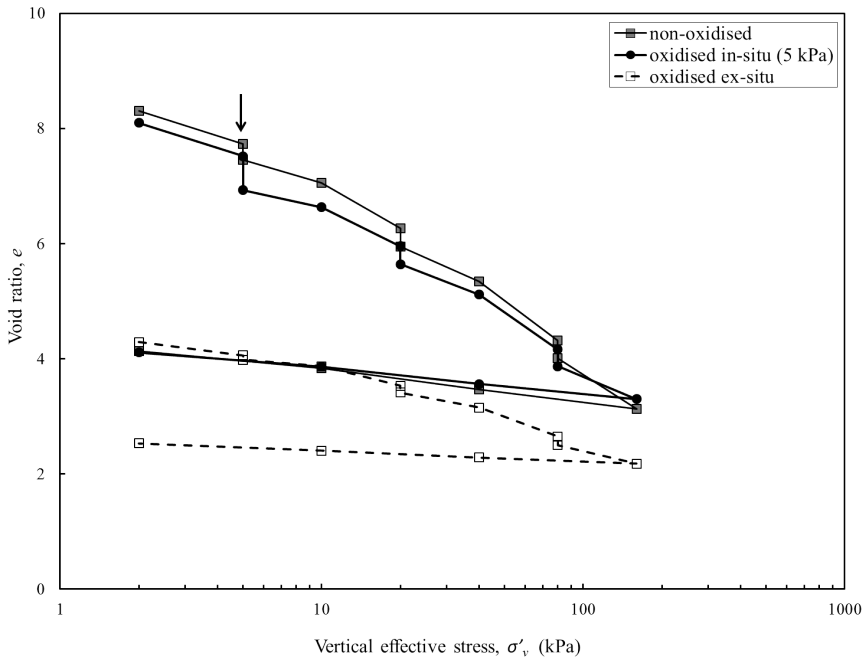
(a) 5 kPa



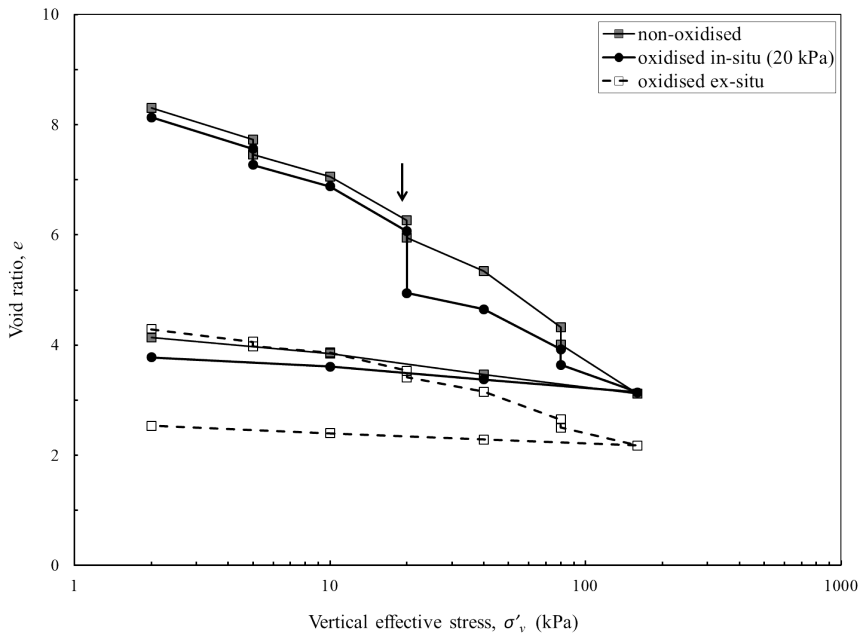
(b) 20 kPa

Figure 3.2: Compression curves for organic soil which is subjected to in-situ oxidation at 5 kPa and 20 kPa in comparison with the non-oxidised and ex-situ oxidised samples starting at high initial liquidity index ($LI_0 = 2.33-2.46$)

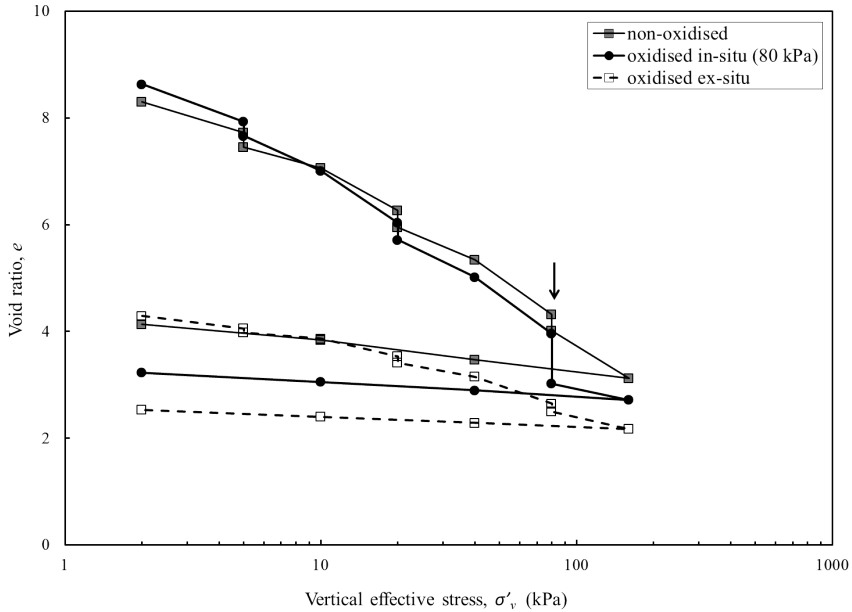
Upon subsequent loading after oxidation the oxidised sample shows the development of an apparent pre-consolidation stress, and a stiffer behaviour until the latter is approached, which is consistent with a stiffer arrangement of the soil fabric after the volumetric collapse has occurred during oxidation. Starting from the stress level corresponding to the previously developed pre-consolidation stress, the compression curve tends to re-align to the one of the non-oxidised sample, apparently showing that the increase in stiffness is only temporary, and can be interpreted as an anticipated void ratio reduction. For the samples tested starting from a high liquidity index, all the curves converge towards the same point at 160 kPa, suggesting that eventually the stress level is dominating the final state of the samples. However, permanent changes of the soil fabric due to oxidation are suggested by the comparison of the behaviour of the samples upon unloading, with the oxidised samples showing higher swelling compared to non-oxidised sample. In Figure 3.3, the companion data are reported for the samples prepared at lower liquidity index. It can be noted that the pattern of behaviour is the same as before, although the compression curves do not converge yet in the stress range investigated.



(a) 5 kPa



(b) 20 kPa



(c) 80 kPa

Figure 3.3: Compression curves for organic soil which is subjected to in-situ oxidation at 5 kPa , 20 kPa and 80 kPa (bottom) in comparison with the non-oxidised and ex-situ oxidised samples starting at low initial liquidity index ($LI_0 = 0.81-0.89$)

By comparing the change in void ratio experienced by oxidation at increasing constant stress, it can be observed that it depends on the stress level, and that the higher the stress, the higher the change in void ratio over the current one. The comparison of the total settlements and strains of the different samples is shown in Table 3.3. The values show that, although oxidation contributes to the total settlement of the organic samples, this contribution becomes less relevant when compared to the settlement (and strains) due to consolidation when the vertical stress is increased, in the stress range investigated.

Table 3.3: Settlements and strains due to compression and oxidation in the oedometer cell and ignition afterwards

Sample	e_0	e at 2 kPa	e_f	H_0 [mm]	H at 2 kPa [mm]	H_f [mm]	$\Delta H/H_0$ [%]	$\Delta H/H_{2kPa}$ [%]	ΔH by CO [mm]	ΔH by CO/ H_0 [%]
<i>Oxidation at 5 & 20 kPa</i>										
non-oxidised	17.0	10.9	4.4	18.9	12.5	5.7	70	55	-	-
oxidised in-situ (5 kPa)	20.0	11.5	3.3	17.9	10.6	3.5	81	67	1.9	11
oxidised in-situ (20 kPa)	22.1	14.1	3.3	20.3	13.3	3.7	82	72	2.7	13
oxidised ex-situ	9.0	6.5	3.0	20.8	15.5	8.2	61	47	-	-
<i>Oxidation at 5, 20 & 80 kPa</i>										
non-oxidised	9.6	8.3	4.5	21.1	18.4	10.8	49	41	-	-
oxidised in-situ (5 kPa)	9.5	8.1	4.4	21.1	18.4	10.8	49	41	1.3	6
oxidised in-situ (20 kPa)	9.5	7.6	4.0	21.1	18.4	10.0	53	45	2.3	11
oxidised in-situ (80 kPa)	9.2	8.6	3.3	20.6	19.4	8.5	58	56	1.9	9
oxidised ex-situ	4.5	4.3	2.5	20.9	20.0	13.4	36	33	-	-

It is worth noting that the volume change due to oxidation is almost entirely due to loss of water holding capacity, while the contribution of solid mass loss is very small. In order to quantify the contribution of decomposition to the total compression of soil, the organic content of oxidised and non-oxidised samples (inside cell) were determined at the end of the oedometer tests. The results are shown in Table 3.4., which show that oxidation using Hydrogen peroxide did not cause significant change to the amount of dry solid. Almost no mass loss was observed for the samples which were oxidised ex-situ for the controlled amount of H_2O_2 used. The mass loss due to in-situ oxidation was around 2-3% on average, with higher values only for the two samples having an initial high liquidity index. Upon further combustion the mass loss is significantly higher, around 50%. Besides, the specific gravity values after H_2O_2 oxidation do not differ much from the original condition, which confirms that no significant modification of the organic compounds had occurred.

Table 3.4: Details of average compression index of NCL and changes of reloading line after oxidation

Sample description	C_r below p_c 2 - 5 kPa	C_c (24 hrs loading) before oxidation	after oxidation	C_s (24 hrs unloading) 160 - 2 kPa	C_r after creep and/or oxidation 5 - 10 kPa	20 - 40 kPa	80 - 160 kPa
High liquidity index							
<i>Oxidation at 5 & 20 kPa</i>							
non-oxidised	-	4.56 (2-160 kPa)	0.77	3.77	3.42	-	-
oxidised in situ at 5 kPa	-	5.85 (2-5 kPa)	3.88 (10-160 kPa)	0.54	2.46	2.35	-
oxidised in situ at 20 kPa	-	6.69 (2-20 kPa)	2.85 (40-160 kPa)	0.38	4.92	0.96	-
oxidised ex situ	-	2.17 (2 - 160 kPa)	0.23	1.38	1.45	-	-
Low liquidity index							
<i>Oxidation at 5, 20 and 80 kPa</i>							
non-oxidised	1.45	3.48 (20-160 kPa)	0.53	1.32	2.03	2.95	-
oxidised in-situ (5 kPa)	1.46	-	2.94 (20-160 kPa)	0.42	1.00	1.75	1.88
oxidised in-situ (20 kPa)	1.44	-	2.51 (40-160 kPa)	0.34	1.31	0.97	1.66
oxidised in-situ (80 kPa)	1.77	3.45	-	0.27	2.16	2.32	1.01
oxidised ex-situ	0.58	1.50 (20-160)	0.19	0.38	0.87	1.08	-

In order to quantify the results by means of parameters, which could be useful in the practice, a simple quantitative interpretation of the results is given, with reference to the compression parameters typically used in the practice. Figure 3.4 schematically depicts the typical experimental results got from the oedometer tests. A normal consolidation line, having a slope C_c can be identified, which is the bounding limit for each sample in the compression plane. The compression index C_c represents the slope of the void ratio-effective stress plot for the normally consolidated part. The slope of the swelling (unloading) lines is indicated with C_s , while the slope of the reloading lines is named C_r . The swelling index C_s and the reloading index C_r describe the behaviour of the samples when they are overconsolidated.

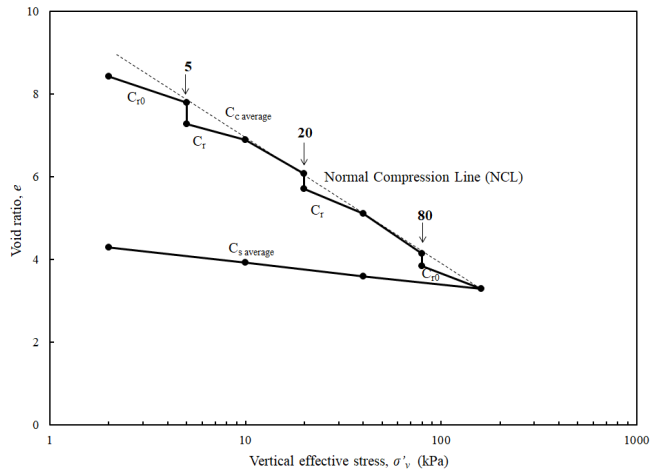


Figure 3.4: Plot of void ratio vs vertical effective stress which shows the definition of compression parameters

For the non-oxidised and ex-situ oxidised samples the compression index and swelling index can be determined from the slope of the compression curves. It is worth noting that at the beginning of the compression tests the samples tend to appear slightly overconsolidated. The initial pre-consolidation pressure for dredged materials can be estimated using empirical relationships by means of the liquidity index. For the samples with a high liquidity index, in the range of 2.33 to 2.46, the expected preconsolidation stress would be lower than the initial load step of 2 kPa. For the samples with an initial liquidity index of 0.81 to 0.89 the corresponding value would be in the range of 5 and 20 kPa. Hence, for the second series the C_c is determined as the average slope of the compression curve between 20 and 160 kPa. The initial reloading slope C_{r0} is defined based on the slope of the compression curve between 2 and 5 kPa. The swelling index C_s is determined based on the average slope of the unloading steps from 160 kPa to 5 kPa. The results are summarised in Table 3.5. Starting from the latter it is interesting to note that oxidation dramatically reduces the swelling amount of the soil upon unloading, indicating that the water holding capacity reduces significantly. In addition, the samples which were oxidised in-situ under load have a lower swelling index compared to the one of the ex-situ oxidised sample. The result seems to suggest that the structure changes

experienced during the collapse of the metastable structure also reduce the swelling potential of the soil. The slope of the reloading lines is not constant, and depends on the stress-oxidation history of the soil. In general, the higher the collapse strain during oxidation, the smaller the C_r upon reloading. A dramatic difference between the C_c of the non-oxidised and the ex-situ oxidised soil can be appreciated. On the contrary, the reference C_c of the in-situ oxidised samples does not differ much from the one of the natural soil. This is an important result, suggesting that the fabric of the in-situ oxidised samples differ significantly from the ex-situ oxidised ones.

Table 3.5: Changes in soil properties as a consequence of compression and oxidation in the oedometer cell and ignition afterwards

Sample	Before compression			After compression			Solid mass loss during compression			Solid mass loss by ignition							
	w [%]	G _s [-]	e [-]	LI [-]	w [%]	G _s [-]	e [-]	LI [-]	before [g]	after [g]	loss [g]	LoI [%]	G _s [-]				
<i>Oxidation at 5 & 20 kPa</i>																	
non-oxidised	1100	1.8	17	2.46	298	1.82	4.4	0.2	5.7	5.6	0.03	0.5	5.62	2.97	52.8	n.d.	
oxidised in-situ (5 kPa)	1086	1.8	20	2.42	252	1.89	3.3	0.07	4.9	4.5	0.4	8.2	4.46	2.13	2.33	52.2	n.d.
oxidised in-situ (20 kPa)	1086	1.8	22.1	2.42	213	1.84	3.3	-0.04	5.6	4.9	0.76	13.6	4.94	2.5	2.44	49.4	n.d.
oxidised ex-situ	460	1.97	9	2.33	149	2.03	3	0.15	12.6	12.4	0.24	1.9	12.2	8.67	3.53	28.9	n.d.
<i>Oxidation at 5, 20 & 80 kPa</i>																	
non-oxidised	514	1.82	9.6	0.81	259	1.82	4.5	0.09	11.1	11	0.11	1	10.82	5.53	5.29	48.9	2.62
oxidised in-situ (5 kPa)	513	1.82	9.5	0.81	245	1.84	4.4	0.05	11.3	11.2	0.09	0.8	11.09	5.79	5.3	47.8	2.74
oxidised in-situ (20 kPa)	513	1.82	9.5	0.81	228	1.83	4	0	11.2	10.9	0.29	2.6	10.88	5.69	5.19	47.7	2.66
oxidised in-situ (80 kPa)	514	1.82	9.2	0.81	205	1.83	3.3	-0.06	11.1	10.9	0.26	2.3	10.79	5.63	5.16	47.8	2.67
oxidised ex-situ	254	1.91	4.5	0.89	148	1.88	2.5	0.14	21.5	21.5	0.01	0	7.95	5.08	2.87	36.1	2.65

For the non-oxidised and ex situ oxidised samples the compression index and swelling index can be determined from the slope of the compression curves. Following the consolidation theory of Terzaghi, the simplified compression curve consists of linear sections, with two distinct values for the slope: the compression index C_c represents the slope of the void-ratio-effective stress plot for the normally consolidated part, whereas the swelling index C_s represents the gradient of the overconsolidated part of the loading curve or the slope of the unloading curve. For normally consolidated soils the preconsolidation pressure (or overconsolidation ratio) can be estimated using empirical relationships with the liquidity index. Hence for the samples with a high liquidity index in the range of 2.33 to 2.46 the expected overburden pressure would be lower than the initial load step of 2 kPa. For the samples with an initial liquidity index of 0.81 to 0.89 the corresponding overburden pressure would be in the range between 5 and 20 kPa. Hence for the second series the C_c is determined as the average slope of the compression curve between 20 and 160 kPa and the C_s is defined based on the slope of the compression curve between 2 and 5 kPa and the average slope during the unloading of the samples.

3.5. DISCUSSION

Overall, the shape of the compression curves suggest that ex-site oxidation changes the initial fabric of the sample, while in-situ oxidation affects the initial fabric of the natural soil by means of structural changes similar to those obtained by loading. The volume change experienced during on-site oxidation under load appear to have a similar effect as secondary compression (creep). The comparison between the effects of natural creep and oxidation upon reloading show that the pattern of behaviour is similar, although oxidation is able to trigger a much higher reduction in void ratio. Understanding the mechanisms responsible of secondary compression (creep) in organic soils is a real challenge to engineers. Many mechanisms have been suggested in an attempt to explain the soil creep deformation in coarse and fine grained soils, such as (1) breakdown of interparticle bonds, (2) jumping of bonds of molecule structures, (3) sliding between particles, (4) water drainage from micropores to macropores, and (5) structural viscosity (Le et al., 2012). However, these mechanisms were mostly suggested based on the observation of volume change under constant applied stress, without investigating the role played by environmental factors.

In organic soils, the development of secondary compression can be induced either by applied stress or an environmental impact such as oxidation. Oxidation is claimed to cause loss of soil integrity and to ultimately transform chemical substances to humic substances. The loss of organic matter can either be in the form of gas or solution (Hobbs, 1986). The fibres of the soil firstly suffer from breakage and reduction in size and strength, and eventually by permanent loss of the solid material (Wardwell et al., 1983). The additional settlement which results from decomposition specifically is a combination of two different mechanism that are (1) the volume loss due to microbial activity, which account the changes of organic substances and (2) fibres compressibility as the organic soil structure losses its integrity (Wardwell & Nelson, 1981). Although oxidation is believed to be slow in the field, it can rapidly increase when a stimulating environment is met. The soil samples used in this study consists of a mixture of visible and non-visible

fine fibres, organic material, fine particles and coarse material. In an effort to better elucidate the role of oxidation, creep due to compression at constant stress was measured to provide a reference for creep under the same applied stress accelerated by oxidation.

Based on the results obtained, the oxidised sample outside the cell show much lower C_c and C_s values compared to non-oxidised sample, suggesting that the two have a substantially different fabric from the beginning. On the contrary, in-situ oxidation acts on the original fabric of the soil, causing a metastable collapse, which however does not bring the state of the sample back to the one characterising the ex-situ oxidised one. The reference virgin compression line of the in-site oxidised samples almost remains the one of the non-oxidised sample. The oxidation process does not significantly change the volume of solids during secondary compression. This is probably due to the resistance of the organic material to decomposition through hydrogen.

These results suggest that the volume change experienced by the material undergoing in-site oxidation is mainly due to the expulsion of water from the macropores and micropores of the soil system. In the solid organic part, there are inner (micropores) and outer (macropores) voids saturated with water. During consolidation, the free water from the macropores is expelled, while under constant vertical effective stress the water which is held within the internal cells (micropores) is reduced, with a rate which depends on the permeability of the material. The time dependent development of settlement and its rate are analysed in more detail in the following chapter. It is worthwhile noting that the formation of gas may also further decrease the void volume, by reducing the amount of liquid inside the soil, and that the clayey constituents of the soil may have contribute to structural creep.

3.6. CONCLUSION

This study successfully was conceived to investigate the role of oxidation on the primary and secondary compression behaviour of the organic soil. Oxidation was accelerated using 10% Hydrogen peroxide solution. In an attempt to investigate the combined effect of fabric and oxidation on the soil compression behaviour, samples were oxidised outside the cell prior to the compression and the results upon loading were compared to the behaviour of the soil when oxidised in-situ under different constant vertical stresses.

The soil pre-oxidised ex-situ shows much lower compressibility and lower swelling capacity compared to non-decomposed soil. However, in-situ oxidation mainly acts on the metastable fabric of the original soil. The void ratio reduces abruptly, but it keeps higher than the void ratio characterising the state of the ex-situ decomposed soil for the same vertical effective stress. In-situ oxidation causes breakdown of the fabric, with a rearrangement of the fabric elements into a more stable arrangement.

At the end of the test, a small amount of mass solid loss occurred after the decomposition process, as a consequence of the resistance of the organic matter to the oxidising agent. This implies that the total volume change as a result of decomposition is not significant compared to other sources of compression, such as water drainage from the macropores and the micropores of the soil matrix and the structural viscosity of the clay minerals. Overall, the volume loss due to on-site oxidation is comparable to that due to loading, and it contributes to a minor part of the total settlement when the soil experi-

ences large changes in the vertical stress.

The study contributes to the understanding of the compression behaviour of organic soils induced by environmental impacts such as decomposition, and it is believed to contribute to improve the models for better predicting in situ settlements. However, as in depth understanding of the oxidation and decomposition mechanisms is not straightforward, a collaborative effort from different disciplines more focussing on the biochemical processes could be of further help in improving models for coupled compression and oxidation. These would allow to reveal the role of specific oxidising agent in relation with the identification of the group components in organic soils that are most susceptible to decomposition. By repeating these tests with different soils and/or oxidising agent, a general modelling tool combining the effects of coupled oxidation and decomposition is expected to become possible.

Notwithstanding its limitations, this study has investigated for the first time the effects of oxidation under constant different load, in an attempt to provide a first indication on the consequences of organic soil degradation on existing constructions and on possible future urban development. Also, the results offer a reference for ground improvement techniques designed to minimise land subsidence, and for assessing the consequences of anthropogenic activities such as groundwater table lowering, land drainage systems, and any other activity potentially leading to a change in the existing environmental conditions.

3.7. ACKNOWLEDGEMENTS

The authors acknowledge the following contributions of Delft University Technology (TU Delft) employee to the mentioned work: Arno Mulder for assisting geotechnical laboratory tests; Jolanda van Haagen with chemical tests and colleagues from geotechnical and geo-environmental research groups. Dr. ir. J.T.C. Grotenhuis, Environmental Technology, Wageningen University for giving the opportunity to involve in the project of Lift up Lowlands which was funded under STW Grant. The first author gratefully acknowledges a research scholarship from the Public Service Department of Malaysia and Universiti Teknologi MARA, Malaysia.

4

OXIDATION EFFECT ON CONSOLIDATION AND CREEP OF ORGANIC SOILS

*After primary consolidation is over in peat,
secondary compression occurs,
at a slower rate.*

Mesri

4.1. INTRODUCTION

Unexpected settlement in organic soils may occur during service life of buildings which may result in loss of service conditions of structures and infrastructures. Accelerated decomposition of organic matter is one of the factors that contribute to the long term settlement (creep) of soil besides imposed mechanical loading. In the Netherlands for instance, settlement problem due oxidation of organic matter is of great importance issue. This is because regular drainage for agricultural activities in organic soils often is performed and soil surface needs to be reclaimed due to subsiding low-lying areas. On the average, the settlement rate as a result of agricultural activities in peatland which induced by decomposition is about 10 mm per year whereas in drained areas of polders in western Netherlands are ranged from 1 to 2 mm per year (Camporese et al., 2006; Hoogland et al., 2012)

4

Under normal condition, decomposition process is regarded to be very slow and not being considered in settlement design calculations. However, it can stimulate significantly when suitable environmental of decomposition is condition is achieved which often neglected by engineers. For this reason, most of the buildings are at high risk for having excessive long-term secondary compression which commonly underestimate during geotechnical design stage. Decomposition is described as a process which involves the loss of solid organic matter by oxidation to either gas or dissolved compounds and disappearance of physical structure and change of chemical state (Hobbs, 1986; O'Kelly & Pichan, 2013). The physical and mechanical properties of organic soil are influenced by oxidation in two ways either by losing actual solid mass due to chemical decomposition that is often catalysed by micro-organisms present in the subsurface or by changes in the original structural fabric .

Based on the literature, several environmental factors can activate and accelerate this process tremendously such as changes in temperature, aeration, pH and nutrients as a result of groundwater fluctuation or human disturbances (Hobbs, 1986; Wardwell et al., 1983). Generally, the total settlement of saturated organic soils is divided into three separate components: immediate settlement, primary consolidation and secondary compression. Immediate settlement is described as a sudden reduction in volume due to expulsion and compression of gas in soil voids. Primary consolidation is the reduction in volume due to outflow of pore water from void spaces accompanied by a transfer of load from soil water to the solid skeleton. Secondary compression is an additional settlement which occurs due to rearrangement of internal soil structure after primary consolidation is completed under constant vertical effective stress (Skempton & Bjerrum, 1957). The factors influence the rate of secondary compression in soil are discussed by Green (1969), among others.

The mechanisms of secondary compression in soft soils have been discussed (Sridharan & Rao, 1982; Le et al., 2012; Takeda et al., 2012; Fatahi et al., 2013). However, all the studies focus on clay soil containing silt but not organic material. The effect of decomposition on the physical and engineering properties of low and highly organic soils are well documented (Al-Khafaji & Andersland, 1981; O'Kelly & Pichan, 2014; Pichan & O'Kelly, 2012; Wardwell & Nelson, 1981).

For organic soils, the secondary compression is based on macropores and microp-

ores concept (Zhang & O'Kelly, 2013). During primary consolidation, pore water is only expelled from the macropores, while during secondary compression stage, pore water is gradually expelled from the micropores into macropores DeJosselin (De Josselin de Jong, 1968). However, none these studies integrate the effect of decomposition. Secondary compression is influenced by decomposition in two ways (1) volume loss associated by microbial mechanism and (2) structure loses its integrity (Wardwell & Nelson, 1981). However, limited information is available looking at the direct effect of accelerated decomposition on the compression properties of organic soils. Al-Khafaji & Andersland (1981) for instance, investigated the settlement of paper pulp fibre-kaolin mixtures during decomposition. The samples were reconstituted at different initial organic content and decomposition was stimulated by nutrients and seed microorganisms before low constant vertical effective stress, 3.42 kPa was applied. Meanwhile, Wardwell & Nelson (1981) compared the settlement-time profile of cellulose fibre-kaolin mixtures with and without decomposition. Samples were firstly added with nutrients to stimulate decomposition and prepared at a vertical stress of 24 kPa in a moulding chamber before placing it in an oedometer under higher constant effective, 48 kPa stress for 6 months.

Settlement prediction model for organic soils which combine the coupling effects of mechanical loading and natural process (decomposition) needs to be established for better design estimation. However, this task is not a straightforward solution as we need to develop an actual measured settlement data for natural soil obtained from the field so that predicted model and measured data are fitting each other. Studies have been carried out to understand how decomposition affects the settlement behaviour, however, limited information is obtained looking at the decomposition effects on real or natural organic soils. This is because most of the samples were reconstituted at different degree of decomposition and also decomposition were stimulated earlier before constant loadings were applied which do not replicate the real condition at the field. Besides, the changes of consolidation properties with respect to different stress levels once accelerated decomposition take place are yet to be known. The loading and unloading response after the occurrence of decomposition in organic material are also still missing in the literature.

In order to fill the missing gap, this paper is structured to answer the following questions;

- How is the time-dependent deformation of dredged organic sediments when decomposed in-situ under normal and accelerated condition ?
- What is the effect of accelerated decomposition on the primary consolidation and secondary compression parameters at different stress levels ?
- Does oxidation at different constant loading influences the consolidation parameters in organic material ?

For this reason, an attempt has been made to study the effect of in-situ oxidation on the compression properties of a natural organic material. Consolidation tests were performed. In-situ decomposition was stimulated inside the consolidation cell using a chemical oxidant Hydrogen Peroxide under selected constant loads. The same tests were

also performed on reconstituted pre-oxidised samples in order to study the influence of soil structure on consolidation behaviour of organic soils.

In the following, a detailed characterisation of the tested organic material with the description of the test procedures are described. Then, the test results will be presented and evaluated based on the questions raised. The term oxidation and decomposition are used interchangeably as both have the same meaning only that oxidation is occurring at a faster rate than natural decomposition due to oxygen interaction in soil.

4.2. MATERIALS AND METHODS

Soil Characterisation

The organic sediments were dredged from the ditches and canals in the peat meadow area of Wormer and Jisperveld, the Netherlands. A series of classification tests were conducted according to the relevant standards (BS 1377-2, 1990; ASTM, 2007b). Particle size distribution was obtained by conducting wet sieving followed by Hydrometer test for fine-grained soils. For Hydrometer test, pre-treatment with 10% Hydrogen peroxide solution was done as the soil contains significant fraction of organic matter as specified in BS1377 (BS 1377-2, 1990). Water content was determined by drying the specimen for at least 24 hours in an oven at 105 °C. As the organic sample contains mostly water and less solid material, the weight of the dried sample should be checked so that there is no change in mass after further drying periods in excess of 1 hour (ASTM, 2008).

For Atterberg limit test, the organic sample was firstly spread on a tray and partially dried at room temperature of 20 °C to 25 °C. To accelerate the drying process of the material, a slow fan was used until sufficient water were removed to enable Liquid Limit test and Plastic Limit tests. The soil was mixed carefully in order to avoid excessive drying and to ensure uniform consistency. Falling cone method was carried out to determine the Liquid limit while Plastic limit was determined by rolling thread method. The specific gravity of solid was determined using gas-expansion pycnometer with 10 number of cycles by measuring the density of dried solids (ASTM, 2014). Organic content of test samples was determined using ignition method by firstly oven-drying at 105 °C for 24 hours and cooling down in a desiccator, to prevent adsorption of moisture from the atmosphere. The powdered dried samples were then placed in a muffle furnace at 500 °C for 4 hours and subsequently the ignited samples weight were measured (R.A.W, 2005). The degree of decomposition was identified by performing fibre content test on original and oxidised sample (ASTM, 2008). The elemental composition and micrograph of the test sample were analysed using Environmental Scanning Electron Microscope (ESEM) and Energy Dispersive X-ray Analysis (EDAX). Soil properties such as water content, fibre content, organic content, Atterberg limit and specific gravity were also performed on the oxidised sample with Hydrogen Peroxide where the details of the treatment are described in the following section.

4.3. SPECIMEN PREPARATION

Preparation of fully oxidised reconstitute sample

Decomposition activity was accelerated using Hydrogen Peroxide (H₂O₂). This chemical

solution is commonly used to remove organic matter as pre-treatment of organic soils in sedimentation test . In order to prepare a fully oxidised sample, 300 ml of 10 %(w/w) H_2O_2 was mixed with 100 g of partially dried organic sample. The amount of H_2O_2 proposed was expected to be sufficient to oxidise all the organic matter. Oxidation was carried out in batches in order to ensure that complete oxidation took place. Using a glass rod, the mixed solution with organic material was stirred gradually from time to time so that all the organic materials were well suspended. Distilled water was added occasionally to avoid excessive frothing and sample loss over the lip of the beaker. Once the froth subsided, the suspended solution was left overnight to allow complete reaction. H_2O_2 was added again the next day to confirm that the oxidation reaction was completed. Once no gas formation and frothing were visually observed, it was assumed that all organic matter had been oxidised. The solid fraction was filtered, washed with distilled water and dried in the oven for 24 hours at 105 °C, cooled down in a desiccator (Schumacher, 2002; Huang et al., 2009).

4.4. TESTING PROGRAMME

1-Dimensional Consolidation Test

Five types of samples were used for consolidation tests that are non-oxidised with creep at 5 and 20 kPa (NO_C5C20), oxidised at 5 kPa with creep at 5 and 20 kPa (O5_C5C20), oxidised at 20 kPa with creep at 5 and 20 kPa (O20_C5C20), fully oxidised with creep at 5 and 20 kPa (FO_C5C20) and non-oxidised subjected to 24 hours of loading (NO_24 hrs). Loading steps of 2, 5, 10, 20, 40, 80 and 160 kPa and unloading steps of 40, 10, 2 and 20 kPa were applied for all the samples. Each step took about 24 hours load duration. Note that the effect of Load increment ratio (LIR) on consolidation behaviour is not covered in this study. In order to study the effect of creep and in-situ oxidation on primary compression behaviour, samples were left under two stages of creep load at 5 and 20 kPa. Soil samples were firstly allowed to complete its end of primary (eop) compression in 24 hours although faster duration of eop is expected in organic soils. This is to avoid difficulties determining the end of primary compression or beginning of secondary compression. After 24 hours loading, secondary compression was already observed. Then, samples were left under the creep loadings for 9 days before continuing to the next incremental load.

For oxidised soils, in-situ oxidation was stimulated in the samples by replacing tap water in the consolidation cell by 10 %(w/w) Hydrogen peroxide during loading for a period of 9 days. This is because, during oxidation, the displacement-time plot showed a significant drop which eventually reached a constant displacement suggesting that oxidation was completed for at least 9 days. After the oxidation stage was ended, samples were allowed to complete the remaining loading and unloading stages in the same chemical solution. For the case of non-oxidised and fully oxidised sample with creep, the samples were left in tap water under creep load at 5 and 20 kPa for 9 days. At the end of consolidation test, the final thickness and water content were measured. The summary of the long-term compression and creep test program for the test samples is given in Table 4.1.

Table 4.1: Long term consolidation tests loading scheme for each sample

Loading stage	Stress level [kPa]	Load duration [days]	Samples identification			
			NO_C5C20	O5_C5C20	O20_C5C20	FO_C5C20
Stage 1	5	9	creep	creep + oxidation	creep	creep
Stage 2	20	9	creep	creep	creep + oxidation	creep

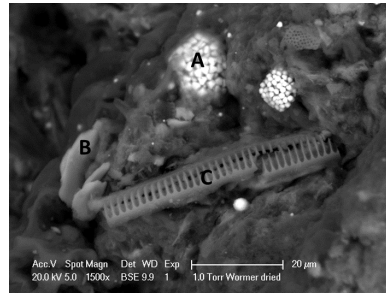
4.5. RESULTS AND DISCUSSIONS

Soil Classification and Physical Properties

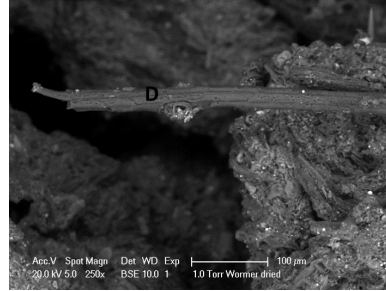
The natural water content of the organic sample is about 1200 % which is in the common range for natural fibrous materials (Mesri & Ajlouni, 2007). Sieving analysis on the original sample indicates that about 8 % of the solid particles (based on dry mass) passes the 63 μm sieve. Some traces of thin dark black plant fibres were observed. The sample has a very strong odour due natural decomposition of organic matter. The X-ray diffraction analysis revealed that the inorganic fraction of the soil contains mainly quartz, a significant amount of pyrite and some clay minerals. The Unified Soil Classification System (USCS) classifies a soil as organic when the ratio of oven dried to air dried liquid limit is less than 0.75. Highly organic soil such as peat are dark in colour with a strong odour and spongy texture.

Huang et al. (2009) proposed a classification system where a soil is classified as mineral if OC is below 3 % and mineral soil with organics if OC is between 3 % to 15 %. The term organic should be used for soils with OC more than 15 %. Soils with 15 % to 30 % OC are called organic soil and highly organic soil or peat when OC > 30 %. The weakness of this classification is that there is no distinction between highly organic soil and peat in terms of percentage of organic content. The ASTM standard proposed that soils with more 75 % OC are defined as peat. For this sample, it is more relevant to use the classification of peat proposed by ASTM D4427 due to the presence of visible fibre roots structure similarly to peat. ESEM analysis with EDAX showed that the inorganic fraction is mostly biogenic, composed of siliceous diatom skeletons, some calcium carbonate (CaCO_3) and in-situ formed pyrite framboids (FeS_2). There is only a very small fraction of clastic clay minerals observed composed of Si, Al, K (4.1). The SEM images of the diatom organics and fibres show surfaces to be finely perforated which are capable of holding relatively large quantities of water (O' Loughlin & Lehane, 2003).

The liquid limit and plastic limit of the original material are 582 % and 228 % respectively. The very high liquid limit is in the range of liquid limit for organic soils and peat (Hobbs, 1986). The plastic limit is below the A-line and within the boundary of peats when plotted in the chart of plasticity index and liquid limit as proposed by Hobbs (1986). The measured specific gravity (G_s) is 1.80 which is much lower than mineral soils. This value is strongly influenced by the amount and type of organic constituent in test samples (den Haan & Kruse, 2007; Hobbs, 1986). Organic compounds such as cellulose have a G_s value of approximately 1.58 and for lignin it is approximately 1.40. These compounds present in the organic soil and affects the compounded specific gravity (den Haan & Kruse, 2007). Based on the G_s value obtained, a preliminary estimation of Loss on ignition (LOI) can be calculated using Equation 4.1 as proposed by Skempton & Petley



(a)



(b)

Figure 4.1: Scanning electron micrograph of organic sediments from Wormer Jisperveld, Netherlands showing the presence of (A)pyrite framboids, (B)Clay minerals, (C)Siliceous diatoms and (D)fibre cellular material

(1970) where $G_{s,organic} = 1.4$, $G_{s,mineral} = 2.7$ and $C = 1.04$ respectively. The calculated LOI is 54 % while LOI measured is 51.2 %, seems agreeable to the corresponding correlation. Overestimation of organic content might occur in organic soil samples due to the loss of structural water present in some clay minerals by evaporation, decomposition of inorganic carbonates and oxidation of FeS_2 (den Haan & Kruse, 2007). The fibre content is 15 % which is classified as sapric / amorphous organic matter which corresponds to von Post scale H₇-H₁₀ (Landva et al., 1983).

$$\frac{1}{G_s} = \frac{1 - C(1 - N)}{G_{s,organic}} + \frac{C(1 - N)}{G_{s,mineral}} \quad (4.1)$$

For the oxidised samples, lower liquid limit and plastic limit are observed. The potential of water holding capacity organic content decreases with increasing oxidation as the plant tissues are broken down which mainly influence the liquid limit results (O'Kelly & Pichan, 2013). Besides, the liquid limit is highly dependent on the chemistry of the water and the cation exchange capacity of the soil (Hobbs, 1986). Slightly higher specific gravity value is obtained for oxidised sample as a result of breakdown, mineralisation of organic matter and increase in particle density. Higher mineral content and (or) higher degree of decomposition will contribute to higher specific gravity values (Huat et al., 2011; Hobbs, 1986). Lower fibre content is observed on the oxidised probably due to remoulding of the sample during specimen preparation causes considerable mechanical tearing

and breakage of the fibres besides the effect of decomposition process which leads to disappearance of the physical texture of the sample and also changing the complex organic composition into simpler forms of organic by-products (Al-Khafaji & Andersland, 1981). The summary of the test results is shown in Table 4.2:

Table 4.2: Summary of selected properties for non-oxidised and oxidised outside the cell samples

Properties	Unit	Non-oxidised	Oxidised ex-situ
Water content	%	1200	940
Liquid limit	%	582	270
Plastic limit	%	228	127
Plasticity index	%	354	143
Specific gravity	[-]	1.80-1.82	1.86-2.03
Fibre content	%	15	7
Organic content	%	49.28	42.7
LOI	%	51.23	44.9

Time-settlement plots

The time-settlement curves for all the samples due to the effect of creep load at 5 and 20 kPa are shown in Figure 4.2. For samples O5_C5C20 and O20_C5C20, it can be clearly observed that the effect of creep and oxidation causes significant settlement which later becomes constant once H₂O₂ was introduced at 24 hours. However, creep alone without oxidation shows almost constant height for NO_C5C20 and FO_C5C20 samples after 24 hours of loading period. Samples O5_C5C20 and O20_C5C20 display constant volume change behaviour after 10000 and 9000 minutes respectively. The flat curve indicates that oxidation process has ended completely which took about 9 days before subsequent load can be applied.

Effect of in-situ oxidation on secondary compression

The rate of settlement under the effect of oxidation is investigated by analysing secondary compression behaviour for both creep stages, 5 and 20 kPa. Secondary compression is defined as the additional compression that occurs after primary consolidation is reached under constant effective vertical stress. The amount of secondary compression is normally expressed in terms of the coefficient of secondary compression, C_α which is linked to the slope of the settlement over time. Different ways were reported to determine C_α either in terms of vertical strain as a function of logarithm of time, $C_\alpha = \Delta\varepsilon_v / \Delta \log t$ (Lambe & Whitman, 1969) or void ratio as a function of logarithm of time, $C_\alpha = \Delta e / \Delta \log t$ (Mitchell & Soga, 2005). In this paper, changes in void ratio is adopted as it refers to constant height of solid. Although the rate of secondary compression is believed to be constant with logarithm of time, it depends on the properties of the soil tested and test conditions (Fox et al., 1992). Figure 4.3 shows the plot of void ratio versus logarithm of time for both creep stages. A detailed analysis is performed on the settlement at the last log curve data of 24 hours loading (before oxidation) and after 24 hours loading (after oxidation) for oxidised and non-oxidised samples.

After 24 hours loading period, samples which are subjected to only creep load at 5 kPa

without oxidation in cell NO_C5C20 and FO_C5C20 show almost constant rate of secondary compression with logarithm of time. However, the oxidised sample O5_C5C20 exhibits tremendous increase in the rate of secondary compression shown by the steep slope of the curve which tends to flatten after 12 000 minutes. Similar behaviour is also observed for creep load at 20 kPa where constant rate of secondary compression are observed for samples without oxidation NO_C5C20 and FO_C5C20 while oxidised sample O20_C5C20 initially displays increase in secondary compression rate and flattens down after 100 000 minutes. The decrease in secondary compression is probably related to constant gas production rate associated with the product of oxidation of organic matter. Nevertheless, secondary compression still occurring probably due to rearrangement of soil particles after oxidation or compression of gas that is developed inside the pores. [Wardwell & Nelson \(1981\)](#) claimed that rapid increase in secondary compression when plotted in terms of vertical strain versus logarithm of time is associated to linear microbial activity and not necessarily related to instantaneous structural breakdown.

In order to provide a quantitative measure of the rate of secondary compression, Table 4.3 shows the summary of C_α values for both creep stages. Apparently, the C_α values at the end of oxidation stage are higher for all oxidised samples O5_C5C20 and O20_C5C20 compared to other remaining samples. Meanwhile, fully oxidised sample FO_C5C20 which is pre-treated with Hydrogen peroxide shows lower C_α values compared to non-oxidised sample NO_C5C20 implying that removal of organic content earlier from the soil before creep loading is applied besides having lower initial water content able to reduce the effect of secondary compression tremendously. It seems that the effect of creep alone may reduce the C_α values for all cases especially for pre-treated sample but the effect of creep and oxidation increases the C_α values. The increase in C_α after oxidation is believed due to decay from oxidation process which creates empty space or voids in soil specimen which subsequently occupied by soil particles causing additional volume reduction. Besides, gas formation as a result of oxidation also creates an empty voids inside the soil for the rearrangement of soil particles ([Boso & Grabe, 2013](#)). The increase in secondary compression rate may also relate to increase in tertiary compression ([Gokhan & Ahmet, 2003](#); [Szymański et al., 2004](#)). Different factors may influence the rate of secondary compression such as consolidation pressure, load increment ratio, temperature, thickness, permeability, organic matter, state of stress and remoulding ([Olson, 1989](#)).

Table 4.3: Changes of the coefficient of secondary compression for creep stages 5 and 20 kPa

Stress level [kPa]	Coefficient of secondary compression, $C_\alpha = \Delta e / \Delta \log t$							
	NO_C5C20		O5_C5C20		O20_C5C20		FO_C5C20	
	before	after	before	after	before	after	before	after
5	0.30	0.23	0.41	0.68	0.46	0.37	0.18	0.12
20	0.36	0.34	0.38	0.28	0.34	0.47	0.16	0.15

The changes of C_α for each vertical effective stress is plotted in Figure 4.4. For this purpose, the slope of void ratio versus log time at the end of 24 hours loading is determined. From the results, the effect of creep and oxidation causes a decrease in C_α in the

next step loading when oxidised at 5 and 20 kPa respectively. However, other samples show an increase in C_α from 5 to 10 kPa and later decrease from 20 to 40 kPa.

Effect of in-situ oxidation on primary consolidation parameters

Based on thorough literature studies, there are very limited data reporting the effects of creep on subsequent consolidation behaviour (Olson, 1989). The work of Olson (1989) on remoulded peat suggested that creep under any stress reduces the amount of primary compression on the next loading and has a similar effect to overconsolidation. Besides, he stated that primary and secondary effects are less easily separated on the second load and disappear altogether for all subsequent loads when referring to settlement-log time plot. Figure 4.5 shows the compression curves of void ratio versus logarithm time for one of the odometer samples.

It is apparent that the curves for non-oxidised sample do not follow the typical one-dimensional consolidation curves like inorganic soils. The typical type 1 ("S") curve is only observed at lowest pressure, 2 kPa with clear end of primary compression (eop). However, compression curves with higher consolidation pressures ranging from 5–160 kPa show almost flat with no clear inflection point. The presence of organic material in the soil with high water holding increases the equilibrium water content and corresponding void ratio at low stress level (Al-Khafaji & Andersland, 1981). Taylor's square root time method is preferred in order to determine the eop time under 24 hours of loading period. Some authors argue that the accuracy of eop time depends on the method used either Taylor square root time or Casagrande log time and pore water pressure measurement (Robinson, 1999). The drawbacks of each method used to evaluate the eop in highly organic soil (peat) is discussed by Colleselli et al. (2000). The eop consolidation time for all the tested samples is evaluated based on Taylor's square root time method in the absence of pore pressure data. Figure 4.6 shows the settlement plot 24 hours loading at oxidation stage 5 kPa and after oxidation stage, 10 kPa. To avoid difficulties in identifying basic parameters, creep is assumed to develop after the end of primary consolidation ends (Fatahi et al., 2013; Zhang & O'Kelly, 2013). Table 4.4 shows the summary of estimated eop consolidation time at 90 % degree of consolidation for all the samples.

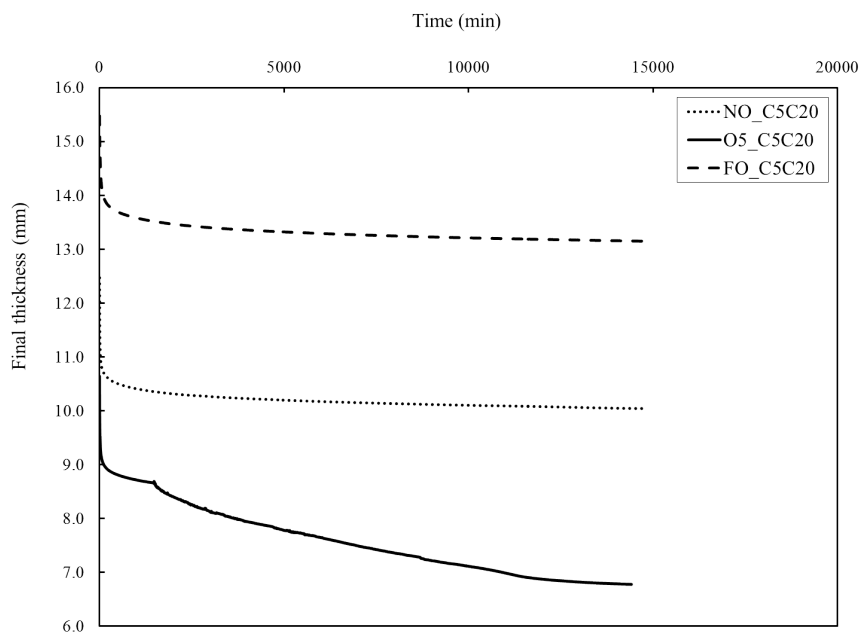
Table 4.4: Summary of end of primary consolidation time (eop) for all the tested samples using Taylor's square root time method

Pressure [kPa]	End of primary consolidation time (minutes)				
	NO_C5C20 $w_o = 1100\%$	O5_C5C20 $w_o = 1086\%$	O20_C5C20 $w_o = 1086\%$	FO_C5C20 $w_o = 460\%$	NO_24 hrs $w_o = 1207\%$
2	15.2	17.6	19.4	153.8	16.0
5	13.0	15.2	16.0	64.0	17.6
10	14.4	1.0	25.0	24.0	25.0
20	25.0	4.0	27.0	54.8	25.0
40	19.4	7.8	2.0	41.0	25.0
60	-	-	-	-	49.0
80	25.0	15.2	9.0	23.0	-
160	27.0	17.6	14.4	27.0	-

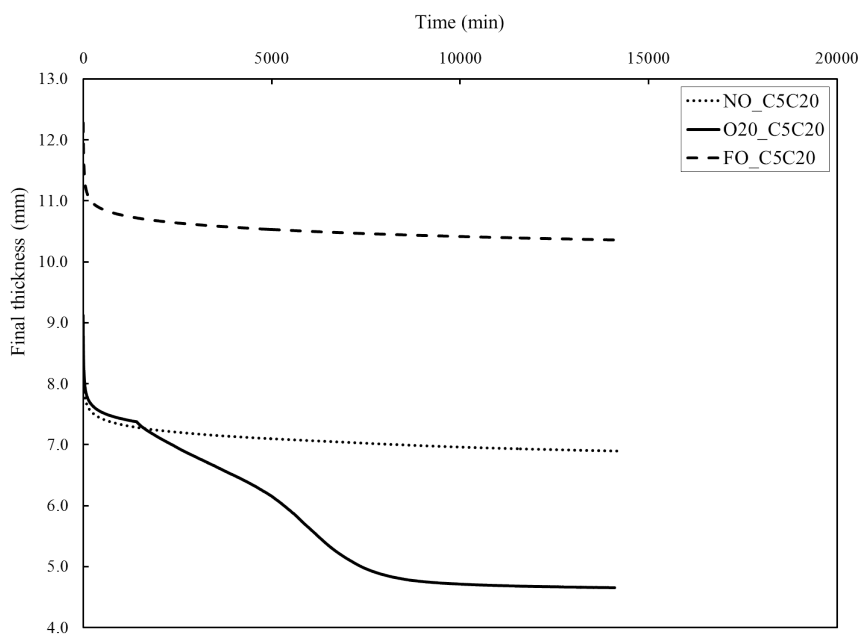
The oxidised sample with creep O5_C5C20 shows a significant drop of eop time from 5 kPa to the next step after oxidation, 10 kPa. Subsequent loadings after 10 kPa result to increasing values of eop time with increasing stress increments. Similar trend is observed for sample O20_C5C20 where shorter eop time is observed from 20 to 40 kPa after oxidation is taking place at 20 kPa and further increases at higher pressures. Meanwhile, the eop time for NO_C5C20 sample slightly change after creep effect at 5 and 20 kPa and also increases with higher pressures. This is probably due to the effect of oxidation causes solid organic materials and fibres to disintegrate into smaller particles and gas production creating empty void spaces before further loading is imposed to the soil. The increase in consolidation pressure and further reduction in void ratio contributes to higher eop time which is typical for all soils (Koti Reddy et al., 2014).

However, FO_C5C20 shows higher eop for all the steps compared to other samples. This seems logical because the pre-oxidised sample has less organic content with smaller soil grains and void spaces which give slower dissipation of pore water pressures compared to the non-oxidised sample which has bigger voids with porous structure (Hobbs, 1986; Mesri & Ajlouni, 2007). NO_24 hrs shows increasing eop time with increasing loading steps.

Settlement components in each sample at different consolidation pressures are gathered in Table 4.5. For sample O5_C5C20, it is striking to see that the effect of creep and oxidation at 5 kPa reduce the amount of primary compression and significantly increase the amount of secondary compression in the next loading, 10 kPa. Similar trend is observed for sample O20_C5C20 where an increase of primary compression is observed at 40 kPa when oxidised at 20 kPa. However, the effect of creep alone also shows the same trend but not significant as the previous case for samples NO_C5C20 and FO_C5C20 especially in secondary compression increment. Meanwhile, NO_24hrs which does not experience neither creep or oxidation has higher primary compression compared to secondary compression for each stress. Highly organic soil (peat) has high initial rate of primary consolidation and significant secondary consolidation where creep component always greater than secondary component (O'Kelly & Pichan, 2013). Oxidation causes breakdown of organic solid particles into smaller mineral grains which results to decrease in void spaces. Besides, it produces gas and creating air pockets around the solid grains. Hence, higher pressure increments cause higher compressibility or higher total settlement.

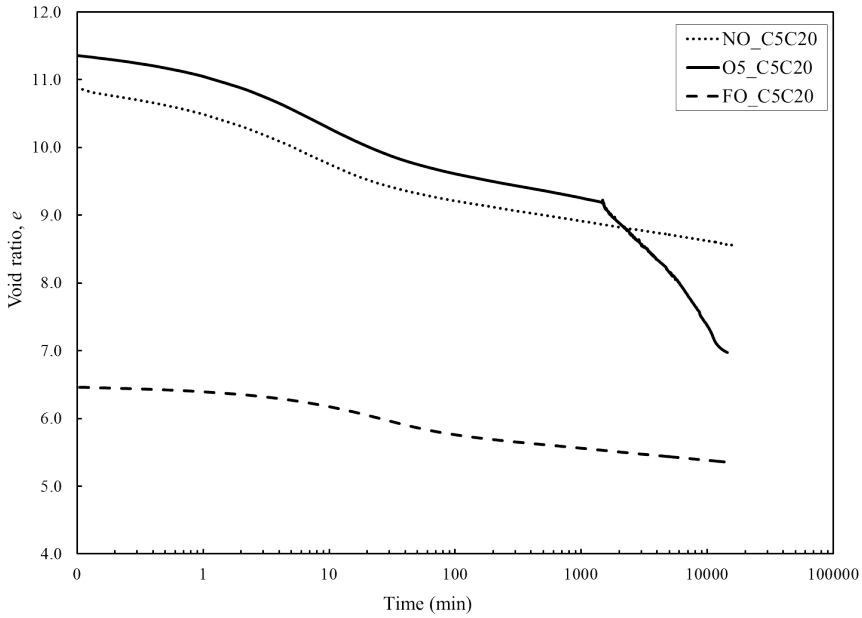


(a) 5 kPa

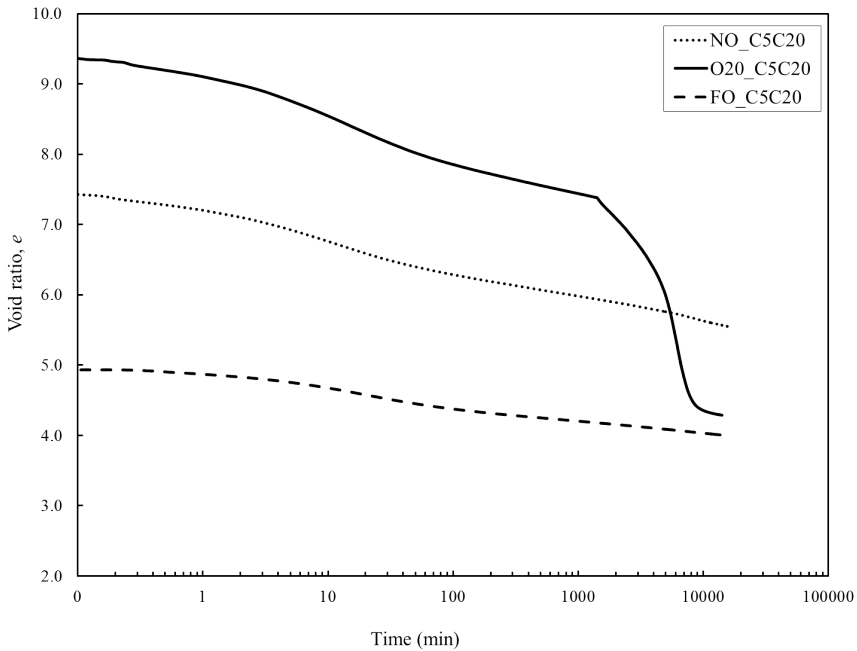


(b) 20 kPa

Figure 4.2: Settlement versus time plot for all oedometer samples during consolidation and creep at vertical stresses of 5 and 20 kPa

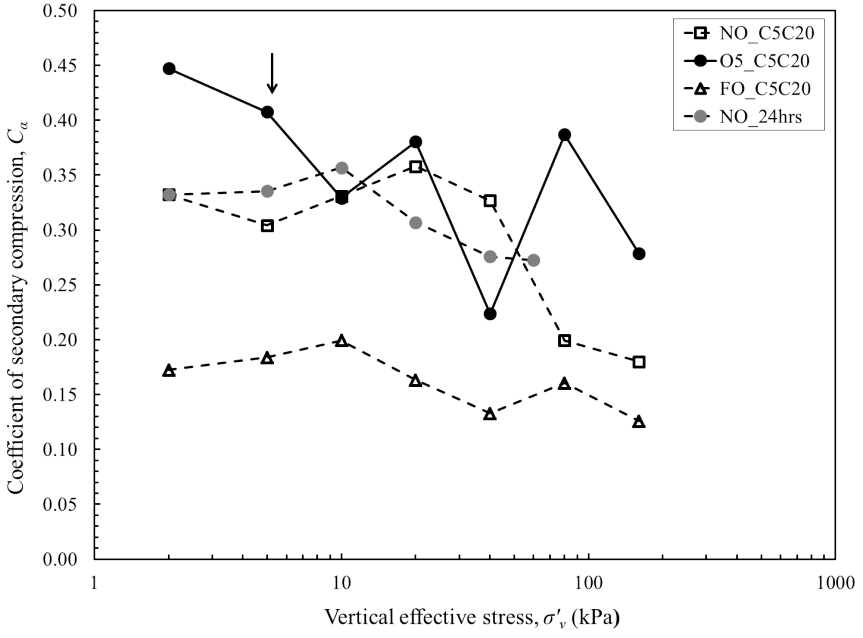


(a) 5 kPa

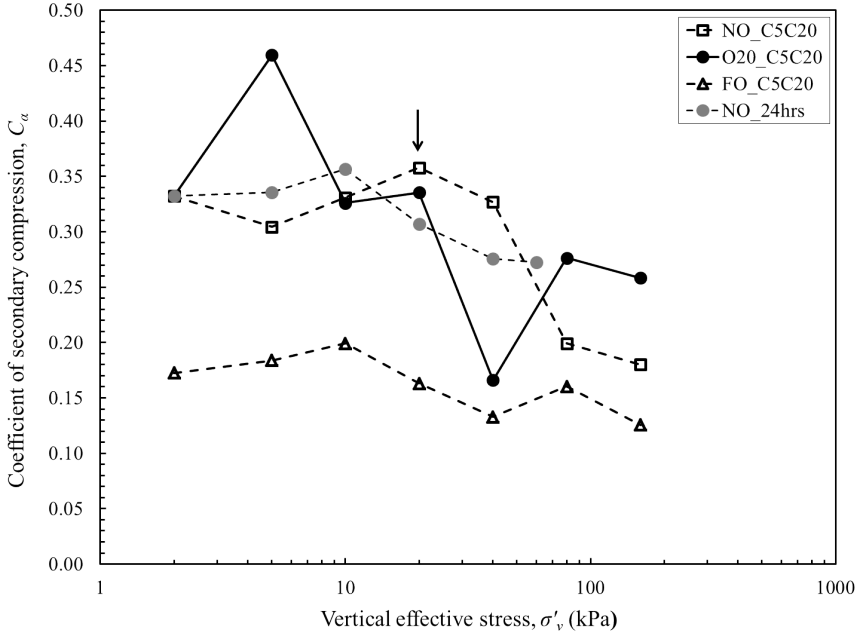


(b) 20 kPa

Figure 4.3: Void ratio versus logarithm time plot for all oedometer samples under constant stress of (a)5 kPa and (b)20 kPa



(a) oxidised at 5 kPa



(b) oxidised at 20 kPa

Figure 4.4: Changes of coefficient of secondary compression with vertical effective stress for all different samples in comparison with sample which is oxidised at 5 and 20 kPa

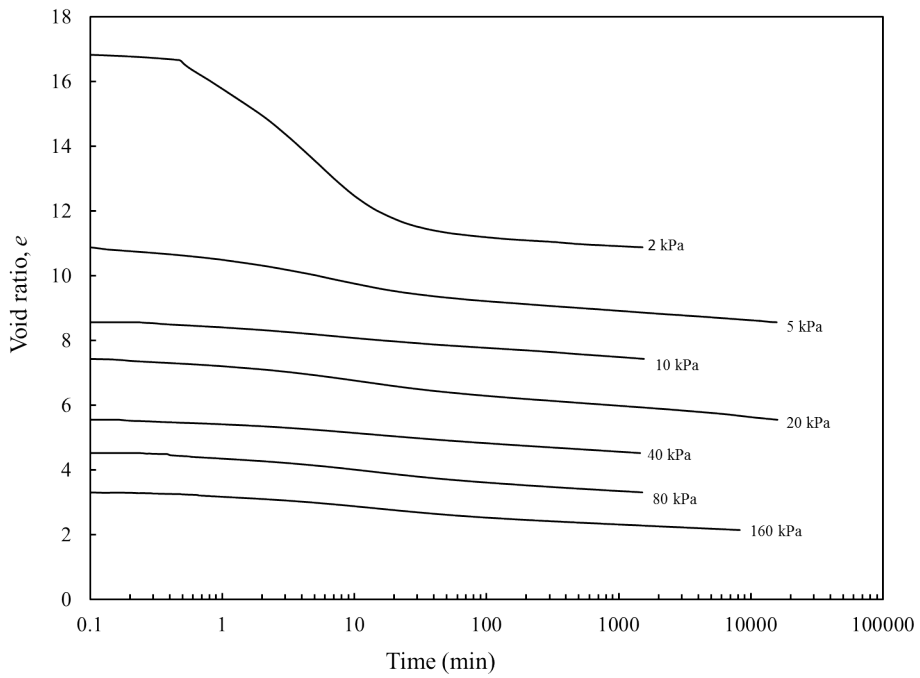
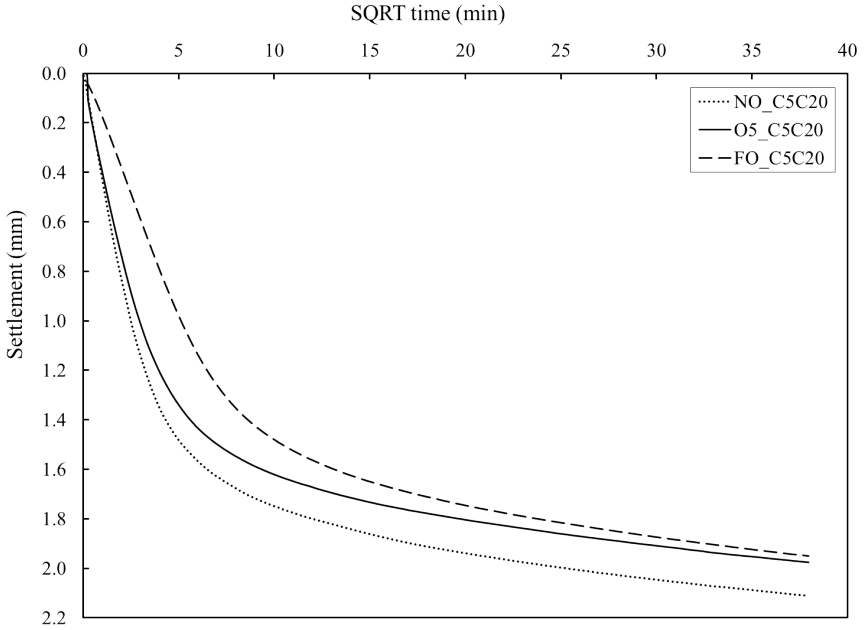
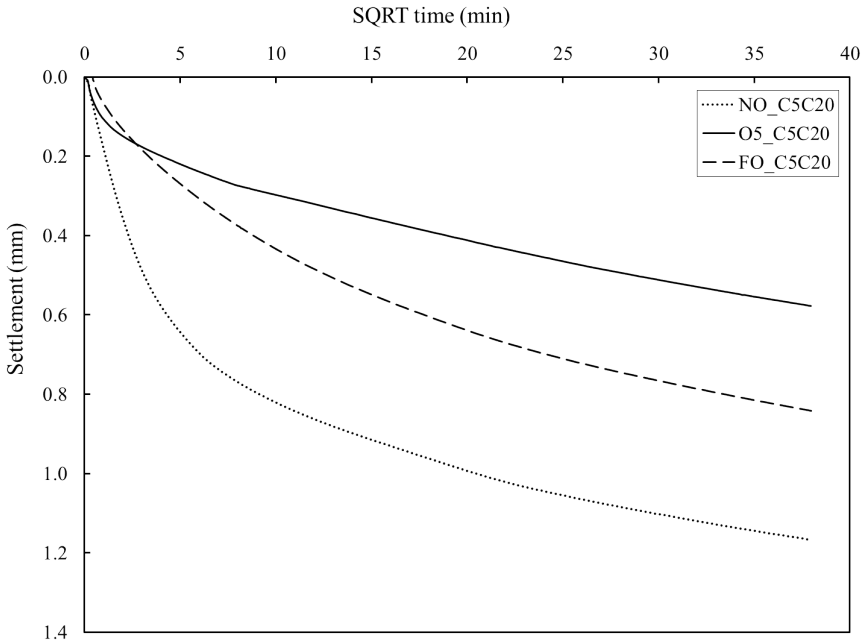


Figure 4.5: Sample of compression curves (e – time) for non-oxidised sample



(a) 5 kPa



(b) 10 kPa

Figure 4.6: Example of settlement-square root time curves at (a) $\sigma'_v = 5$ kPa and (b) after creep and oxidation stages at 5 kPa ($\sigma'_v = 10$ kPa) for 24 hours loading period

(a) Samples subjected to creep and oxidation and creep without oxidation

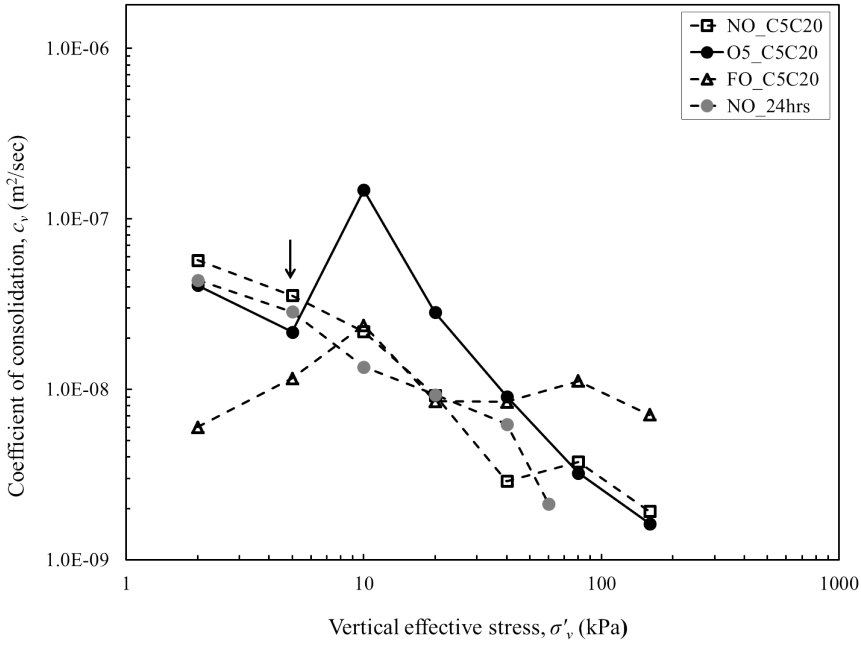
Vertical stress (kPa)	Different settlement components breakdown (mm)															
	NO_C5C20			DS_C5C20			O20_C5C20			FO_C5C20						
	S_i	S_p at 100%	S_s after 100%	S_i	S_p at 100%	S_s after 100%	S_i	S_p at 100%	S_s after 100%	S_i	S_p at 100%	S_s after 100%				
2	0.40	5.30	0.68	6.44	0.05	6.28	0.92	7.25	2.50	4.11	0.40	7.01	0.05	1.01	4.22	5.28
5	0.05	1.30	0.67	2.11	0.10	1.22	0.66	1.99	0.06	1.00	0.83	2.49	0.05	1.46	0.45	1.95
10	0.05	0.36	0.91	1.51	0.05	0.08	2.35	2.48	0.05	0.71	0.91	1.67	0.03	0.29	0.92	1.24
20	0.10	0.83	0.53	1.57	0.05	0.31	0.69	1.05	0.10	1.06	0.61	1.76	0.10	0.99	0.48	1.57
40	0.05	0.54	0.89	1.49	0.03	0.16	0.74	0.93	0.02	0.62	2.32	2.96	0.05	0.43	0.80	1.28
80	0.05	0.76	0.47	1.27	0.02	0.48	0.46	0.96	0.02	0.20	0.42	0.64	0.03	0.79	0.75	1.57
160	0.05	0.64	0.53	1.22	0.03	0.44	0.33	0.80	0.02	0.34	0.47	0.84	0.05	0.46	0.47	0.97

(b) Sample without creep and oxidation

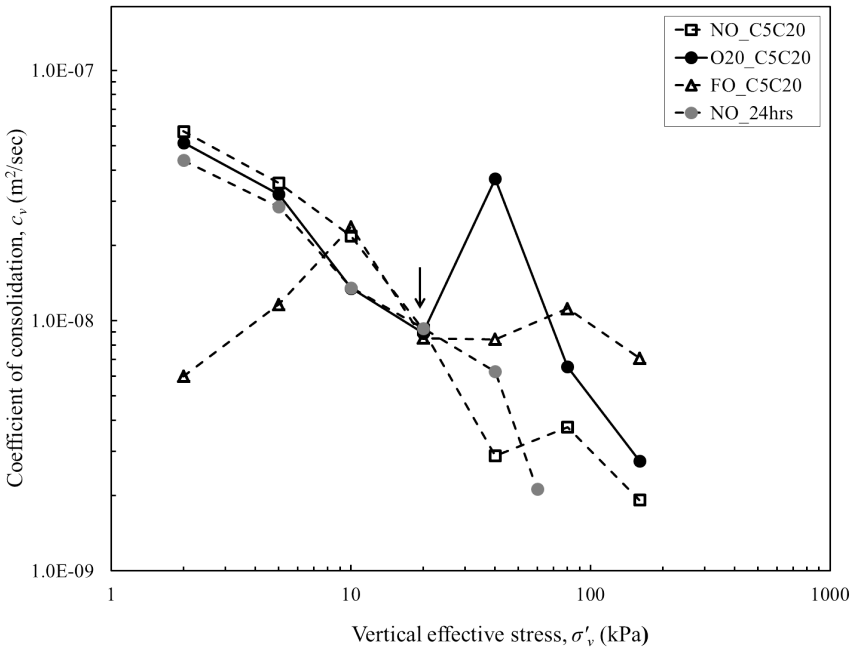
Pressure (kPa)	Different settlement components breakdown (mm)		
	S_i	S_p at 100%	S_s after 100%
2	0.05	1.00	8.00
5	0.10	1.67	0.24
10	0.05	1.11	0.29
20	0.05	0.89	0.21
40	0.05	0.83	0.06
60	0.05	0.47	0.36

Table 4.5: Summary of settlement components for different samples experiencing creep, creep and oxidation and without creep and oxidation effects

The coefficient of consolidation, c_v is used in order to describe the rate of compression in a particular soil and it depends on coefficient of permeability, k_v and coefficient of volume compressibility, m_v . It relates the change in excess pore water pressures with time and the amount of water expelled from the voids during consolidation. There is a wide variation in the value and trend of c_v reported for organic soils depending on which method is used to estimate the eop time. The relationships of coefficient of consolidation, c_v with vertical effective stress, σ'_v for all different sample conditions are shown in Figure 4.7. It is somehow surprising to see that sample O5_C5C20 shows a tremendous increase in c_v from $2.2 \times 10^{-8} \text{ m}^2/\text{s}$ to $1.5 \times 10^{-7} \text{ m}^2/\text{s}$ once creep and oxidation occurred at 5 kPa although these values at higher stresses. Similar pattern is observed for O20_C5C20 sample where higher c_v value is observed in the next step after creep and oxidation stage at 20 kPa from $8.9 \times 10^{-9} \text{ m}^2/\text{s}$ to $3.7 \times 10^{-8} \text{ m}^2/\text{s}$. This behaviour is also observed in FO_C5C20 sample. It seems that the effect of creep and oxidation increases the c_v values in the next pressure step. Meanwhile, NO_C5C20 sample shows decreasing c_v value after the effect of creep alone without oxidation at 5 and 20 kPa which is similar like NO_24hrs sample. Comparison is made with data presented by [Al-Khafaji & Andersland \(1981\)](#) on reconstituted sample which indicates that c_v decrease as decomposition occurred and this reduction is caused by formation of gas bubbles and reduction in the coefficient of hydraulic conductivity. This totally not the case for natural sample which was oxidised in-situ. The findings obtained by [Nie et al. \(2012\)](#) which stated that c_v increases with decreasing organic content seems to better agree with the results.



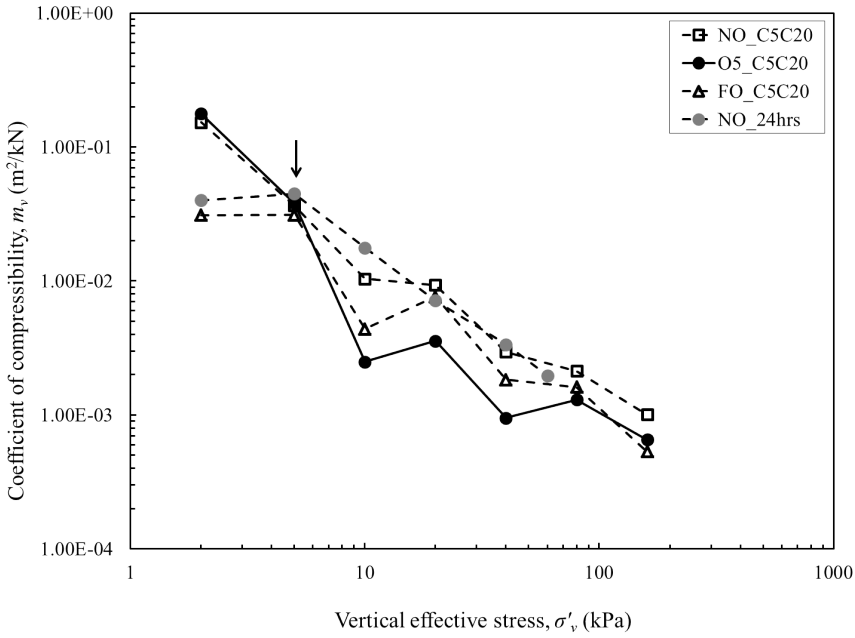
(a) 5 kPa



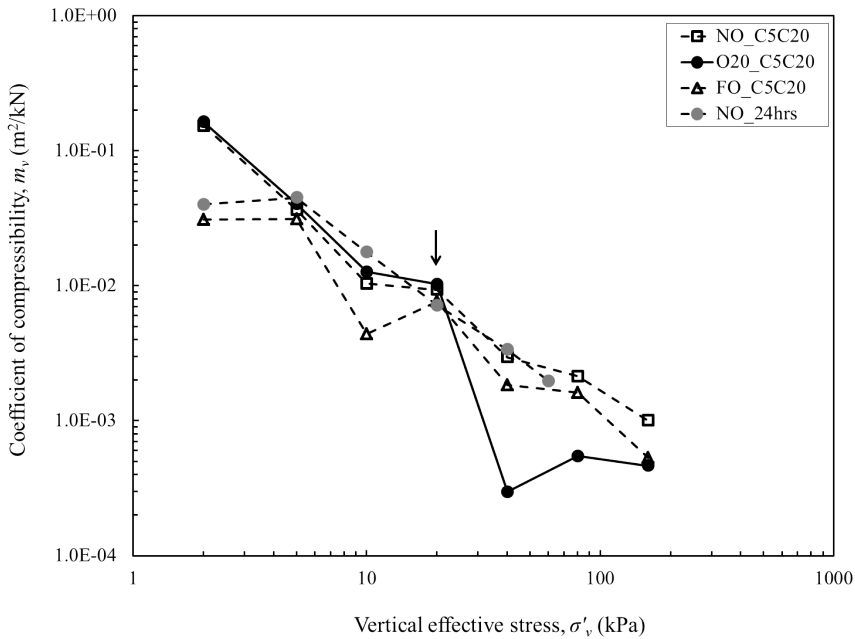
(b) 20 kPa

Figure 4.7: The change of coefficient of consolidation, c_v at different effective vertical stresses for all samples in comparison with oxidised at 5 and 20 kPa samples

The compressibility of samples can be described by coefficient of volume change, m_v . Figure 4.8 shows the comparison of coefficient of volume change $m_v - \log \sigma'_v$ for each sample. For sample which undergoes creep and oxidation, a significant change of m_v is observed compared to creep only. For instance, O5_C5C20 shows a sharp decrease in m_v value from 5 to 10 kPa while sample O20_C5C20 shows similar response from 20 to 40 kPa. For NO_C5C20, the creep effect at 5 and 20 kPa contribute to a slight decrease in m_v which is less influential compared to creep and oxidation effect. This implies that samples which are subjected to creep and oxidation show stiffer material response compared to creep only when further loaded. Meanwhile, sample FO_C5C20 shows lower compressibility compared to NO_C5C20 after creep at 5 and 20 kPa while NO_24hrs samples has the highest compressibility. It is claimed by that increase in degree of decomposition and effective stress in highly organic soils result to lower m_v values which justify the results (Badv & Sayadian, 2012; O'Kelly & Pichan, 2013). Organic soil such as peat decomposes, the void ratio declines and becomes stiffer and its structure is deformed steadily under secondary strain (Bell, 2000).



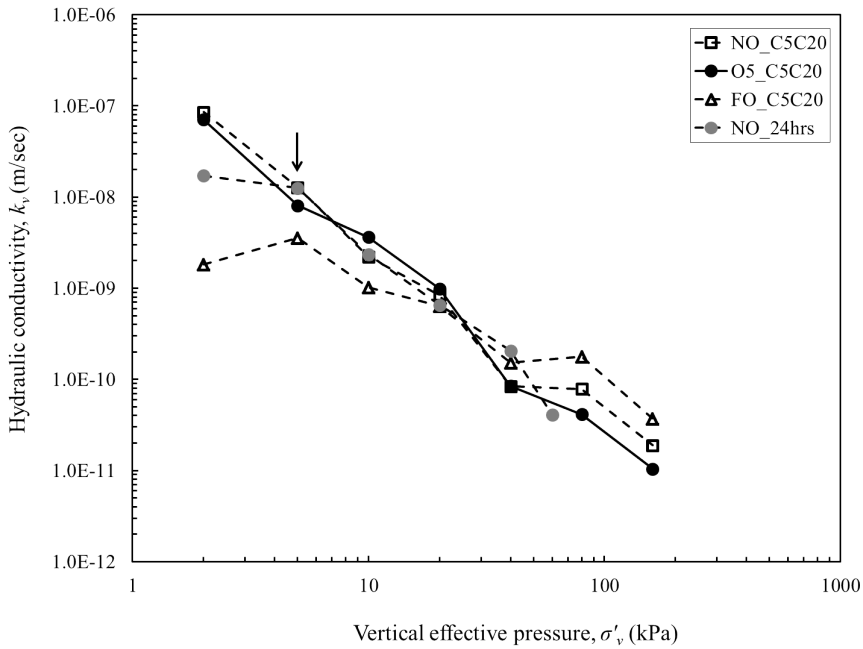
(a) 5 kPa



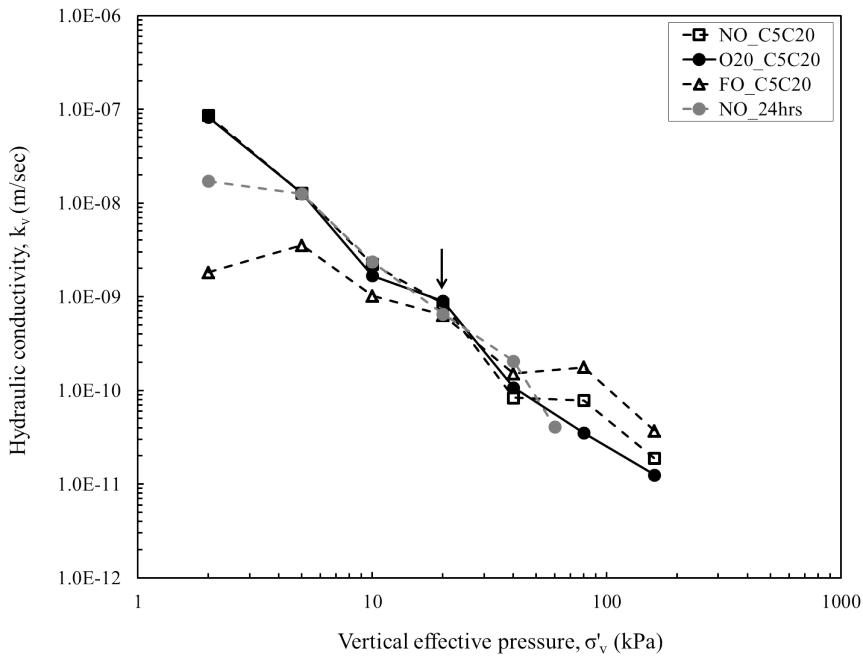
(b) 20 kPa

Figure 4.8: The change of coefficient of volume compressibility, m_v at different effective vertical stress for all samples in comparison with oxidised at 5 and 20 kPa samples

By substituting the c_v and m_v values, the coefficient of permeability, k_v for each load step of the tested soils can be estimated. O'Kelly & Pichan (2013) highlighted that the k_v values that based on the eop consolidation time are preferably estimated from pore-water pressure measurements rather than the typical settlement or volume change response. However, in this study pore pressure measurement is outside the scope of this paper. Figure 4.9 presents the plot of $k_v - \log \sigma'_v$ for all different samples. O5_C5C20 sample shows a decrease in k_v value from loading step at 5 to 10 kPa and subsequently decreases from 20 to 160 kPa. Similar behaviour is observed for sample O20_C5C20 where there is a reduction of k_v value after creep and oxidation occurred from step 20 to 40 kPa. Lower k_v value is observed in the remaining steps of the loading. The effect of creep alone also causing a decrease in k_v values together with other remaining samples. Many factors governing the permeability of organic soils such as expulsion of water from macro- and micro-pores due to primary and secondary compression, increase in volume of entrapped gas bubbles in macro-and micro-pores as a results of decomposition and clogging of the pores by bacterial mass or nongaseous products of bacterial respiration (O'Kelly & Pichan, 2013). Permeability of soil decreases when the volume of entrapped of gas bubble increases as a consequence of oxidation process.



(a) 5 kPa



(b) 20 kPa

Figure 4.9: The change of hydraulic conductivity, k_v , at different vertical effective stress for all tested samples in comparison with oxidised at 5 and 20 kPa samples

It is reported by Santagata et al. (2008) that for highly organic content soil (OC = 40-60 %), c_v is ranging between $9.2 \times 10^{-5} \text{ m}^2/\text{s}$ to $5 \times 10^{-8} \text{ m}^2/\text{s}$ and k_v is ranging between $2.1 \times 10^{-7} \text{ m/s}$ to $6.66 \times 10^{-11} \text{ m/s}$. The results obtained seem reasonable with the values reported.

4.6. CONCLUSION

In this paper, the effect of creep with and without oxidation on the primary consolidation and secondary compression behaviour is investigated through the performance of a series of conventional and long duration of one-dimensional compression tests. These tests are performed on five different types of sample which are NO_C5C20, O5_C5C20, O20_C5C20, FO_C5C20 and NO_24 hrs with different testing conditions. Creep at 5 and 20 kPa are applied for each case except for NO_24 hrs which follows 24hrs normal loading. The coefficient of secondary compression, C_α is determined for each stress level together with primary consolidation parameters such as coefficient of consolidation, c_v , coefficient of volume of compressibility, m_v and hydraulic conductivity, k_v . The following conclusions are drawn from the experimental data and analysis:

- (a) Physical properties of organic sediments are significantly different from those of inorganic soils and vary in a wide range due to oxidation process.
- (b) Given the limitation of the method, it can be stated that it is impossible to identify the end of primary compression using Casagrande's log time method due to the flat shape of the curves. Therefore, Taylor's square root time method is adopted in the analysis.
- (c) After creep and oxidation at both stress levels, the primary settlement is reduced significantly but secondary settlement increases significantly in the following loading step. Similar behaviour is observed for creep effect only but not as influential as the previous case.
- (d) There is an increase in C_α after oxidation especially for samples O5_C5C20 and O20_C5C20. Although oxidation comes to the end, secondary compression still occurs with constant logarithm of time. The other remaining samples show a decrease in C_α at the same period with NO_24 hrs having the slowest rate.
- (e) The changes of C_α with stress levels indicate that creep and oxidation show a decrease in C_α in the next step loading for samples O5_C5C20 and O20_C5C20. However, other samples show an initial increase of C_α from 5 to 10 kPa and later decrease from 20 to 40 kPa.
- (f) Samples with creep and oxidation O5_C5C20 and O20_C5C20 show higher c_v values compared to creep sample without oxidation NO_C5C20. Although in general it is expected that c_v value to be dominated by the permeability of the soil, this is not the case from the results obtained as the permeability values decrease once creep and oxidation have taken place. The increase in c_v is due to a much stiffer response possibly related to the rearrangement of the soil particles as a result of

entrapped gas escape and change in fabric. This behaviour is also observed in FO_C5C20 sample. Meanwhile, NO_C5C20 sample shows decreasing c_v value after the effect of creep at 5 and 20 kPa which is similar to NO_24hrs sample.

- (g) Samples O5_C5C20 and O20_C5C20 which undergo creep and oxidation have the lowest compressibility which results in significant drop in m_v in the step after oxidation followed by FO_C5C2, NO_C5C20 and NO_24 hrs.
- (h) After oxidation step at 5 kPa to 20 kPa, a small decrease in k_v values is observed for creep with oxidation samples. The decrease in permeability results from the reduction in void ratio, .

Overall, the results suggest that the decrease in hydraulic conductivity, decrease in compressibility and increase in settlement rate after creep and oxidation effect are mostly related to entrapped gas bubbles. Until now, the understanding on the effect of entrapped gas on the compressibility behaviour of organic soil is very limited. Even, some authors believe that conversion of organic substrate into gases due to decomposition process is not responsible for the compressibility of organic deposits. However, the results suggest that gas plays an important role when looking to settlement of organic soils. This study provides a possible explanation to the combined effect of creep and in-situ oxidation. However, it does not tackle to the gas production rate during oxidation. Therefore, further study looking on the relation of settlement and gas production as a consequence of oxidation is worthwhile.

4.7. ACKNOWLEDGEMENTS

The authors acknowledge Arno Mulder and Jolanda van Haagen for assisting laboratory test at Delft University of Technology (TU Delft). Dr. ir. J.T.C. Grotenhuis, Environmental Technology, Wageningen University for giving the opportunity to involve in the project of Lifting up the Lowlands which was funded under STW Grant. The first author gratefully acknowledges a research scholarship from the Public Service Department of Malaysia and also home institute Universiti Teknologi MARA, Malaysia.

5

EVALUATING THE KINETICS OF OXIDATION OF ORGANIC MATTER IN PEATLANDS

*The rate of oxidation of organic matter,
depends on aeration, temperature,
nutrients and pH.*

O'Kelly

5.1. ABSTRACT

Aerobic oxidation of organic matter in organic soils and peatlands results in the loss of organic matter, which induces subsidence of soil layers causing structural damage to buildings and infrastructure and the emission of carbon dioxide which increases global warming. The rate of oxidation may be limited due to insufficient oxygen supply in the upper zone. However, when there is a significant drop in groundwater level, the oxidation rate may increase as soil loses its moisture and the zone of aeration becomes deeper.

Different methods have been proposed to estimate the rate of oxidation and resulting carbon dioxide production in peatlands. Most of these methods are based on empirical relationships with measured settlement rates, or on direct measurements carbon dioxide emission from the site. However, these methods do not provide a closed mass balance required to directly link the actual loss in organic matter and the observed settlement and reported carbon dioxide emissions. Also they do not investigate whether or how the observed rates may be affected by the limited supply of oxygen. Therefore, the actual loss of organic matter and potential carbon dioxide production that can be expected without any limitation of oxygen is yet to be known.

The aim of this paper is to compare different methods to measure the rate of aerobic oxidation and improve understanding about link between loss of organic matter, volume change, surface subsidence and carbon dioxide emission. The oxidation rate is measured in a bioreactor containing suspended organic matter, where it is derived from the oxygen depletion rate and evaluated under varying oxygen concentrations and it is measured in a one-dimensional consolidation test set-up, where it is derived from measured settlement and organic mass loss during chemical oxidation using hydrogen peroxide. For each approach the corresponding carbon dioxide emissions are calculated and the results and differences are discussed. The results of these experiments improve insight about the factors controlling oxidation, settlement and carbon dioxide emissions in peatlands and the effectiveness of proposed mitigation measures.

5.2. INTRODUCTION

Peat soils and organic soils are problematic material for engineered applications due to their high water and organic content, which results in poor bearing capacity and high compressibility. Due to scarcity of land, these soils are normally drained and reclaimed to meet societal demands in agricultural, recreational and urban development. In the Netherlands for instance, draining the groundwater table is performed regularly to allow agricultural activities such as dairy farming.

However, regular drainage and lowering groundwater levels will induce significant land subsidence which can damage buildings and infrastructure during service. Water management schemes resulting in fluctuating groundwater levels are considered to be the dominant process controlling the settlement rates for peat land (Dawson et al., 2010).

Subsidence rates in the Netherlands are reported ranging from 1-2 mm yr⁻¹ in the polders of the western part of the Netherlands for shallow drainage depth (0.1-0.2 m), up to 6-17 mm yr⁻¹ in areas with deeper groundwater levels (0.25-1 m) (Schothorst, 1977; Beuving & Van den Akker, 1996). Worldwide subsidence rates up to 2-3 cm yr⁻¹ are re-

ported in the temperate Sacramento-San Joaquin delta in California and more than 5 cm yr⁻¹ in tropical peatlands such as Malaysia (Camporese et al., 2006; Gambolati et al., 2003). According to Wösten et al. (1997), the total settlement of peatlands induced by drainage can be explained by three different mechanisms which are shrinkage, oxidation and consolidation. The mechanism for each component is described as follows:

Consolidation is the mechanical compression of the saturated peat layer below groundwater level as a result of an increase in overburden pressure from drained soil. A drop in groundwater level will increase the overburden pressure, due to loss of buoyancy force; *Oxidation* is the loss of organic matter, which directly results in solid volume loss. Aerobic oxidation, in which oxygen is used as oxidising agent, is considered the dominant process causing loss of organic matter in peatlands. A drop in groundwater level increases the depth at which oxygen can penetrate and aerobic oxidation can occur. *Shrinkage* is the volume reduction of peat above groundwater level as a result of desiccation induced by evapotranspiration.

Each time drainage occurs, primary consolidation occurs in the layer below groundwater level and shrinkage in the layer above groundwater table. After a few years, secondary compression will occur in the area above groundwater table as a result of oxidation (Kasimir-Klemedtsson et al., 1997). Until today, there is still a debate on which of these processes is the dominant process controlling the settlement of peatlands and how these processes are linked to one and another.

According to Schothorst (1977), several early studies in the Netherlands claimed that oxidation was not the dominant process contributing to peatland settlement compared to shrinkage when examining peat soil under grass with shallow drainage. However, in areas with very deep drainage, oxidation could become dominant. He claimed that of the total settlement of 6 to 10 cm, 65 % are related to oxidation of organic matter and shrinkage above the groundwater level, while 35 % (1 to 4 cm) was attributed to compression below the groundwater table.

When looking at the upper layer (above groundwater table) in the past 1000 years, he claimed that 85 % of the total settlement of 2 m were from oxidation of organic matter due its higher bulk density and mineral content while 15 % were from shrinkage. The effect of deeper drainage was less significant in deep peat because compression of this area had contributed to little settlement. For countries outside the Netherlands, in temperate and tropical peatlands, oxidation is seen as the major process contribution to land settlement. Various authors claimed that oxidation of organic matter in the aerated upper layer was the major mechanism causing irreversible long term settlement of drained peat soil (Ingebritsen et al., 1999; Camporese et al., 2006; Dawson et al., 2010).

Besides causing settlement, the oxidation of organic matter in peatland is also a source of carbon dioxide emissions. According to Hoogland et al. (2012), peatlands with subsidence rates of 10 mm per year produce 22 tonnes of carbon dioxide per hectare per year.

Estimation of these carbon dioxide emissions are made either from field measurements or laboratory experiments. Three methods to determine the rate of oxidation in terms of carbon dioxide emissions from farmed organic soils are reported. These methods are (a) by estimation from settlement rates; (b) by modelling using precipitation and temperature as input variable; and (c) by direct measurement carbon dioxide emissions

(van den Akker et al., 2008). Nevertheless, each method has its own drawbacks.

The first method uses an empirical relation between settlement and carbon dioxide emissions as described by Armentano & Menges (1986):

$$\frac{dm_{CO_2}}{dt} = F \cdot S_{mv} \cdot \rho_{so} \cdot f_{os} \cdot f_c \cdot \frac{M_{CO_2}}{M_C} \cdot 1000 \quad (5.1)$$

where;

dm_{CO_2}/dt = CO_2 emission [kg ha yr⁻¹]

F = fraction subsidence due to oxidation of organic matter compared to total subsidence

S_{mv} = subsidence rate [m yr⁻¹]

ρ_{so} = dry bulk density of the soil [kg m⁻³]

f_{os} = organic matter fraction of the soil [-]

f_c = carbon fraction in the organic matter. Considering glucose represents organic matter this value is 0.4 [-]

M_{CO_2} = the molar mass of carbon dioxide, i.e. 44 [g/mol]

M_C = the molar mass of carbon, i.e. 12 [g/mol]

This relation requires to estimate the fraction of settlement, which is attributed to oxidation. Armentano & Menges (1986) found that there is no fixed value for this fraction, but indicated it varied between 0.33 to 0.67. However, van den Akker et al. (2008) using the same formula, considered that shrinkage and consolidation are relatively fast processes and suggested attributed all settlement was solely due to oxidation ($F=1$).

The second method uses an empirical relation between the annual loss of height by oxidation and climate expressed as rain factor. The rain factor is calculated as a function of annual rainfall (mm) divided by annual mean temperature (°C). The lower the rain factor, the higher the peat oxidation (Kasimir-Klemedtsson et al., 1997). The carbon dioxide emissions calculated this way are unrealistically high compared to the other methods (van den Akker et al., 2008).

The last method involves direct field measurement of carbon dioxide emissions. Kasimir-Klemedtsson et al. (1997) used this method to compare carbon dioxide fluxes from cropped and uncropped land and indicated that carbon dioxide emissions from cropped land can be 38% lower than from uncropped land. However, when using this method it is complicated to distinguish contributions from different sources, such as photosynthetic and respiration activity of freshly growing plants or other microbes and fauna in the rhizosphere, or the aerobic or anaerobic oxidation of deeper and older organic peat material. It is not possible to separate the carbon dioxide fluxes for each of these sources and sinks based on measurement of the surface flux alone or link the carbon dioxide emissions directly to loss of organic matter and settlement in the organic soil.

Although it is evident that settlement rate, loss in organic matter and carbon dioxide emissions correlate and depend on groundwater fluctuations and climate, all three suggested methods fail to provide sufficient evidence for a mechanistic relationship leading to a closed mass and volume balance. It is clear from field measurements that settlement is not always completely due to oxidation and measurement of carbon dioxide emissions cannot directly be related to loss of organic matter through aerobic oxidation, the actual oxidation rate in the field cannot be directly determined. The oxidation rate

in soils is limited by the supply of oxygen. In case the oxidation rate is limited due to lack of oxygen supply, higher rates of oxidation and consequent settlement and carbon dioxide emissions can be expected when oxygen supply is stimulated for example during ploughing, through bioturbation by roots or burrowing fauna or as a result of ground water fluctuations. So far, the literature sources discussed in this study did not investigate the potential effect of transport limitation or substrate availability.

Hence, the objective of this paper is to quantify the oxidation rate under varying conditions and improve understanding about the kinetics of aerobic oxidation and the relationship between loss of organic matter, surface subsidence and carbon dioxide emissions. First, a conceptual model is presented to explain the different oxidation processes and the effect of oxygen availability and mixing conditions on the degradation rate and secondly laboratory experiments are performed under varying oxidising conditions (biological or chemical) and mixing regimes using a batch reactor containing suspended organic sediments and in a one-dimensional consolidation test set-up (oedometer). The rates of aerobic oxidation are quantified in terms of oxygen depletion rate, settlement rate and loss of solid mass. Consequently, these rates are converted to carbon dioxide emission rates using the simplified conceptual model for aerobic oxidation and the empirical correlation used by [van den Akker et al. \(2008\)](#). The results are compared with reported rates in literature.

5.3. CONCEPTUAL MODEL OF AEROBIC OXIDATION OF ORGANIC MATERIAL

Degradation of organic matter in peatland areas can take place on land or in the water both under aerobic and anaerobic conditions. The oxygen, which is used for aerobic oxidation comes from the atmosphere. The soil column can be divided in two zones. At the top zone, above the ground water level, sufficient oxygen is transferred from the atmosphere into the soil to allow for aerobic oxidation and below the ground water level the oxygen is depleted and anaerobic decomposition processes take place as illustrated in Figure 5.1. Fluctuations in groundwater level and presence of capillary water may cause the boundary between the anaerobic and aerobic zone to vary spatially and in time.

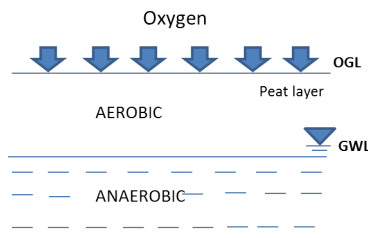
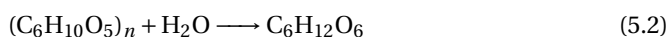
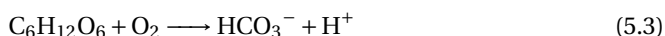


Figure 5.1: The subsurface can be divided in two zones based on the availability of oxygen

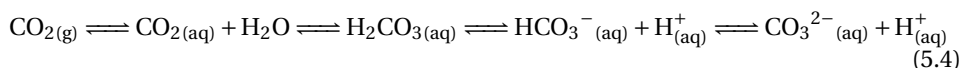
The aerobic degradation of organic matter in peatlands undergoes several steps. Plant materials are composed of a complex mixture of carbohydrates, mainly polysaccharides. These polysaccharides are polymers, which mean they are composed of a long chain of monomers, such as glucose, that are linked together covalently by glycosidic bonds. The three major types of organic matter, which are normally found in soil organic matter are all polysaccharides: cellulose, hemicellulose and lignin (Kogel-Knabner, 2002). Cellulose is reported to be the most abundant biopolymer. It forms the major structural component in plants, is described by the generic formula of $(C_6H_{10}O_5)_n$ and is formed by many units of glucose $C_6H_{12}O_6$ monomers. The first step in the degradation process is a hydrolysis reaction in which the polysaccharides are broken down in the smaller monomers, by reacting with water. The hydrolysis reaction is catalysed by acid forming bacteria (Pichan & O'Kelly, 2012). For cellulose breaking down to glucose the hydrolysis reaction can be written as follows:



The conversion of glucose to fully mineralised products is rather simple because oxygen respiring bacteria (aerobic bacteria) can degrade monomers completely to dissolved inorganic carbon (DIC) (Megonigal et al., 2004). Dissolved inorganic carbon is a weak acid and forms several equilibria in water. At neutral, pH bicarbonate HCO_3^- is the dominant DIC species, hence the oxidation reaction can be described as follows:



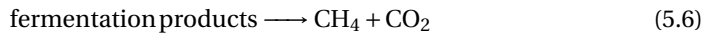
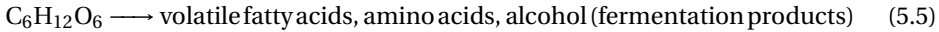
The produced bicarbonate is in equilibrium with carbonate CO_3^{2-} and carbonic acid H_2CO_3 . The carbonic acid is in equilibrium with carbon dioxide in the gas phase through Henry's law. The chain of equilibrium reactions can be written as follows:



As a result of the acid production at neutral pH the reaction shifts towards the left and most of the produced bicarbonate dissociates to carbonic acid of which a part transfers to the gas phase as carbon dioxide. The release of carbon dioxide to the atmosphere is related to the loss of solid organic mass and eventually leads to a volume loss, which in turn is related to land subsidence. Following the stoichiometry of the oxidation reaction, the availability of oxygen will influence the rate of aerobic oxidation and hence the settlement rate. Due to the limited solubility of oxygen in water, the availability of oxygen highly depends on the degree of water saturation in soil. Fluctuation of groundwater level will change the degree of saturation in the upper layer and increases the exchange of air from the atmosphere with the groundwater, which will stimulate the oxidation process. However, in many fine grained soils capillary suction allows the groundwater to rise significantly above the phreatic surface, hence the major part of the soil remains anaerobic.

The soil also degrades under anaerobic conditions. Anaerobic decomposition also involves a hydrolysis reaction to transform the solid organic matter (cellulose) into degrad-

able organic monomers (e.g. glucose). But after that these monomers undergo primary fermentation to low molecular weight products such as alcohol and volatile fatty acids. These primary fermentation products are either mineralised to CO_2 and CH_4 or undergo secondary fermentation to smaller volatile fatty acids. Secondary fermentation products are mineralised by respiratory organisms using inorganic terminal electron acceptors, such as sulphate SO_4^{2-} , nitrate NO_3^- or ferric iron Fe^{3+} , a process that yield CO_2 or CO_2 and CH_4 (Magonigal et al., 2004; Mer & Roger, 2001). The simplified scheme of reaction is as follows:



Anaerobic degradation of organic matter also causes soil mass loss and consequent layer compaction and subsidence and release of carbon dioxide and methane, however these processes are much slower and out of scope for this study.

5.3.1. EFFECT OF OXYGEN AVAILABILITY ON THE AEROBIC OXIDATION RATE

The reaction rate for aerobic degradation of organic matter is controlled by many factors, which may be biotic factors such as the type and degradability of organic material, the presence and composition of soil micro-organisms (bacteria, fungi, archaea) or biotic factors such as temperature, pH, oxygen availability, hydrology and pore water quality (Camporese et al., 2006; Brouns, 2016). The degradation process involves multiple enzymatic reactions. The overall reaction rate is determined by the slowest or rate limiting step. In most cases when sufficient oxygen is available, the hydrolysis of the macromolecular organic matter is considered the rate limiting step (Arndt et al., 2013). In case of aerobic oxidation of the organic matter, the overall oxidation rate depends on the availability of the oxygen and can be described using the Michaelis-Menten equation (Longmuir, 1954; Greenwood, 1961). This equation states that the rate, r , will eventually reach a plateau with increasing substrate concentration, $[S]$, provided that enzyme concentration is at steady state. The equation is given by:

$$r = \frac{V_{max}[S]}{K_m + [S]} \quad (5.7)$$

where V_{max} denotes the maximum reaction rate and K_m is the affinity or half saturation constant (i.e. the substrate concentration at which $r = 1/2 V_{max}$). Assuming a closed system to which no oxygen is supplied and oxygen is the limiting substrate, the rate at which oxygen is being consumed, i.e. the oxygen uptake rate (OUR), can be considered to be directly related to the rate at which organic matter is being degraded.

In an open system, oxygen may be transferred from the atmosphere to the ground-water. In that case, the oxygen concentration in the water phase depends the balance between oxygen transfer rate (OTR) and oxygen uptake rate (OUR):

$$\frac{dC_{O_2}}{dt} = OTR - OUR \quad (5.8)$$

The oxygen transfer rate, OTR, from the gas to the liquid phase can be calculated using:

$$OTR = k_L A (C^* - C_L) \quad (5.9)$$

Where k_L is the molar transfer coefficient, A is the surface area of the interface between the gas and the liquid phase, C_L is the oxygen concentration in the liquid phase and C^* is the oxygen concentration in the liquid phase when it is in equilibrium with the gas phase. The equilibrium oxygen concentration can be calculated using Henry's law:

$$C_{O_2}^* = \frac{p_{O_2}}{K_H} \quad (5.10)$$

where $C_{O_2}^*$ is the equilibrium concentration of the dissolved phase at the given temperature and ambient pressure, K_H is Henry's constant for oxygen and p_{O_2} is the partial pressure of oxygen in gas phase. With a partial pressure of oxygen in the air typically being about 0.21 atm and Henry's constant at 25 °C of 770 atm L/mol the equilibrium concentration of oxygen in the liquid phase is calculated at 2.72×10^{-4} mol/L.

In partially saturated conditions, the surface area of the interface between the gas and the liquid phase is large, which may cause the oxygen transfer rate to increase. Once the oxygen is transferred from the gas to the liquid phase, the concentration and distribution of oxygen in the liquid phase depends on the mixing conditions. In soil, the liquid phase is not stirred, consequently the oxygen is mostly transported by molecular diffusion, which is described by Fick's law.

$$J = -D \frac{dC}{dx} \quad (5.11)$$

As the diffusion coefficient is rather small (i.e. $D \approx 2 \times 10^{-9} \text{ m}^2 \text{ s}^{-1}$), diffusive transport is rather slow. Hence, it is expected that the oxygen is not able to penetrate deep into saturated soil, before it is being consumed by aerobic oxidation processes.

Ground water fluctuations, crack formation due to swelling and shrinkage, bioturbation by burrowing animals or root growth as observed in the field after 3 years of drying as shown in Figure 5.2 may enhance oxygen transport in the soil surface.

In shallow open water, the oxygen concentrations may be higher as waves, currents and wind or human interference through lake recreation and dredging activities enhance the mixing conditions and cause convective transport of oxygen rich water. These enhanced mixing conditions may also cause the settled sediments at the water bottom to resuspend and mix with oxygen in the water. It is expected that under these enhanced mixing conditions oxidation rates are higher.

5.3.2. CHEMICAL OXIDATION WITH HYDROGEN PEROXIDE

In order to accelerate oxidation of organic matter hydrogen peroxide is being used as a chemical oxidant. For example, when assessing the grain size distribution of fine grained

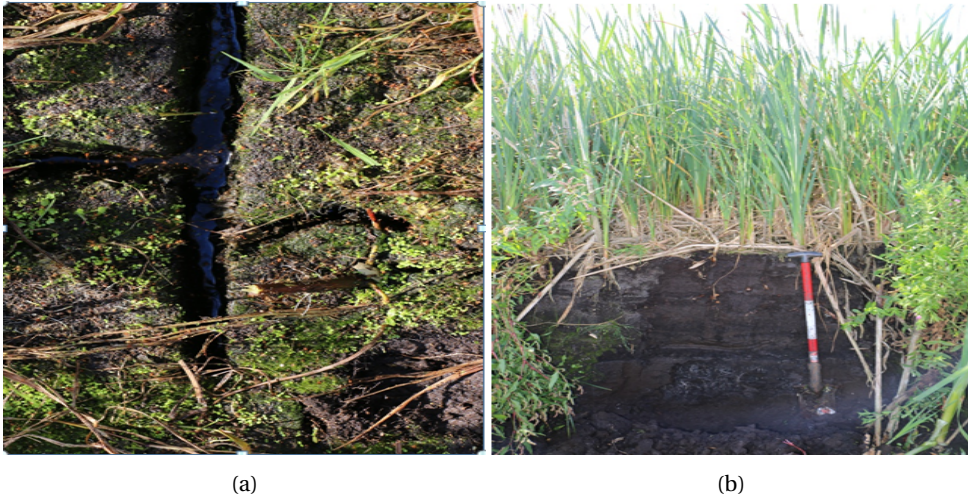
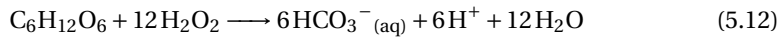
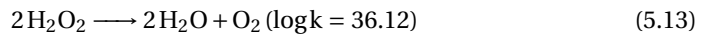


Figure 5.2: The dredged sediments from Wormer & Jisperveld after 3 years of drying through evaporation and downward drainage

soils using the hydrometer, oxidation with hydrogen peroxide is suggested as a pre-treatment method to remove the organic material (e.g. (BS 1377-2, 1990)). However, the efficiency of this method for organic matter removal is debated (Mikutta et al., 2005). Organic matter is chemically oxidised with hydrogen peroxide according:



However, hydrogen peroxide itself is thermodynamically unstable and can also decompose into oxygen (O_2) and water (H_2O) without oxidising organic matter. The decomposition of hydrogen peroxide can be written as below (Mikutta et al., 2005):



The oxygen produced by hydrogen peroxide decomposition consequently raises the oxygen concentration and may also stimulate the aerobic oxidation process.

5.4. MATERIALS AND METHODS

In order to evaluate the kinetics of oxidation and determine the effect of oxygen concentration on the oxidation rate, experiments are performed in a liquid batch reactor using two different oxidising agents and variable mixing conditions:

1. Oxidation under aerobic conditions in which oxygen is supplied by sparging and oxygen transfer between the headspace and the liquid.
2. Oxidation under controlled dosage of hydrogen peroxide.

Both regimes have been operated in stirred and unstirred conditions. The oxidation rate was determined based on the oxygen depletion rates in the liquid phase and based on the total mass loss during the entire experiment.

Secondly, oxidation experiments were performed to evaluate the kinetics of oxidation in the solid state using an oedometer set-up under accelerated oxidation conditions using a concentrated hydrogen peroxide solution. The oxidation rate was determined based on settlement rate and mass loss.

5.4.1. SOIL MATERIAL

In all the experiments an organic soil was used which was dredged from the lakes and ditches in the peat meadow area of Wormer & Jisperveld in the Netherlands as shown in Figure 5.3. The soil is characterised according to relevant standard methods BS 1377-2 (1990); ASTM (2007a), by determining its water content, specific gravity, organic matter content, pH and electrical conductivity (EC). The water content is determined by drying the soil in 105 °C oven ASTM (2010a). After drying, the sample is then transferred in the high temperature oven 500 °C for 4 hours to determine the organic matter content through loss on ignition (LOI) (R.A.W, 2005). The specific gravity of the solid phase, both after drying and after loss on ignition test is determined using gas-expansion pycnometer (ASTM, 2014). The elemental and mineralogical composition was determined by XRF and XRD and ESEM analysis using a Phillips XL30 Environmental Scanning Electron Microscope, with EDX spot analysis capability to detect the elemental composition as shown in Figure 5.4. The sample for pH measurements are prepared by putting 10 g of air dried organic soil in 10 ml demi water and 10 ml of 0.1 M NaCl respectively for a period of 1 hr (ASTM, 2004). Then, the pH and EC are checked using the Consort Data logger (SP10 and ST10 electrodes with C3010 datalogger).

The samples used in all experiments had a loss on ignition between 51 to 54%. Considering, this amount is the total organic matter, the amount of total organic carbon (TOC) can be calculated, which is 0.4 times the loss on ignition. Total organic carbon is often used as an indicator to describe the chemical components of organic matter in soil and sediments due to complexity measuring other components in organic matter. XRD, XRF and ESEM with EDX analysis showed that besides the organic fibers, inorganic minerals were also present in the oxidised sample and included such as quartz, pyrite, calcium carbonate and clay minerals.

BIOREACTOR SET UP

A 2 Litre – Bioreactor with electrodes and in-Control process controller (Applikon Biotechnology) was used. Electrodes measuring Dissolved oxygen (dO), pH and electrical conductivity (EC) were connected to the controller, calibrated and installed in the reactor. The pH sensor is calibrated using two different buffers having pH 7.0 and pH 4.0. The EC sensor is calibrated using a 0.1 M Potassium Chloride (KCl) solution. For the dO sensor a two-point calibration was performed using a beaker containing demi water under conditions of 0% dO by sparging with nitrogen gas and 100% dO by sparging with air. 100% dO corresponds to the dissolved oxygen concentration in equilibrium with the atmosphere at ambient pressure and a temperature of 25 °C, 2.72×10^{-4} mol/L. Using this factor, the

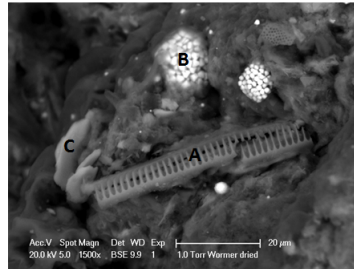


Figure 5.3: Image from ESEM analysis identifying the different components of the dredged organic sediments: A) siliceous diatoms; B) pyrite framboids; C) clay minerals embedded in a matrix of organic fibers

Element	C	O	Si	Al	Fe	S	Ca	K	Mg	Na
Bulk	59	31	5.1	1.9	0.8	0.9	0.6	0.4	0.4	0.2
Organic fibers	70 ↑	25 ↑	1.0	0.6	0.3	1 ↑	1 ↑	0.1	0.4	0.3 ↑
Diatom skeletons	56	36 ↑	6 ↑	0.8	0.2	0.4	0.3	0.1	0.2	<0.1
Pyrite framboids	51	14	2	0.8	11 ↑	20 ↑	0.3	0.1	<0.1	<0.1
Clay minerals	44	33 ↑	10 ↑	7 ↑	0.8	0.5	0.5	3 ↑	0.6 ↑	0.6 ↑

Figure 5.4: Elemental composition in atomic weight percentage for the different components in the dredged organic material

recorded dissolved oxygen concentrations (%) are measured and later converted back to concentrations in mol/L. After calibration, the sensors are transferred in the reactor containing demi water. The temperature in the reactor was controlled at 25 °C. The soil sample is added by mixing it with demi water and pouring it as a suspension in the reactor. Table 5.1 shows the initial properties of organic sample in the bioreactor.

After adding the soil, the reactor was filled with additional demineralised water up to a total liquid volume of 1.2 L. The composition of the bioreactor is described in Table 5.2.

After all sensors are installed and fixed tightly, the lid of the reactor and all ports are closed, except for the air inlet and outlet. The outlet is connected to a gas volume clock, which is composed of two glass measuring cylinders, places on a weight scale. The biggest measuring cylinder is filled with water and the other smaller one is placed upside down in the bigger one. The gas is allowed to flow into the small measuring cylinder and the weight of displaced water is representative for the produced gas volume. An air pump is connected to the inlet. Figure 5.5 shows an image the bioreactor with all relevant accessories connected to it.

EXPERIMENTAL PROCEDURE FOR BIOREACTOR EXPERIMENTS

Once reactor is set-up, stirring is started at a rate of 400 rpm. Using an air pump, the soil suspension is sparged with air. When all ports in the lid were closed, careful attention must be given to open the tube connected to the gas volume clock to avoid overpressure

Table 5.1: Selected properties of soil sample in Bioreactor

Properties	Unit	
Gravimetric water content	%	531
Organic content	%	53.7
Inorganic content	%	46.3
Mass of soil	g	100.0
Mass of dry solid	g	15.85
Total organic matter (TOM)	g	8.5
Total organic carbon (TOC)	g	4.9
	mol/C	0.4
Initial pH	-	6.7
Initial Electrical conductivity (EC)	$\mu\text{S}/\text{cm}$	835

Table 5.2: Composition inside the bioreactor

Component	Unit	Amount
Total volume reactor	L	2.2
Headspace	L	1
Soil	g	100(15.85 g dry mass)
Demiwater	L	1.2

in the reactor during sparging. Once achieving a maximum dO concentration, the air injection was stopped, the inlet gas tube was closed and the outlet was connected to a gas clock. However, based on the lack of produced gas volume observed in the gas clock, it appeared the reactor was not completely closed and they may have been some leakage. Consequently, in the remainder of the experiments the gas volume was not measured. Next, the organic material is allowed to react under stirring conditions, and at regular time intervals the stirring was stopped and the organic matter was allowed to oxidise under non-stirring conditions for several hours. During this stirring and non-stirring periods the dO, pH and EC were continuously monitored. In this experiment, 7 cycles of stirring and non-stirring cycles were performed. After the 4th non-stirring cycle the liquid was sparged with air a second time. After the 7th cycle stirring and sparging cycles were continued however the oxygen probe was malfunctioning, hence the dO values were not correctly registered.

The experimental procedure of the chemical oxidation using hydrogen peroxide was similar to the oxidation under aerobic conditions, with some adjustments. Before adding hydrogen peroxide to the suspension, the reactor was sparged with air, followed by a period of stirring without sparging and a period of non-stirring, during which the non-stirring was performed. Consequently, after the second stirring was started again and once a stable dO was reached, a solution containing 10 % (w/w) of H_2O_2 was added with a pump rate of 0.05 ml/min until a set point of 200 % dO was reached. A significant increase of dO is observed immediately after addition of H_2O_2 in the sample. The time of adding H_2O_2 from the beginning until reaching a set point of 200 % was recorded using a stopwatch. Once dO reached 200 %, the sample was allowed to react with H_2O_2 until

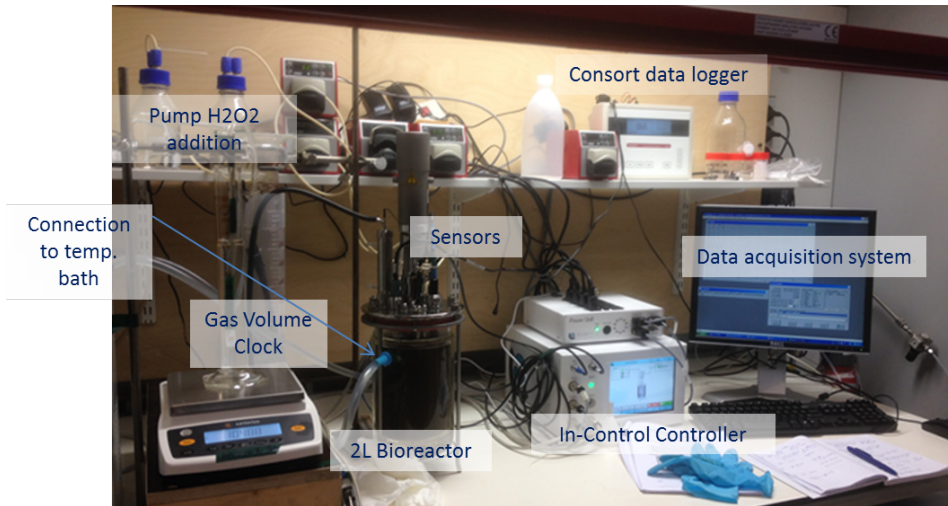


Figure 5.5: Bioreactor equipment with relevant configurations

almost reaching a stable dO value. Then, the stirring was stopped again for several hours, and the oxygen was allowed to deplete until 0% dO was reached. The same procedure was repeated six times. During the 6th dosage an overdose of hydrogen peroxide was added, and the mixed suspension was allowed to react until no further change in pH, EC and dO was observed.

At the end of both experiments, about half the volume of liquid was extracted, the solids were filtered out and the specific gravity, organic content of the solid fraction were measured. To the second half of the liquid a 1M sodium hydroxide NaOH solution was added, to bring back the pH to its original value around 6.5, after which the liquid was sampled and filtered and the solid fraction was analysed for specific gravity and organic content. Both solid fractions were also analysed using ESEM.

ONE-DIMENSIONAL CONSOLIDATION (OEDOMETER) SET UP

Oxidation experiments were carried out using a one-dimensional consolidation set-up or oedometer. Three sets of oedometer tests were performed simultaneously, in which each of the samples was allowed to oxidise at a different overburden pressure, namely 5, 20 and 80 kPa. Table 5.3 shows the initial properties of all the samples for oedometer tests.

The oedometer tests were performed following standard procedure (CEN, 2004c). The load was applied in incremental steps of 2, 5, 10, 20, 40, 80 and 160 kPa. During each load increment, the sample was allowed to drain for at least 24 hours, until the next load increment was applied. This was to ensure that the primary consolidation phase is not included in the calculation of settlement as a result of oxidation. For organic soils, primary consolidation occurs rapidly and secondary compression is considered more significant.

Analysis of the time dependent settlement indicated that within these 24 hours, end

Table 5.3: Selected properties of soil sample in Oedometer

Properties	Unit	Sample		
		O5	O20	O80
Gravimetric water content	%	513	513	514
Organic content	%	51.3	51.3	51.3
Inorganic content	%	48.7	48.7	48.7
Total soil mass	g	69.2	68.5	68.4
Mass of dry solid	g	11.3	11.2	11.1
Mass of water	g	57.9	57.3	57.3
Initial void ratio	-	9.3	9.3	9.4
Initial dry density	gcm^{-3}	0.176	0.176	0.176
Initial bulk density	gcm^{-3}	1.08	1.08	1.08
Total organic matter (TOM)	g	5.8	5.7	5.7
Total organic carbon (TOC)	g	2.3	2.3	2.3
	mol/C	0.3	0.3	0.3

of primary consolidation was reached and the samples experienced secondary compression (Zain et al., 2017). At 5, 20 and 80 kPa, one of the three samples was oxidised. At these pressure steps all samples were allowed to consolidate for a period of 10 days. For the sample, which was oxidised, the water in the oedometer cell, which was about 300 ml, was taken out rapidly and replaced by a 10% (w/w) hydrogen peroxide solution. Based on the amount of organic carbon and the stoichiometry of the oxidation reaction in Equation 5.3, it was calculated that 300 ml of 10% hydrogen peroxide solution was sufficient to oxidise all organic matter in the sample. During each oxidation period, the settlement was measured and compared with the other two samples which were not oxidised or already oxidised at an earlier time step. After consolidating the samples to 160 kPa, the load was removed in three steps of 40, 10 and 2 kPa, the samples were removed from the load frame and the change in mass, loss on ignition and specific gravity before and after oxidation were measured and compared.

5.4.2. ESTIMATING CARBON DIOXIDE PRODUCTION FROM OXIDATION AND SETTLEMENT RATES

The amount of carbon dioxide production was calculated differently for the different experiments. From the bioreactor experiments, the carbon dioxide production rate was calculated from the measured oxygen depletion rate per gram of dry soil.

From the oxidation experiments in the oedometer set-up the carbon dioxide emissions were determined in two ways: 1) from the measured settlement using the equation presented by Armentano & Menges (1986) and assuming that 100% of the settlement was caused by oxidation of organic matter according to van den Akker et al. (2008); and 2) from the measured loss in organic matter.

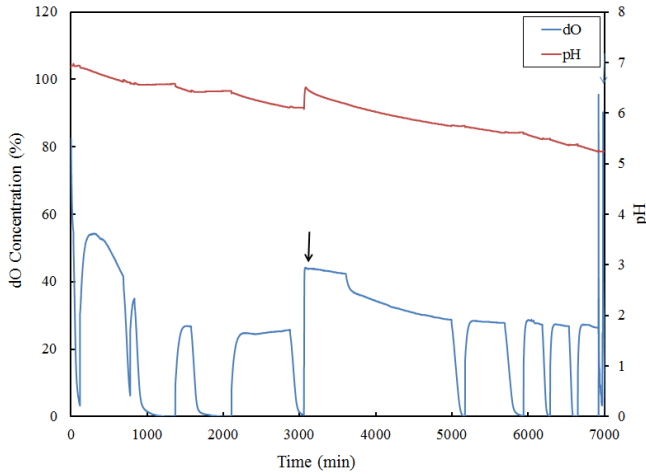
5.5. RESULTS AND DISCUSSION

BIOREACTOR EXPERIMENTS

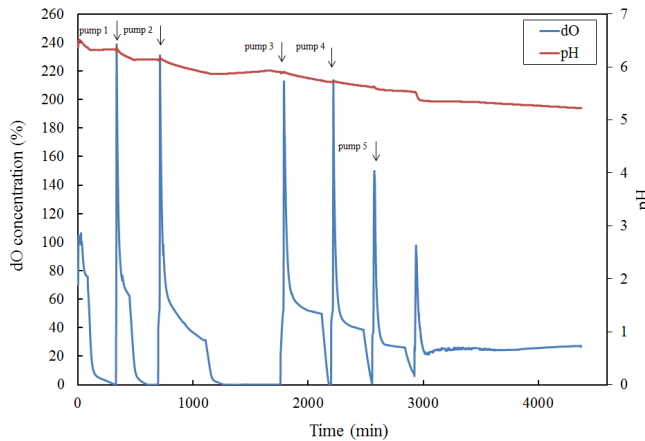
During the aerobic oxidation experiment, the dissolved oxygen (dO) concentration varied depending on the whether or not the suspension was aerated or stirred as shown in in Figure 5.6a. Each time when stirring was stopped, the suspended organic matter settled in the reactor and the oxygen level dropped rapidly at a relatively constant rate. The rate of oxygen depletion decreased when the dO level approached zero. When stirring was started again, a rapid increase of dO was observed until a maximum value was obtained. In the subsequent stirring and non-stirring cycles similar patterns were observed. Each time after stirring was stopped the dO level decreased to zero and when stirring was started again it increased to a constant level. The maximum dO concentration during stirring gradually decreased from 100 % at the start of the experiment to about 24 % after 1500 minutes in which 3 non-stirring cycles were performed. Since the reactor was not aerated during this time, it is assumed that the reduction in dO concentration is either the result of an increased oxidation rate or due to a partially depleted oxygen concentration in the headspace of the reactor. After 3000 minutes the reactor was sparged with air again replacing the air in the headspace. The maximum dO level initially went back to 43 %, but when sparging was stopped, and stirring continued, dO gradually dropped again. Several non-stirring periods were performed, showing patterns similar to the earlier non-stirring cycles.

The decrease in oxygen concentration during the non-stirring cycles indicated that the oxygen transfer from the headspace is limited by the diffusion through the water column from the headspace to the settling organic matter. As a result, the oxygen concentration gradually decreases until eventually the reaction rate goes to zero due to lack of oxygen. When stirring is started again, the organic matter is resuspended and in direct contact with the air in the headspace. The drop in oxygen concentration during stirring phases may indicate an increase in the oxidation rate or a gradual drop of the partial pressure of oxygen in the headspace and related equilibrium concentration in the liquid phase.

Figures 5.6b shows the results of chemical oxidation in stirred and non-stirred conditions. In the first period, the reactor was sparged with air and no hydrogen peroxide was added. A drop of dO was observed immediately after sparging was stopped. Once a constant dO was reached, at about 78 % stirring was stopped and a steep drop of dO was observed similar to Figure 5.6a. At the second stirring cycle, a first dosage of H_2O_2 was added, which resulted in an immediate increase in dO. The duration of adding H_2O_2 until reaching the dO setpoint of 200 % was recorded. After reaching the setpoint, the sample was allowed to react under stirring conditions in which the dO level showed a rapid decrease again. Part of this decrease may be due to degradation of organic matter, but considering that as a result of H_2O_2 decomposition into oxygen and water, the oxygen concentration is higher than its equilibrium value with the headspace, part of the rapid decrease in oxygen may be due to gas transfer from the liquid to the gas phase. The rate of oxygen depletion reduced when the dO level dropped below 100 % and the dO level continued to drop gradually during stirring conditions reaching values between 40 % and 20 %. In total, five H_2O_2 dosages were added. The amount of H_2O_2 added to



(a)



(b)

Figure 5.6: Measurement data of dissolved oxygen concentration and pH under stirring and non-stirring conditions with time under the influence of (a) aerobic oxidation and (b) chemical oxidation

reach the set point for each cycle increased with time as shown in Table 5.4. In cycle 6, it was not possible to reach the setpoint dO value of 200% although a high volume of H_2O_2 was added. Similar to the aerobic oxidation test several non-stirring cycles were performed in which the dO level showed similar patterns as for aerobic degradation.

During aerobic oxidation the pH gradually dropped from 7.0 to 5.6. Each time when the dO level was 0% the pH remained constant, which confirmed that the oxidation reaction was stopped. When stirring was started again, the pH continued to decrease further. When the reactor was sparged with fresh air, the pH went back up from 6.11 to 6.44, but

after sparging was stopped the gradual descent continued. After the 7th cycle, the dO probe was malfunctioning, hence no reliable dO values were recorded.

During chemical oxidation the pH showed a similar profile as observed during aerobic oxidation. The initial pH was lower, but the pattern was similar gradually decreasing from 6.4 to 5.2, except for the last dosage of H₂O₂. The large dosage during the 6th cycle caused a significantly faster drop in pH, which seemed to indicate an acceleration of the reaction rate.

Table 5.4: The amount of Hydrogen peroxide added to reach dissolved oxygen setpoint

Cycle	Pump number	Amount of H ₂ O ₂ added [ml]	Dissolved oxygen level setpoint [%]
2	1	0.49	200 %
3	2	0.54	200 %
4	3	0.62	200 %
5	4	0.79	200 %
6	5	2.71	140 %

Assuming that during non-stirring conditions the oxygen transfer approaches zero due to a limited diffusion rate, the change in oxygen concentration in the volume which contains organic matter is equal to the reaction rate (whereas close to the water surface in the volume which does not contain organic matter the concentration is slowly rising. As the dO electrode remains in the volume, which contains organic matter, the slope of the dO concentration profiles during the non-stirring cycles is considered equal to the reaction rate. In Figures 5.6a and 5.6b, this slope is plotted as a function of oxygen concentration.

The results for all non-stirring periods for aerobic and chemical oxidation are presented in Figures 5.7 and 5.8. Interestingly, these curves take approximately the form of a Michaelis-Menten saturation curve, which is used to describe the kinetics of enzymatic reactions. Consequently the reaction rate (or oxygen depletion rate) can be described using equation above and the experimental data can be used to determine the kinetic constants, i.e., the maximum reaction rate, V_{max} and substrate affinity constant, K_m . In cycle 1, V_{max} is higher than for the other non-stirring cycles. It is assumed that during this cycle the rate is higher due to availability of more easily degradable organic matter. In the 2nd and 3rd cycle V_{max} significant decrease with respect to the 1st cycle. In the remaining cycles the value for V_{max} still decreases reaching a stable value around 6.4×10^{-7} mol/L.min. A constant value for V_{max} probably indicates that the hydrolysis reaction is the rate limiting process.

The oxygen depletion rates during the non-stirring cycles decrease with decreasing oxygen concentration. As K_m is defined as the concentration at which the reaction rate is 50 % of V_{max} , K_m is dependent on V_{max} and decreases each cycle with decreasing V_{max} , decreasing from 4×10^{-5} mol/L for the first cycle to 1×10^{-5} mol/L for the last cycle.

For chemical oxidation, similar patterns were observed in Figure 5.8. The first non-stirring cycle showed the highest V_{max} , while for all the following cycles the V_{max} gradually decreased. Also all cycles showed a decreasing oxygen depletion rate with decreasing oxygen concentration, following the trend of the Michealis-Menten equation, except for

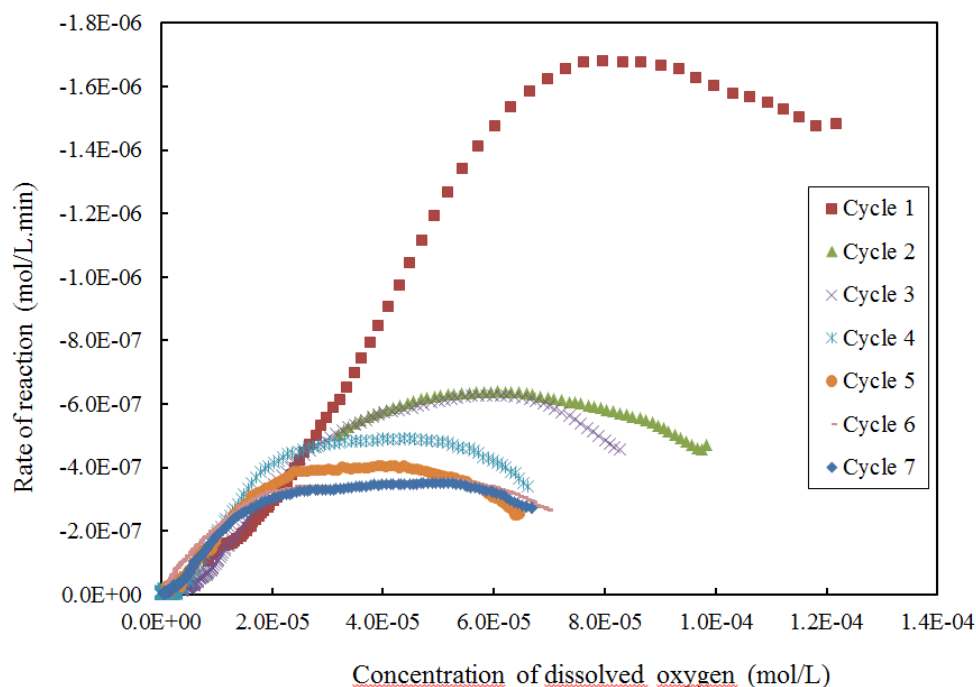


Figure 5.7: Oxygen depletion rates versus concentration of dissolved oxygen during non-stirring cycles obtained from the aerobic oxidation tests

the 6th cycle, which seemed to fluctuate and was not continued long enough to allow the oxygen concentration to drop to 0%.

Figures 5.9 and 5.10 show the maximum reaction rate, V_{max} and Michaelis-Menten constant, K_m for aerobic and chemical oxidation respectively. Both V_{max} and K_m values decreased with the number of cycles.

The measured specific gravity and organic matter content before and after the oxidation experiments are presented in Table 5.5. The specific gravity is influenced by the type and amount of organic matter (Hobbs, 1986) and also the type and amount of oxidation. The results show that aerobic oxidation did not influence the specific gravity as compared to chemical oxidation after drying at 105 °C. Faster oxidation is expected using H_2O_2 compared to aerobic oxidation which results to faster breakdown and mineralisation of organic matter and eventually higher specific gravity. However, in this experiment, lower specific gravity from chemical oxidation is obtained probably due to dissolution of minerals or error in measurements. Organic matter removal by Hydrogen peroxide may affect mineral phase as it promote dissolution of poorly crystalline minerals such as sulphide minerals from pyrite at low pH, disintegration of expandable clay minerals and transformation of vermiculite into mica-like products due to NH_4^+ fixation (Mikutta et al., 2005).

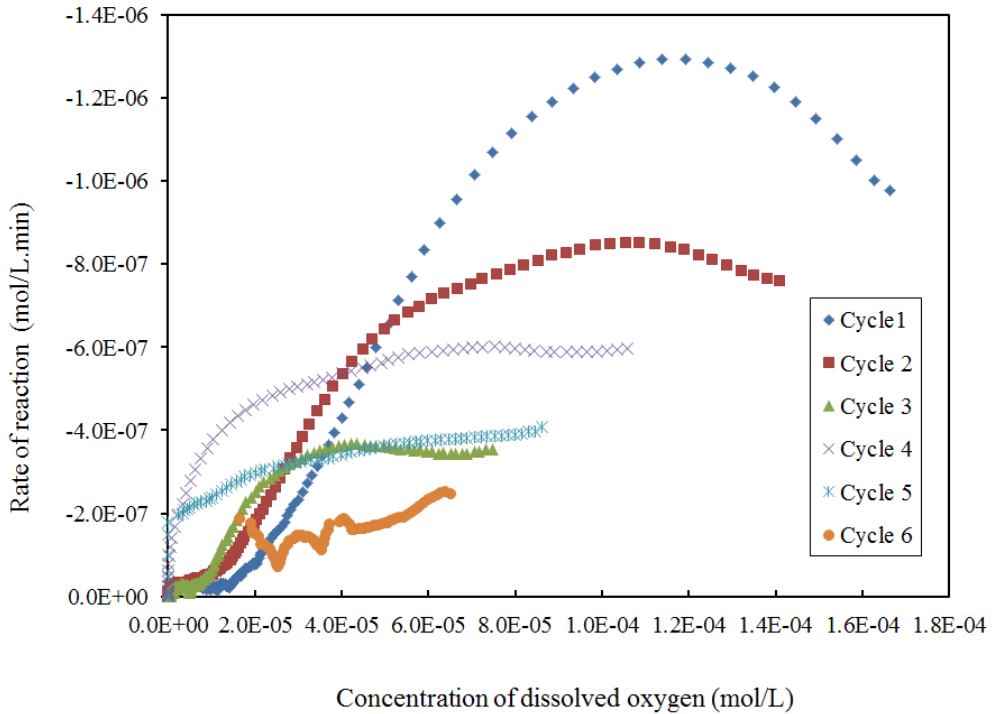


Figure 5.8: Oxygen depletion rate versus concentration of dissolved oxygen during non-stirring cycles obtained from the chemical oxidation tests

Lower organic content is obtained after chemical oxidation which result from removed dissolved organic carbon. However, unexpected higher organic content is obtained after aerobic oxidation probably as a consequence of loss of structural water from clay minerals or hydroxyl OH group at high combustion temperature which increases the total carbon loss. As the sample contained a significant quantity of pyrite, precipitation of Ferric hydroxide $\text{Fe}(\text{OH})_3$ may have occurred in this experiment as a result of the oxidation of ferrous iron Fe^{2+} (Thorsten, 2013). Both oxidising conditions seem to lower the pH values. The relevant reactions which may involve in this experiment is described in the appendix.

Table 5.5: Effect of specific gravity, organic content and pH subjected to different oxidising conditions in reactor

Types of oxidation	Specific gravity			Organic content [%]		pH	
	Initial 105 °C	Final 105 °C	Final 500 °C	Initial 500 °C	Final 500 °C	Initial	Final
Aerobic oxidation	1.8	1.8	2.76	53.7	56.21	6.5	3.5
Chemical oxidation	1.8	1.74	2.15	53.7	40.16	6.4	2.3 /2.5

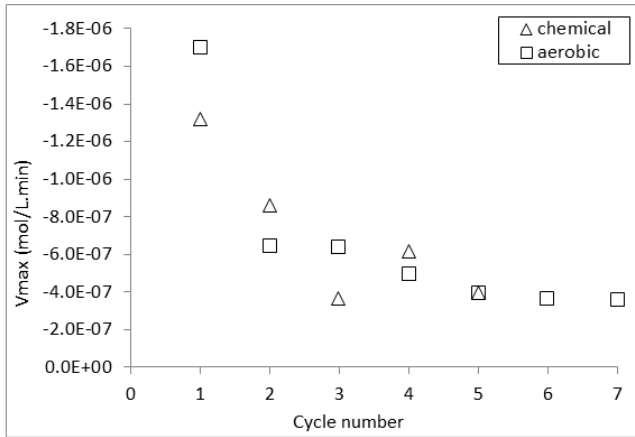


Figure 5.9: The change of maximum reaction rate, V_{max} for each non-stirring cycle under the influence of aerobic oxidation and chemical oxidation through H_2O_2 dosage

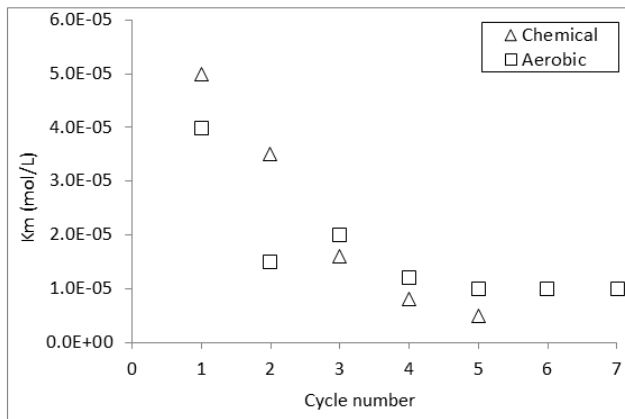


Figure 5.10: The change of substrate affinity constant, K_m for each non-stirring cycle under the influence of aerobic oxidation and chemical oxidation by H_2O_2 dosage

5.5.1. OEDOMETER RESULTS

Figure 5.11 shows the settlement profiles during oxidation at constant effective vertical stresses of 5, 20 and 80 kPa. At all pressure levels addition of 10 % (w/w) Hydrogen peroxide resulted in significant settlement. Most settlement took place during the first 4 to 6 days after which the settlement rate decreased gradually to zero. The decrease in settlement rate could indicate that 1) all available organic matter was oxidised, 2) all H_2O_2 was depleted either by oxidising the organic matter or due to decomposition and transfer of the resulting oxygen to the gas phase or 3) transport limitation of H_2O_2 , for example, the H_2O_2 may have oxidised all organic matter in the top layer of the sample leaving non-

degradable material, which could have reduced the hydraulic conductivity. According to O'Kelly & Pichan (2014), oxidation causes transformation of organic material into finer grains that pack more tightly which results to lower void ratio, a higher bulk density and contribute to a lower hydraulic conductivity.

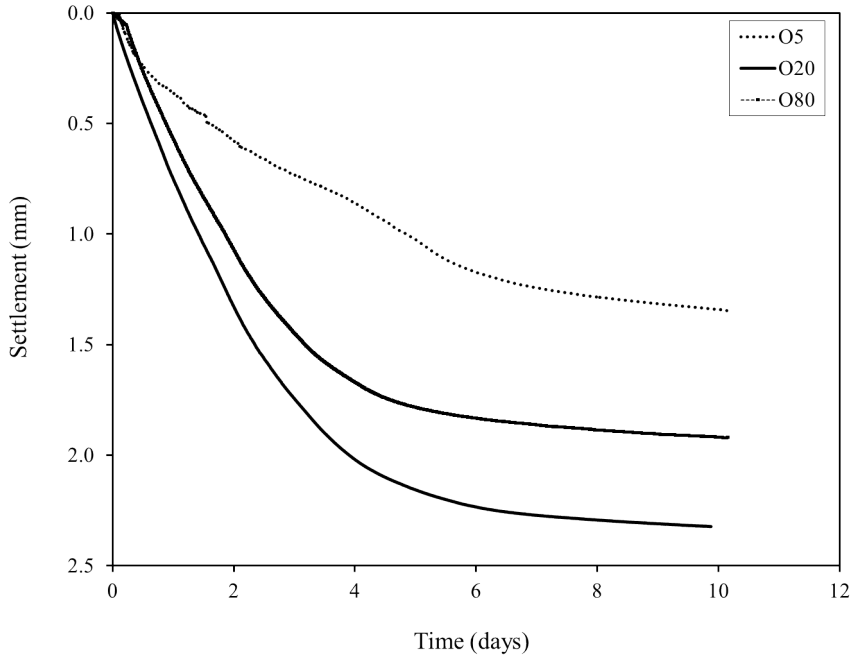


Figure 5.11: Settlement versus time plot at oxidation stage level

Figure 5.12 shows the settlement rates in time for the three oedometer samples. As proposed by van den Akker et al. (2008), the settlement rate associated to oxidation can be used to calculate the potential carbon dioxide emissions. The samples at 20 and 80 kPa showed similar profile, a linearly decreasing settlement rate over a period of 5 days after which it went gradually to zero. The sample at 5 kPa showed a rapid decrease in settlement rate in the beginning after which it remained constant for about 5 days after which it eventually gradually dropped to zero.

This changes in specific gravity, organic content and density are shown in Table 5.6. There is a slight change in the specific gravity values for all oedometer samples once oxidation and consolidation has completed. The organic content reduces after oxidation due to loss of organic matter after treatment with H_2O_2 and an increase in dry density is observed attributed to a higher mineral content as a result of mineralisation. The efficiency to remove organic matter using H_2O_2 appeared to be low as only 4 % of organic matter was lost, while sufficient hydrogen peroxide was supplied to oxidise all organic matter. The efficiency of H_2O_2 to oxidise organic matter depends on soil reaction, presence of carbonates, chemically resistant organic compounds and protection of organic compound by mineralised coatings (Mikutta et al., 2005).

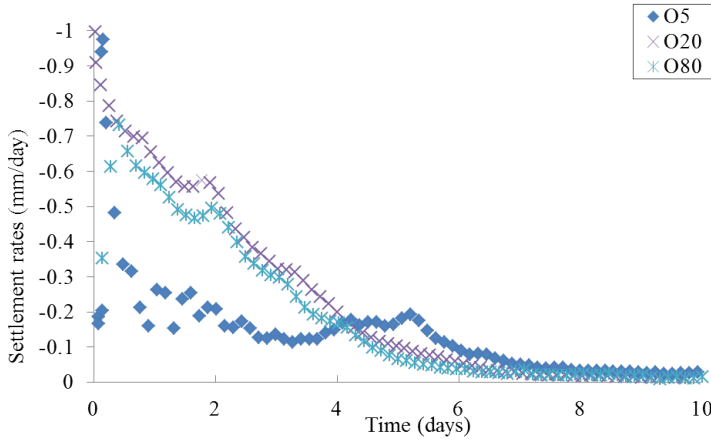


Figure 5.12: Plot of settlement rates versus time for all oedometer samples

Table 5.6: Effect of oxidation on specific gravity, organic content and mass loss at different oxidation pressure

Sample	Specific gravity		Organic content [%]		Dry density [Mg/m ³]	
	Initial	Final	Initial	Final	Initial	Final
O5	1.82	1.84	51.28	47.79	0.17	0.34
O20	1.82	1.83	51.28	47.7	0.17	0.37
O80	1.82	1.83	51.28	47.82	0.18	0.43

CALCULATING CARBON DIOXIDE EMISSIONS IN THE BIOREACTOR

The carbon dioxide emissions can also be estimated for the bioreactor experiments. Considering that according to the simplified chemical reaction equation, the oxygen depletion rate is equal to the carbon dioxide production rate, the carbon dioxide production rate can be calculated from the measured oxygen depletion during the non-stirring cycles in the bioreactor experiments. As shown in Figure 5.9 and Figure 5.10, the maximum oxygen depletion rate, V_{max} , decreases with the number of cycles, but the difference between the aerobic and chemical oxidation experiments is rather small. Consequently, the carbon dioxide emission rates are calculated based on the maximum and minimum values for V_{max} according to:

$$\frac{dm_{CO_2}}{dt \cdot m_{SO}} = \frac{V_{max} \times V_T \times M_{CO_2}}{m_{SO}} \quad (5.14)$$

The results are presented in Table 5.7

The oxidation reaction in the bioreactor shows a CO₂ emission rate ranging from 0.63 to 2.98 g-CO₂ g-dry soil⁻¹ yr⁻¹, likely depending on the degradability of the organic matter and potentially on the pH of the liquid. These rates are a bit lower than observed in the chemical oxidation tests in the oedometer, which indicates that chemical oxidation using a concentrated H₂O₂ solution results in higher oxidation rates than the max-

Table 5.7: Predicted carbon dioxide emissions from bioreactor experiments

		Min	Max
Oxygen depletion rate (V_{max})	[mol $L^{-1} min^{-1}$]	3.6E-07	1.7E-06
Specific CO ₂ emission rate	[g-CO ₂ g-dry soil ⁻¹ yr ⁻¹]	0.63	2.98

imum oxidation rate observed in the bioreactor. A possible explanation for the high reaction rates observed in the oedometer, could be an increase in temperature as a result of the exothermic effect of the oxidation reaction. A similar rise in temperature is observed when organic soils are suspended in concentrated H₂O₂ solution for the removal of organic material. Another explanation for the high oxidation rates is that at high concentrations of H₂O₂, the Michaelis-Menten equation is not valid anymore and chemical oxidation follows different kinetics.

The oxidation rates in the bioreactor seem to be higher than observed in the field considering the oxidation rates in the bioreactor are of the same order of magnitude as in the oedometer tests, whereas the rates in the oedometer tests are at least 1 order of magnitude higher than observed in the field. This makes sense as the oxidation rate in the field is expected to be limited by the supply in oxygen. However, a direct comparison of total carbon dioxide emissions per hectare is difficult as the thickness of the zone in which oxidation takes place is unknown.

CALCULATING CARBON DIOXIDE EMISSIONS FROM SETTLEMENT ANALYSIS

Using the provided equation by van den Akker et al. (2008), and taking the same assumption that the fraction of subsidence due to oxidation of organic matter compared to total subsidence is 100%, (i.e., $F = 1$), the total carbon dioxide emissions per gram of dry soil and the extrapolated emission rate per hectare of surface area is calculated from the settlement measurements during oxidation. As the settlement rate varies in time, the average settlement rate is determined from the moment the oxidation starts to the moment when 90% of the final settlement is reached, t_{90} . In order to compare the data between different experiments, the carbon dioxide emissions are also calculated per gram of dry soil. The total specific CO₂ emission, i.e., the CO₂ emission per gram of dry soil is calculated using:

$$\frac{m_{CO_2}}{m_{SO}} = \frac{F \times \Delta H \times A \times \rho_d \times M_{CO_2}}{m_{SO} \times M_{CH_2O}} \quad (5.15)$$

Whereas the specific CO₂ emission rate is calculated using:

$$\frac{dm_{CO_2}}{m_{SO} \cdot dt} = \frac{0.9 \times F \times \Delta H \times A \times \rho_d \times M_{CO_2}}{t_{90} \times m_{SO} \times M_{CH_2O}} \quad (5.16)$$

The results are presented in Table 5.8.

The calculated CO₂ emission rates from settlement analysis are 10 to 36 times higher than the 22,000 kg-CO₂ yr⁻¹ ha⁻¹ reported by van den Akker et al. (2008), which clearly indicates that the oxidation rate in the field is limited by oxygen supply. The analysis

Table 5.8: Predicted carbon dioxide emissions from settlement rate (F=1)

Overburden pressure at oxidation step	[kPa]	5	20	80
Initial total soil mass, m_{t0}	[g]	69.2	68.5	68.4
Initial water content	[-]	5.13	5.13	5.14
Initial dry mass, m_{s0}	[g]	11.29	11.17	11.14
Initial organic matter content (LOI)	[-]	0.513	0.513	0.513
Initial mass of organic matter, m_{o0}	[g]	5.79	5.73	5.71
Height at the start of oxidation	[cm]	1.86	1.54	1.08
Void ratio at the start of oxidation	[-]	7.5	6.1	4
Water volume at the start of oxidation	[cm^{-3}]	46.5	37.5	24.5
Total volume at the start of oxidation	[cm^{-3}]	52.7	43.6	30.6
Total mass at the start of oxidation	[g]	57.8	48.6	35.6
Dry density at start of oxidation	[$g\ cm^{-3}$]	0.214	0.256	0.364
Total settlement, ΔH	[mm]	1.35	2.32	1.92
Time to reach 90% settlement, t_{90}	[days]	6.5	4.45	4.3
Average settlement rate, $0.9\Delta H/t_{90}$	[$cm\ day^{-1}$]	0.019	0.047	0.04
Settlement rate	[$cm\ yr^{-1}$]	6.8	17.1	14.7
F	[-]	1	1	1
Total CO ₂ emission	[$g\text{-CO}_2\ g\text{-dry}\ soil^{-1}$]	0.05	0.11	0.13
CO ₂ Emission rate	[$kg\ yr^{-1}\ ha^{-1}$]	214259	643884	783071
Specific CO ₂ emission rate	[$g\ g\text{-dry}\ soil^{-1}\ yr^{-1}$]	2.75	8.36	10.2

also illustrated how CO₂ emissions increase with increasing settlement and density. For example, although the settlement (rate) at 80 kPa is smaller than at 20 kPa, still the CO₂ emissions are higher due to a higher dry density.

CALCULATING CARBON DIOXIDE EMISSIONS FROM MASS LOSS

A second and third estimate of the carbon dioxide emissions can be made from the measured loss in dry mass or the measured loss in organic mass during oxidation. To determine the CO₂ emission rate in these cases it is assumed that the rate of settlement is directly correlated to the rate of mass loss. Hence, the specific CO₂ emission, and specific CO₂ emission rate from mass loss, Δm_s , can be calculated using:

$$\frac{m_{CO_2}}{m_{s0}} = \frac{\Delta m_s \times M_{CO_2}}{m_{s0} \times M_{CH_2O}} \quad (5.17)$$

$$\frac{dm_{CO_2}}{dt \cdot m_{s0}} = \frac{0.9 \times \Delta m_s \times M_{CO_2}}{t_{90} \times m_{s0} \times M_{CH_2O}} \quad (5.18)$$

And the specific CO₂ emission, and specific CO₂ emission rate from loss in organic mass, Δm_o , can be calculated using:

$$\frac{m_{CO_2}}{m_{SO}} = \frac{\Delta m_o \times M_{CO_2}}{m_{SO} \times M_{CH_2O}} \quad (5.19)$$

$$\frac{dm_{CO_2}}{dt \cdot m_{SO}} = \frac{0.9 \times \Delta m_o \times M_{CO_2}}{t_{90} \times m_{SO} \times M_{CH_2O}} \quad (5.20)$$

The results are presented in Table 5.9 and Table 5.10.

Table 5.9: Predicted carbon dioxide emissions from change in dry mass

Overburden pressure at oxidation	[kPa]	5	20	80
Initial dry mass	[g]	11.29	11.17	11.14
Final dry mass	[g]	11.20	10.91	10.85
Total mass loss	[g]	0.09	0.26	0.29
Time to reach 90% reaction	[days]	6.50	4.45	4.30
Total CO ₂ emission	[g-CO ₂ g-dry soil ⁻¹]	0.012	0.034	0.038
CO ₂ emission rate	[g-CO ₂ g-dry soil ⁻¹ yr ⁻¹]	0.73	3.11	3.60
F		0.27	0.37	0.35

Table 5.10: Predicted carbon dioxide emissions from change in organic mass (LOI)

Overburden pressure at oxidation	[kPa]	5	20	80
Initial dry mass	[g]	11.29	11.17	11.14
Initial organic matter content (LOI)	[-]	0.51	0.51	0.51
Initial organic mass (TOM)	[g]	5.79	5.73	5.71
Final dry mass	[g]	11.20	10.91	10.85
Final organic matter content (LOI)	[-]	0.478	0.477	0.478
Final organic mass (TOM)	[g]	5.35	5.21	5.19
Total loss organic mass	[g]	0.44	0.53	0.53
Time to reach 90% reaction	[days]	6.50	4.45	4.30
Total CO ₂ emission	[g-CO ₂ g-dry soil ⁻¹]	0.057	0.069	0.069
CO ₂ emission rate	[g-CO ₂ g-dry soil ⁻¹ yr ⁻¹]	3.56	6.30	6.54
F		1.29	0.75	0.64

Comparing the different approaches to calculate the CO₂ emissions from the oedometer tests shows that calculations based on mass loss result in 3 to 4 times smaller CO₂ emissions than based on settlement analysis. The calculations based on loss of organic mass are in the same range as based on settlement. For the oxidation test at 5 kPa, the calculated CO₂ emissions based on organic mass loss are higher than the values based on settlement, but for 20 and 80 kPa they are lower.

The discrepancy in calculated CO₂ emission rates between methods based on settlement, loss of dry mass and loss of organic mass may be the result of other chemical

reactions involving the inorganic mineral fraction. Organic matter removal by Hydrogen Peroxide may also affect the inorganic fraction as it may promote dissolution of poorly crystalline minerals at low pH, disintegration of expandable clay minerals and transformation of vermiculite into mica-like products due to NH_4^+ fixation Mikutta et al. (2005). Also inorganic minerals may be oxidised in presence of oxygen or Hydrogen Peroxide. For example, pyrite may be oxidised when exposed to oxygen and water, to form sulphate and ferric iron (Thorsten, 2013). The ions resulting from oxidation and reduction reactions may consequently precipitate and alter the fraction of inorganic minerals and effect the total and organic dry mass before and after oxidation.

Another explanation for the observed discrepancy may be the fact that settlement and mass loss are not necessarily directly related. Part of the settlement may be due to deformation of the soil fabric and structure. Partial oxidation of the organic fibrous material may cause structural collapse, resulting in more settlement than expected based on mass loss.

5.6. CONCLUSIONS

The kinetics of oxidation of dredged organic sediments from a peatland meadow area in the Netherlands has been compared in terms of oxygen depletion rate, settlement rate, loss of dry mass or loss of organic mass for varying oxidation conditions.

Bioreactor tests allowed to determine the oxidation rate as a function of oxygen concentration. They showed the oxidation kinetics could be described using a Michealis-Menten enzyme kinetics model, in which the maximum rate of oxidation under sufficient oxygen availability, V_{max} , and affinity constant, K_m were determined through multiple non-stirring cycles. Chemical oxidation using controlled addition of hydrogen peroxide showed similar values for V_{max} and K_m compared to aerobic oxidation.

Chemical oxidation tests in the oedometer set-up showed that although the oxidation was very inefficient based on the observed mass loss still significant settlement was observed during oxidation. Comparing the maximum oxidation rates per gram of dry soil in the bioreactor with the chemical oxidation rates per gram of dry soil in the oedometer confirmed that the oxidation rate in the oedometer is limited by a limited oxygen availability.

Secondly the oedometer tests showed that the fraction of settlement attributed to the oxidation is not necessarily equal to 100% as proposed by van den Akker et al. (2008), but depends on the method by which it is determined. Hence, a direct correlation between measured settlements and carbon dioxide production involves significant uncertainty.

5.7. ACKNOWLEDGEMENTS

The authors acknowledge Arno Mulder and Jolanda van Haagen for assisting laboratory test at Delft University of Technology (TU Delft). Dr. ir. J.T.C. Grotenhuis, Environmental Technology, Wageningen University for giving the opportunity to involve in the project of Lifting up the Lowlands which was funded under STW Grant. The first author gratefully acknowledges a research scholarship from the Public Service Department of Malaysia and also home institute Universiti Teknologi MARA, Malaysia.

6

EFFECT OF OXIDATION ON SHRINKAGE AND WATER RETENTION BEHAVIOUR

*The soil shrinkage curve can be divided,
into 4 phases which are structural, normal,
residual and zero.*

Schindler

6.1. ABSTRACT

Peatlands and organic soils in Delta areas suffer from continued surface subsidence, while at the same time accumulation of suspended sediments originating from these peatlands leads to poor water quality. Many researchers attribute the majority of surface subsidence of peatlands to decomposition of organic matter, particularly as a result of aerobic oxidation during periods of low groundwater level. The sediments which settle in the ditches and lakes are regularly dredged, deposited in depots where they are left to ripen, after which they are spread over the meadows. Spreading these sediments on land may partially compensate for surface subsidence. An experimental study was performed to improve understanding about the ripening of organic dredged sediments and to determine the efficiency of these sediments to mitigate subsidence in peatlands. Sediments collected from the peatland Wormer & Jisperveld in The Netherlands, were exposed to aerial drying in a laboratory environment. In order to investigate the effect of organic matter on the shrinkage and water retention behaviour, some of the samples were chemically oxidised using hydrogen peroxide before drying. Samples were placed in a modified Hyprop device, which was used to measure the suction development during drying. By placing the device including the sample inside an X-ray CT scanner, the shrinkage could be determined accurately, including the formation of gas voids and desiccation cracks. The results demonstrate that oxidation of organic matter significantly reduces the water holding capacity of the dredged organic sediments, which is also reflected by a change in liquid and plastic limit. Both samples show significant shrinkage upon drying, but the non-oxidised sample shows much more volume change than the oxidised soil. The soil water retention curves (SWRC) show similar patterns as one-dimensional compression tests, in which the slope of the SWRC is equal to the compression index. However, considering the stress conditions during soil shrinkage are closer to isotropic conditions the SWRC is below the normal consolidation line and closer to the critical state line. When starting the drying process with a slurry, a large part of the shrinkage occurs before suction can be measured. A correction procedure is suggested to extend the measuring range of the HYPROP device to low suction values. The CT scans indicate that apart from some gas bubbles which appear in the non-oxidised soil at a pressure below 1 kPa and shrinkage cracks which occur at a later stage in the drying process, both soils remain close to full saturation.

6.2. INTRODUCTION

During the Holocene period, peat formation took place in the Netherlands above the Pleistocene layers. These peatlands were either excavated or used as fuel or drained and reclaimed from the 12th century for agricultural purposes. Ever since the reclamation of these lands, the peat meadows have been subsiding. Peatlands initially were on average between one to three meters above sea level but now peatlands have subsided to one to two meters below average sea level (Ven, 2003).

Surface subsidence of peat is triggered by drainage of the land and can be attributed to three different mechanisms (Wösten et al., 1997): consolidation, shrinkage and oxidation. Consolidation is the mechanical compression of a saturated soil layer below groundwater level as a result of an increase in overburden pressure from the soil above.

A drop in groundwater level will increase the overburden pressure, due to loss of buoyancy force. Shrinkage is the volume reduction of peat above groundwater level as a result of desiccation induced by evapotranspiration. Oxidation is the loss of organic matter, which directly results in solid volume loss. A drop in groundwater level increases the depth at which oxygen can penetrate and may accelerate aerobic oxidation, but it also induces capillary suction causing shrinkage.

Although a lot of research has been carried on peat subsidence, there is still no consensus on which of these contributing factors is dominant. Pons & Zonneveld (1965) stated that half of the total moisture loss and consequently half of the settlement was caused by oxidation of organic matter. Schothorst (1977) assumed that higher content of mineral elements in the top layers was due to oxidation of the organic matter. By comparing the bulk density of mineral elements in the layers above and below groundwater level he could estimate the amount of oxidation. He concluded that approximately 15 % of the total subsidence could be attributed to shrinkage of the upper layer, which subsequently leaves 85 % to be ascribed to oxidation of organic matter. van den Akker et al. (2008) assumed that the long term subsidence can be mainly attributed to oxidation of organic material. This assumption allowed him to establish a direct correlation between surface subsidence and CO₂ emissions in peatlands.

Although aerobic oxidation may be considered the dominant process causing subsidence in peatlands (van den Akker et al., 2008; Gebhardt et al., 2010), when examining the composition of organic soils, it appears that 90 % to 95 % of the total volume consists of water. Hence, it is impossible to attribute the majority of peat subsidence directly to oxidation and loss of organic matter. However, indirectly the loss of organic matter causes volume change, as by degradation of the organic matter the soil may lose its water retention capacity (Pichan & O'Kelly, 2012). Hence, the water, which cannot be retained by the degraded soil will drain off or evaporate, resulting in volume loss and consequent surface subsidence. Considering the lack of consensus, there is a need to investigate and quantify the relative contribution of each of these factors to the amount of surface subsidence.

This study aims to quantify the effect of shrinkage induced by evaporation and investigate the effect of organic matter on the shrinkage and water retention behaviour of dredged organic sediments. Soil shrinkage is defined as loss of moisture in soil due to drying which may lead to decrease in soil volume. The weight and volume of a soil decrease during drying as the soil shrinks (Oleszczuk & Truba, 2013). The potential shrinkage depends on soil type and stress history. Gebhardt et al. (2012) reported that potential shrinkage ranged from 2 % of the initial volume for a clean sand to 65 % for a peaty clay. The shrinkage curves for organic soils may differ from mineral soils. Initially peat soils may show less shrinkage upon drying than a fine-grained mineral soil, as water drains through the larger pores, desaturating the soil. However, further drying and partial degradation of the fibrous material deteriorates the soil structure. Consequently, after multiple wetting and drying cycles and as a result of structural degradation organic soils may show significant shrinkage, in which the major part of this shrinkage is irreversible (Gebhardt et al., 2012; Peng & Horn, 2007; Szatylowicz et al., 1996).

The shrinkage behaviour of a soil is described by two empirical correlations: the soil shrinkage characteristic curve (SSCC) and the soil water retention curve (SWRC). The

shrinkage curve relates the void ratio or specific to the gravimetric or volumetric water content (Yao, 2016). According to Schindler et al. (2015), soil shrinkage as a results of soil evaporation can be divided into various phases. The first phase is structural shrinkage is when the loss of water due to draining of macropores is larger than the volume changes, so that the soil structure behaves stable. Followed by normal shrinkage (proportional shrinkage), where the volume change caused by shrinkage is proportional to the water loss from smaller voids. The third phase, residual shrinkage is when the loss of water volume is greater than the total decrease in sample's volume. In the final phase, zero shrinkage, the sample's volume does not decrease any further, while the final amount of water evaporates and the soil only desaturates.

The SWRC or soil water characteristic curve (SWCC) relates the water content to the soil suction. Soil suction, which is the driving force causing soils to shrink and desaturate, can be described using a capillary model, which represents a pore where at the interface between air and water develops a pressure difference between pore air pressure and pore water pressure which termed as matric suction. As the matric suction increases the water content decreases, which causes the soil to shrink or desaturate. There are three zones distinguished in this curve, which is boundary effect zone, transition zone and residual zone (Fredlund et al., 2012). Lab measurements on water retention of peat have been reported, but still the shrinkage and water retention behaviour are not well understood (Schwärzel et al., 2002).

According to Gebhardt et al. (2012), shrinkage increases with degree of decomposition and decreases with ash content. Water holding capacity decreases as decomposition degree state increases (Campos et al., 2011). Brandyk et al. (2002) mentioned that the shrinkage intensity depends on the type of organic matter. As the soil shrinks, soil volume and porosity decrease, while the bulk density increases (Schindler et al., 2015). The rate of shrinkage depends on type of peat, degree of decomposition, bulk density and ash content (Oleszczuk et al., 2003). Contrary to clays, for peats not all four shrinkage zones can be identified, but primarily structural and proportional shrinkage (Oleszczuk et al., 2003). In order to measure the shrinkage properties of soil, different laboratory methods have been reported such as measuring the displacement of mercury of artificial formed clay balls (Bohne & Kretschmer, 1984), coating soil samples with paraffin and measure the displacement of water (Lauritzen & Stewart, 1942), saran resin method (Reeve & Hall, 1978; Bronswijk, 1988), measure the displacement of petroleum for small samples (Monnier et al., 1973) and wrapped soil clods in a flexible rubber membrane (Tariq & Durnford, 1993). However, all these direct methods only allow the volume to be measured for a single water content. Continuous observation of the volumetric change of a sample is not possible with these methods. The vertical and radial deformation of a cylinder shaped soil sample can be measured using a Vernier Caliper (Peng & Horn, 2005). However, this method is rather time consuming and error-prone due to measurement uncertainties and soil variability Braudeau et al. (1999) and the occurrence of shrinkage cracks.

There are various methods to measure the SWRC of soils (Fredlund & Rahardjo, 1993). Schindler et al. (2010, 2015) developed a device known as Hyprop, which enabled automatic determination of the soil water retention curve, based on the evaporation method proposed by Wind (1966) and later modified by Schindler (1980). In this method, a satu-

rated soil sample is placed in a ring on a sensor unit, which contains two tensiometers. The whole set-up is placed on a balance and the loss in water mass by evaporation was recorded while pressure transducer tensiometers are used to obtain corresponding suctions. Although the device was designed to measure the SWRC for non-shrinking soils, Schindler et al. (2015) suggested to use a membrane to prevent the sample to stick to the ring measure the change in height and diameter of the sample using a caliper. Some other authors also combined evaporation experiments with shrinkage measurements, in which shrinkage and water retention curves were measured directly (Boivin et al., 2004, 2006). However, these methods do not account for shrinkage cracks or internal air voids and consequently are unable to accurately measure soil volume and saturation. In contrast, X-ray computed tomography (CT) can be used to scan a material in high resolution and reconstruction of the scanned images allows to create a 3D image of the soil sample and determine the volume of different materials based on differences in unit weight. Kettridge & Binley (2008), used X-ray CT scanning were able to identify the amount and volume trapped gas bubbles and measure fibrous structure in peat soil. Using X-ray CT scanning will enable a more accurate determination of the actual soil volume and structure and even in case of irregular shrinkage or occurrence of desiccation cracks.

The main objective of this study was to assess how organic matter and water content influence the shrinkage and soil water retention curves of dredged organic sediments and to quantify the potential contribution of shrinkage to subsidence under natural drying conditions. In order to answer these questions, a series of tests was performed in which organic dredged sediments were exposed aerial drying in the laboratory. In order to investigate the effect of organic matter on the shrinkage and water retention behaviour some of the samples were chemically oxidised using hydrogen peroxide before drying. Samples were placed in a modified Hyprop device, which was used to measure the suction development during drying. By placing the device including the sample inside an X-ray CT scanner, the shrinkage could be determined accurately, including the formation of gas voids and desiccation cracks.

6.3. MATERIALS AND METHOD

6.3.1. PROJECT AREA, FIELD MEASUREMENTS AND SOIL COLLECTION

The organic sediments used in this study were collected in the area of Wormer & Jisperveld. Wormer & Jisperveld is a peat wetland and nature reserve of about 2400 ha. It lies in the Dutch province Noord-Holland between Wormer, de Rijk, Purmerend and Wormerveer. The area consists of a network of ditches and 3 shallow lakes, namely: De Poel, Het Zwet and De Marken. Of the total area, 240 hectares is constructed on, 500 hectares is water and 1660 hectares are peatlands. The area is independently preserved and maintained by the organisations Natuurmonumenten and Natura 2000, with Natura 2000 maintaining the majority of the region. Main use of the land is for dairy farming (cattle and sheep) serving secondly as a nature reserve for preserving its unique wildlife and for recreational activities. The project area is shown in Figure 6.1. Between 2005 and 2013, about 750,000 m^3 of dredged material was removed from about 200 km of ditches to improve water quality and deepen the waterways to enable recreation. Most of these dredged materials were placed in deposits, in which they were allowed to ripen before

being spread out over the meadows and raise the surface level of the land (Oliveira et al., 2018).

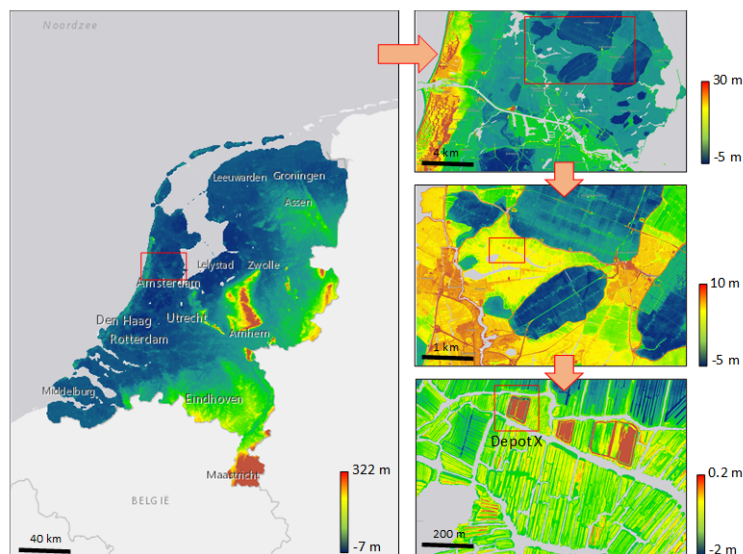


Figure 6.1: Project location: Depot X in the peatlands of Wormer & Jisperveld, The Netherlands. Colours indicate surface elevation relative to Amsterdam Ordnance Datum (NAP) derived from AHN (2019). Elevation measurements were taken by LIDAR measurements in spring 2016

Dredged sediment samples were retrieved from a slurry deposit (Depot X) in Wormer & Jisperveld. Depot X was filled with dredged sediments in two stages: In spring 2014 the deposit was filled up to about 1.75 m with dredged slurry, which was exposed to atmospheric drying during the summer. In autumn 2014 another 0.75 m of slurry was added, after which the deposit was allowed to dry, accelerated by evapotranspiration from excessive reed growth for a time period of 2 years. The level of the top and bottom of the drying sediments were regularly monitored and samples were taken to determine water and organic content (Oliveira et al., 2018). The monitoring results showed that after a time period of 2.5 years, only 0.70 m was left of the original 2.5 m of dredged sediments, a total volume change of 62%. The average water content reduced from an average 1200% to about 500%, while the organic content remained constant. An additional 0.2 m of settlement was measured, due to consolidation of the underlying peat soil. The field measurements indicated that most of the total subsidence could be attributed to shrinkage and some to consolidation of the underlying layers.

A month after the first phase of filling of Depot X, the samples were taken for the laboratory experiments described in this study. The samples were stored in large air tight containers and placed in a 10 °C climate room. The dredged sediments were a thick brown slurry, as shown in Figure 6.2. Before usage the slurry was mixed well, to acquire representative samples.



Figure 6.2: Dredged sediment from storage container

6.3.2. CLASSIFICATION TEST

The sediments were characterized by a series of standard classification tests following ASTM and RAW standards [ASTM \(2007a\)](#); [R.A.W \(2005\)](#), including particle size distribution, Atterberg limits, water content, fibre content, and loss on Ignition (LOI) to determine the organic content. Particle size distribution by means of wet sieving and hydrometer tests were particularly difficult to carry out as the majority of the sludge consisted of water with fine organic fibrous material. Hydrometer tests are typically carried out on samples after removal of organic matter. The test assumes particles to be spherical when deriving the particle size distribution, based on differences in settling velocity. The large amounts of organic fibrous material in the dredged sediment made hydrometer test unreliable. Additional test were performed, including, X-ray diffraction (XRD) and X-ray fluorescence (XRF) for the mineralogy and elemental composition, environmental scanning electron microscope (ESEM) for microscopic imaging of the material, and Rock-Eval (RE) tests for measuring the type and amount of organic carbon. Results of these tests are reported by [Oliveira et al. \(2018\)](#). Finally, settling column tests were performed to determine settling velocity and equilibrium volume and water content after settling, prior to consolidation or shrinkage.

6.3.3. OXIDATION PROCEDURE

The oxidised organic slurry was prepared by pretreating a sample of the organic sediments with hydrogen peroxide (following British Standard 1377-2:1990). The sediments were air dried to around the liquid limit (546%), a concentrated hydrogen peroxide solution was then slowly added to the slurry while being mixed gently with a glass rod. The amount of hydrogen peroxide needed was calculated based on the total organic carbon (TOC) content as determined through LOI test. A conversion factor of 1.724 was used to convert organic matter to organic carbon ([Schumacher, 2002](#)). The amount of hydrogen peroxide was scaled according to the weight of the batch of partially dried slurry, 275 ml H₂O₂ 10% (wt/wt) per 100 g partially dried soil. Immediate frothing occurred when hydrogen peroxide was added. The oxidising slurry occasionally stirred was done to subdue the excessive frothing.

After excessive frothing stopped the sample was covered with a glass dish and left

to stand overnight. The lack of visible frothing and bleached soil colour indicated a complete reaction, but frothing may have continued due to the decomposition of excess H_2O_2 at mineral surfaces (Mikutta et al., 2005). The next day, once the frothing ceased, the oxidised slurry was filtered with the help of a vacuum pump, 20 μ m filter paper and washed with demineralised water. The pH of the filtered oxidised slurry was then checked using a CONSORT pH meter. Levels of pH ranged from 2 - 2.5 after oxidation, which is considered to be highly acidic and unsafe to work with. The acidic slurry was neutralised with sodium hydroxide (NaOH 2M). Small amounts of NaOH 2M of around 1 ml were added to the oxidised material and mixed thoroughly. After mixing the pH was rechecked with the Consort pH meter and the process was repeated until the mixture reached a pH of 5.5 - 7.

6.3.4. HYPROP TESTS

SWRC curves were determined using a modified Hyprop device (Mergroup). The Hyprop procedure is based on the evaporation method described by Wind (1966) and later modified to the extended evaporation method (EEM) by Schindler (1980). The standard Hyprop system consists of a sensor unit, which contains two tensiometers of different length (1.25 and 3.75 cm). A steel sampling ring containing a soil sample 5 cm in height and 8 cm in diameter is placed on the sensor unit. The sensor and soil sample are placed on a scale. As the soil dries out, water inside of the tensiometer's shaft is sucked out through the ceramic tip, creating a suction inside of the tensiometer. Suction and weight loss are measured continuously. The water retention curve is derived by calculating the volumetric water content from the measured weight loss and plotting it against the measured average suction. The suction difference between the two tensiometers, can be used to estimate the unsaturated hydraulic conductivity according to Darcy Buckingham's law (Schindler, 1980). For this study some modifications were required to use the Hyprop system in combination with CT scanning. The metal components had to be removed from the Hyprop to minimize the amount of artefacts for CT images. Thus, the metal fastening clips and metal sampling ring were replaced with a new PVC system. The PVC fastening system consists of a PVC base, two plastic screw threads through the base and a PVC top beam to fasten the Hyprop to the base with 2 plastic screws, as shown in Figure 6.3.

The height of the new PVC sampling ring has been extended to 12 cm to accommodate for the large amount of expected shrinkage and prevent punching of the top tensiometer through the soil surface as it shrinks. The new sampling rings were slightly thicker than the original, which results in a slight decrease of the inner diameter to approximately 7.5 cm. The sampling ring is filled with slurry up to a column height of approximately 10 cm.

6.3.5. MACRO CT SCANS

CT scans were made at regular time intervals to monitor the shrinkage of the soil in the Hyprop, using a macro CT scanner (Siemens Somatom). In this scanner a motorised X-ray source rotates around a circular opening, called a gantry, in which the Hyprop device is placed. The source shoots beams of X-rays through the soil sample. As X-rays leave



Figure 6.3: Modified Hyprop set-up

the soil, they are then picked up by the detectors and transmitted to a computer. Each time the X-ray source completes a full rotation a 2D greyscale image of the soil is constructed. The CT scanning is repeated to generate multiple 2D slices, in which the distance between the slices can be set. The stack of 2D images can be used to reconstruct a 3D image. The greyscale value depends on the X-ray attenuation, which in turn depends on the density and the atomic number of the chemical element(s) present in each pixel and the incident photon energy (Ngan-Tillard, D. J. M. Huisman et al., 2018). The lighter the pixel color is, the higher the material attenuation and the higher the material density is. Careful attention needs to be taken to minimize the effects of artefacts in CT images. Common issues with CT scans are undesired artefacts in the image slices. There are many different CT artefacts such as noise, ring, beam hardening, scatter, pseudo-enhancement, motion, cone beam, helical, out of field artefacts and metal artefacts. In depth knowledge of all these artefacts are outside the scope of this study. However, discerning the major influence of artefacts in the CT scans is of importance. In this case, metal components in the Hyprop causes significant amount of artefacts in the CT images. These metal components cause beam hardening and scatter artefacts on the CT images, discernible by dark streaks between two high attenuation objects such as metal. An example is shown in Figure 6.4. A high attenuation object is presented as white on an image, due to absorption of X-ray photons. Beam hardening can be explained as the loss of X-ray energy more quickly as it passes it through metal, where scatter is caused by X-ray photons to change directions and miss the detector (Boas & Fleischmann, 2012).

Using the 3D image analysis software Avizo 9.0 3D images were reconstructed from the stacked 2D slices and further processed for quantitative analysis. Image processing involved several steps. First the “Interactive Thresholding” module was used to convert the greyscale images are into a binary images, in which the separation of different mate-

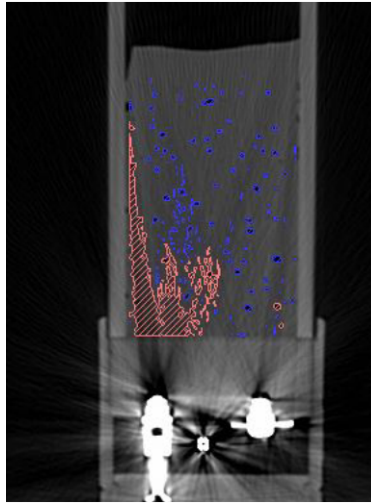


Figure 6.4: Metal components in the Hyprop device cause beam hardening artefacts, which show up as dark streaks in the image. These artefacts are identified (in red) and removed manually from the 3D reconstructed volume

6

rials is based on the density dependent attenuation of X-rays. Two greyscale thresholds were used to separate gas filled voxels and the wet soil filled voxels from other materials (Figure 6.5).

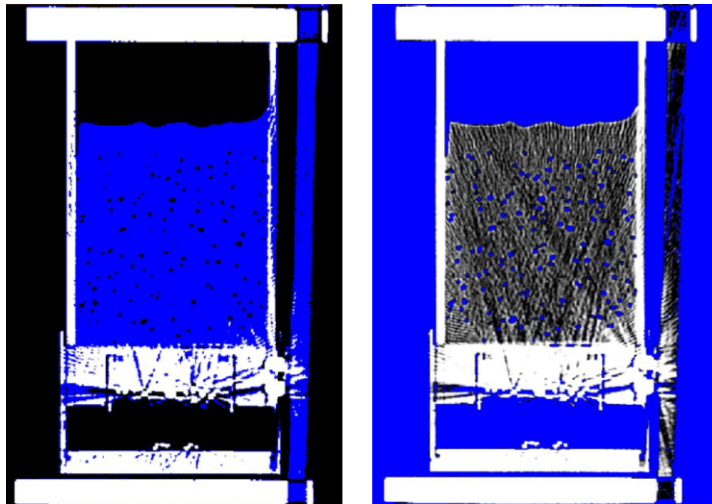


Figure 6.5: Separating the soil (left) and gas (right) from the other materials with interactive thresholding (the separated phase is indicated in blue)

Due to a limited resolution of the macro CT scanner and the fine pore sizes of the drying material, the liquid and solid phase and small potentially trapped gas bubbles

cannot be separated. The threshold values were manually selected in each scan based on visual interpretation of the greyscale histograms. The thresholds varied in each scan, as the bulk density of the soil is increasing during the desiccation process. Undesired objects such as the Hyprop device and surrounding air were removed from the image with the “Volume Edit” module. Then a 3D object is generated with the “Generate Surface” module, which encloses the total lump of soil and the “Label Analysis” module is used to calculate the bulk volume of soil. The “Separate Object” module had to be used to separate connected gas bubbles, artefact errors and exposed cavities to the atmosphere. Manual image segmentation was employed to remove the artefact errors caused by the metal disturbance of the Hyprop device, remove other unwanted objects (such as surrounding air) that the Volume Edit failed to remove, and differentiate between gas completely enclosed by the sediments and cavities exposed to the atmosphere. An example of the resulting 3D objects is shown in Figure 6.6.

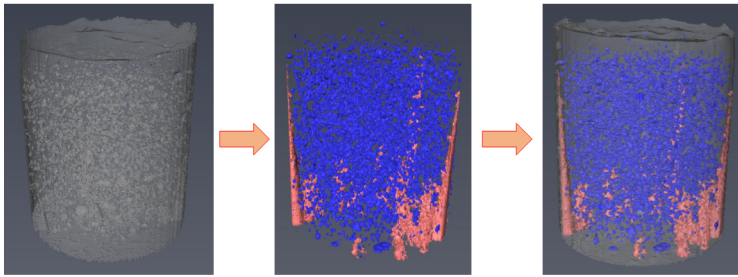


Figure 6.6: 3D objects of the soil, gas and beam hardening artefacts were combined to create the final images

Finally the “Label Analysis” module was used again to calculate the total volume of enclosed gas bubbles and artefacts. Final images, which show the volumes of soil, gas and removed artefacts are obtained by overlapping the two generated 3D images.

6.4. RESULTS AND DISCUSSION

6.4.1. SOIL CLASSIFICATION AND PHYSICAL PROPERTIES

Selected physical properties for the non-oxidised and oxidised material are presented in Table 6.1. The natural (gravimetric) water content of the organic sample was about 1600%. The soil is considered a slurry for having water content exceeding the liquid limit. Dark black in color with traces of thin plant fibres were observed. The measured specific gravity (G_s) is strongly influenced by the amount and type of organic matter in the test sample (den Haan & Kruse, 2007; Hobbs, 1986). A higher specific gravity is obtained after chemical oxidation due to oxidation of organic matter. Oxidation significantly reduced the liquid and plastic limit and also caused a significant drop in pH. Settling tests provided the composition of the slurry after settling prior to consolidation or shrinkage in terms of void ratio, e_0 or water content, w_0 .

Table 6.1: Selected classification properties

Properties	Unit	Non-oxidised	Oxidised
Gravimetric water content	%	1600	282
Sand fraction	%	8	n.d.
Fines fraction	%	92	n.d.
e_0	-	45.6	n.d.
w_0	%	2536	n.d.
Organic content (LOI)	-	51.44	28.1
pH	%	7-7.5	2-2.5
Fibre content	%	15	7
Specific gravity	-	1.75-1.82	1.86-2.03
Liquid limit	%	546	171
Plastic limit	%	205	127

6.4.2. HYPROP TEST RESULTS

Four Hyprop tests were performed on oxidised and no-oxidised samples, in which the initial water content was varied. The properties of these samples are shown in Table 6.2 below:

Table 6.2: Selected soil properties for Hyprop tests

Sample	Initial water content (%)		Dry mass (g)	Organic content (%)
	Gravimetric	Volumetric		
Non-oxidised 3 x LL		1296	7.16	51.44
Non-oxidised 3 x LL		997	9.12	48.7
Oxidised 2 x LL		282	26.2	28.1
Oxidised LL		172	36.73	29.95

Figure 6.7 shows the results of the Hyprop measurements. Some of the samples displayed some irregular values at the start of the experiment due to assembly procedure of the Hyprop, which caused some initial tension build up. These tensions gradually dissipated after which the suction followed its regular path. Similar to Tollenaar et al. (2018), it was found that when testing soils which demonstrate significant shrinkage, the presence of two tensiometers may induce vertical cracks within the sample or can cause the long tensiometer to bend and get damaged. Secondly, it was found that during a large part of the drying process the measured suction values were negative or close to zero. Similarly, Tollenaar (2017) found that when drying clayey soils with an initial water content above liquid limit, the suction remained negative for a long time period up to several days, even though significant shrinkage took place. They considered that the measured suction should be corrected for the loss in hydrostatic head and the initial offset (van Paassen et al., 2018; Tollenaar, 2017). The correction was applied on the measured suctions, by calculating the hydrostatic head loss from the measured weight loss and the surface area of the ring and taking the sample height as initial offset.

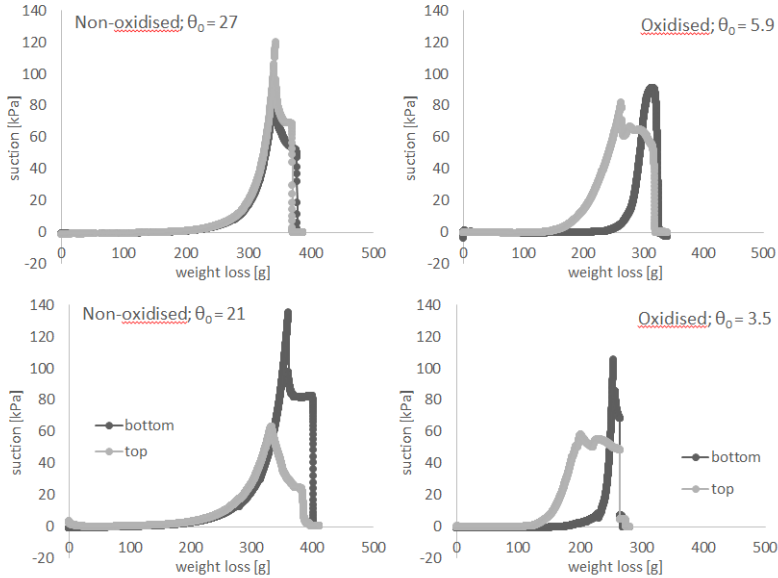


Figure 6.7: Measured weight loss and suction for the Hyprop tests

When comparing the measured suction in the top and bottom tensiometer, the oxidised soils showed that the measured suction in the long tensiometer started to rise earlier than the suction in the short tensiometer. For the non-oxidised soils the suction in both tensiometers showed similar patterns. According to [UMS \(2012\)](#) the hydraulic conductivity can be calculated based on the evaporation rate and the suction difference between the long and short tensiometer. However, as the soil is shrinking irregularly both in the vertical and radial direction, the flow rate cannot be accurately calculated. Still the increase in suction difference in the oxidised soil may indicate a reduced hydraulic conductivity.

Figure 6.8 shows the SWRC curves for all the Hyprop samples. The suction profile was calculated based on the average suction of the top and bottom tensiometers. Correcting the suction for the initial offset and the loss in hydraulic head increased the suction values, particularly in the range of suctions below 2 kPa. Above 2 kPa the correction did not affect the suction curve. SWRC curves for the non-oxidised samples aligned very well at suction levels above 10 kPa as the difference in initial water content did not change the location nor the slope of the curve. Removal of organic matter significantly reduced the water retention capacity and reduced the slope of the SWRC curve. For the oxidised samples correcting the measured suction for the initial offset resulted in a small but positive suction values during the initial stage of drying. The oxidised material with lower initial water content had a lower water retention capacity and reduced the slope of the SWRC compared to the oxidised material with high water content, but the two curves converged at about 1000 kPa, i.e., the end of the measurable suction range for the Hyprop equipment.

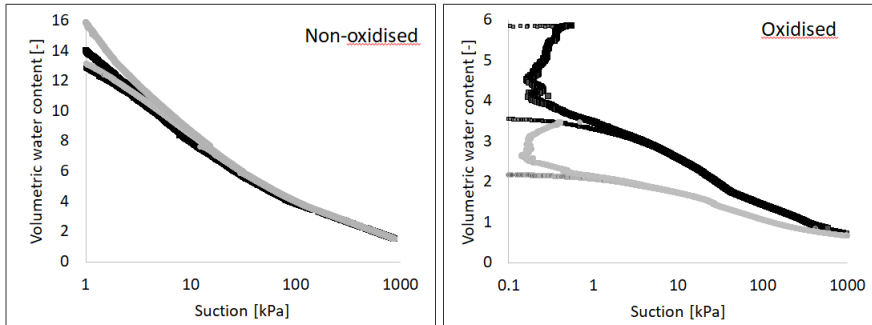


Figure 6.8: SWRC curves for non-oxidised soil (left) with initial VWC of 2723% (grey) and 2147% (black) and oxidised soil (right) with initial VWC of 586% (grey) and 348% (black)

6.4.3. CT SCAN MEASUREMENT AND SOIL SHRINKAGE CURVES

Figure 6.9 shows a selection of the reconstructed 3D images of the shrinking soil samples. The grey transparent color represents the soil volume, blue represents the entrapped gas, pink represents artefacts created by beam hardening caused by the metal components in the Hyprop system and the red indicates air pockets, which are in contact with the atmosphere and excluded from the volume analysis. The soil volume, i.e., the fraction of solids and water, was determined from the CT scans and from the measured mass of water during the experiment and the measured dry mass at the end of each experiment assuming an average specific gravity of 1.8 for the non-oxidised sample and 1.86 for the oxidised sample. Comparison between these two volume estimates showed an average error of about 2%.

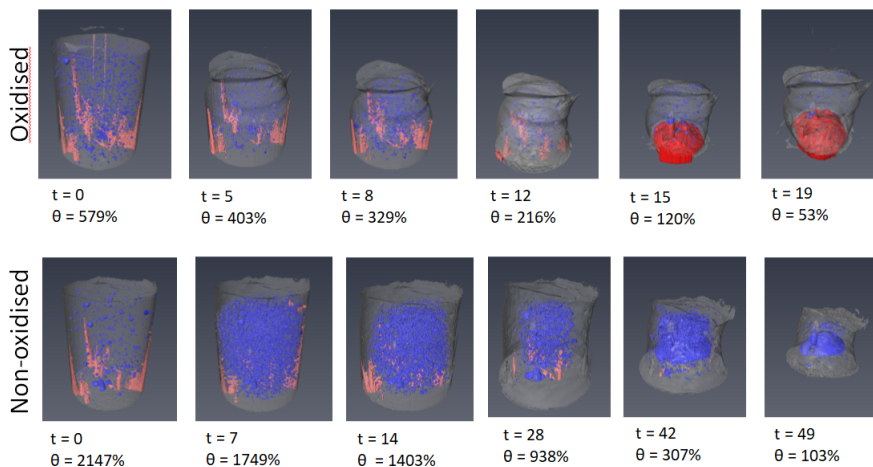


Figure 6.9: 3D reconstruction images of non-oxidised and oxidised samples

Both Figure 6.10 shows an increase in gas volume during the initial stage of drying for the non-oxidised soil. Peak gas volume for the partly dried non-oxidised sample was around 1 kPa. The non-dried, non-oxidised soil also showed an increase in gas volume, but the location of the peak could not be detected due a limited number of CT scan images. The entrapped gas bubbles gradually migrated and agglomerated into larger gas bubbles to form eventually a large gas pocket. In some cases these gas pockets got in contact with atmosphere, causing an exposed crack in the soil surface, after which the gas volume was excluded from the volume analysis. The oxidised soil initially showed slightly higher gas volumes, which gradually decreased during the drying process.

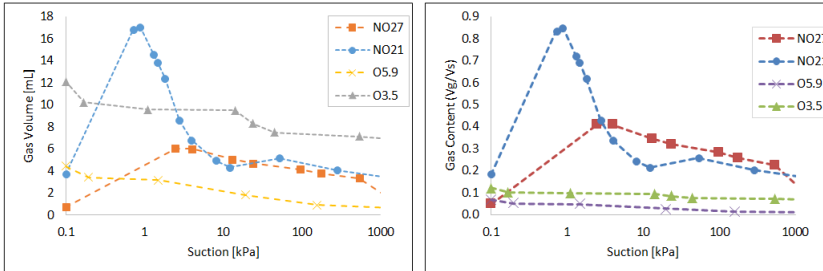


Figure 6.10: Gas volume and gas content versus suction plot for non-oxidised soil

The increase in gas volume in the non-oxidised soil may be attributed to exsolution of dissolved gas as a result of an increase in suction. Figure 6.10 shows the change in gas volume (left) and gas content (right) as a function of the average suction. As the gas solubility is directly related to the water pressure according to Henry's law, an increase in suction corresponds to a drop in water pressure and reduces the solubility for dissolved gases. Assuming that at the start of the experiment the dissolved gas phase is in equilibrium with the atmospheric or hydrostatic pressure a drop in pore water pressure will create an oversaturated solution, which may result in exsolution and gas bubble formation (Leroueil et al., 2015). Similarly, exsolution of gas has been attributed to drops in atmospheric pressure (Young, 1992; Gebert & Groengroeft, 2006). Another possible contribution to the increase gas volume is the production of gas due to oxidation of organic matter. The lack of gas formation in the oxidised samples may indicate that after oxidation and neutralizing the pH the dissolved gas was not yet in equilibrium with the atmosphere or the smaller available porosity and presence of existing gas bubbles, preventing new bubbles to form within the pores. Except for the initial increase in gas volume for the oxidised samples all samples showed a gradual decrease in the occluded gas volume. Gradual decrease of gas volume in time may be caused by diffusion of gas through the pore-water and venting to the atmosphere (LeBihan & Serge, 2002). In the final stages of a number of Hyprop experiments, sudden gas volume decrease is attributed to formation of cracks that are open to the atmosphere, causing episodic release of gas bubbles, also referred to as ebullition.

The Soil Shrinkage Curves (SCC) are constructed by plotting the void ratio over the volumetric water content. Both void ratio and volumetric water content are derived from

volume analysis of the CT scan data. The void volume is the summation of volume of water V_w and volume of occluded gas V_g , in which the volume of water is determined by subtracting the solid volume from the measured soil volume in the CT scan. measurements. The volume of solid V_s is assumed fixed and unchanged throughout the test and is calculated by final dry mass of the sample and the end of test and the specific gravity. The resulting shrinkage curves and the related degree of saturation (V_w/V_v) are shown in Figure 6.11

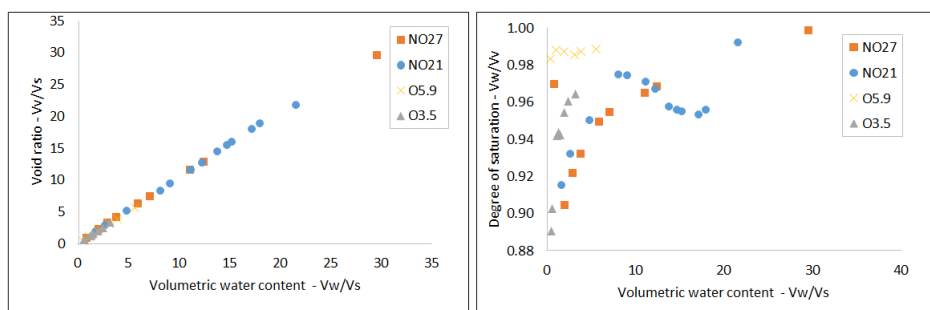


Figure 6.11: Shrinkage curves (left) and degree of saturation (right)

6

All shrinkage curves for the various Hyprop follow approximately straight lines close to saturation line, indicating that during the desiccation process, only proportional shrinkage is observed at near saturated conditions, where the loss of water volume is almost equal to the loss of bulk volume. If desiccation would have been allowed to continue, it is expected that eventually inflection points would appear, marking a clear point of air entry. However, experiments were stopped at a maximum suction of 880 kPa, corresponding to the air entry point of the ceramic tensiometer tips. The degree of saturation remained constant and close to full saturation during the complete tests, the gas fraction could be completely attributed to the gas bubbles or pockets, which were either present from the start of the experiment (for the oxidised samples) or formed during the initial stage of drying.

6.5. CONCLUSION

Chemical oxidation of organic matter reduces the water retention capacity of soils, which is reflected by a decrease in liquid and plastic limit and a reduction in the onset and slope of the Soil Water Retention Curves. At any given suction level, the volumetric water content is significantly reduced for oxidised samples. Varying the initial water content change the onset or the beginning of the water retention characteristic curve. When starting in a slurry state a large part of soil shrinkage takes place before significant levels of suction can be measured. For non-oxidised sample formation of occluded gas is observed at the initial drying stage. Peak gas volume is observed at low suction values of about 1 kPa. The formation of gas may be related to the increase in suction or drop in water pressure, which reduces the solubility of dissolved gas, to the degradation of

organic matter, increasing the amount of dissolved gas or a combination of both. Afterwards, the gas volume decreases as the sediment shrinks, which may be due to diffusion in pore water and escape to the atmosphere. Aggregation of gas bubbles into larger pockets and ebullition of gas bubbles and crack formation is also observed during the experiment. However the amount of entrapped gas does not significantly affect the shrinkage characteristics for the range of water contents observed during the major part of the desiccation process in the field. Only proportional shrinkage is observed at near saturated conditions, where the loss of water volume is equal to the loss of bulk soil volume.

7

CONCLUSIONS AND RECOMMENDATIONS

7.1. CONCLUSIONS

In this study the effect of oxidation on the compression behaviour of organic soils has been investigated. The total settlement of organic soils and peat as a result of groundwater lowering can be divided into three different mechanisms which are consolidation, oxidation and shrinkage (Wösten et al., 1997). The mechanism for each component is described as follows:

Consolidation is the mechanical compression of the saturated peat layer below groundwater level as a result of an increase in overburden pressure from drained soil. A drop in groundwater level will increase the overburden pressure, due to loss of buoyancy force; Oxidation is the loss of organic matter, which directly results in solid volume loss. Aerobic oxidation, in which oxygen is used as oxidising agent, is considered the dominant process causing loss of organic matter in peatlands. A drop in groundwater level increases the depth at which oxygen can penetrate and aerobic oxidation can occur. Shrinkage is the volume reduction of peat above groundwater level as a result of desiccation induced by evapotranspiration.

Several authors claim that oxidation of organic matter in the upper layer (aerobic oxidation) is the major mechanism causing irreversible long term settlement of drained peat soil (Ingebritsen et al., 1999; Campoprese et al., 2006; Dawson et al., 2010). However where there is consensus that groundwater lowering causes subsidence, there is still a debate about the relative contribution of the different mechanisms. The objective of this study was to quantify the relative contribution of consolidation, oxidation and shrinkage to the total settlement of organic soils and identify the factors which affect the rate of aerobic oxidation. Organic sediments, dredged from the ditches in at the peatland area of Wormer & Jisperveld in The Netherlands. were sampled and characterised. One dimensional consolidation tests were used to assess the compression behaviour (Chap-

ter 3) and consolidation behaviour (Chapter 4) of the sediments under various oxidising conditions: 1) non-oxidised, 2) chemically oxidised prior to the consolidation tests and 3) chemically oxidised inside the consolidation cell at various load steps. A chemical oxidant Hydrogen Peroxide which is normally used in soil classification test to remove organic matter was used to accelerate the oxidation process. The maximum oxidation rate under aerobic conditions and the effect of oxygen availability on the oxidation rate, was evaluated using a continuously stirred tank reactor (CSTR) (Chapter 5). Finally evaporative drying tests have been performed on oxidised and non-oxidised samples to study the shrinkage behaviour of organic soils (Chapter 6). The conclusions of each of these studies are summarised here chapter by chapter.

(Chapter 3): The effect of oxidation on compression behavior of organic soils. The results of the one dimensional consolidation tests showed that in situ oxidation of organic soils (under constant loading conditions) results in significant volume reduction. However the contribution of oxidation on the total volume reduction in organic soils is less significant than volume loss due to (primary) consolidation.

The (ex-situ) chemically oxidised sample has a lower initial void ratio (after settling), a lower compressibility and lower swelling capacity than the non-oxidised sample as expressed by a lower compression index C_c and swelling index C_s , which corresponds to the most observations in the literature.

When the organic soil is oxidised in-situ, it shows initially a higher stiffness upon further loading. When the compression curve approaches the virgin compression curve (VCC) of the non-oxidised soil, the compressibility increases to value similar to the non-oxidised curve. The observed behaviour appeared to be independent of the stress level at which the soil is oxidised. Upon unloading the in situ oxidised soils show a lower swelling capacity than the non-oxidised soil.

The compression and swelling behaviour of the in-situ chemically oxidised soil can be attributed to the fact that decomposition of organic soil results in the partial removal of organic matter, but does not immediately destroy the soil fabric. As the soil fabric remains (partly) intact, the metastable structure may initially provide higher stiffness, however the weakening or partial destruction of the fabric reduces the swelling capacity upon unloading.

In situ chemical oxidation resulted in a loss in solid mass, particularly for the samples had a high initial water content. However the loss in solid mass was less than expected, which may be attributed to a limited amount of oxidizing agent. Loss on ignition tests showed that the in situ chemically oxidised samples had slightly lower organic content than the non-oxidised sample. However the ex-situ oxidised sample still showed significant organic content, indicating that a significant fraction of organic matter could not be chemically oxidised or that chemical oxidation may result in other solid products.

(Chapter 5): Kinetics of oxidation in organic soils and peat The rate of aerobic oxidation in the field is limited by the limited availability of oxygen. Aerobic decomposition is a complex process, but can be simplified in two steps: 1) hydrolysis of large organic polymers (cellulose), process glucose and 2) the glucose reacts with oxygen to form water and carbon dioxide. When sufficient oxygen is present the oxidation rate is limited by

the hydrolysis step, which depends on environmental conditions, type of organic matter (size, surface area chemical composition), the amount and type of micro-organisms and the rate at which they are able to hydrolyze. In this study, the rate of aerobic oxidation is determined under varying conditions. Bioreactor experiments allowed to determine the oxidation rate of organic sediments dredged from the lakes in Wormer & Jisperveld as a function of oxygen concentration. They showed that the oxidation rate can be described using the Michaelis-Menten equation, which is a model commonly used to describe enzyme kinetics. The maximum rate of oxidation, which occurs under conditions of sufficient oxygen availability, V_{max} , and the affinity or half-saturation constant, K_m , were determined during multiple stirring and non-stirring cycles. Aerated experiments and the oxidation experiments using controlled addition of hydrogen peroxide as chemical oxidant showed similar kinetics in the same concentration range. Both V_{max} and K_m showed decreasing trends with the number of cycles. For aerobic oxidation V_{max} ranged from 1.6×10^{-7} to 0.3×10^{-7} mol/L/min and K_m from 4×10^{-5} to 1×10^{-5} mol/L, respectively, while under chemical oxidation V_{max} ranged from 1.2×10^{-6} to 0.3×10^{-6} mol/L.min and K_m from 5×10^{-5} to 0.5×10^{-5} mol/L.

A drop in pH is observed for both aerobic and chemical oxidation. The drop in pH may be attributed to the increase in carbonic acid concentration or the potential oxidation of iron sulfide minerals.

The carbon dioxide production rates were estimated from the oxygen depletion rates in the bioreactor test, and from the rates of settlement, solid mass loss and organic mass loss during the oxidation step in the one-dimensional consolidation experiments, using an empirical formula proposed by [van den Akker et al. \(2008\)](#). The results showed that carbon dioxide production estimates based on settlement rate are higher than other estimates. Hence the fraction of settlement attributed to the oxidation is expected to be smaller than 100% as proposed by [van den Akker et al. \(2008\)](#).

(Chapter 6): The effect of organic matter on the shrinkage behaviour. The effect of organic matter on the shrinkage and water retention behaviour of organic soils is evaluated by performing evaporative drying tests using the Hyprop device on non-oxidised and oxidised samples. Oxidation significantly affected the water retention behavior, but did not significantly influence the shrinkage curve. The oxidised soil showed significantly lower water retention capacity. Reducing the initial water content of the sample reduced the onset of the water retention characteristic curve. These results confirm earlier findings e.g., by [Oleszczuk et al. \(2003\)](#). Both samples showed significant shrinkage, but during most of this shrinkage the samples remained close to full saturation, while loss of water volume is almost equal to the loss of bulk soil volume. The non-oxidised samples showed gas formation at the initial stage of drying which was not the case for oxidised samples. Peak gas volume was observed at low tension values of 10 hPa and later decreases as tension increased, which may be due to diffusion of gas in the pore water. The mechanisms of gas formation are thought to be either exsolution of dissolved methane, oxidation of organic matter or a combination of both. The total volume of trapped gas within the soil is still relatively small. Hence it does not affect the shrinkage curve.

7.2. RECOMMENDATIONS

The results may be used to extend the theoretical framework for settlement prediction and incorporate the effect of oxidation as an important mechanism causing secondary compression. A modelling tool which couples the effects of consolidation, decomposition and reactive transport can be established. As the understanding of the underlying mechanisms and their interaction is not straightforward, it requires a collaborative effort from different disciplines in order to understand the properly describe the hydro-mechanical behaviour and chemical conversions in organic soils. The performed experiments should be repeated by using a larger quantity or other types of oxidising agent, which are more stable in nature and also identifying different components in organic soil that have different susceptibility to decomposition. Similar test series can also be repeated on different types of organic soils.

REFERENCES

- AHN (2019). Actueel Hoogte Bestand Nederland. URL: www.ahn.nl.
- Akagi, H. (1994). A physico-chemical approach to the consolidation mechanism of soft clays. *Soils Found*, 34, 43–50.
- van den Akker, J. J. H., Kuikman, P. J., de Vries, F., Hoving, I., Pleijter, M., Hendriks, R. F. A., Wolleswinkel, R. T. L., Simoes, R. T. L., & Kwakernaak, C. (2008). Emission of CO₂ from agricultural peat soils in the netherlands and ways to limit this emission. In *Proceedings of the 13th International Peat Congress After Wise Use The Future of Peatlands* (pp. 645–648). volume 1.
- Al-Khafaji, A. W. N. (1979). *Decomposition effects on engineering properties of fibrous peats*. Ph.D. thesis Michigan State University.
- Al-Khafaji, A. W. N., & Andersland, O. B. (1981). Compressibility and strength of decomposing fibre–clay soils. *Géotechnique*, 31, 497–508.
- Andersland, O. B., & Al-Khafaji, A. W. N. (1984). Estimating failure probabilities for California levees. *Journal Geotechnical Engineering*, 110, 993–994.
- Andersland, O. B., Khattak, A. S., & Al-Khafaji, A. W. N. (1980). Effect of organic material on soil shear strength. In R. Yong, & F. Townsend (Eds.), *ASTM STP 740 Laboratory Shear Strength of Soil* (pp. 226–241). Chicago: American Society for Testing and Materials.
- Andrejko, M. J., Fiene, F., & Cohen, A. D. (1983). Comparison of ashing techniques for determination of the inorganic content of peats. *Testing of Peats and Organic Soils, ASTM STP 820*, (pp. 5–20).
- Arman, A. (1970). Engineering classification of organic soils. *Highway Research Record*, 310.
- Armentano, T. V., & Menges, E. S. (1986). Patterns of change in the carbon balance of organic soil-wetlands of the temperate zone. *Journal of Ecology*, 74, 755–774.
- Arndt, S., Jørgensen, B. B., LaRowe, D. E., Middelburg, J. J., Pancost, R. D., & Regnier, P. (2013). Quantifying the degradation of organic matter in marine sediments: A review and synthesis. *Earth-Science Reviews*, 123, 53–86.
- ASTM (2004). D2976-71: Standard Test Method for pH of Peat Materials. *ASTM International*, 71, 1–2.

- ASTM (2007a). D2974-07a: Standard Test Methods for Moisture, Ash and Organic Matter of Peat and Other Organic Soils. *ASTM International*, (pp. 1–4).
- ASTM (2007b). D4427-07: Standard Classification of Peat Samples by Laboratory Testing. *ASTM International*, (pp. 1–3).
- ASTM (2008). D1997-91: Standard Test Method for Laboratory Determination of the Fiber Content of Peat Samples by Dry Mass. *ASTM International*, 91, 1–2.
- ASTM (2010a). D2216-10: Standard Test Methods for Laboratory Determination of Water (Moisture) Content of Soil and Rock by Mass 1. *ASTM International*, (pp. 1–7).
- ASTM (2010b). D4318-10: Standard Test Methods for Liquid Limit, Plastic Limit and Plasticity Index of Soils. *ASTM International*, (pp. 1–15).
- ASTM (2011). D2434-68: Standard Practice for Classification of Soils for Engineering Purposes (Unified Soil Classification System). *ASTM International*, 11, 1–12.
- ASTM (2013). C618-12a: Standard Specification for Coal Fly Ash and Raw or Calcined Natural Pozzolan for Use. *ASTM International*, (pp. 1–5).
- ASTM (2014). D5550-14: Standard Test Method for Specific Gravity of Soil Solids by Gas Pycnometer. *ASTM International*, (pp. 1–5).
- Badv, K., & Sayadian, T. (2012). An investigation into the geotechnical characteristics of Urmia peat. *Iranian Journal of Science and Technology - Transactions of Civil Engineering*, 36, 167–180.
- Barden, L. (1968). Primary and secondary consolidation of clay and peat. *Geotechnique*, 18, 1–24.
- Barden, L. (1969). Time dependent deformation of normally consolidated clays and peats. *Journal of the soil mechanics and foundations division*, 95, 1–31.
- Bell, F. G. (2000). *Engineering Properties of Soils and Rocks*. (4th ed.). Oxford, London: Blackwell Science.
- Berry, P. L., & Poskitt, T. J. (1972). The consolidation of peat. *Geotechnique*, 22, 27–52.
- Beuving, J., & Van den Akker, J. J. H. (1996). *Maaiveldsdaling van veengrasland bij twee slootpeilen in de polder Zegvelderbreek. Vijfentwintig jaar zakkingsmetingen op het ROC Zegveld. Rapport, vol. 377. DLO-Staring Centrum, Wageningen (in Dutch)*. Technical Report DLO-Staring Centrum Wageningen.
- Bjerrum, L. (1967). Engineering geology of Norwegian normally-consolidated marine clays as related to settlement of buildings. *Geotechnique*, 17, 81–118.
- Blackford, J. J., & Chambers, F. M. (1993). Determining the degree of peat decomposition for peat-based palaeoclimatic studies. *International Peat Journal*, 5, 7–24.

- Boas, F. E., & Fleischmann, D. (2012). CT artifacts: causes and reduction techniques F Edward. *Imaging Med*, 4, 229–240.
- Bohne, K., & Kretschmer, H. (1984). Untersuchung zum Schrumpfung und Quaelungsverhalten. *Arch.Acker.Pfl.Boden*, 28, 577–584.
- Boivin, P., Garnier, P., & Tessier, D. (2004). Relationship between clay content, clay type, and shrinkage properties of soil samples. *Soil Science Society of America Journal*, 68, 1145–1153.
- Boivin, P., Schäffer, B., Temgoua, E., Gratier, M., & Steinman, G. (2006). Assessment of soil compaction using soil shrinkage modelling: Experimental data and perspectives. *Soil and Tillage Research*, 88, 65–79.
- Bord na Mona (1985). *Fuel peat in developing countries*. Technical Report Irish Peat Development Authority Washington, DC. URL: <http://documents.worldbank.org/curated/en/1985/06/439714/fuel-peat-developing-countries>.
- Boso, M., & Grabe, J. (2013). Long term compression behaviour of soft organic sediments. In A. Laloui, L.Ferrari (Ed.), *Multiphysical Testing of Soils and Shales* (pp. 249–254). Springer Berlin Heidelberg.
- Brandyk, T., Szatyłowicz, J., Oleszczuk, R., & Gnatowski, T. (2002). Water-related physical attributes of organic soils. In L. E. Parent, & P. Ilnicki (Eds.), *Organic soils and peat materials for sustainable Agriculture* (p. 224). CRC Press.
- Braudeau, E., Costantini, J. M., Bellier, G., & Colleuille, H. (1999). New device and method for soil shrinkage curve measurement and characterization. *Soil Science Society of America Journal*, 63, 525–535.
- Bronswijk, J. J. B. (1988). Modelling of water balance, cracking and subsidence of clay soils. *Journal Hydrology*, 97, 199–212.
- Brouns, K. (2016). *The effects of climate change on decomposition in Dutch peatlands : an exploration of peat origin and land use effects*. Ph.D. thesis Utrecht University.
- BS 1377-2 (1990). Methods of test for soils for civil engineering purposes (classification tests).
- Campanella, R. G., & Mitchell, J. K. (1968). Influence of temperature variations on soil behaviour. *Journal of the soil mechanics and foundations division, Proceedings of the American society of civil engineers*, 94, 709–734.
- Camporese, M., Gambolati, G., Putti, M., & Teatini, P. (2006). Peatland subsidence in the Venice watershed. *Peatlands: Evolution and Records of Environmental and Clmate Changes*, 9, 529–550.
- Campos, J. R. R., Silva, A. C., Fernandes, J. S., Ferreira, M. M., & Silva, D. V. (2011). Water retention in a peatland with organic matter in different decomposition stages. *Revista Brasileira de Ciência do Solo*, 35, 1217–1227.

- CEN (2004a). ISO/TS 17892-1: Geotechnical investigation and testing - Laboratory testing of soil - Part 1: Determination of water content. *Nederlands Normalisatie-Instituut*, (pp. 1–6).
- CEN (2004b). ISO/TS 17892-4: Geotechnical investigation and testing - Laboratory testing of soil - Part 4: Determination of particle size distribution. *Nederlands Normalisatie-Instituut*, (pp. 1–31).
- CEN (2004c). ISO/TS 17892-5: Geotechnical investigation and testing - Laboratory testing of soil - Part 5: Incremental loading oedometer test. *Nederlands Normalisatie-Instituut*, (pp. 1–25).
- Chandler, C. J., & Chartress, F. R. D. (1988). Settlement measurement and analysis of three trial embankments on soft peaty ground. In *Baltic Conference*. Tallin.
- Chesworth, W. (2008). *Encyclopedia of Soil Science*. The Netherlands: Springer.
- Chin A Moei, S. A. (2016). Effects of organic matter on shrinkage and water retention behaviour of organic dredged sediment.
- Christensen, R. W., & Wu, T. H. (1964). Analysis of clay deformation as a rate process. *Journal Soil Mechanics Foundation*, 90, 125–157.
- Christie, I. F., & Tonks, D. M. (1985). Developments in the time line theory of consolidation. In *The 11th international conference on soil mechanics and foundation Engineering* (pp. 423–426). San Francisco.
- Colleselli, F., Cortellazzo, G., & Cola, S. (2000). Laboratory testing of Italian peaty soils. In T. Edil, & P. Fox (Eds.), *Geotechnics of High Water Content Materials, ASTM STP 1374* (pp. 226–240). West Conshohocken, PA: American Society for Testing and Materials.
- Couwenberg, J. (2009). Methane emissions from peat soils (organic soils, histosols). In *Wetlands International, Proceedings for UN-FCCC* (pp. 1–16). Bonn.
- Craig, R. F. (2004). *Craig's Soil Mechanics* volume 53. (Seventh ed.). Taylor & Francis.
- Crooks, J. H. A., Becker, D. E., Jerreries, M. G., & McKenzie, K. (1984). Yield behaviour and consolidation. I: pore water response. In R. Yong, & T. F.C. (Eds.), *Proceedings, Symposium on sedimentation consolidation models: prediction and validation* (pp. 356–381). San Francisco: ASCE.
- Dawson, Q., Kechavarzi, C., Leeds-Harrison, P. B., & Burton, R. G. O. (2010). Subsidence and degradation of agricultural peatlands in the Fenlands of Norfolk, UK. *Geoderma*, 154, 181–187.
- De Jong, G. J., & Verruijt, A. (1965). Primary and secondary consolidation of a spherical clay sample. In *Proceeding of the 6th international conference soil mechanic and foundation engineering* (pp. 254–258). Montreal.
- De Josselin de Jong, G. (1968). Consolidation models consisting of an assembly of viscous elements or a cavity channel network. *Geotechnique*, 18, 195–228.

- Dhowian, A. W., & Edil, T. B. (1980). Consolidation behavior of peats. *Geotechnical Testing Journal*, 3, 105–114.
- Drexler, J. Z., de Fontaine, C. S., & Deverel, S. J. (2009). The legacy of wetland drainage on the remaining peat in the Sacramento-San Joaquin Delta, California, USA. *WETLANDS*, 29, 372–386.
- Duraisamy, Y., Huat, B. B. K., & Aziz, A. A. (2007). Engineering properties and compressibility behavior of tropical peat soil. *American Journal of Applied Sciences*, 4, 768–773.
- Edil, T. B. (1997). Construction over peats and organic soils. In *Proceedings Conference on Recent Advances in Soft Soil Engineering*. Kuching, Sarawak, Malaysia.
- Elsayed, A., Paikowsky, S., & Kurup, P. (2011). Characteristics and engineering properties of peaty soil underlying cranberry bogs. *Geo-Frontiers 2011*, (pp. 2812–2821).
- Fao (2015). The main characteristics of tropical peat. URL: <http://www.fao.org/docrep/x5872e/x5872e06.htm>.
- Farrell, E. R., O'Neill, C., & Morris, A. (1994). Changes in the mechanical properties of soils with variations in organic content. In T. den Haan, E.J., Termaat, R., Edil (Ed.), *Advances in Understanding and Modelling the Mechanical Behaviour of Peat* (pp. 19–25). Rotterdam.
- Fatahi, B., Le, T. M., Le, M. Q., & Khabbaz, H. (2013). Soil creep effects on ground lateral deformation and pore water pressure under embankments. *Geomechanics and Geoengineering*, 8, 107–124.
- Force, E. A. (1998). *Factors controlling pore-pressure generation during K0-consolidation of laboratory tests*. Ph.D. thesis MIT.
- Fox, P., Edil, T., & Lan, L. (1992). $C\alpha/Cc$ concept applied to compression of peat. *Journal of Geotechnical Engineering*, 118, 1256–1263.
- Fredlund, D. G., & Rahardjo, H. (1993). *Soil Mechanics for Unsaturated Soils*. Canada: John Wiley & Sons, Inc.
- Fredlund, D. G., Rahardjo, H., & Fredlund, M. D. (2012). *Unsaturated soil mechanics in engineering practice*. Canada: John Wiley & Sons, Inc.
- Fredlund, M. D., Wilson, G. W., & Fredlund, D. G. (2002). Representation and estimation of the shrinkage curve. In *UNSAT 2002, Proceedings of the Third International Conference on Unsaturated Soils* (pp. 145–149).
- Gambolati, G., Putti, M., Teatini, P., & Gasparetto Stori, G. (2003). Subsidence due to peat oxidation and impact on drainage infrastructures in a farmland catchment south of the Venice Lagoon. *Materials and Geoenvironment*, 50, 125–128.
- Garlanger, J. E. (1972). The consolidation of soils exhibiting creep under constant effective stress. *Giotechnique*, 22, 71–78.

- Gebert, J., & Groengroeft, A. (2006). Passive landfill gas emission - Influence of atmospheric pressure and implications for the operation of methane-oxidising biofilters. *Waste Management*, 26, 245–251.
- Gebhardt, S., Fleige, H., & Horn, R. (2010). Shrinkage processes of a drained riparian peatland with subsidence morphology. *Journal of Soils and Sediments*, 10, 484–493. doi:10.1007/s11368-009-0130-9.
- Gebhardt, S., Fleige, H., & Horn, R. (2012). Anisotropic shrinkage of mineral and organic soils and its impact on soil hydraulic properties. *Soil & Tillage Research*, 125, 96–104.
- Gibson, R. E., & Lo, K. Y. (1961). A theory of consolidation exhibiting secondary compression. *Norwegian Geotechnical Institute*, .
- Gofar, N., & Sutejo, Y. (2007). Long term compression behaviour of fibrous peat. *Malaysian Journal of Civil Engineering*, 19, 104–116.
- Gokhan, C., & Ahmet, S. (2003). Effects of organic content on secondary and tertiary compression behaviour of soft clay. In *International Workshop on Geotechnics of Soft Soils-Theory and Practice* (pp. 403–408). Noordwijkerhout, The Netherlands: Vemeer, P.A., Schweiger, H.F., Karstunen, M., Cudny, M.
- Goldberg, D. (1965). Discussion of Jonas 'Subsurface stabilisation of organic silty clay by precompression'. *Journal of the soil mechanics and foundation division, American society of civil engineers*, 91.
- Graham, J., Crooks, H. A., & Bell, A. L. (1983). Discussion: Time effects on the stress-strain behaviour of natural soft clays. *Geotechnique*, 33, 327–340.
- Graham, J., & Yin, J. H. (2001). On the time-dependent stress-strain behaviour of soft soils. In C. F. Lee, C. K. Lau, C. W. W. Ng, A. K. Kwong, P. L. R. Pang, J. H. Yin, & Z. Q. Yue (Eds.), *Proceedings of the Third International Symposium on Soft Soil Engineering* (p. 13). The Netherlands: A.A. Balkema.
- Gray, H. (1936). Progress report on research on the consolidation of fine-grained soils. *Proceedings international conference on soil mechanics and foundation engineering*, 2, 138–141.
- Green, W. J. (1969). *The influence of several factors on the rate of secondary compression of soil*. Ph.D. thesis University of Missouri.
- Greenwood, D. J. (1961). The effect of oxygen concentration on the decomposition of organic materials in soil. *Plant and Soil*, 14, 360–376.
- Grim, R. E. (1962). *Applied clay mineralogy, International series in the earth and planetary sciences*. (2nd ed.). New York, NY: McGrawHill.
- Gupta, B. (1964). *Creep of saturated soil at different temperatures*. Ph.D. thesis University of British Columbia, Canada.

- Guven, N. (1993). Molecular aspects of clay of clay-water interactions. In N. Guven, & R. Pallastro (Eds.), *Clay water interface and its rheological properties, CMS workshop lectures* (pp. 2–79). Clay minerals society.
- den Haan, E. J. (1997). An overview of the mechanical behaviour of peats and organic soils And some appropriate construction techniques. In B. et al. Huat (Ed.), *Proceedings Conference on Recent Advances in Soft Soil Engineering* (pp. 17–45). Kuching, Sarawak, Malaysia: CRC Press.
- den Haan, E. J., & Kruse, G. A. M. (2007). Characterisation and engineering properties of Dutch peats. In S. Phoon, K.K., Hight, D.W., Leroueil, S. & Tan (Ed.), *Proceedings of the Second International Workshop on Characterisation and Engineering Properties of Natural Soils* (pp. 2101–2133). Singapore: Taylor & Francis.
- Hanrahan, E. T. (1954). An investigation of some physical properties of peat. *Geotechnique*, (pp. 108–123).
- Hardin, B. O., & Black, W. L. (1968). Vibration modulus of normally consolidated clay. *Journal of the soil mechanics and foundation division, Proceedings of the American society of civil engineers*, 94, 353–370.
- Heidarian, P. (2012). *Effect of initial water content and stress history on water-retention behaviour of mine tailings*. Ph.D. thesis Carleton University Ottawa.
- Hobbs, N. B. (1986). Mire morphology and the properties and behaviour of some British and foreign peats. *Quarterly Journal of Engineering Geology and Hydrogeology*, 19, 7–80.
- Hobbs, N. B. (1987). A note on the classification of peat. *Geotechnique*, 37, 405–407.
- Hoogland, T., van den Akker, J. J. H., & Brus, D. J. (2012). Modeling the subsidence of peat soils in the Dutch coastal area. *Geoderma*, 171-172, 92–97.
- Huang, P. T., Patel, M., Santagata, M. C., & Bobet, A. (2009). *Classification of Organic Soils*. 1.
- Huat, B. B. K., Asadi, A., & Kazemian, S. (2009). Experimental Investigation on Geomechanical Properties of Tropical Organic Soils. *American Journal of Engineering and Applied Sciences*, 2, 184–188.
- Huat, B. B. K., Kazemian, S., Prasad, A., & Barghchi, M. (2011). State of an art review of peat : General perspective. *International Journal of the Physical Sciences*, 6, 1988–1996.
- Huat, B. B. K., Prasad, A., Asadi, A., & Kazemian, S. (2014). *Geotechnics of Organic Soils and Peat*. CRC Press.
- Humphries, W. K., & Wahls, H. E. (1968). Stress history effects on dynamic modulus of clay. *Journal of the soil mechanics and foundations division*, 94, 371–390.

- Ingebritsen, S. E., Ikenhara, M. E., McVoy, C., Glaz, B., & Park, W. (1999). Drainage of Organic Soils: Sacramento-San Joaquin Delta; Florida Everglades. *Land subsidence in the United States: US Geological Survey Circular 1182*, (pp. 79–106).
- Jinming, H., & Xuehui, M. (1998). Physical and Chemical Properties of Peat. *Coal, oil shale, natural bitumen, heavy oil and peat, II*.
- Jonas, E. (1964). Subsurface stabilisation of organic silty clay by precompression. *Journal of the soil mechanics and foundation division, proceedings of the American society of civil Engineers*, 90, 363–376.
- Joosten, H., & Clarke, D. (2002). *Wise Use of Mires and Peatlands - Background and Principles Including a Framework for Decision-Making*. Saarijarvi, Finland: International Mire Conservation Group and International Peat Society.
- Kasimir-Klemedtsson, A., Klemedtsson, L., Berglund, K., Martikainen, P., Silvola, J., & Oenema, O. (1997). Greenhouse gas emissions from farmed organic soils: a review. *Soil Use and Management*, (pp. 245–250).
- Kazemian, S., & Huat, B. B. K. (2010). Assessment of stabilization methods for soft soils by admixtures. In *2010 International Conference on Science and Social Research (CSSR 2010)* (pp. 118–121). Kuala Lumpur, Malaysia.
- Kazemian, S., Huat, B. B. K., Prasad, A., & Bargchi, M. (2011a). A state of art review of peat: Geotechnical engineering perspective. *International Journal of the Physical Sciences*, 6, 1974–1981.
- Kazemian, S., Huat, B. B. K., Prasad, A., & Barghchi, M. (2011b). Effect of peat media on stabilization of peat by traditional binders. *International Journal of the Physical Sciences*, 6, 476–481.
- Kettridge, N., & Binley, A. (2008). X-ray computed tomography of peat soils: measuring gas content and peat structure. *Hydrological Processes*, 22, 4827–4837.
- Khattak, A. S. (1978). *Mechanical behaviour of fibrous organic soils*. Ph.D. thesis Michigan State University.
- Klavins, M., Sire, J., Purmalis, O., & Melecis, V. (2008). Approaches to estimating humification indicators for peat. *Mires and Peat*, 3, 1–15.
- Kogel-Knabner, I. (2002). The macromolecular organic composition of plant and microbial residues as inputs to soil organic matter. *Soil Biology and Biochemistry*, 34, 139–162.
- Koti Reddy, B. H., Sahu, R. B., & Ghosh, S. (2014). Consolidation Behavior of Organic Soil in Normal Kolkata Deposit. *Indian Geotechnical Journal*, 44, 341–350.
- Kuhn, M. R., & Mitchell, J. K. (1993). New perspective on soil creep. *Journal Geotechnical Engineering*, 119, 507–524.

- Kwok, C. Y., & Bolton, M. D. (2010). DEM simulations of thermally activated creep in soils. *Geotechnique*, 60, 425–433.
- Lambe, T. W., & Whitman, R. V. (1969). *Soil mechanics*. New York, NY: Wiley.
- Landva, A. O., Korpjiaakko, E. O., & Pheeneey, P. E. (1983). Geotechnical Classification of Peats and Organic Soils. In P. Jarrett (Ed.), *STP 820 Testing of Peats & Organic Soils* (pp. 37–51). Toronto, Canada: American Society for Testing and Materials.
- Landva, A. O., & Pheeneey, P. E. (1980). Peat fabric and structure. *Canadian Geotechnical Journal*, 17, 416–435.
- van der Lans, R. G. J. M. (2009). Gas-liquid interface transport.
- Lauritzen, C. W., & Stewart, A. J. (1942). Soil volume changes and accompanying moisture and pore-space relationships. *Soil Science Society of America*, (pp. 113–116).
- Le, T. M., Fatahi, B., & Khabbaz, H. (2012). Viscous Behaviour of Soft Clay and Inducing Factors. *Geotechnical and Geological Engineering*, 30, 1069–1083.
- LeBihan, J. P., & Serge, L. (2002). A model for gas and water flow through the core of earth dams. *Canadian Geotechnical Journal*, 39, 90–102.
- Leonards, G. A., & Altschaeffl, A. G. (1964). Compressibility of Clay. *Journal of soil mechanics and foundations division, American society of civil engineers*, 90, 133–154.
- Leonards, G. A., & Girault, P. (1961). A study of the One-dimensional Consolidation Tests. In *Proceedings 9th ICSMFE* (pp. 116–130). Paris volume 1.
- Leroueil, S., Hight, D. W., & Cabral, A. R. (2015). *Practical implications of gas-water interactions in soils*.
- Lo, K. Y. (1961). Secondary compression of clays. *Journal of the soil mechanics and foundations division, American society of civil engineers*, 87, 61–87.
- Long, M. (2005). Review of peat strength, peat characterisation and constitutive modelling of peat with reference to landslides.
- Longmuir, I. S. (1954). Respiration rate of bacteria as a function of oxygen concentration. *Biochemical Journal*, 57, 81–87.
- Low, P. F. (1962). Influenced of adsorbed water on exchangeable ion movement. In *Proceedings of the 9th national conference on clays and clay mineral*. New York, NY.
- Macfarlane, I. C. (1969). *Muskeg Engineering Handbook*. University of Toronto Press.
- McDougall, J. R. R., Pyrah, I. C. C., Yuen, S. T. S. T. S., Monteiro, V. E. D. E. D., Melo, M. C. C., Jucá, J. F. T., & Juca, J. F. (2004). Decomposition and settlement in landfilled waste and other soil-like materials. *Geotechnique*, 54, 1–5.
- McGeever, J. (1987). *The strength parameters of an organic silt*. Msc thesis Trinity College, University of Dublin.

- Megonigal, J. P., Hines, M. E., & Visscher, P. T. (2004). Anaerobic Metabolism: Linkages to Trace Gases and Aerobic Processes. In W. Schlesinger, H. Holland, & K. Turekian (Eds.), *Biogeochemistry* chapter 8.08. (pp. 317–424). Elsevier volume 8.
- Mer, J. L., & Roger, P. (2001). Production, oxidation, emission and consumption of methane by soils: A review. *European Journal of Soil Biology*, 37, 25–50.
- Mesri, G. (1973). Coefficient of secondary compression. *Journal of the Soil Mechanics and Foundations Division*, 99, 123–137.
- Mesri, G. (2003). Primary compression and secondary compression In: Soil behaviour and soft ground construction. In *Geotechnical special publication, ASCE* (pp. 122–166). Reston: ASCE volume 119. doi:[http://dx.doi.org/10.1061/40659\(2003\)5](http://dx.doi.org/10.1061/40659(2003)5).
- Mesri, G., & Ajlouni, M. (2007). Engineering Properties of Fibrous Peats. *Geotechnical and Geoenvironmental Engineering*, 133, 850–866.
- Mesri, G., & Castro, A. (1987). C_{α}/C_c concept and K_0 during secondary compression. *Journal of Geotechnical Engineering*, 113, 230–247.
- Mesri, G., & Godlewski, P. M. (1977). Time and stress compressibility interrelationship. *Journal Geotechnical Engineering*, 103, 417–430.
- Mesri, G., Stark, T. D., Ajlouni, M. A., & Chen, C. S. (1997). Secondary Compression of Peat with or without Surcharging.pdf. *Journal of Geotechnical and Geoenvironmental Engineering*, 123, 411–421.
- Mikutta, R., Kleber, M., Kaiser, K., & Jahn, R. (2005). Review : Organic Matter Removal from Soils using Hydrogen Peroxide , Sodium Hypochlorite and Disodium Peroxodisulfate. *Soil Science Society of America*, 69, 120–135.
- Mitchell, J. K. (1964). Shearing resistance of soils as a rate process. *Journal soil mechanics foundation division*, 90, 29–61.
- Mitchell, J. K., & Campanella, R. G. (1968). Soil creep as a rate process. *Soil creep as a rate process*, 94, 1–26.
- Mitchell, J. K., & Soga, K. (2005). *Fundamentals of Soil Behaviour*. (3rd ed.). JOHN WILEY & SONS, INC.
- Miyakawa, I. (1960). Some aspects of road construction in peaty or mashy areas in Hokkaido. In *Civil Engineering Research Institute, Hokkaido Development Bureau*. Sapporo, Japan.
- Monnier, G., Stengel, P., & Fies, J. C. (1973). Une methode de mesure de la densite apparente de petits agglomerats terreux: application a l'analyse des systemes de porosite du sol. *Annales agronomiques*, (pp. 533–545).
- Murayama, S., & Shibata, T. (1961). Rheological properties of clays. In *Proceedings of the 5th international conference soil mechanics* (pp. 269–273). Paris volume 1.

- Navarro, V., & Alonso, E. E. (2001). Secondary compression of clays as a local dehydration process. *Geotechnique*, *51*, 859–869.
- Newland, P. L., & Allely, B. H. (1960). A study of the consolidation characteristics of a clay. *Geotechnique*, *10*, 62–74.
- Ngan-Tillard, D. J. M. Huisman, D. J., Corbella, F., & Van Nass, A. (2018). Over the rainbow? Micro-CT scanning to non-destructively study Roman and early medieval glass bead manufacture. *Journal of Archaeological Science*, *98*, 7–21.
- Nie, L., Lv, Y., & Li, M. (2012). Influence of organic content and degree of decomposition on the engineering properties of a peat soil in NE China. *Quarterly Journal of Engineering Geology and Hydrogeology*, *45*, 435–446. doi:10.1144/qjegh2010-042.
- Nie, L., Su, Z.-D., Xia, J., Lv, Y., & Li, Z.-C. (2013). Study on mineral distribution of peat soil in northeast china. *Asian Journal of Chemistry*, *25*, 10150–10152.
- O’ Loughlin, C. D., & Lehane, B. M. (2003). A STUDY OF THE LINK BETWEEN COMPOSITION AND COMPRESSIBILITY OF PEAT AND ORGANIC SOILS. In B. Huat, H. Omar, S. Maail, & E. Mahsun (Eds.), *Proceedings of 2nd International Conference on Advances in Soft Soil Engineering and Technology* (pp. 135–152). Putrajaya, Malaysia.
- O’Kelly, B. C. (2008). Effect of biodegradation on the consolidation properties of a dewatered municipal sewage sludge. *Waste Management*, *28*, 1395–1405. doi:10.1016/j.wasman.2007.08.004.
- O’Kelly, B. C., & Pichan, S. P. (2013). Effects of decomposition on the compressibility of fibrous peat — A review. *Geomechanics and Geoengineering*, *8*, 286–296.
- O’Kelly, B. C., & Pichan, S. P. (2014). Effect of decomposition on physical properties of fibrous peat. *Environmental Geotechnics*, *1*, 22–32.
- Oleszczuk, R., Bohne, K., Szatyłowicz, J., Brandyk, T., & Gnatowski, T. (2003). Influence of load on shrinkage behavior of peat soils. *Journal of Plant Nutrition and Soil Science*, *166*, 220–224.
- Oleszczuk, R., & Truba, M. (2013). The analysis of some physical properties of drained peat-moorsh soil layers. *Land Reclamation*, *45*, 41–48.
- Oliveira, B. R., Smit, M. P., Veld, H., & van Paassen, L. A. Rijnaarts, H. H. Grotenhuis, T. (2018). Subsidence of organic dredged sediments in an upland deposit in Wormer-en Jisperveld: North Holland, the Netherlands. *Environmental earth sciences*, *77*, 131.
- Olson, R. E. (1989). Unit 7: Secondary consolidation.
- van Paassen, L. A., Tollenaar, R. N., Jommi, C., Steins, A., & von Unold, G. (2018). Investigating some irregularities observed during suction measurements using the Hyprop device. In *7th International Conference on Unstaurated Soil Mechanics, At Hongkong*.

- Paaswell, R. E. (1967). Temperature effects on clay soil consolidation. *Journal of the soil mechanics and foundations division, Proceedings of the American Society of Civil Engineers*, 93, 9–21.
- Pankratov, T. A., Ivanova, A. O., Dedysh, S. N., & Liesack, W. (2011). Bacterial populations and environmental factors controlling cellulose degradation in an acidic Sphagnum peat. *Environmental microbiology*, 13, 1800–14.
- Peng, X., & Horn, R. (2005). Modeling soil shrinkage curve across a wide range of soil types. *Soil Science Society of America*, 69, 584–592.
- Peng, X., & Horn, R. (2007). Anisotropic shrinkage and swelling of some organic and inorganic soils. *European Journal of Soil Science*, 58, 98–107.
- Pichan, S., & O’Kelly, B. C. (2012). Effect of Decomposition on the Compressibility of Fibrous Peat. *ASCE GeoCongress 2012*, (pp. 4329–4338).
- Pichan, S. P., & O’Kelly, B. C. (2013). Stimulated decomposition in peat for engineering applications. *Proceedings of the Institution of Civil Engineers - Ground Improvement*, 166, 168–176.
- Plum, R. L., & Esrig, M. I. (1969). Some temperature effects on soil compressibility and pore water pressures. *48th Annual Meeting of the Highway Research Board*, .
- Pons, L. J., & Zonneveld, I. S. (1965). Soil ripening and soil classification: Initial soil formation in alluvial deposits and a classification of the resulting soils. *International Institute for Land Reclamation and Improvement*, (pp. 1–128).
- Price, J. S., Cagampan, J., & Kellner, E. (2005). Assessment of peat compressibility: is there an easy way? *Hydrological Processes*, 19, 3469–3475.
- Radforth, N. W. (1969). Classification of Muskeg. In I. Macfarlane (Ed.), *Muskeg Engineering Handbook*. Toronto, Ontario: University of Toronto Press.
- R.A.W (2005). R.A.W. proef 124: Standaard RAW Bepalingen, Identificatie: 300-W-H1.01-F1, Versienummer: 2005.0002, Ingangsdatum: februari 2005.
- Reeve, M. J., & Hall, D. G. (1978). Shrinkage in Clayey Subsoils of Contrasting Structure. *Journal of Soil Science*, 29, 315–323.
- Robinson, R. G. (1999). Consolidation analysis with pore water pressure measurements. *Geotechnique*, 49, 127–132.
- Santagata, M., Bobet, A., Johnston, C. T., & Hwang, J. (2008). One-Dimensional Compression Behavior of a Soil with High Organic Matter Content. *Journal of Geotechnical and Geoenvironmental Engineering*, 134, 1–13.
- Schiffman, R. L., Ladd, C. C., & Chen, A. T. (1966). The secondary consolidation of clay. *I.U.T.A.M. Symp. Rheol. Soil Mech.*, (p. 273).

- Schindler, U. (1980). Ein Schnellverfahren zur Messung der Wasserleitfähigkeit im teilgesättigten Boden and Stechzylinderproben. *Archiv für Acker- und Pflanzenbau und Bodenkunde*, 21, 1–7.
- Schindler, U., Doerner, J., & Mueller, L. (2015). Simplified method for quantifying the hydraulic properties of shrinking soils. *Journal of Plant Nutrition and Soil Science*, 178, 136–145.
- Schindler, U., Durner, W., Von Unold, G., Mueller, L., & Wieland, R. (2010). The evaporation method: Extending the measurement range of soil hydraulic properties using the air-entry pressure of the ceramic cupitile. *Journal of plant nutrition and soil science*, 173, 563–572.
- Schmidt, N. O. (1964). Secondary consolidation review of literature. Personal notes, .
- Schothorst, C. J. (1977). Subsidence of low moor peat soils in the western Netherlands. *Geoderma*, 17, 265–291.
- Schumacher, B. A. (2002). *Methods for the Determination of Total Organic Carbon (TOC) in Soils and Sediments*. Technical Report April Ecological Risk Assessment Support Center, U.S. Environmental Protection Agency Las Vegas.
- Schwärzel, K., Renger, M., Sauerbrey, R., & Wessolek, G. (2002). Soil physical characteristics of peat soils. *Journal of Plant Nutrition and Soil Science - Zeitschrift für Pflanzenernährung und Bodenkunde*, 165, 479–486.
- Šimůnek, J., Kodešová, R., Gribb, M. M., & van Genuchten, M. T. (1999). Estimating hysteresis in the soil water retention function from cone permeameter experiments. *Water Resources Research*, 35, 1329–1345.
- Skempton, A. W., & Bjerrum, L. (1957). A contribution to the settlement analysis of foundations on clay. *Geotechnique*, 7, 168–178.
- Skempton, A. W., & Petley, D. J. (1970). Ignition Loss and Other Properties of Peats and Clays from Avonmouth, King's Lynn and Cranberry Moss. *Géotechnique*, 20, 343–356.
- Slneiderink, M. (2016). *Dynamic characterisation of SOM degradation with an aerobic reaction network*. Msc thesis Delft University of Technology.
- Sridharan, A., & Prakash, K. (1998). Secondary Compression Factor. In *Proceedings of the ICE - Geotechnical Engineering* (pp. 96–103). volume 131.
- Sridharan, A., & Rao, A. S. (1982). Mechanisms controlling the secondary compression of clays. *Géotechnique*, 32, 249–260.
- Stirk, G. B. (1954). Some aspects of soil shrinkage and the effect of cracking upon air entry into the soil. *Australian Journal of Soil Research*, 5, 279–290.
- Swift, R. G. (1996). *Organic matter characterization*. Soil Science Society of America.

- Szatyłowicz, J., Oleszczuk, R., & Brandyk, T. (1996). Shrinkage characteristics of some fen peat soils. In *Proceedings of the 10th International Peat Congress* (pp. 327–338). Bremen, Germany volume 2.
- Szymański, A., Sas, W., & Drozd, A. (2004). Secondary compression in organic soils. *Annals of Warsaw Agricultural University, Land Reclamation*, (pp. 221–228).
- Takeda, T., Sugiyama, M., Akaishi, M., & Chang, H. (2012). Secondary Compression behavior in One-Dimensional Consolidation Tests. *Journal of GeoEngineering*, 7, 53–58.
- Tariq, A. U. R., & Durnford, D. S. (1993). Soil volumetric shrinkage measurements: a simple method. *Soil Science*, 155, 325–330.
- Taylor, D. W. (1942). *Research on consolidation of clays..* Ph.D. thesis Massachusetts Institute of Technology, Cambridge, Massachusetts.
- Taylor, D. W., & Merchant, W. A. (1940). A theory of clay consolidation accounting for secondary compression. *Journal Math Physics*, 19, 167–185.
- Terzaghi, K. (1941). Undisturbed clay samples and undisturbed clays. *Journal Boston Soc. Civil Eng*, 29, 211–231.
- Terzaghi, K., Peck, R. B., & Mesri, G. (1996). *Soil Mechanics in Engineering Practice*. (3rd ed.). New York, NY: John Wiley & Sons, Inc.
- Thomas, M. B., & Spurway, M. I. (1998). A Review of Factors Influencing Organic Matter Decomposition and Nitrogen Immobilisation in Container Media. *Combined Proceedings International Plant Propagators' Society*, 48, 66–71.
- Thorsten, C. (2013). Some Chemistry of Acid Mine Drainage (AMD).
- Tollenaar, R. N. (2017). *Experimental Investigation on the Desiccation and Fracturing of Clay*. Phd dissertation Delft University of Technology.
- Tollenaar, R. N., van Paassen, L. A., & Cristina, J. (2018). Small-scale evaporation tests on clay: influence of drying rate on clayey soil layer. *Canadian Geotechnical Journal*, 55, 437–445.
- Tremblay, H., Duchesne, J., Locat, J., & Leroueil, S. (2002). Influence of the nature of organic compounds on fine soil stabilization with cement. *Canadian Geotechnical Journal*, 39, 535–546.
- UMS (2012). *User manual Hyprop, version 02.13*. Munich, Germany: UMS GmBH.
- Ven, G. (2003). *Leefbaar laagland: geschiedenis van de waterbeheersing en landaanwinning in Nederland*. Matrijs. Fifth edition.
- Venmans, A. A. M. (2004). Organic soils: Power Point Presentation TU Delft course (TA4130).
- Verruijt, A. (2001). *Soil Mechanics*. Delft, The Netherlands.

- Wahls, H. E. (1962). Analysis of primary and secondary consolidation. *Journal of the soil mechanics and foundations division*, 88, 207–231.
- Waksman, S. A. (1930). Chemical composition of peat and the role of microorganisms in its formation. *American Journal of Science*, 19, 32–54.
- Wang, Y. H., & Xu, D. (2006). Dual porosity and secondary consolidation. *Journal Geotechnical Geoenvironment Engineering*, 133, 793–801.
- Wardwell, R. E., Charlie, W. A., & Doxtader, K. A. (1983). *Test method for determining the potential for decomposition in organic soils*. West Conshohocken, PA.
- Wardwell, R. E., & Nelson, J. D. (1981). Settlement of Sludge Landfills with Fibre Decomposition. *Proc. 10th Int. Conf. Soil Mech. Found. Engng*, 2, 397–401.
- Whitlow, R. (2004). *Basic Soil Mechanics*. (4th ed.). Singapore: Prentice Hall.
- Wikipedia (2016). Organic Matter, Wikipedia, The Free Encyclopedia. URL: [https://en.wikipedia.org/w/index.php?title=Organic{_{}}matter{&}oldid=726278785](https://en.wikipedia.org/w/index.php?title=Organic_{_}matter{&}oldid=726278785).
- Wind, G. (1966). Capillary conductivity data estimated by a simple method. In *Proceedings of the Wageningen Symposium: Water in the Unsaturated Zone* (pp. 181–191).
- Wong, L. S., Hashim, R., & Ali, F. H. (2009). A Review on Hydraulic Conductivity and Compressibility of Peat.pdf. *Journal of Applied Sciences*, 9, 3207–3218.
- Wösten, J. H. M., Ismail, A. B., & Van Wijk, A. L. M. (1997). Peat subsidence and its practical implications: A case study in Malaysia. *Geoderma*, 78, 25–36.
- Yao, Y. (2016). *Dewatering behaviour of fine oil sands tailings*. Ph.D. thesis Delft University of Technology.
- Yin, J. H., Zhu, J. G., & Graham, J. (2002). A new elastic viscoplastic model for time-dependent behaviour stress-strain behaviour of normally and overconsolidated clays: theory and verification. *Canadian Geotechnical Journal*, 39, 157–173.
- Yong, R. N., Pusch, R., & Nakano, M. (2010). *Containment of high level radioactive and hazardous solid wastes with clay barriers*. Taylor & Francis.
- Young, A. (1992). The effects of fluctuations in atmospheric pressure on landfill gas migration and composition. *Water, Air and Soil Pollution*, 64, 601–616.
- Zain, N. H. M., van Paassen, L. A., & Jommi, C. (2017). Effects of in-situ oxidation on the compression behaviour of organic soils. *In preparation*, .
- Zainorabidin, A., & Wijeyesekera, D. C. (2007). Geotechnical Challenges with Malaysian Peat. In *Proceedings of the Advances in Computing and Technology* (pp. 252–261).
- Zeeuw, J. d. (1978). Peat and the dutch golden age. *The historical meaning of energy attainability. AAG Bijdragen*, 21, 3–31.

- Zeevaart, L. (1986). Consolidation in the intergranular viscosity of highly compressible soils. *Consolidation of soils: testing and evaluation*, 892, 257–281.
- Zhang, L., & O’Kelly, B. C. (2013). CONSTITUTIVE MODELS FOR PEAT — A REVIEW. In B. Onate, E., Owen, D.R.J., Suarez (Ed.), *12th International Conference on Computational Plasticity* (pp. 1294–1304). Barcelona, Spain: International Center for Numerical Methods in Engineering (CIMNE).
- Zulkifley, M. T. M., Ng, T. F., Raj, J. K., & Hashim, R. (2013). Definitions and engineering classifications of tropical lowland peats. *Bulletin of Engineering Geology and the Environment*, 72, 547–553.
- Zumdahl, S. S., & Zumdahl, S. A. (2007). *Chemistry*. (Seventh ed.). Boston, USA: Houghton Mifflin Company.



AMOUNT OF HYDROGEN PEROXIDE

Given soil properties as below:

Gravimetric water content = 530.9%

Organic content = 53.7%

Inorganic content = 46.3%

Amount of original soil = 100 g

Dry solid = 15.85 g

The amount of organic matter (in grams) contains in 100 g of wet soil is calculated based on organic content and dry solid obtained from water content where:

$$\text{Organicmatter}(OM) = \frac{53.7}{100} \times 15.85\text{g} = 8.5\text{g} \quad (\text{A.1})$$

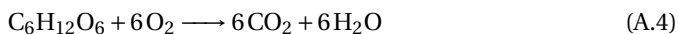
A conversion factor of 1.724 suggested by [Schumacher \(2002\)](#) and [Skempton & Petley \(1970\)](#) is used to convert organic matter to organic carbon. This is based on the assumption that organic carbon contains 58% of organic matter. However, this factor can range from 1.724 to as high as 2.5 ([Schumacher, 2002](#)). The conversion from organic matter to organic carbon as described below:

$$\text{Organicmatter}(OM) = 1.724 \times \text{Organiccarbon} \quad (\text{A.2})$$

$$\text{Organiccarbon} = \frac{8.5\text{g}}{1.724} = 4.94\text{g} \quad (\text{A.3})$$

Organic carbon (in grams) is then converted to mol by referring to molecular formula of carbon. In organic soils, three major biomass group are normally found that are cellulose, hemicellulose and lignin ([Kogel-Knabner, 2002](#)). Cellulose is reported to be

the most abundant biopolymer and comprises of the major structural component with generic formula of $(C_6H_{10}O_5)_n$ which is formed by different unit of glucose $C_6H_{12}O_6$ monomers. Consider aerobic oxidation of glucose which can be written as follows:



The equation can be written in a more simple biomass form (per mol of organic carbon) where;



This shows that one mol of organic carbon requires one mol of oxygen to allow complete oxidation of organic matter. If 4.94 g organic carbon contains in the soil, there is 0.4 mol of organic carbon in the soil by taking 1 mol of carbon is equivalent to 12 g of soil. Hence, 0.4 mol of oxygen is required to oxidise 0.4 mol of organic carbon.

Meanwhile, the amount of 10% (w/w) Hydrogen peroxide H_2O_2 required to oxidise organic matter in oedometer test can be determined by firstly understanding the Hydrogen peroxide reaction mechanisms. The reaction of Hydrogen peroxide and other chemical oxidants is described in detail by Mikutta et al. (2005). Hydrogen peroxide is chemically unstable and the reaction can be written as follows:



If the reaction is written per mol of H_2O_2 , Equation above can be simplified as:



This describes that one mol of H_2O_2 produce 0.5 mol of O_2 . In order to produce 0.4 mol of O_2 , 0.8 mol of H_2O_2 is required. Molecular weight of H_2O_2 is given by 34 g. Hence, 0.8 mol of H_2O_2 contains 27.2 g.

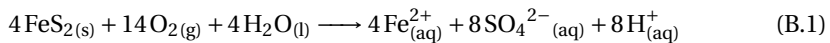
In this experiment, 10% (w/w) H_2O_2 is used which can be defined as 10 g of H_2O_2 / 100 L total solution. As the stock is prepared in 1 Litre volume with given H_2O_2 relative density of 1.11 g/cm³ which almost similar to the density of water, it can also be expressed as 100 g of H_2O_2 / 1000 g total volume. Hence, 27.2 g of H_2O_2 requires around 300 ml total 10% (w/w) H_2O_2 solution.

B

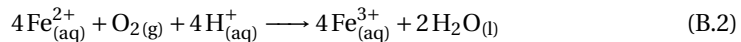
CHEMICAL REACTIONS

B.1. PYRITE OXIDATION REACTION

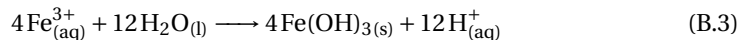
According to [Thorsten \(2013\)](#), when pyrite FeS_2 is exposed to oxygen and water, the mineral partly dissolves and the sulphide is oxidized to sulphate according to:



The dissolved sulphate ions increase the acidity of the solution and the produced ferrous iron Fe^{2+} can be further oxidized to ferric iron:

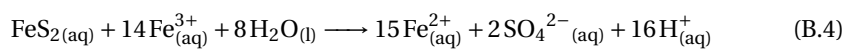


The produced acidity is partly consumed in this reaction. The rate of this inorganic oxidation reaction can be catalysed by several bacteria and is pH dependant. Under acidic conditions (pH 2-3) the reaction is proceeding slowly, with limited number of bacteria able to be active, but at pH values near 5 or higher the reaction can be several orders of magnitude faster. This reaction is referred to as the "rate determining step" in the overall acid-generating sequence. Once ferric iron is formed it may react with water and form ferric hydroxide.



The ferric hydroxide formed in this reaction also called "yellow boy", a yellowish-orange precipitate (solid) which formed when pH is above 3.5 but when pH is below 3.5, little or no solids will precipitate. Other reactions can also occur due to oxidation of additional pyrite by ferric ion. This is the cyclic and self-propagating part of the overall

reaction and takes place very rapidly. The reaction continues until either ferric iron or pyrite is depleted. Note that in this reaction, iron is the oxidising agent, not oxygen.



SUMMARY

Organic soils and peat soils are widely distributed across the world, particularly in the Northern hemisphere in countries like Canada and Russia having 170 and 150 million hectares respectively and in tropical regions such as Indonesia and Malaysia, which contain 26 million and 3 million hectares respectively. Organic soils and peat are considered problematic materials for construction. Due to their high water content and high compressibility, they are unsuitable material to support any foundation and other type of loading in their natural state. However, as population grows every year, land becomes scarce and the need to use this land for agriculture or construction is rising. In practice, these waterlogged soils are drained before any potential usage for construction. However, drainage requires significant time and leads to settlements or subsidence. Subsidence in organic soils may cause damage or high maintenance costs to buildings and infrastructure or require significant amount of materials to raise or maintain surface level, which may be costly or have significant environmental impact. Subsidence of peat also occurs in rural areas. Peat meadows are drained through networks of ditches and waterways to enable farming or agriculture. These waterways require regular dredging to keep them open from plant growth and prevent them to fill up with partly degraded organic matter. In this project 'Lift up Lowlands' the potential of using these dredged organic sediments to compensate surface subsidence in peatlands is investigated.

Drainage induced subsidence of peatlands or organic soils is attributed to three different mechanisms, which are oxidation, consolidation and shrinkage. Currently there is no consensus worldwide, which of these mechanisms is the main cause of surface subsidence. Some authors claimed that oxidation of organic matter in the upper layer (aerobic oxidation) is the major mechanism causing irreversible long term settlement of drained peat soil. The oxidation process is considered to be very slow under limited oxygen or anaerobic conditions, but it can be accelerated under aerobic conditions, when oxygen is allowed to penetrate the upper layer as a result of drainage. Oxidation of organic matter can cause settlement normally unaccounted for during service life of buildings due to development of secondary compression and it is considered to be a large source of greenhouse gas emissions. The main aim of this thesis is to investigate the role of oxidation in influencing the compression behaviour of organic soils and peat.

The research starts with a literature review on organic soils and peat, which covers their distribution, classification, physical and engineering properties in comparison with other similar soils and includes some background on the different types of organic matter together and their structural and chemical properties.

The effect of oxidation on the compression behaviour of organic soil is investigated by performing One Dimensional Consolidation Tests. Oxidation of organic matter is stimulated prior to loading (ex-situ) and inside the oedometer cell (in-situ) under different constant loads in order to simulate conditions in the field using Hydrogen Peroxide.

This reagent has the ability to accelerate the oxidation process and is commonly used to remove organic matter in soil classification test. The results show that a sample, which is oxidised in-situ develops a metastable structure as the void ratio under a given effective stress does not reach the virgin compression line of the ex-situ decomposed soil. With subsequent loading, a stiff response is observed, until the virgin compression line of the non-oxidised soil is reached. Upon unloading, the in situ oxidised soil shows a reduced swelling capacity similar to the ex-situ oxidised soil.

The following chapter discusses on the effect of in-situ oxidation on consolidation and creep parameters at different stress levels. Consolidation parameters include coefficient of consolidation, c_v , coefficient of volume compressibility, m_v and hydraulic conductivity, k_v while creep parameter is the secondary compression, C_α . The results show that C_α and m_v and k_v decrease in the step after oxidation, while c_v increases. Using Taylor's square root time method, the time to reach the end of primary compression during the load step after oxidation was significantly shorter when compared to the effect of creep alone. The primary compression reduced significantly, while secondary compression increased significantly after creep and oxidation took place.

In the next chapter the kinetics or rate of aerobic oxidation in organic soil and peatlands are discussed. Different methods were used to measure the kinetics of oxidation: by measuring the oxygen depletion rate in a bioreactor, and by measuring the settlement rate, loss in dry mass or loss of organic matter in the one dimensional consolidation tests. The rate of oxidation is expressed in terms of carbon dioxide emissions assuming a simplified chemical reaction equation and using an empirical relation suggested by [van den Akker et al. \(2008\)](#) to relate deformation to oxidation. Organic matter was suspended in a bioreactor, which was initially sparged with air and consequently subjected to cycles of stirring and non-stirring. Based on oxygen depletion rate during non-stirring cycles, the rate of oxidation could be determined based on the oxygen depletion rate. The oxygen depletion rate could be described with the Michaelis-Menten equation, which is used to determine the effect of substrate limitation on enzyme kinetics. The maximum oxidation rate in terms of carbon dioxide emissions ranged between 0.63 and 2.98 gram CO₂ per gram of dry soil per year. Chemical oxidation with hydrogen peroxide showed similar oxygen depletion rates at similar measured dissolved oxygen concentrations. Higher oxidation rates could be obtained by increasing the Hydrogen Peroxide concentration. For the settlement data, the rate of oxidation was estimated using an empirical relationship described by [van den Akker et al. \(2008\)](#), which links settlement rate, dry bulk density, organic matter fraction, carbon fraction and carbon dioxide emissions and uses a fraction which relates the settlement due to oxidation of organic matter compared to total settlement. Finally, the difference in dry mass and mass of organic matter before and after in-situ oxidation in oedometer cell was used to estimate the oxidation rate. For each approach, the corresponding carbon dioxide emissions are calculated and the results and differences are discussed. The results showed that although the oxidation in the oedometer was very inefficient (based on the observed mass loss), still significant settlement was observed during oxidation. Comparing the maximum oxidation rates per gram of dry soil in the bioreactor with the chemical oxidation rates in the oedometer confirmed that the oxidation rate in the oedometer is limited by a limited oxygen availability. Secondly, the oedometer tests showed that the fraction of settlement attributed

to the oxidation is not necessarily equal to 100% as proposed by [van den Akker et al. \(2008\)](#), but depends on the method by which it is determined. Hence, a direct correlation between measured settlements and carbon dioxide production involves significant uncertainty.

The last chapter describes the effect of organic matter and initial water content on shrinkage and water retention behaviour. The shrinkage and water retention behaviour were compared between oxidised and non-oxidised material. Hyprop tests were carried out to measure the water tension and soil weight as the sample dries. At regular time intervals, the Hyprop system was placed in an X-ray CT scanner, which was used to determine the shrinkage in soil volume during drying. The results showed that oxidation of organic matter significantly reduces the water holding capacity of the dredged organic sediments. Both the oxidised and non-oxidised samples showed significant shrinkage upon drying, but the non-oxidised sample showed much more volume change than the oxidised soil. The soil water retention curves (SWRC) show similar patterns as the one-dimensional consolidation tests, in which the slope of the SWRC is equal to the compression index. However, considering the stress conditions during soil shrinkage are closer to isotropic conditions the SWRC is expected to be slightly below the normal consolidation line derived from the oedometer tests and closer to the critical state line. When starting the drying process with a slurry, a large part of the shrinkage occurs before suction can be measured. A correction procedure is suggested to extend the measuring range of the HYPROP device to low suction values. The CT scans indicate that apart from some gas bubbles (which particularly appear in the non-oxidised soil at a suction pressure below 1 kPa) and shrinkage cracks which occur at a later stage in the drying process, both soils remain close to full saturation.

SAMENVATTING

Organische bodems en veengronden zijn wijd verspreid over de wereld, vooral op het noordelijk halfrond in landen als Canada en Rusland met respectievelijk 170 en 150 miljoen hectare en in tropische regio's zoals Indonesië en Maleisië, die respectievelijk 26 miljoen en 3 miljoen hectare bevatten. Organische bodems en veen worden beschouwd als problematische grond voor constructie activiteiten. Vanwege hun hoge watergehalte en hoge samendrukbaarheid zijn ze ongeschikt materiaal om een fundering of ander soort lading in hun natuurlijke staat te dragen. Naarmate de bevolking elk jaar groeit, wordt het land schaars en neemt de behoefte om dit land te gebruiken voor constructie of landbouw activiteiten toe. In de praktijk worden deze drassige bodems gedraineerd voordat ze kunnen worden gebruikt voor constructie van gebouwen en infrastructuur. Drainage vergt echter veel tijd en leidt tot bodemdaling. Bodemdaling in organische bodems kan schade of hoge onderhoudskosten veroorzaken of een aanzienlijke hoeveelheid materialen vereisen om het maaiveldniveau te verhogen of te handhaven, wat kostbaar kan zijn of aanzienlijke milieueffecten kan hebben. Veenweiden worden ook gedraineerd via netwerken van sloten en waterwegen om landbouw of landbouw mogelijk te maken. Deze waterwegen moeten regelmatig gebaggerd worden om ze open te houden en plantengroei en gedeeltelijk afgebroken organisch materiaal te verwijderen. In het project 'Lift up Lowlands' is onderzocht of dit gebaggerd organische materiaal gebruikt kan worden om bodemdaling in veengebieden tegen te gaan.

Door drainage veroorzaakte bodemdaling van veengronden of organische bodems wordt toegeschreven aan drie verschillende mechanismen, namelijk oxidatie, consolidatie en krimp. Momenteel is er wereldwijd geen consensus, welke van deze mechanismen de belangrijkste oorzaak is van bodemdaling. Sommige auteurs beweren dat oxidatie van organisch materiaal in de bovenste laag (aerobe oxidatie) het belangrijkste mechanisme is dat onomkeerbare langdurige daling van gedraineerde veengrond veroorzaakt. Het oxidatieproces wordt beschouwd als zeer langzaam onder beperkt aerobe of anaërobe omstandigheden, maar het kan worden versneld onder aerobe omstandigheden, wanneer zuurstof de bovenlaag kan binnendringen als gevolg van drainage. Oxidatie van organisch materiaal wordt normaal gezien niet beschouwd, bij de voorspelling van bodemdaling gedurende de levensduur van gebouwen of infrastructuur. Oxidatie wordt wel beschouwd als een grote potentiële bron van broeikasgasemissies. Het belangrijkste doel van dit proefschrift is om de rol van oxidatie in het beïnvloeden van het compressiegedrag van organische bodems en veen te onderzoeken.

Het onderzoek begint met een literatuurstudie over organische bodems en veen, waarbij de globale verspreiding, classificatie, fysische en technische eigenschappen worden beschouwd in vergelijking met andere bodems. Ook is de samenstelling van verschillende soorten organisch materiaal en hun structurele en chemische eigenschappen bestudeerd.

Het effect van oxidatie op het compressiegedrag van organische grond is bestudeerd door het uitvoeren van eendimensionale consolidatietesten. Oxidatie van organisch materiaal is gestimuleerd voorafgaand aan het belasten (ex situ) en onder verschillende constante belastingen in de oedometercel (in-situ) met behulp van waterstofperoxide. Waterstofperoxide is een sterke oxidator en wordt vaak gebruikt om organisch materiaal te verwijderen voorafgaand aan geotechnische grondclassificatietesten. De testresultaten laten zien dat bij in situ oxidatie een metastabiele structuur ontstaat, die in eerste instantie een stijve respons vertoont bij verdere verhoging van de belasting, totdat de maagdelijke compressielijn van de niet-geoxideerde grond is bereikt, waarna de in situ geoxideerde grond een vergelijkbaar samendrukkingsgedrag als de niet geoxideerde grond vertoont. Bij het verlagen van de belasting van de belasting vertoont de in situ geoxideerde grond een verminderd zwelvermogen vergelijkbaar met de ex situ geoxideerde grond.

In het volgende hoofdstuk wordt het effect van in-situ oxidatie op de consolidatieparameters consolidatiecoëfficiënt, c_v , samedrukkingscoëfficiënt, m_v en hydraulische geleidbaarheid, k_v en de kruipparameter, C_α , beschreven. De resultaten laten zien dat C_α , m_v en k_v in de stap na oxidatie afnemen, terwijl c_v toeneemt. Met behulp van Taylor's methode is aangetoond dat de tijd om het einde van de primaire compressie te bereiken tijdens de belastingstap na oxidatie significant korter is dan in de test zonder oxidatie. De primaire compressie vermindert aanzienlijk, terwijl secundaire compressie aanzienlijk toeneemt nadat kruip en oxidatie hebben plaatsgevonden.

In het volgende hoofdstuk wordt de kinetiek van aërobe oxidatie in organische bodem en veengronden besproken. Verschillende methoden werden gebruikt om de oxidatiesnelheid te meten. De oxidatiesnelheid wordt uitgedrukt als CO₂ emissie in gram CO₂ per gram droge grond per jaar, met behulp van een simpele reactievergelijking en een empirische correlatie tussen deformatie en massaverlies beschreven door [van den Akker et al. \(2008\)](#). Organisch materiaal werd gesuspendeerd in een bioreactor, die aanvankelijk werd doorgeblazen met lucht en vervolgens werd onderworpen aan cycli van roeren en niet-roeren. Door de concentratie opgelost zuurstof in de suspensie te meten tijdens niet-roerende cycli, kon de snelheid van oxidatie worden bepaald op basis van de snelheid waarmee de zuurstofconcentratie afneemt. De zuurstofdepletiesnelheid kan worden beschreven met de Michaelis-Menten-vergelijking, die wordt gebruikt om het effect van substraatbeperking op enzymkinetiek te beschrijven. De maximale oxidatiesnelheid onder zuurstorijke omstandigheden in de bioreactor varieert van 0.63 tot 2.98 gram CO₂ per gram droge grond per jaar. Chemische oxidatie met waterstofperoxide in de bioreactor vertoont vergelijkbare zuurstofdepletiesnelheden bij vergelijkbare gemeten opgeloste zuurstofconcentraties. Verhoging van de waterstofperoxide concentratie resulteert in hogere oxidatiesnelheden. Bij in situ oxidatie in de oedometer cel kan de oxidatiesnelheid op drie manieren worden bepaald. Allereerst is de hoeveelheid oxidatie gerelateerd aan de hoeveelheid vervorming (bodemdaling), waarbij verondersteld is dat alle vervorming een gevolg is van oxidatie van het organisch materiaal, overeenkomstig met de aanname ([van den Akker et al., 2008](#)). Daarnaast is het verschil in droge massa en de massa van organisch materiaal vóór en na in-situ oxidatie in oedometercellen gebruikt om de oxidatiesnelheid te schatten. Voor elke benadering zijn de overeenkomstige kooldioxide-emissies berekend en de resultaten en verschillen zijn besproken. De resul-

taten tonen aan dat, hoewel de oxidatie in de oedometer zeer inefficiënt was (op basis van het waargenomen massaverlies), er nog steeds aanzienlijke vervorming is waargenomen tijdens oxidatie. Het vergelijken van de maximale oxidatiesnelheden per gram droge grond in de bioreactor met de chemische oxidatiesnelheden in de oedometer bevestigt dat de oxidatiesnelheid in de oedometer beperkt is door een beperkte beschikbaarheid van zuurstof (op basis van massaverlies). Ten tweede is aangetoond dat de vervorming die wordt toegeschreven aan de oxidatie van het organische materiaal niet noodzakelijkerwijs gelijk is aan 100%, zoals voorgesteld door [van den Akker et al. \(2008\)](#), maar hangt af van de methode waarmee deze wordt bepaald. Op basis van deze observatie is geconcludeerd dat een directe correlatie tussen gemeten vervorming en berekende koolstofdioxide emissies aanzienlijke onzekerheid met zich meebrengt.

Het laatste hoofdstuk beschrijft het effect van organisch materiaal en het initiële watergehalte op het krimp- en waterretentiegedrag van organische grond tijdens drogen. Het krimp- en waterretentiegedrag van ex situ geoxideerd sediment is vergeleken met niet-geoxideerd materiaal. Proeven zijn uitgevoerd met behulp van een Hyprop systeem, waarin de zuigspanning en het gewicht van de grond tijdens het uitdrogen continu kunnen worden gemeten. Op regelmatige tijdstippen is het Hyprop-systeem in een röntgen-CT-scanner geplaatst, waarmee het volume van de krimpende, uitdrogende grond kan worden bepaald. De resultaten tonen aan dat oxidatie van organisch materiaal de wateropname capaciteit van de gebaggerde organische sedimenten aanzienlijk vermindert. Zowel de geoxideerde als de niet-geoxideerde monsters vertonen veel krimp tijdens het drogen, maar het niet-geoxideerde materiaal vertoont veel meer volumeverandering dan het geoxideerde materiaal. De waterretentiekaracteristieke curves (SWRC) vertonen vergelijkbare patronen als de eendimensionale consolidatie tests, waarbij de helling van de SWRC gelijk is aan de compressie-index. Bij hoge initiële watergehalten, kenmerkend voor opgebaggerd en verpompt fijnkorrelig of organisch materiaal, vindt een groot deel van de krimp plaats voordat enige zuigspanning kan worden gemeten. Om het meetbereik van het Hyprop systeem uit te breiden tot lage zuigspanningswaarden, is een voorgestelde correctieprocedure toegepast. De CT-scans geven aan dat de totale volumeverandering vrijwel gelijk is aan het waterverlies. Afgezien van enkele gasbellen, die vooral ontstaan in de niet-geoxideerde materiaal bij een zuigspanning lager dan 1 kPa) en krimpscheuren die zich in een later stadium van het droogproces voordoen, blijven zowel het geoxideerde als het niet-geoxideerde materiaal tijdens het droogproces vrijwel volledig verzadigd met water.

ACKNOWLEDGEMENTS

First and above all, I praise to Allah S.W.T, the Most Gracious and Most Merciful for the strength He has given me and also His blessings in completing my PhD dissertation. I never expect to reach until this far and it is a miracle to deliver my work especially when I need to obliged myself to three different jobs as of being a student, a mother and also a wife. Initially, I almost losing myself in this battle but with the help of supportive people around me now I do believe that nothing is impossible. I know words cannot replace the support that you have showered me throughout my journey. With that, I would like to this opportunity to extend my deepest appreciation to the following people that I will mention here explicitly.

First of all to my PhD supervisors, Professor Cristina Jommi and Dr Leon van Paassen. They have been very supportive and always challenge me to work on something that is beyond my comforting zone. It may be difficult for me but I know it benefits me in a certain way. I know both of you have a very tight schedule but you never fail to listen to my research progress either verbally or virtually.

Laboratory technicians: Arno Mulder and Yolanda van Haagen for your good cooperation assisting my laboratory works until completion.

To my parents for their continuous encouragement and support. My father, Md. Zain bin Abdul Jalil who has been monitoring my whereabouts from far. My mother, Napsiah Mohd who has never given up praying for my success and always be a good listener during my difficult times. I know how much you miss talking to me and thousand apology for not having time for you.

My beloved daughter, Azwa Safrina who always there to cherish my day with her sweet character and funny jokes. Thank you for colouring my life and behaving well when i am busy with my work. I hope you will remember your great moments here and especially your Dutch language and friends. You have been a good Dutch translator for me during our times here. My husband, Muhammad Adib Bin Haron for helping me to take care of my daughter when i was busy with my lab tests.

I also would like to appreciate the assistance and support from my current and former colleagues: Vu Minh Ngan, Partick Arnold, Hongfen Zhou, Andre van Turnhout, Di-anne den Hamer, Vinh Pham, Roderick Tollenaar, Elisa Ponziani, Yajun Li, Rui Rui, Leon Acousta, Jiani, Laura Amelia, Basyarah Hamat and Balqis Mohd Yunus.

Not to forget to my scholarship funders, Ministry of Education Malaysia and Universiti Teknologi MARA for providing me an opportunity to study in Delft University of Technology.

*Nor Hazwani Md. Zain
2019
Delft*

CURRICULUM VITÆ

Nor Hazwani Md. ZAIN

01-09-1983 Born in Kuala Lumpur, Malaysia.

EDUCATION

2000–2002 Pre-university Matriculation Programme
College TAJ Matriculation Centre, Perak, Malaysia

2002–2005 Bachelor of Civil Engineering
University of Malaya, Malaysia

2005–2007 Master of Science in Geotechnical Engineering
Universiti Teknologi MARA, Malaysia

2019 PhD Geotechnical Engineering
Delft University of Technology
Thesis: Effect of Oxidation on the Compression Behaviour of
Organic Soils
Promotor: Prof. dr. ir. C. Jommi
Copromotor: Dr. ir. L.A. van Paassen